DEVELOPMENT OF THE MODIFIED STRUCTURED CAM CLAY MODEL AND FINITE ELEMENT IMPLEMENTATION

Jirayut Suebsuk

A Thesis Submitted in Partial Fulfillment of the Requirements for the Degree of Doctor of Philosophy in Civil Engineering

Suranaree University of Technology

Academic Year 2010

การพัฒนาแบบจำลองโมดิไฟด์ สตัคเจอร์ด แคม เคลย์ และการนำไปใช้ในวิธีไฟไนท์อิลลิเมนต์

นายจิระยุทธ สืบสุข

วิทยานิพนธ์นี้เป็นส่วนหนึ่งของการศึกษาตามหลักสูตรปริญญาวิศวกรรมศาสตรดุษฎีบัณฑิต
สาขาวิชาวิศวกรรมโยธา
มหาวิทยาลัยเทคโนโลยีสุรนารี
ปีการศึกษา 2553

DEVELOPMENT OF THE MODIFIED STRUCTURED CAM CLAY MODEL AND FINITE ELEMENT IMPLEMENTATION

Suranaree University of Technology has approved this thesis submitted in partial fulfillment of the requirements for the Degree of Doctor of Philosophy.

Thesis Examining Committee

_____
(Prof. Dr. Dennes T. Bergado)
Chairperson

_____
(Prof. Dr. Suksun Horpibulsuk)
Member (Thesis Advisor)

_____
(Dr. Martin D. Liu)
Member

_____
(Asst. Prof. Dr. Pornpot Tanseng)
Member

_____
(Asst. Prof. Dr. Avirut Chinkulkijniwat)
Member

_____
(Assoc. Prof. Dr. Suched Likitlersuang)
Member

_____
(Asst. Prof. Dr. Pornkasem Jongpradist)
Member

_____	_____
(Prof. Dr. Sukit Limpijumnong)	(Assoc. Prof. Dr. Vorapot Khompis)
Vice Rector for Academic Affairs	Dean of Institute of Engineering

จิระยุทธ สืบสุข : การพัฒนาแบบจำลองโมดิไฟด์ สตัคเจอร์ด แคม เคลย์ และการนำไปใช้ในวิธีไฟไนท์อิลลิเมนต์ (DEVELOPMENT OF THE MODIFIED STRUCTURED CAM CLAY MODEL AND FINITE ELEMENT IMPLEMENATION) อาจารย์ที่ปรึกษา : ศาสตราจารย์ ดร.สุขสันติ์ หอพิบูลสุข, 224 หน้า

วิทยานิพนธ์นี้นำเสนอแบบจำลองพฤติกรรม (constitutive model) สำหรับดินเหนียวพันธะเชื่อมประสาน (structured clays) ซึ่งประกอบด้วยสามส่วนหลัก ส่วนแรก กล่าวถึง การพัฒนาแบบจำลองพฤติกรรมทั่วไปสำหรับดินเหนียวไร้พันธะเชื่อมประสาน (destructured clay) ดินเหนียวพันธะเชื่อมประสานธรรมชาติ (naturally structured clay) และดินเหนียวพันธะเชื่อมประสานสังเคราะห์ (artificially structured clay) แบบจำลองนี้พัฒนาจากแบบจำลองสตัคเจอร์ด แคม เคลย์ (Structured Cam Clay: SCC) แบบจำลองที่พัฒนาขึ้นใหม่ให้ชื่อว่า แบบจำลองโมดิไฟด์ สตัคเจอร์ด แคม เคลย์ (Modified Structured Cam Clay: MSCC) อิทธิพลของพันธะเชื่อมประสาน (soil structure) และการสลายของพันธะเชื่อมประสาน (destructuring) ต่อพฤติกรรมทางกลของดินเหนียวสามารถอธิบายได้โดยหลักการความเค้นประสิทธิผลดัดแปลง (modified effective stress) ซึ่งเป็นผลรวมของความเค้นประสิทธิผลปัจจุบัน (current effective stress) และความเค้นประสิทธิผลเนื่องจากอิทธิพลของพันธะเชื่อมประสาน (structure strength) พันธะเชื่อมประสานส่งผลต่อการเพิ่มขึ้นของความเค้นประสิทธิผลดัดแปลง และขนาดของผิวคราก (yield surface) อีกทั้งยังเพิ่มแรงยึดเหนี่ยว (cohesion) กำลัง ณ จุดยอด (peak strength) และความแข็งแกร่ง (stiffness) อีกด้วย การแตกสลายของพันธะเชื่อมประสานเริ่มเกิดขึ้นเมื่อสถานะความเค้น (stress state) อยู่บนผิวคราก กฎการแตกสลายของพันธะเชื่อมประสาน (destructuring law) ได้ถูกพัฒนาตามหลักการดังนี้ คือ การแตกสลายของพันธะเชื่อมประสานเกิดทันทีหลังจากจุดวิบัติ (failure) กระบวนการนี้เป็นผลจากการแตกหัก (crushing) ของพันธะเชื่อมระหว่างอนุภาคเม็ดดิน (soil-cementation structure) ซึ่งส่งผลต่อการเกิดพฤติกรรมอ่อนตัวลงเมื่อความเครียดเพิ่มขึ้น (strain softening) พันธะเชื่อมประสานจะแตกสลายอย่างสมบูรณ์เมื่อสถานะความเค้นอยู่ที่สถานะวิกฤต (critical state) ผิวครากของดินพันธะเชื่อมประสาน และดินไร้พันธะเชื่อมประสานจะเป็นผิวเดียวกันที่สถานะวิกฤต รูปร่างผิวครากสำหรับแบบจำลอง MSCC ยังคงใช้รูปร่างเดียวกันกับแบบจำลองโมดิไฟด์ แคม เคลย์ (Modified Cam Clay: MCC) ในขณะที่พลาสติคโพเทนเชียล (plastic potential) พัฒนาขึ้นโดยการรวมอิทธิพลของพันธะเชื่อมประสานที่มีต่อทิศทางของความเครียดพลาสติค (plastic strain direction) ในการคำนวณพฤติกรรมการแกร่งขึ้น (hardening) และพฤติกรรมการอ่อนลง (softening) พารามิเตอร์ของแบบจำลอง MSCC แบ่งออกได้เป็นสองส่วน คือ พารามิเตอร์สำหรับอธิบาย

พฤติกรรมที่ไม่เกี่ยวข้องกับพันธะเชื่อมประสาน (destructured properties) และพารามิเตอร์สำหรับอธิบายอิทธิพลของพันธะเชื่อมประสาน (structured properties) พารามิเตอร์ทั้งหมดของแบบจำลองนี้มี นัยทางกายภาพ (physical meaning) และสามารถหาได้จากผลการทดสอบแรงอัดแบบสามแกน

งานวิจัยในส่วนที่สอง คือ การปรับปรุงแบบจำลอง MSCC สำหรับการทำนายพฤติกรรมของดินพันธะเชื่อมประสานในสถานะอัดตัวมากกว่าปกติ (overconsolidated structured clays) แบบจำลองนี้ได้รับการพัฒนาให้สอดคล้องตามหลักการพื้นฐานของแบบจำลอง SCC โดยให้ชื่อว่า แบบจำลองโมดิไฟด์ สตัคเจอร์ด แคม เคลย์ ร่วมกับทฤษฎีขอบเขตผิว (Modified Structured Cam Clay with Bounding Surface Theory: MSCC-B) แบบจำลองที่ปรับปรุงขึ้นนี้สามารถอธิบายกระบวนการแกร่งขึ้น และกระบวนการแตกสลายของพันธะเชื่อมประสานของดินพันธะเชื่อมประสานอัดตัวมากกว่าปกติ ค่าโมดูลัสความแกร่งขึ้นแบบพลาสติค (plastic hardening modulus) ซึ่งมีค่าเปลี่ยนแปลงตลอดการให้น้ำหนักบรรทุกสามารถคำนวณได้โดยอาศัยเทคนิคภาพฉายเชิงรัศมี (radial mapping technique) พารามิเตอร์ h ซึ่งเป็นพารามิเตอร์ที่ขึ้นกับชนิดของวัสดุ ถูกนำเสนอขึ้นเพื่อแสดงอิทธิพลของสถานะความเค้นสำหรับดินพันธะเชื่อมประสานอัดตัวมากกว่าปกติในสมการคำนวณโมดูลัสความแกร่งขึ้นแบบพลาสติค ผลการคำนวณจากแบบจำลอง MSCC-B ได้รับการตรวจสอบความถูกต้องและประสิทธิภาพโดยการเปรียบเทียบกับผลการทดสอบของตัวอย่างดินเหนียวพันธะเชื่อมประสานธรรมชาติ และดินเหนียวพันธะเชื่อมประสานสังเคราะห์ ภายใต้การทดสอบการอัดตัวแบบเท่ากันทุกทิศทาง (isotropic compression test) และการทดสอบการรับแรงเฉือนแบบอัดตัว (compression shearing test) จากผลการศึกษาปรากฏว่าแบบจำลอง MSCC-B สามารถทำนายผลการตอบสนองทางกล (mechanical response) ของดินพันธะเชื่อมประสานอัดตัวมากกว่าปกติภายใต้สถานะระบายน้ำ (drained condition) และไม่ระบายน้ำ (undrained condition) ได้เป็นอย่างดี

งานวิจัยในส่วนสุดท้ายศึกษาผลกระทบของพันธะเชื่อมประสานต่อความเค้น (stress) ความเครียด (strain) และกำลัง (strength) แบบเฉพาะจุด (local element) ที่ไม่เป็นแบบเดียวกัน (inhomogeneous) ในการทดสอบการรับแรงเฉือนภายใต้แรงอัดแบบสามแกน โดยวิธีไฟไนท์อิลลิเมนต์ร่วมกับแบบจำลอง MSCC ในการศึกษานี้แบบจำลอง MSCC ถูกจัดให้อยู่ในรูปแบบคอนทินัม จาโคเบียน (continuum Jacobian) และถูกเขียนเป็นรหัสภาษาคอมพิวเตอร์เพื่อใช้คำนวณร่วมกับโปรแกรมไฟไนท์อิลลิเมนต์เชิงพานิชย์ ชื่อว่า ABAQUS การศึกษาทำโดยการเปรียบเทียบผลการวิเคราะห์พฤติกรรมของตัวอย่างดินเหนียวพันธะเชื่อมประสานสังเคราะห์ภายใต้การทดสอบแรงอัดแบบสามแกน โดยใช้พารามิเตอร์ของแบบจำลองสำหรับดินเหนียวพันธะเชื่อมประสานสังเคราะห์ที่ปริมาณซีเมนต์ต่าง ๆ ทั้งในสภาวะระบายน้ำ และไม่ระบายน้ำ การวิเคราะห์โดยวิธีไฟไนท์อิลลิเมนต์เป็นแบบ couple hydro-mechanic ความเค้น และความเครียดเฉพาะที่ของ

ตัวอย่างดินเหนียวพันธะเชื่อมประสานสังเคราะห์ที่ปริมาณซีเมนต์ต่าง ๆ ถูกนำมาพิจารณาเปรียบเทียบกับตัวอย่างดินเหนียวไร้พันธะเชื่อมประสาน ในส่วนท้าย นัยสำคัญที่ได้จากการวิเคราะห์เปรียบเทียบโดยวิธีไฟไนท์อิลลิเมนต์ได้รับการสรุปและวิจารณ์

สาขาวิชาวิศวกรรมโยธา
ปีการศึกษา 2553

ลายมือชื่อนักศึกษา _____
ลายมือชื่ออาจารย์ที่ปรึกษา _____
ลายมือชื่ออาจารย์ที่ปรึกษาร่วม _____

JIRAYUT SUEBSUK : DEVELOPMENT OF MODIFIED STRUCTURED CAM CLAY MODEL AND FINITE ELEMENT IMPLEMENTATION.
THESIS ADVISOR : PROF. SUKSUN HORPIBULSUK, Ph.D., 224 PP.

CONSTITUTIVE EQUATION/STRUCTURED CLAY/PLASTICITY/
CRITICAL STATE MODEL/SOIL STRUCTURE/DESTRUCTURING/BOUNDING SURFACE THEORY/FINITE ELEMENT ANALYSIS

With the advances in the calculation by a numerical method and computer hardware, it becomes more common to predict the response of geotechnical material using a constitutive model in numerical analysis. The constitutive models for structured clay have been developed in this research. The thesis is composed of three consecutive parts. First part presents a generalised constitutive model for destructured, naturally structured and artificially structured clays that extends the Structured Cam Clay (SCC) model. This model is designated as “Modified Structured Cam Clay (MSCC) model”. The influence of structure and destructuring on the mechanical behaviour of clay can be explained by the change in the modified effective stress, which is the sum of the current mean effective stress and the additional mean effective stress due to structure (structure strength). The presence of structure increases the modified mean effective stress and yield surface, enhancing the cohesion, peak strength and stiffness. The destructuring begins when the stress state is on the virgin yield surface. After the failure (peak strength) state, the abrupt destructuring occurs as the soil-cementation structure is crushed; hence the strain softening. The soil structure is completely removed at the critical state when the yield surface becomes identical to

the destructured surface. The destructuring law is proposed based on this premise. In the MSCC model, the yield function is the same shape as that of the Modified Cam Clay (MCC) model. A plastic potential is introduced so as to account for the influence of structure on the plastic strain direction for both hardening and softening behaviours. The required model parameters are divided into those describing destructured properties and those describing structured properties. All the parameters have physical meaning and can be simply determined from the conventional triaxial tests.

Second part presents a generalised critical state model with the bounding surface theory for simulating the stress-strain behaviour of overconsolidated structured clays. The model is formulated based on the framework of the Structured Cam Clay (SCC) model and is designated as the Modified Structured Cam Clay with Bounding Surface Theory (MSCC-B) model. The hardening and destructuring processes for structured clays in the overconsolidated state can be described by the proposed model. The image stress point defined by the radial mapping technique is used to determine the plastic hardening modulus, which varies along loading paths. A new proposed parameter h, which depends on the material characteristics, is introduced into the plastic hardening modulus equation to take the soil behaviour into account in the overconsolidated state. The MSCC-B model is evaluated in light of the model performance by comparisons with the measured data of both naturally and artificially structured clays under isotropic compression and compression shearing tests. From the comparisons, it is found that the MSCC-B model gives an excellent prediction of mechanical response in both drained and undrained conditions.

Last part presents the study of the inhomogeneous stress-strain-strength behaviour influenced by the structure strength by using the finite element analysis

with the MSCC model. The MSCC model formulated with a continuum Jacobian has been coded into the commercial finite element program, ABAQUS by the user subroutine, UMAT. The generalised MSCC model has been used to study a triaxial compression test of artificially structured clay specimens with various cement contents under drained and undrained conditions by a couple hydro-mechanic finite element analysis. The influence of structural properties on the inhomogeneity is studied. The local stress and strain of the artificially structured specimens is compared with those of the destructured specimen under various isotropic yield stress ratio (YSRiso). The key aspects of finite element simulation of artificially structured clay are summarised and discussed.

School of Civil Engineering

Academic Year 2010

Student's Signature _____

Advisor's Signature_____

Co-advisor's Signature _____

ACKNOWLEDGEMENTS

Seven years ago, I have entered the School of Civil Engineering, Suranaree University of Technology, which led to a big change in my life. I have pursued my Master's and Ph.D. studies in the Field of Geotechnical Engineering. It was my great opportunity to work under the supervision of Professor Dr. Suksun Horpibulsuk for both Master's and Ph.D. studies. I would like to express my deepest gratitude and appreciation to Professor Dr. Suksun Horpibulsuk for his invaluable guidance, encouragement and enthusiasm throughout my studies at the Suranaree University of Technology.

I also wish to acknowledge Dr. Martin D. Liu, my co-advisor, for his insights into geotechnical modelling, valuable comments, suggestions, and support during my 6-month visit to the University of Wollongong, New South Wales, Australia.

The examining committee has also played an important role in the completion of this thesis. I am grateful to Professor Dr. Dennes T. Bergado for serving as a chair of the Ph.D. thesis examining committee. I would like to thank Assistant Professor Dr. Avirut Chinkulkijniwat, Assistant Professor Dr. Pornpot Tanseng, Assistant Professor Dr. Pornkasem Jongpradist, and Associate Professor Dr. Suched Likitlersuang for serving as Ph.D. thesis examiner. Their valuable constructive and useful comments have improved the quality of this thesis.

I would like to thank Dr. Tanongsak Bisarnsin and Associate Professor Dr. Sittichai Seangatith, School of Civil Engineering, Suranaree University of Technology, for their excellent lectures, which provided the inspiration for this research.

I wish to thank all the staff and faculty members at the School of Civil Engineering, Suranaree University of Technology, for the academic, administrative and technical support during my study. I acknowledge Mr. Wangkraew Boonsaun, a Ph.D. student for his friendship and valuable support. I also acknowledge Mr. Apichit Kumpala, my classmate, for the excellent discussion and encouragement up till the completion of this thesis. I would like to thank Mr. Kittipong Ekintumas, Worley Parsons (Thailand) Co. Ltd., for valuable discussions on the finite element program, ABAQUS.

I am indebted to my family. My parents are a source of encouragement since I was young. My parents are my first teachers. They taught me the most important things in life. My girl friend, Nantaporn, has been my important companion during my Ph.D. study. She is my dearest friend, confidant, partner and advisor. She believed in me even when I had doubts. I am forever grateful to her.

Finally, I would like to acknowledge the Higher Education Commission Office in Thailand for the financial support under the Strategic Scholarships Programme for Frontier Research Network. Facilities, equipment, and financial support provided by the Suranaree University of Technology are also very much appreciated.

Jirayut Suebsuk

TABLE OF CONTENTS

Page

TABLE OF CONTENTS (Continued)

Page

TABLE OF CONTENTS (Continued)

Page

TABLE OF CONTENTS (Continued)

Page

TABLE OF CONTENTS (Continued)

Page

TABLE OF CONTENTS (Continued)

Page

LIST OF TABLES

Table **Page**

LIST OF FIGURES

Figure **Page**

LIST OF FIGURES (continued)

Figure **Page**

LIST OF FIGURES (continued)

Figure **Page**

LIST OF FIGURES (continued)

Figure **Page**

LIST OF FIGURES (continued)

Figure **Page**

LIST OF FIGURES (continued)

Figure **Page**

LIST OF FIGURES (continued)

Figure **Page**

LIST OF FIGURES (continued)

Figure **Page**

LIST OF FIGURES (continued)

Figure **Page**

LIST OF FIGURES (continued)

Figure **Page**

SYMBOLS AND ABBREVIATIONS

A_w	=	Cement content
CSL	=	Critical state line
E'	=	Modulus of elasticity in terms of effective stress
F	=	Yield function
G	=	Plastic potential function
G'	=	Shear modulus in terms of effective stress
H	=	Hardening modulus
H_j	=	Hardening modulus at image stress point for bounding surface model
H_s	=	Hardening modulus for Gen and Nova's model
ICL	=	Intrinsic compression line (of destructured soil)
K'	=	Bulk modulus in terms of effective stress
K_0	=	Lateral earth pressure coefficient at rest
R^*	=	Degree of structure for Asaoka et al.'s model
T	=	Pseudo time
YSRiso	=	Isotropic yield stress ratio, p'_y / p'
b	=	Destructuring index due to volumetric deformation for the MSCC and MSCC-B models
	=	Bonding for Gen and Nova's model

SYMBOLS AND ABBREVIATIONS (continued)

e	=	Voids ratio
e^*_{IC}	=	Voids ratio at a reference pressure (1 kPa) of the ICL
e^*_{λ}	=	Reference voids ratio for normal compression line at p' = 1 kPa
e^*_{Γ}	=	Reference voids ratio for critical state line at p' = 1 kPa
dh	=	Rate of hardening parameter
$d\sigma$	=	Increment of stress
$d\varepsilon$	=	Increment of strain
$d\lambda$	=	Plastic multiplier
h	=	Damage for Gen and Nova's model
	=	1st material constant for hardening modulus for Yu et al.'s model
	=	Non-dimensional parameter, describing the effect of material characteristics on the hardening modulus for the MSCC-B model
k	=	Flow rule multiplier for the SCC model
m	=	2nd material constant for the hardening modulus for Yu et al.'s model
n	=	Model parameter for the plastic stiffness for bounding surface model
p'	=	Mean effective stress
$\overline{p}'$	=	Modified mean effective stress

SYMBOLS AND ABBREVIATIONS (continued)

p'_0	=	Reference size of yield surface (stress history)
p'_{0j}	=	Reference size of the structural bounding surface
p'_b	=	Mean effective stress increasing due to structure or structure strength
p'_{b0}	=	Initial structure strength in the $q - p'$ plane
p'_c	=	Reference size of the loading surface for the MSCC-B model
	=	Stress history for Gen and Nova's model
p'_{c0}	=	Initial stress history for Gen and Nova's model
p'_e	=	Equivalent pressure on the isotropic compression line at the same voids ratio
p'_j	=	Mean effective stress at image stress point
p'_p	=	Parameter for describing the size of plastic potential
p'_s	=	Isotropic virgin yielding stress for the SCC model
p'_t	=	Tension strength for Gen and Nova's model
$p'_{y,i}$	=	Initial yield stress of isotropic compression line of structured soil
q	=	Deviatoric stress
q_j	=	Deviatoric stress at image stress point
t_0	=	Time at the start of the load increment

SYMBOLS AND ABBREVIATIONS (continued)

$t_0 + \Delta t$	=	Time at the end of the load increment
u	=	Pore pressure
Δe	=	Additional voids ratio sustained by soil structure
Δe_i	=	Additional voids ratio sustained by soil structure at the initial virgin yielding
Δu	=	Excess pore pressure
Λ	=	Plastic multiplier
M	=	Gradient of critical state line in the $q - p'$ plane
M^*	=	Gradient of critical state line in the $q - p'$ plane of reconstituted soil
α	=	Image stress ratio
δ	=	Distance from the origin to the current stress point for bounding surface model
δ_0	=	Distance from the origin to the image stress point for bounding surface model
δW	=	Energy dissipated per unit volume of soil
δk	=	Increment of hardening parameter
$\delta p'$	=	Increment of mean effective stress
$\delta p'_0$	=	Increment of isotropic yield stress
δq	=	Increment of deviatoric strain

SYMBOLS AND ABBREVIATIONS (continued)

$\delta\varepsilon_d$	=	Deviatoric strain increment
$\delta\varepsilon_d^e$	=	Elastic deviatoric strain increment
$\delta\varepsilon_d^p$	=	Plastic deviatoric strain increment
$\delta\varepsilon_v$	=	Volumetric strain increment
$\delta\varepsilon_v^e$	=	Elastic volumetric strain increment
$\delta\varepsilon_v^p$	=	Plastic volumetric strain increment
$\varepsilon_1, \varepsilon_2, \varepsilon_3$	=	Principal strain
ε_d	=	Deviatoric strain
ε_d^p	=	Plastic deviatoric strain
ε_v	=	Volumetric strain
ε_v^p	=	Plastic volumetric strain
γ	=	Ratio between the image stress and the current stress for Yu et al.'s model
η	=	Stress ratio
$\overline{\eta}$	=	Modified stress ratio
κ	=	Gradient of unloading or swelling line of structured clay
κ^*	=	Gradient of swelling or reloading line of reconstituted soil in the $e - \ln p'$ plane

SYMBOLS AND ABBREVIATIONS (continued)

λ^*	=	Gradient of normal compression of reconstituted soil in the $e-\ln p'$ plane
μ'	=	Poisson ratio in terms of effective stress
θ	=	Lode angle
$\sigma'_1, \sigma'_2, \sigma'_3$	=	Principal stress
σ'_c	=	Effective confining pressure
$\sigma'_x, \sigma'_y, \sigma'_z$	=	Normal stress
$\tau'_{xy}, \tau'_{zx}, \tau'_{yz}$	=	Shear stress
ω	=	Non-dimension parameter control effect of soil structure on the flow rule for the SCC model
ξ	=	Destructuring index due to shear deformation
ψ	=	Parameter defining shape of the plastic potential
$\left[D_{ep}\right]$	=	Elastoplastic stiffness matrix
$\left[J\right]$	=	Jacobian matrix
∂	=	Partial derivative of a function

CHAPTER I

INTRODUCTION

1.1 Background

There are myriad problems associated with the engineering construction in soft clay deposits of the Southeast Asian region, especially in coastal regions such as Chao Phayra Plain in Thailand, Mekong Delta in Vietnam and Cambodia, Central Plains of the Philippines, Coastal Plains of Malaysia, Indonesia, Singapore, Hong Kong, Korea, Japan and Taiwan. These coastal regions are generally covered with very soft clays. The clay behaviour is significantly influenced by its structure, which is determined by both the particle and arrangements (fabric) and the inter-particle forces (soil-cementation or bonding). The soil structure is formed by various processes such as natural deposition, which is affected by the chemical bonding between soil particles during sedimentation process and human design, which is known as chemical stabilised soil. The stress-strain-strength predictions are nescessary for geotechnical engineer in practice. The soil structure causes the difference in the mechanical behaviour of clays between the intact and reconstituted states. Therefore, the plastic deformational response due to the destructuring cannot be explained by the conventional critical state model, which is developed based on the clay behaviour in reconstituted state.

There have been great progresses in constitutive modelling of clay behaviour with consideration of soil structure. One of them is the famous work proposed by Gen and Nova (1993). Their concept has influenced to the development of model for bonding material recently. Some frontier researches in modelling the destructuration of soil structure following the Gen and Nova's concept are the kinematic hardening model for structured clay (Kavvadas and Amorosi, 2000; Rouainia and Muir Wood, 2000; Gajo and Muir Wood, 2001; Baudet and Stallebrass, 2004), an extension of Cam Clay model with superloading surface for structured soil (Asaoka et al., 2000), and etc. Although those models can predict impressively the ordinary behaviour of structured soft clay, however some salient characteristics of structured stiff and artificially structured clays are overlooked. Some advanced models have been developed based on the complex theories for better prediction of mechanical behaviour of artificially structured clay. Consequently their model parameters are difficult for practical identification; it is one problem for limited use of the advanced soil models.

Liu and Carter (2002) presented an extended version of Cam Clay model with consideration of the effect of soil structure, 'Structured Cam Clay (SCC) model'. The SCC model was formulated based on the simple critical state plasticity theory in the conventional triaxial space. The different voids ratio between structured and destructured compression line has been adopted as a state parameter for the identification of the effect of soil structure on the volumetric deformation. The structure and destructuring laws were implicated following the simple volumetric hardening and softening model formulation. Liu and Carter's model is a successful model for the natural clay behaviour with the simple pattern recognition inherited

from the Cam Clay model (Roscoe and Burland, 1968). The SCC model has been extended to the generalised stress space and implemented to a finite element analysis for solving geotechnical boundary value problems (Liyanapathirana et al., 2009). However, some features of structured clay have been ignored for its simplicity (i.e., cohesion effect, strain softening behaviour and etc.). This leads to the limitations of the SCC model for predicting the strongly structured clay behaviour, especially structured stiff clay and artificially structured clay. It is necessary to have a simple model for describing the clay behaviour in reconstituted, naturally structured and artificially structured states by a single rational theory with parameters obtained from conventional laboratory. This leads to the development of the constitutive model in this research.

1.2 Aims of the study

This thesis presents the development of a generalised critical state model for describing the behaviour of structured clay in three different states: destructured, naturally structured and artificially structured states. The proposed models are formulated based on the theoretical framework of the SCC model (Liu and Carter, 2002). The compression model of structured clay, which is a key feature in the formulation of the SCC model, was adapted together with a proposed modified effective stress concept and a destructuring law due to shear deformation. Two versions of soil models are presented for the different purposes. First version is a generalised critical state model for structured clay, named ‘Modified Structured Cam Clay (MSCC) model’. In this model, the soil is modelled as the elastic-virgin yielding material by considering the cohesion effect, strain softening and the effect of soil

structure on the plastic direction. Some additional model parameters were introduced based on the derivation of conventional compression and triaxial test results. The second version is an extended MSCC model for better prediction of stress-strain-strength of soil in overconsolidated state. The bounding surface plasticity theory was incorporated into the generalised MSCC model. The radial mapping rule was presented for describing the hardening/softening and destructuring during loading inside the boundary surface. The verification of the proposed model in triaxial space was carried out by simulating compression tests and undrained and drained shearing tests under a wide range of effective mean stress. Various clays from many parts of the world were used in the verification. Finally, an extension of MSCC model into the generalised stress space was presented and implemented into the finite element code for solving the boundary value problems in geptechnical practice.

1.3 Structure of presentation

This thesis consists of six chapters and outlines of each chapter are presented as follows:

Chapter II presents the review of previous research on the constitutive modelling for structured clay. Topic discussion includes: the basis critical state soil mechanics and the model of Cam Clay family, conceptual framework for modelling the bonding materials, recent models developed for structured clay, theory for modelling soil in overconsolidated state, and the framework of the SCC model.

Chapter III presents the formulation of the MSCC model in conventional triaxial space. The elastoplastic formulation with considering the effect of soil structure is presented based on the critical state framework. It is implemented into a

single element calculation for simulating the conventional compression and triaxial test results. The parametric study of the proposed parameters is discussed. The validation of MSCC model is done under various test results and different conditions.

Chapter IV presents an extended version of the MSCC model for overconsolidated structured clay. The MSCC model is adopted together with the bounding surface plasticity formulation. A parametric study of the additional parameter is discussed. Essential features of extended model are presented by simulating the compression and shear tests of overconsolidated structured clay.

Chapter V presents the application of the MSCC model formulated in the generalised stress space for using to study the influence of soil-cementation structure on the inhomogenouse behaviour of triaxial compression shearing specimen. The finite element implimentation of the MSCC model is presented and also coded in the generised finite element program, ABAQUS. The numerical study of axisymetric triaxial compression shearing test under drained and undrained condition are demonstrated and discussed.

Chapter VI concludes the present work and suggestion of the topics for further study. The list of input parameters and the souce code of the model developed in this thesis are summarised in the appendices.

1.4 Definition of stress and strain variables

The critical state framework has been carried out in the conventional triaxial stress space in order to confine attention to the conventional laboratory consolidation and triaxial test conditions. The simple critical state plasticity model formulations detailed in Chapter III and IV are presented in triaxial stress space and the extension

of proposed model for solving geotechnical boundary value problem is presented in the generalised stress space (in Chapter V).

In formulation of constitutive model in this research, the state of soil is defined by three parameters; those are the mean effective stress, p', deviatoric stress, q, and voids ratio, e. They are defined as follows,

$$p' = \frac{1}{3}\left(\sigma_1' + \sigma_2' + \sigma_3'\right) = \frac{1}{3}\left(\sigma_x' + \sigma_y' + \sigma_z'\right) = \frac{1}{3}\left(\sigma_x + \sigma_y + \sigma_z\right) - u, \tag{1.1a}$$

$$p' = \frac{1}{3}\left(\sigma_1' + 2\sigma_3'\right) \qquad \text{for conventional triaxial space,} \tag{1.1b}$$

$$q = \left[\frac{\left(\sigma_1' - \sigma_2'\right)^2 + \left(\sigma_2' - \sigma_3'\right)^2 + \left(\sigma_3' - \sigma_1'\right)^2}{2}\right]^{\frac{1}{2}}, \tag{1.2a}$$

$$q = \left[\frac{\left(\sigma_x' - \sigma_y'\right)^2 + \left(\sigma_z' - \sigma_x'\right)^2 + \left(\sigma_y' - \sigma_z'\right)^2}{2} + 3\left(\tau_{xy}^2 + \tau_{zx}^2 + \tau_{yz}^2\right)\right]^{\frac{1}{2}}, \tag{1.2b}$$

$$q = \sigma_1' - \sigma_3' \qquad \text{for conventional triaxial space.} \tag{1.2c}$$

The other parameter required for defining the state of stress in deviatoric plane is the Load angle θ, which is defined as:

$$\theta = \tan^{-1}\left[\frac{1}{\sqrt{3}}\left(2\frac{\sigma_2' - \sigma_3'}{\sigma_1' - \sigma_3'} - 1\right)\right] = -\frac{1}{2}\sin^{-1}\left(\frac{27}{2}\frac{\det s}{q^3}\right), \tag{1.3}$$

where

$$\det s = \begin{vmatrix} \sigma_x' - p' & \tau_{xy} & \tau_{zx} \\ \tau_{xy} & \sigma_y' - p' & \tau_{yz} \\ \tau_{zx} & \tau_{yz} & \sigma_z' - p' \end{vmatrix}. \tag{1.4}$$

Corresponding stress parameters, p' and q are the strain parameters, which are volumetric strain, ε_v and deviatoric strain, ε_d:

$$\varepsilon_v = \varepsilon_1 + \varepsilon_2 + \varepsilon_3 = \varepsilon_x + \varepsilon_y + \varepsilon_z, \tag{1.5a}$$

$$\varepsilon_v = \varepsilon_1 + 2\varepsilon_3 \qquad \text{for conventional triaxial space,} \tag{1.5b}$$

$$\varepsilon_d = \frac{\sqrt{2}}{3}\left[\left(\varepsilon_1 - \varepsilon_2\right)^2 + \left(\varepsilon_2 - \varepsilon_3\right)^2 + \left(\varepsilon_3 - \varepsilon_1\right)^2\right]^{\frac{1}{2}}, \tag{1.6a}$$

$$\varepsilon_d = \frac{2}{3}\left(\varepsilon_1 - \varepsilon_3\right) \qquad \text{for conventional triaxial space.} \tag{1.6b}$$

1.5 References

Asaoka, A., Nakano, N., and Noda, T. (2000). Superloading yield surface concept for highly structured soil behaviour. **Soils and Foundations**. 40(2): 99-110.

Baudet, B., and Stallebrass, S. (2004). A constitutive model for structured clays. **Geotechnique**. 54(4): 269-278.

Gajo, A., and Muir Wood, D. (2001). A new approach to anisotropic, bounding surface plasticity: general formulation and simulations of natural and reconstituted clay behaviour. **International Journal for Numerical and Analytical Methods in Geomechanics**. 25: 207-241.

Gens, A., and Nova, R. (1993). Conceptual bases for constitutive model for bonded soil and weak rocks. **Geotechnical Engineering of Hard Soil-Soft Rocks**: Balkema.

Kavvadas, M., and Amorosi, A. (2000). A constitutive model for structured soils. **Geotechnique**. 50(3): 263-273.

Liu, M. D., and Carter, J. P. (2002). A structured Cam Clay model. **Canadian Geotechnical Journal**. 39: 1313–1332.

Liyanapathirana, D. S., Carter, J. P., and Airey, D. W. (2009). Drained bearing response of shallow foundations on structured soils. **Computers and Geotechnics**. 36: 493-502.

Roscoe, K. H., and Burland, J. B. (1968). On the generalised stress-strain behaviour of wet clay. **Engineering plasticity**. 535-609.

Rouainia, M., and Muir Wood, D. (2000). A kinematic hardening constitutive model for natural clays with loss of structure. **Geotechnique**. 50(2): 153-164.

CHAPTER II

MODELLING THE STRUCTURED CLAY BEHAVIOUR

2.1 Introduction

The simplest material model is linear elastic, which is completely described by the generalisation of the Hooke's law (a response between stress and strain is linear relationship). However, for many geomaterials, the overall stress-strain response cannot be condensed into a unique relationship. Hence, it is necessary to have more complicated models to predict real soil behaviour. This leads to the development of elastic-perfectly plastic model (e.g. Tresca, Mohr-Coulomb models) and elastoplastic hardening model (e.g. The Drucker-Prager model) as well as the critical state plasticity model (e.g. Cam Clay model), and etc.

The soil models can implement into geotechnical practice via the numerical techniques. Three governing equations for the solution of the load deformation problems of soil mass are an equilibrium equation that all forces (body, surface, inertia and stress) must be in equilibrium, a compatibility equation, which is the relationship between strains and displacements and a constitutive equation, which is stress and strain relation.

The influence of material type on the mechanical behaviour of soil is reflected by the constitutive equation. Recent soil models have been developed based on two trends of the philosophy. First employs very simple models with relatively few parameters (often with physical meaning), each for a specific application and for

specific type of soil such as normally and lightly overconsolidated clays, sands or rocks. The other trend is to use all-embracing models with a relatively large number of parameters (some may have no physical meaning) for excellent stress and strain prediction. The model selection is dependent on their features, which are suitable for different problems. The desirable soil model for the geotechnical practitioner is a simple model with parameters obtained from the conventional laboratory. The Cam Clay model is one of the most famous models for clays. It was formulated based on the critical state framework. The remoulded clay behaviour is successfully described by this model. The main shortcoming of Cam Clay model is the limitation on modelling the effect of soil structure for natural and cemented clays. There are great progresses for solving this topic during last decade. The complex theories have been developed based on the ordinary Cam Clay model. Some of them are complicated and the parameters have no physical meaning.

This chapter reviews the salient features of structured clay compared with destructured (reconstituted) clay and the conceptual framework for modelling the effect of soil structure on the behaviour of clays. The critical state theory and Cam Clay model are presented briefly and some discussions are made. The recent works on the constitutive modelling for structured clay are reviewed. In particularly the Liu and Carter's model, adopted as fundamental in model development, is presented in details. Moreover, the extensive studies for modelling soil in overconsolidated state are summarised.

2.2 A critical state soil mechanics

2.2.1 Introduction

The critical state soil mechanics is a famous theory for clays, which is developed from the application of theory of plasticity. The formulations of the series of Cam Clay model were proposed by Roscoe and his co-workers at the University of Cambridge. The original formulation of critical state model was presented in the conventional triaxial space (q, p', e) for verification with the conventional test on triaxial condition (Roscoe and Schofield, 1963; Schofield and Wroth, 1968; Atkinson and Bransby, 1978; Muir Wood, 1990). After that the model in the generalised stress space ($\sigma_1', \sigma_2', \sigma_3'$) was formulated for implementation of the model into a numerical analysis (Roscoe and Burland, 1968; Britto and Gunn, 1987; Gens and Potts, 1988; Borja and Lee, 1990).

2.2.2 Concept of critical state soil mechanics

The theory of critical state soil mechanics has been used widely as fundamental for the development of many models. The purpose of all of these models is to achieve a better agreement between predicted and observed soil behaviour. The theory of critical state soil mechanics essentially combine the work of Rendulic (1937) for normally consolidated clays and that of Hvorslev (1937) for overconsolidated clays. The original works were carried out from the test results on the reconstituted clays. To avoid the confusion, the soil parameter referred to reconstituted state in this study is denoted by an asterisk (Burland, 1990). The following is its main hypotheses:

a) The state of the soil, described by the parameters q, p' and e, always lies within or on a unique state boundary surface.

b) In the $e - \ln p'$ plane, the locus of isotropically consolidated states for reconstituted clays, which is called here the isotropic normal compression line is shown in Figure 2.1. It is assumed to be a straight line of the form:

$$e = e_{\lambda}^{*} - \lambda^{*} \ln p' , \tag{2.1}$$

where e_{λ}^{*} is the reference voids ratio for normal compression line at p' = 1 kPa and λ^{*} is the gradient of normal compression (straight line) in the $e - \ln p'$ plane. A swelling line passing through the point (e, p') is described by the following equation:

$$e_{\kappa} = e_{\kappa}^{*} - \kappa^{*} \ln p' , \tag{2.2}$$

where e_{κ}^{*} is the reference voids ratio for swelling or reloading line at p' = 1 kPa and κ^{*} is the gradient of swelling or reloading line in the $e - \ln p'$ plane.

c) All soils ultimately reach a critical state as a unique state of constant volume and effective stress. For a given specific volume, the critical state occurs at a unique stress, and the locus of critical state in the $q - p' - e$ space coincides with line with equation:

$$q = \pm M^{*} p' , \tag{2.3}$$

$$e = e_{\Gamma}^{*} - \lambda^{*} \ln p' , \tag{2.4}$$

where M^* is the gradient of the critical state line in the $q - p'$ plane and e_Γ^* is the reference voids ratio for the critical state line at p' = 1 kPa. Schofield and Wroth (1968) have described the critical state as "flow of the soil like a frictional fluid", with the energy dissipated as friction. The M^* is a simple constant modelling frictional behaviour at the macroscopic scale. It defines the deviatoric stress needed to keep the soil flowing at the critical state for any given mean effective stress.

d) A unique state boundary surface exists, which separates possible from impossible states. The state of the soil described by the stress parameters q, p' and e always lies within or on the state boundary surface. When a clay is sheared, its stress path rises up to the state boundary surface and then travels on the surface until reaching the critical state line. The two surfaces meet at the critical state line presented in the $q - p' - e$ space as shown in Figure 2.2. The unique state boundary surface can be presented in the normalised stress space shown in Figure 2.3 where p'_e is the equivalent pressure on the isotropic compression line at the same voids ratio. It consists of the Hvorslev surface for heavily overconsolidated clays, the Roscoe surface for normally consolidated and lightly overconsolidated clays and the tension cut off for tension failure. The region extending from the swelling line to the state boundary surface is defined as an elastic wall. In the theory of critical state soil mechanics, the response of the soil on an elastic wall is considered to be purely elastic, and after reaching the state boundary surface to be a less stiff combination of elastic and plastic behaviour.

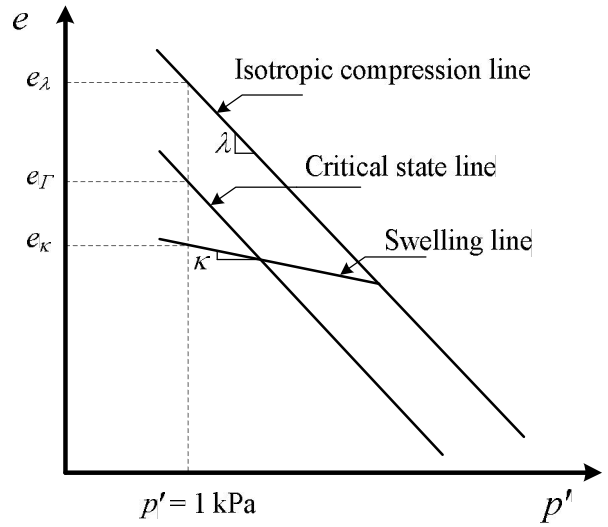

Figure 2.1 Isotropic compression line, swelling line and critical state line

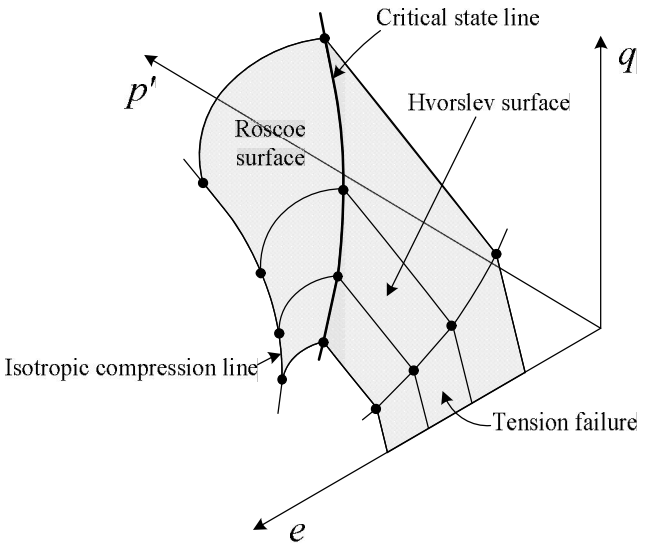

Figure 2.2 State boundary surface of the critical state framework in *q*-*p*′-*e* space (modified from Atkinson and Bransby, 1978)

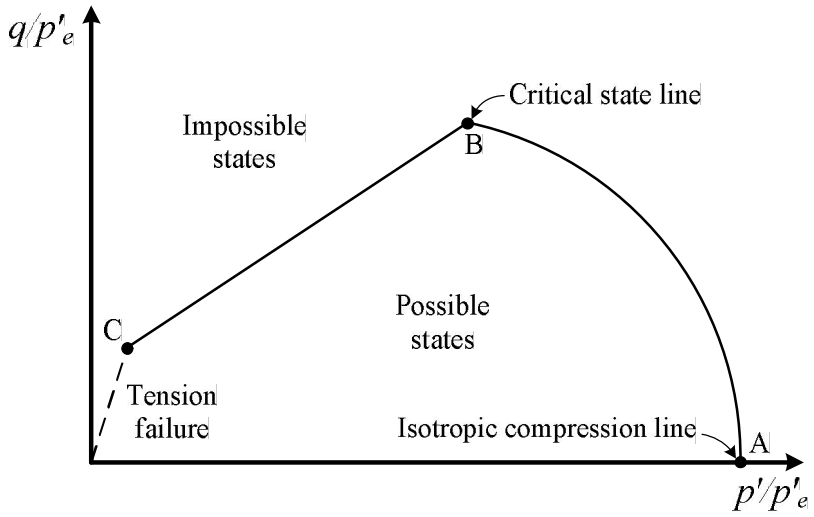

Figure 2.3 State boundary surface in the normalised stress space (After Atkinson and Bransby, 1978)

2.2.3 Cam Clay model

The Cam Clay model was originated by Roscoe and Schofield (1963) for normally and lightly overconsolidated clay following the assumptions that the change in size current yield surface is related to the change in volume of soil sample or volumetric hardening material. The Cam Clay model is the elastoplastic model with the isotropic volumetric hardening.

The elastic volumetric unloading/reloading is accompanied to the variation of p' according to the linear relationship as follows:

$$\delta\varepsilon_v^e = \frac{\delta p'}{K'} = \kappa^* \frac{\delta p'}{(1+e)\,p'}, \tag{2.5}$$

and the recoverable change in deviatoric strain is given by,

$$\delta\varepsilon_d^e = \frac{\delta q}{3G'}, \tag{2.6}$$

where K' is bulk modulus and G' is shear modulus.

The Cam Clay model was derived based on the work equation and the logarithm function was adopted as the yield surface. The equation of the yield surface is,

$$F = q - M^* p' \ln\left(\frac{p_0'^*}{p'}\right) = 0, \tag{2.7}$$

where $p_0'^*$ is the reference size of yield surface (stress history). The energy dissipated at any infinitesimal increment of plastic work of the Cam Clay yield surface is only a function of the plastic deviatoric strain. Following the critical state concept, the Cam Clay yield surface is consistent to the work equation as,

$$\delta W = p'\delta\varepsilon_v^p + q\delta\varepsilon_d^p = M^* p'\delta\varepsilon_d^p, \tag{2.8}$$

where δW is an energy dissipated per unit volume of soil. In the Cam Clay model, it is assumed that the plastic flow obeys the principle of normality and an associated model. Thus, the plastic potential and the yield surface coincide ($G = F$). The plastic flow rule is presented in terms of stress ratio, η, as follows:

$$\frac{\delta\varepsilon_v^p}{\delta\varepsilon_d^p} = \frac{\partial G / \partial p'}{\partial G / \partial q} = M^* - \eta \,. \tag{2.9}$$

The yield surface is assumed to expand with a constant shape and the change in size of the yield surface $\delta p_0'$ is assumed to be directly related to the changes in plastic volume deformation $\delta\varepsilon_v^p$, according to the hardening rule following linear equation:

$$\delta p_0' = \frac{(1+e)\, p_0'}{\left(\lambda^* - \kappa^*\right)} \delta\varepsilon_v^p \,. \tag{2.10}$$

The elastic and plastic stress-strain relationship for the Cam Clay plasticity model is defined in the compliance relationship as:

$$\begin{Bmatrix} \delta\varepsilon_v^e \\ \delta\varepsilon_d^e \end{Bmatrix} = \begin{bmatrix} \frac{1}{K'} & 0 \\ 0 & \frac{1}{3G'} \end{bmatrix} \begin{Bmatrix} \delta p' \\ \delta q \end{Bmatrix}, \tag{2.11}$$

$$\begin{Bmatrix} \delta\varepsilon_v^p \\ \delta\varepsilon_d^p \end{Bmatrix} = \frac{1}{H} \begin{bmatrix} \frac{\partial F}{\partial p'}\frac{\partial G}{\partial p'} & \frac{\partial F}{\partial q}\frac{\partial G}{\partial p'} \\ \frac{\partial F}{\partial p'}\frac{\partial G}{\partial q} & \frac{\partial F}{\partial q}\frac{\partial G}{\partial q} \end{bmatrix}$$

$$= \frac{\left(\lambda^* - \kappa^*\right)}{(1+e) M^* p' \left(M^* - \eta\right)} \begin{bmatrix} \left(M^{*2} - \eta^2\right) & \left(M^* - \eta\right) \\ \left(M^* - \eta\right) & 1 \end{bmatrix} \begin{Bmatrix} \delta p' \\ \delta q \end{Bmatrix}, \tag{2.12}$$

where $H = -\frac{1}{\Lambda}\frac{\partial F}{\partial k}\delta k = -\frac{1}{\Lambda}\frac{\partial F}{\partial p_0'}\delta p_0' = -\frac{\partial F}{\partial p_0'}\frac{\partial p'}{\partial \varepsilon_v^p}\frac{\partial G}{\partial p'}$.

One of the shortcomings of the Cam Clay model is the prediction of the coefficient of the earth pressure at rest, K_0. For one-dimensional normal compression, the Cam Clay model predicts the plastic strain as same as that of the isotropic compression test, so it cannot distinguish between isotropic and one-dimensional normal compression. Furthermore, the discontinuity of the Cam Clay yield surface at q = 0 causes difficulties because the associated flow rule will predict an infinite number of possible strain increment vectors for isotropic compression. Burland (1965) have proposed a modified work equation, which considers the work dissipates in plastic volume change. The energy dissipated in the Cam Clay model is modified as follows,

$$\delta W = p'\left(\delta\varepsilon_v^{p2} + \left(M^*\delta\varepsilon_d^p\right)^2\right)^{\frac{1}{2}}. \tag{2.13}$$

Based on the modified work equation, the Modified Cam Clay (MCC) model proposed by Roscoe and Burland (1968) overcomes these problems by adopting an elliptical yield surface, which has the following expression:

$$F = q^2 - M^{*2}p'\left(p_0'^* - p'\right) = 0. \tag{2.14}$$

When the stress state stays within the current yield surface, the elastic properties of the MCC are the same as those in the original Cam Clay model. The

plastic potential is the same as the yield function for the associated model. The flow rule for the MCC model is then calculated by the application of the normality condition as follows:

$$\frac{\delta\varepsilon_v^p}{\delta\varepsilon_d^p} = \frac{M^{*2} - \eta^2}{2\eta}. \tag{2.15}$$

The hardening relationship for the MCC model is the same as that for original Cam Clay model (Equation 2.10). The elastic and plastic stress-strain response of the MCC model can be written in the compliance relationship as follows:

$$\begin{Bmatrix} \delta\varepsilon_v^e \\ \delta\varepsilon_d^e \end{Bmatrix} = \begin{bmatrix} \frac{1}{K'} & 0 \\ 0 & \frac{1}{3G'} \end{bmatrix} \begin{Bmatrix} \delta p' \\ \delta q \end{Bmatrix}, \tag{2.16}$$

$$\begin{Bmatrix} \delta\varepsilon_v^p \\ \delta\varepsilon_d^p \end{Bmatrix} = \frac{\left(\lambda^* - \kappa^*\right)}{\left(1+e\right)p'\left(M^{*2} + \eta^2\right)} \begin{bmatrix} \left(M^{*2} - \eta^2\right) & 2\eta \\ 2\eta & \frac{4\eta^2}{\left(M^{*2} - \eta^2\right)} \end{bmatrix} \begin{Bmatrix} \delta p' \\ \delta q \end{Bmatrix}. \tag{2.17}$$

2.2.4 Beyond the Cam Clay model

The Cam Clay model can predict the behaviour of normally and lightly overconsolidated clay quite well. However, there are several imperfections for the Cam Clay theory. The Cam Clay model was developed based on the assumption that soils are considered as isotropic hardening and softening material. It is well known

that soils in reality are anisotropic due to the mode of deposition. Many soils have been deposited over areas of large lateral extent and the deformations they have experienced during and after deposition have been essentially one-dimensional. Some further works on the critical state model for soils with an anisotropic consideration have been presented by Whittle (1993), Wheeler et al. (2003) and Dafalias et al. (2006), and etc. Although the anisotropy affects the evolution of the yield surface of structured clay, some simple model considers only the isotropic hardening for simplicity of the model formulation (e.g., Liu and Carter, 2002; Lee et al., 2004 and etc.).

Following the traditional elastoplastic model, the Cam Clay assumes that the plastic strain develops instantaneously and that time does not enter into any consideration. Thus the rate independent Cam Clay model cannot explain time dependent behaviour, such as creep, stress relaxation, strain rate effect, and etc. The further work of critical state models with rate dependent effect have been proposed by Adachi and Oka (1982); Borja and Kavazanjian (1985); Kutter and Sathialingam, (1992) and etc.

The Cam Clay model overestimates the failure stresses on the 'dry' side (i.e. states to the left of the critical state line). The Cam Clay model overestimates the peak strength in undrained heavily overconsolidated clay. The some extended critical state models for overconsolidated clay were developed by using the bounding surface plasticity theory (i.e., Whittle, 1993; Whittle and Kavvadas, 1994; Stallebrass and Taylor, 1997, and etc.).

The other main problem of Cam Clay is the limitation on soil-cementation structure consideration, which is the main topic of research study. The literature review on the modelling the structured soils is presented in the next section.

2.3 Conceptual framework for modelling the structured soils

The Cam Clay model (Roscoe and Schofield, 1963; Roscoe and Burland, 1968) have successfully explained the clays behaviour without soil structure consideration. However the resistance of soil structure is responsible for the difference in the mechanical behaviour of clay in natural between the structured and the destructured states (Leroueil et al., 1979; Hanzawa and Adachi, 1983; Leroueil et al., 1983; Leroueil and Vaughan, 1990; Mitchell, 1996; Shibuya, 2000; Horpibulsuk et al., 2007). Callisto and Rempello (2004) have presented the stress and strain behaviour of three different natural clays that most of them cannot be explained by the MCC model. Based on the examination of a large body of experimental data on structured soils (i.e., Wissa et al., 1965; Burland, 1990; Leroueil and Vaughan, 1990; Cotecchia and Chandler, 1997; Huang and Airey, 1998; Cotecchia and Chandler, 2000; Liu and Carter, 2000; Ismail et al., 2002; Rotta et al., 2003; Callisto and Rampello, 2004; Lorenzo and Bergado, 2004; Horpibulsuk et al., 2005), the mechanic behaviours of structured soils were summarised as follows:

a) A comparison of the compression behaviour of high water content clay in reconstituted, naturally structured and cemented states based on the test data by Lorenzo and Bergado (2004) is shown in Figure 2.4 (A_w stands for cement content by weight). It is seen that the basic feature of the compression behaviour of cemented clay is similar to that of a naturally structured clay (Liu and Carter, 2000). Due to the

effect of soil-cementation, the voids ratio sustained by artificially structured clay is higher than that of the naturally structured clay. During virgin yielding, break-down of soil-cementation takes place, and the additional voids ratio sustained by soil-cementation structure decreases. However, quantitatively speaking, for high water content clay, the additional voids ratio sustained by cementation structure is much higher than that sustained by natural soil structure; the rate of break-up of cementation of cemented clays is generally higher than that of naturally structured clays as indicated by the larger compression.

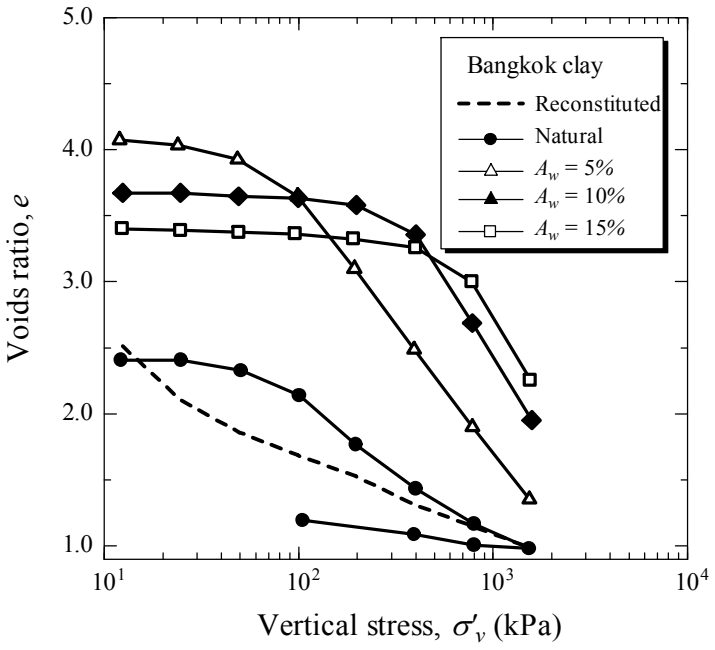

Figure 2.4 One-dimensional compression behaviour of Bangkok clay with various structures (after Lorenzo and Bergado, 2004)

b) Even with the break-up of cementation in virgin yielding, the isotropic compression curve of structured clay is asymptotic to the reconstituted compression curve of natural clay (Cotecchia and Chandler, 2000). The reconstituted compression

curve of the artificially structured clay might be different from that of natural clay since cement or lime and clay might form a new material due to the chemical reaction process. However, this reconstituted compression curve can be used as reference for modelling compression curve of structured clay (Liu and Carter, 1999; Desai, 2001; Liu and Carter, 2003).

c) The size of the initial yield surface increases with soil-cementation, so does the tensile strength of the soil. Due to soil-cementation effect, the highly structured clay mainly exhibits the elastic behaviour when stress state is inside the state boundary surface like concrete.

d) The resistance to elastic deformation and yield stress increase with degree of cementation as shown by the lower swelling index, κ. Even with the increase in the yield stress, the resistance to plastic deformation decreases with the cementation bonds. In other words, the greater the degree of cementation, the higher the virgin yielding compression index, λ. This is due to the sudden break-down of cementation bond for high cementation bond (Horpibulsuk et al., 2004).

e) The strain softening behaviour is investigated for soil loaded on both dry and wet sides of critical state line. This is attributed to the crushing of soil-cementation structure. This feature of softening behaviour of cemented clays is fundamentally different from that of reconstituted clays. The softening behaviour of reconstituted clay occurs only for heavily overconsolidated soil in drained condition and is caused by the interlocking (dismembering of clay clusters) (Srinivasa Murthy et al., 1988; Srinivasa Murthy et al., 1991).

f) A comparison of the shear behaviour of artificially structured clay and that of naturally structured clay shows that the final strength of artificially structured clay,

both in terms of shear stress and shear stress ratio, is generally higher than that of the naturally structured clay.

g) It appears that the variation of mechanical properties of artificially structured clays is basically isotropic (Huang and Airey, 1998; and Rotta et al, 2003).

Based on the recent work on the mechanical behaviour of structured clay, the various approaches for development of constitutive models for structured clay are proposed. One is proposed by Oka et al. (1989). They have presented a constitutive model for soft natural clay incorporated with a damage of soil structure in the plastic formulation. Soil structure is modelled as an extra strength that reduces with plastic strain to the destructured state which is controlled by frictional resistance only. In contrast, Chazallon and Hicher (1995) have presented a damage of soil structure as a change in the elastic properties. The fabric and bonding at microscopic scale are modelled separately. The mechanical behaviour of the fabric is modelled by elastoplastic law, while a bonding is modelled by an elastic law which takes into account the damage spreading inside the material and degradation by means of a damage law.

Vatsala et al. (2001) have presented an elastoplastic model for structured soil, considering its response as the sum of the strength of the soil structure and the cementation bond strength, and modelling these two components separately. The MCC model has been adopted for destructured soil component, and a new elastoplastic model has been proposed for the cementation bond component. A simple associated flow rule is used for both the components.

The classical hardening plasticity is firstly extended to structured soil by Gen and Nova (1993). They have presented the two features of the structured soils, which

should be considered in modelling soil behaviour. First is that the variation of the yield surface is affected by destructuring and second is that the structured soil behaviour must be considered with respect to its behaviour in reconstituted state. The effect of soil structure on the initial elastic domain by using a lager yield surface and allowing for tensile strength and true cohesion have been presented in the work by Gen and Nova as shown in Figure 2.5. They have suggested that the increased yield stress and tensile strength are directly proportional to the yield stress of the reconstituted soil by a factor which is a function of the degree of bonding as shown in Figure 2.6.

The destructuration is modelled by soil structure variables, which are related to plastic strain rate. The variation of yield locus is controlled by a conventional volumetric hardening associated with destructuration. The evolution of the yield surface when hardening of the destructured soil dominated with respect to decrease in the effect of soil structure as shown in Figure 2.7a. Figure 2.7b shows the shrinking of the yield surface which respect to the volumetric softening of destructured soil. The degree of soil structure is defined as a function of the measure of damage, h, Figure 2.8, which is a function of both plastic volumetric and deviatoric strain. The isotropic compression of structured soil can be computed by the concept of destructuration as presented above as shown in Figure 2.9.

Although the model proposed by Gen and Nova (1993) cannot predict advanced features of soil behaviour such as small strain non-linearity, stress-induced anisotropy, effect of recent stress history, etc, but their methodology is simple and clear enough for incorporating with existing soil models. However, a key issue was

not addressed by Gen and Nova (1993) which are the determination of the relation between destructuration and plastic strain or destructuring law.

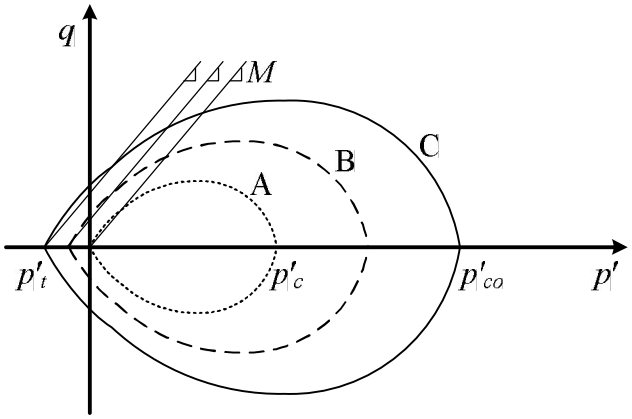

Figure 2.5 Successive yield surfaces for increasing degree of bonding (after Gen and Nova, 1993)

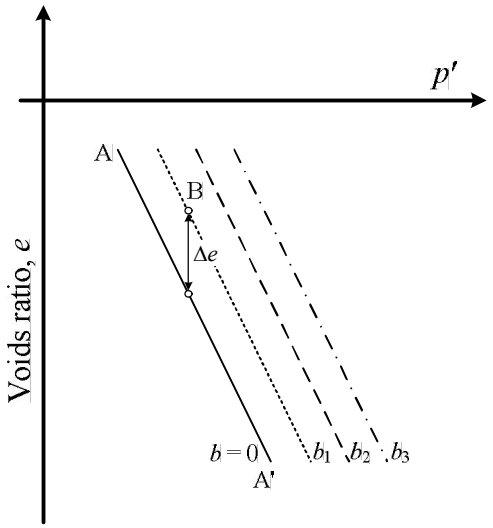

Figure 2.6 Isotropic normal compression curves for material with various degree of bonding (after Gens and Nova, 1993)

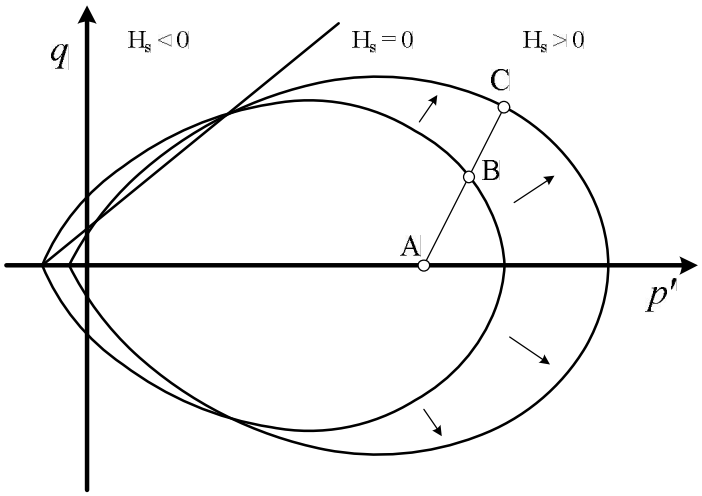

(a) Soil behaviour dominated by strain hardening

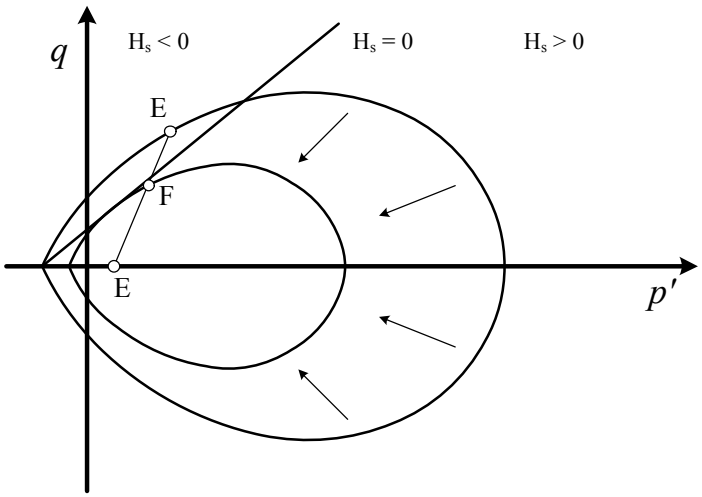

(b) Soil behaviour dominated by strain softening

Figure 2.7 Evolution of the yield surface (after Gens and Nova, 1993)

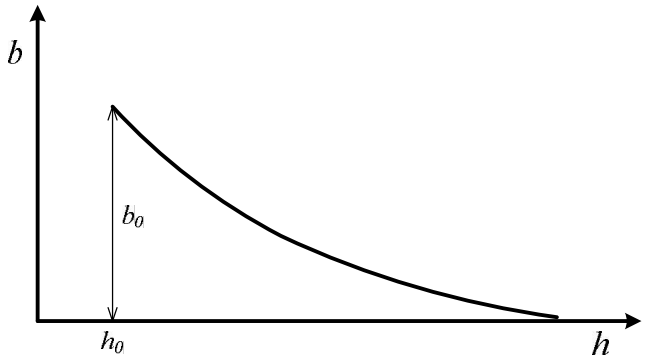

Figure 2.8 Reduction of bonding, *b*, with increasing damage, *h* (after Gen and Nova, 1993)

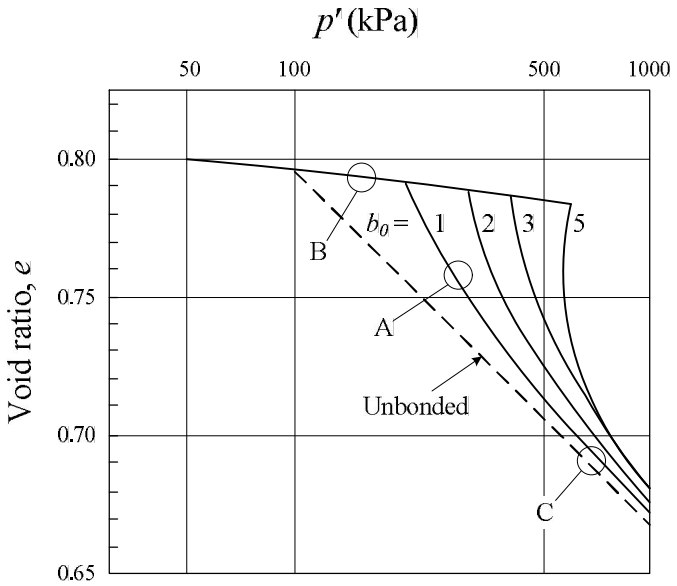

Figure 2.9 Computed isotropic compression curves for materials with different amounts of bonding (after Gens and Nova, 1993)

2.4 Soil models for structured clay based on critical state framework

Various soil models have been developed recently with the framework of critical state soil mechanics to predict the behaviour of structured clays (e.g. Asaoka et al., 2000; Kasama et al., 2000; Kavvadas and Amorosi, 2000; Rouainia and Muir Wood, 2000; Liu and Carter, 2002; Baudet and Stallebrass, 2004; Lee et al., 2004, etc.). Those model follow the presented concepts for modelling the bonded material by Gen and Nova (1993) as discussion in the previous section. Some advanced models with special features and the simple extended MCC model for taking care of the effect of soil structure are presented during last decade. The advanced soil models have been formulated based on the complex theory for the better simulation of special soil behaviour such as structural anisotropy, small strain stiffness, soil in overconsolidated state, and etc (Asaoka et al., 2000; Kavvadas and Amorosi, 2000; Rouainia and Muir Wood, 2000; Gajo and Muir Wood, 2001; Baudet and Stallebrass, 2004).

In the development of the soil models for structured clay, the effect of soil structure is considered by the increase in the size of the bounding surface. Although those models are based on the same concept, evolutions of bounding surface are presented in two different ways. First is that the increased strength (structure strength) is added to the reconstituted material (Asaoka et al., 2000; Rouainia and Muir Wood, 2000; Gajo and Muir Wood, 2001; Baudet and Stallebrass, 2004). The other is the gross yield curve of the structured clays, which is simply determined directly in laboratory as shown in Figure 2.10 (Kavvadas and Amorosi, 2000). Rouainia and Muir Wood (2000) and Gajo and Muir Wood (2001) have described the size of the bounding surface of the naturally structured clay as the size of the structured bounding

surface of the reconstituted clay multiplied by the degree of structure. This approach is similar to the concept of sensitivity framework (Cotecchia and Chandler, 2000) that the state boundary surface of structured clay is defined by the preconsolidation pressure at the intersection of an elastic wall and the natural compression line (apparent yield stress). Asaoka et al. (2000) have presented the size of superloading surface in the same way that it is related to the size of Cam Clay model by the degree of structure, R^*, as shown in Figure 2.11. Liu and Carter (2002) have presented the size of structural yield surface, which is defined by the isotropic virgin yielding stress, p'_s. The elliptical yield surface of the MCC model is adopted in SCC model by Liu and Carter (2002) with a constant aspect ratio, *M*.

In some models, the tensile strength is included in the size of the bounding surface, so that the origin of stress plane is inside the boundary surface (Kasama et al., 2000; Kavvadas and Amorosi, 2000; Lee et al., 2004). The tensile strength caused by structure is not relevant for natural clays but is the main component for controlling the behaviour of structured clay (Horpibulsuk, 2001; Callisto and Rampello, 2004).

The elliptical bounding surface has been adopted for almost models for structured clay inherited from the MCC model (Kasama et al., 2000; Kavvadas and Amorosi, 2000; Rouainia and Muir Wood, 2000; Liu and Carter, 2002; Baudet and Stallebrass, 2004; Lee et al., 2004). In contrast, there are some models use the logarithm function as the shape of bounding surface such as super-subloading model by Asaoka et al. (2000), etc. Asaoka et al. (2000) have introduced the three yield surfaces concept into the Cam Clay model (*vide* Figure 2.11). The relation between each surfaces are presented via parameters dependent on the degree of soil structure. Rouainia and Muir Wood (2000) have modelled the structured clays by an extended

bubble model, which have proposed by Al-Tabbaa and Muir Wood (1989). The kinematic hardening is adopted for describing the stiffness of soil in small strain. The structural and reference surfaces are illustrated in Figure 2.12.

Most models assume that the destructuration is a function of plastic strain. Some models assume that the soil structure do not degrade in elastic region. In other words, there is no destructuration inside the state boundary surface caused by using a single yield surface formulation (Kasama et al., 2000; Liu and Carter, 2002; Lee et al., 2004). However, some advanced soil models allow destructuration to start inside the boundary surface, by using kinematic hardening plasticity (Kavvadas and Amorosi, 2000; Rouainia and Muir Wood, 2000; Gajo and Muir Wood, 2001) or bounding plasticity mapping rule (Tamagnini and D'Elia, 1999) or subloading yield surface concept (Asaoka et al., 2000). However, those models have some limitation that the size of the elastic region is quite difficult to measure directly. The destructuring law for structured models have presented in different ways. Asaoka et al. (2000); Baudet and Stallebress (2004); Rouainia and Muir Wood (2000) have presented the destructuration as a function depended directly on both plastic volumetric strain and plastic deviatoric strain by different proportions.

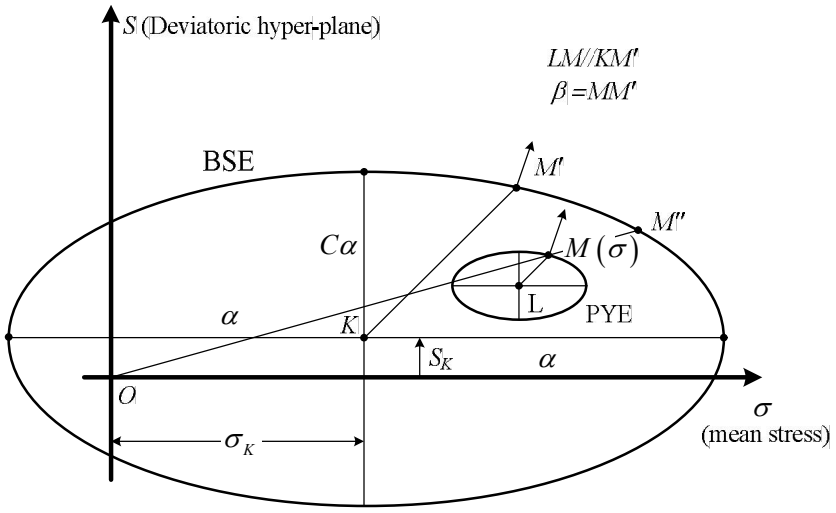

Figure 2.10 Characteristic surfaces for the model for destructuration clays (after Kavvadas and Amorosi, 2000)

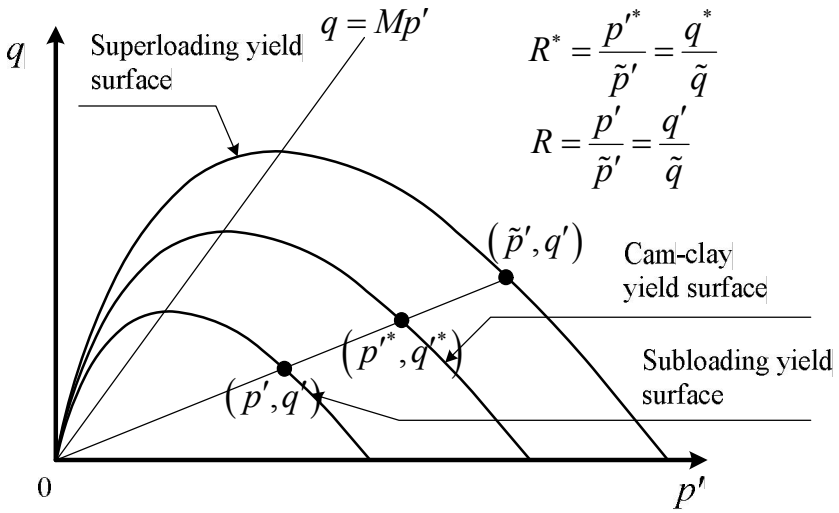

Figure 2.11 The Cam Clay model with the super-subloading yield surface (after Asaoka et al., 2000)

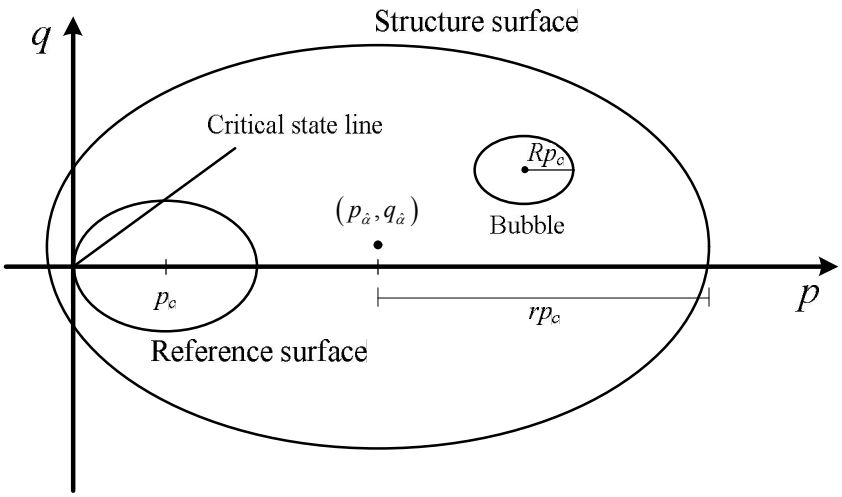

Figure 2.12 Characteristic surfaces for the model for structured clays (after Rouainia and Muir Wood, 2000)

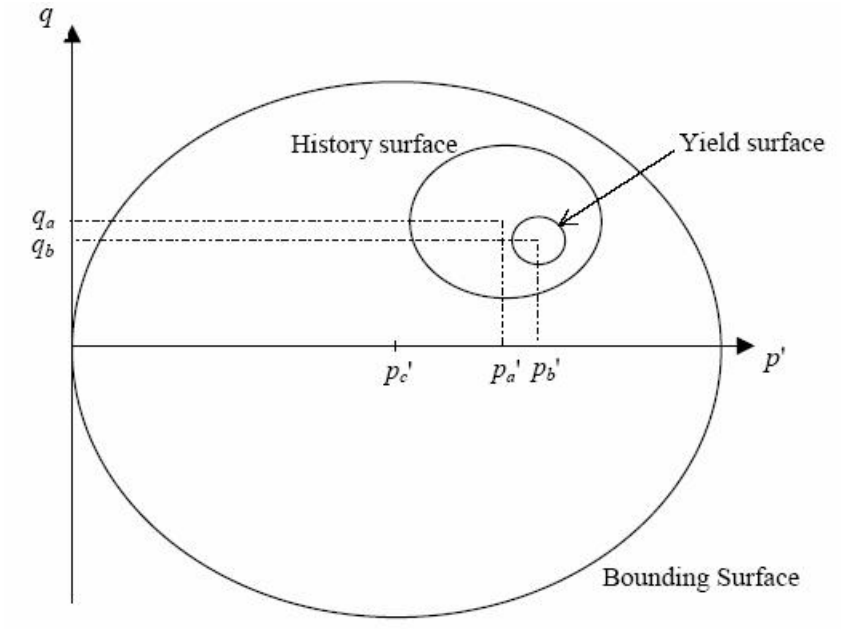

Figure 2.13 The three surface kinematic hardening (3-SKH) model in the triaxial stress space (after Stallebrass, 1990)

2.5 Modelling the overconsolidated soil

The Cam Clay model is based on the assumption that the interior of the yield surface is an elastic domain with no plastic deformation. As discussed earlier, this leads to the limitation of conventional plasticity models to predict plastic deformations during unloading/reloading stages of cyclic loading. Another main problem, which is the topic of this study, is the lack of transition between elastic and plastic behaviour of lightly overconsolidated clay and the destructuration for overconsolidated clay during loading inside the boundary surface. For the structured clay, although the destructuration during loading inside the boundary surface is too small which can be ignored for highly cemented clay, however it produces the plastic volumetric strain, which affects the effective stress path and the development of the excess pore pressure in undrained condition (Horpibulsuk et al., 2004). Moreover, the elastic to failure behaviour of heavily overconsolidated soil predicted by the MCC model is overestimated from the test result caused by the elliptical shape of yield surface which is adopted as the failure envelope (Suebsuk et al., 2008). There are many theories developed for correcting those problems such as multi-surface or kinematic hardening plasticity theory, bounding surface plasticity theory. Those theories are reviewed in this section. In this research, a developed model was extended for explanation of the volumetric hardening and destructuring during loading inside the boundary surface, however for simplicity, the cyclic loading is not focused in this study.

The multi-surface plasticity model has been introduced by Mrŏz (1967). This model incorporates multiple yield surfaces and introduces the kinematic hardening concept to describe cyclic plasticity in metals (Mrŏz, 1967; Mrŏz, 1969). Later, Mrŏz et al. (1978) have extended the application of the multi-surface model to cyclic

loading of soils by taking into account both isotropic hardening due to changes in voids ratio and anisotropic effects induced by preconsolidation. The earlier version of the multi surface plasticity model is based on a finite number of nesting sub-yield surfaces, with the inner most surface enclosing the elastic domain and the outer most surface representing the degree of consolidation. The nesting sub-yield surfaces become active and translate in stress space when intercepted by the current stress state. The hardening modulus is defined by the size of the active nesting surface and varied in a piecewise linear function between consecutive surfaces. A similar kinematic hardening model with multiple nested translating yield surfaces has also developed by Prévost (1977) for undrained cyclic analysis of clays.

To achieve a continuous variation of the hardening modulus, Mrŏz et al. (1978; 1981) have refined the multi-surface model by assuming an infinite number of nesting subyield surfaces. In the infinite-surface model, the hardening modulus depends on the ratio of the size of the instantaneous loading surface on which the stress state lies and the outer most yield surface. Mrŏz et al. (1978; 1979) have also presented a modified two surface model as an alternative simplification to the multi-surface formulation. This formulation avoids the tracing of the evolution of the nesting surfaces by interpolating the hardening modulus using the distance of the stress point from its conjugate point on the outermost yield surface.

More recently, some similar soil models have been formulated based on the critical state framework by Al-Tabbaa and Wood (1989), Stallebrass (1990) and Stallebrass and Taylor (1997) (with three surfaces called 3SKH model, *vide* Figure 2.13). McDowell and Hau (2003) extended Stallebrass and Taylor's work by introducing a new plastic potential to get better predictions of the $K_{0,nc}$ value and

deviatoric strain. A similar model has also been proposed with the consideration of soil structure by Rouainia and Muir Wood (2000); Gajo and Muir Wood (2001).

Dafalias and Popov (1975) have introduced the bounding surface plasticity concept for describing the nonlinear hardening of materials under complex loading. Bounding surface plasticity theory is based on the observation that plastic deformations occur even when a stress state lies inside a conventional yield surface. Bounding surface models provide an inherent extension to conventional constitutive models by assuming a smooth transition of stiffness from elastic to plastic state. In the bounding surface formulation, plastic deformation at any stress point inside the bounding surface is computed by defining the plastic modulus as a decreasing function of the distance of the stress point from its "image point" on the bounding surface.

Mathematical foundation of the general bounding surface theory and its application to isotropic cohesive soils have been presented by Dafalias (1986); Dafalias and Hermann (1986). The bounding surface plasticity model proposed by Dafalias and Hermann (1980); Dafalias (1986) is a simple model within the framework of critical state soil mechanics. It uses a three segment bounding surface with a simple radial mapping rule and a distance dependent additive plastic modulus. This idea can be applied to the existing critical state model as following the diagram illustrated in Figure 2.14. The state boundary surface is defined as the MCC yield surface and a radial mapping rule is adopted to define the image stress point (q_j, p'_j) from the current stress state (q, p'). A smooth transition between elastic and plastic behaviours is described by the modified hardening rule as follows:

$$H = H_j + H_0 \frac{\delta}{\delta_0 - \delta}\left[1 + \left|\frac{M}{n}\right|^n\right], \tag{2.18}$$

where H_j is the plastic stiffness at image stress point, δ and δ_0 are the distance between current stress point and image stress point.

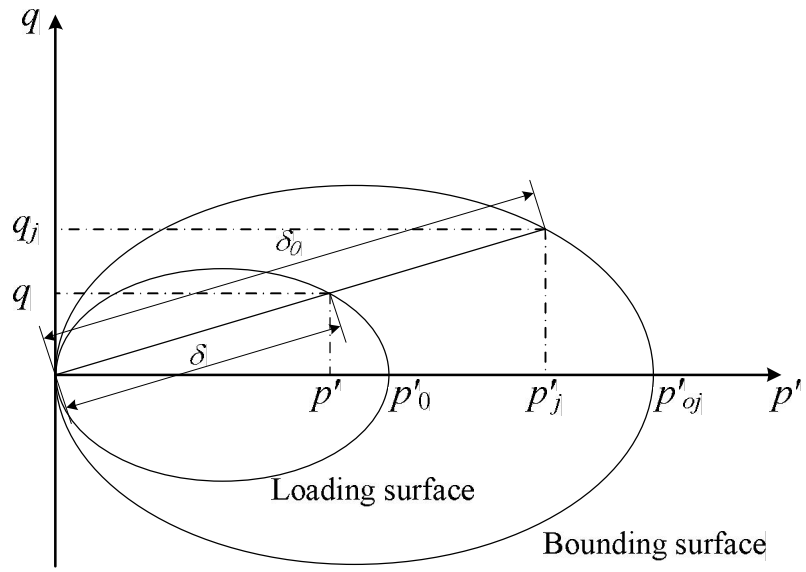

Figure 2.14 A typical bounding surface model in the *q*-*p'* space

Yu et al. (2007) and Khong (2004) have introduced their model named as CASM for predicting the cyclic loading of clay and sand incorporating with the bounding surface formulation. The unified radial mapping rule for clay and sand have been presented in the simple form as follows:

$$\frac{p'_j}{p'} = \frac{q_j}{q} = \frac{p'_{0j}}{p'_0} = \frac{1}{\gamma}, \tag{2.19}$$

$$H = +\infty \text{ if } \gamma = 0, \tag{2.19b}$$

$$H = H_j \text{ if } \gamma = 1, \tag{2.19c}$$

where γ is a ratio between the image stress and the current stress.

The hardening modulus for virgin yielding has been presented following the radial mapping in the form:

$$H = H_j + \frac{h}{p'} \frac{(1-\gamma)^m}{\gamma}, \tag{2.20}$$

where *h* and *m* are two material constants.

The sub-loading surface model proposed by Hashiguchi and Ueno (1977) has similar characteristics to the bounding surface plasticity models. This model employs two similar surfaces, an interior sub-loading surface on which the current stress state lies and an outer conventional yield surface. The hardening modulus in this model is computed using an extended consistency condition on the sub-loading surface. Hashiguchi (1980; 1989); Hashiguchi and Chen (1998) modified this model to incorporate translation of the similarity-centre and rotation of the sub-loading and yield surfaces. The model requires a greater number of hardening variables to account for rotation and translation of the sub-loading surface. The sub-loading surface has been adopted in the formulation of the model for structured clay by Asaoka et al. (2000) for describing the clay behaviour in overconsolidated state.

The bounding surface plasticity has attracted a great deal of attention due to its simplicity and efficiency in modelling unloading/reloading behaviour. The significance of bounding surface formulation is to improve the predictive capability for stress states inside the bounding surface through successive development of plastic strains as the stress point approaches the surface by avoiding abrupt changes from elastic to plastic behaviour. This method is computationally simple, uses fewer model parameters and gives a reasonable accuracy.

2.6 A framework of Structured Cam Clay model

The extended critical state model for structured clays has proposed by Liu and Carter (2002), namely as 'Structured Cam Clay (SCC) model'. The SCC model has been formulated by introducing the influence of soil structure into the MCC model. The destructured soil behaviour is assumed to be described adequately by the MCC model. The different features between structured and destructured soil are encompassed in terms of soil structure. The SCC model parameters are obtained from the destructured samples, which are intrinsic properties (Burland, 1990) and the structured (intact) samples. The influences of soil structure are described by comparing structured soils behaviour with the intrinsic behaviour.

The compression behaviour of structured clay shows the progressive destructuring after the virgin yielding occurs. The gradient of compression line of structured clay is not constant along the virgin yielding as shown by Leroueil and Vaughan (1990), and Burland (1990), etc. The compression equation with the destructuration for structured clay proposed by Liu and Carter (1999; 2000) is adopted in the formulation of SCC model. The difference in voids ratio between a structured

soil and the corresponding destructured soil at the same stress state in compression line (Δe) is introduced to be the key parameter for modelling the influence of soil structure as illustrated in Figure 2.15. The compression equation for structured clay is defined by the standard parameters (e_λ^*, λ^* and κ^*) from the MCC model and three additional parameters (Δe_i, $p'_{y,i}$ and b) as follows:

$$e = e^* + \Delta e = e_\lambda^* - \left(\lambda^* - \kappa^*\right) \ln p'_s - \kappa^* \ln p' + \Delta e_i \left(\frac{p'_{y,i}}{p'_s} \right)^b , \tag{2.21}$$

where $p'_{y,i}$ is the initial yield stress on the normal compression line, Δe_i is an additional voids ratio sustained by soil structure at $p' = p'_{y,i}$, p'_s is stress history on normal compression of structured clay and b is a destructuring index due to volumetric deformation. The value of b depends on soil type and structure and generally $b > 1$ for soft structured clays and $b < 1$ for stiff clays and generally $0 \leq b \leq 30$ (Liu and Carter, 1999; 2000). However the value of b is directly determined from plotting the compression test result in the $\ln\left(\Delta e / \Delta e_i\right) - \ln\left(p'_{y,i} / p'_s\right)$ plane that the b is the gradient of straight line pass through the origin.

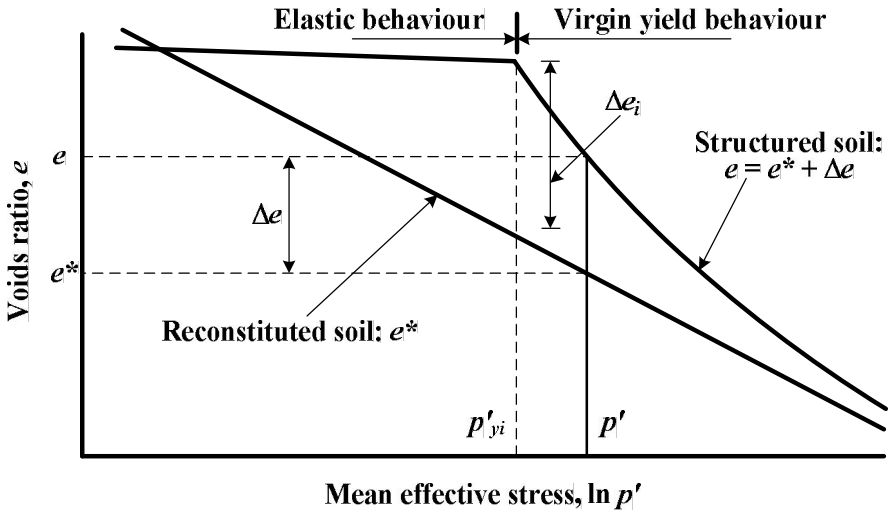

Figure 2.15 Idealisation of the isotropic compression behaviour of reconstituted and structured soils (after Liu and Carter, 2002)

Following the tradition of MCC model, the structured clay behaviour is also divided into elastic and virgin yielding behaviours by its current yield surface, which is dependent on soil structure as well as stress history. Hence, the current yield surface of structured clay, named the structural yield surface, is defined by its current stress state, voids ratio, stress history, and soil structure. Similar to the original proposal by Roscoe and Burland (1968), the yield surface of a structured soil in $q - p'$ plane is assumed to be elliptical in shape and it passes through the origin of the stress coordinates as illustrated in Figure 2.16. The yield function, for structured clays is given by,

$$F = q^2 - M^2 p' \left(p'_s - p' \right) = 0 . \tag{2.22}$$

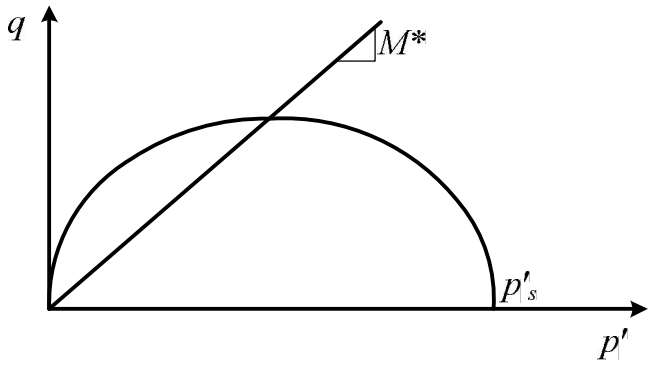

Figure 2.16 The yield surface for structured soils (after Liu and Carter, 2002)

Based on the compression equation (2.20), the total volumetric strain increment for isotropic compression path is obtained as follows:

$$\delta\varepsilon_v = \left(\lambda^* - \kappa^*\right)\frac{\delta p'_s}{\left(1+e\right)p'_s} + b\Delta e\frac{\delta p'_s}{\left(1+e\right)p'_s} + \kappa^*\frac{\delta p'}{\left(1+e\right)p'}. \tag{2.23}$$

For the general stress path, the elastic and plastic volumetric strain increment are rewritten as:

$$\delta\varepsilon_v^e = \kappa^*\frac{\delta p'}{\left(1+e\right)p'}, \tag{2.24}$$

$$\delta\varepsilon_v^p = \left(\lambda^* - \kappa^*\right)\frac{\delta p'_s}{\left(1+e\right)p'_s} + b\Delta e\left(\frac{M^*}{M^* - \eta}\right)\frac{\delta p'_s}{\left(1+e\right)p'_s}, \tag{2.25}$$

where $\left(\frac{M^*}{M^* - \eta}\right)$ represents the effect of anisotropic shearing path on the soil structure. The terms of soil structure in plastic volumetric strain increment is diminished at critical state line. Effect of the b on the compression and shearing behaviour were studied by Liu and Cater (2002) as shown in Figures 2.17 and 2.18.

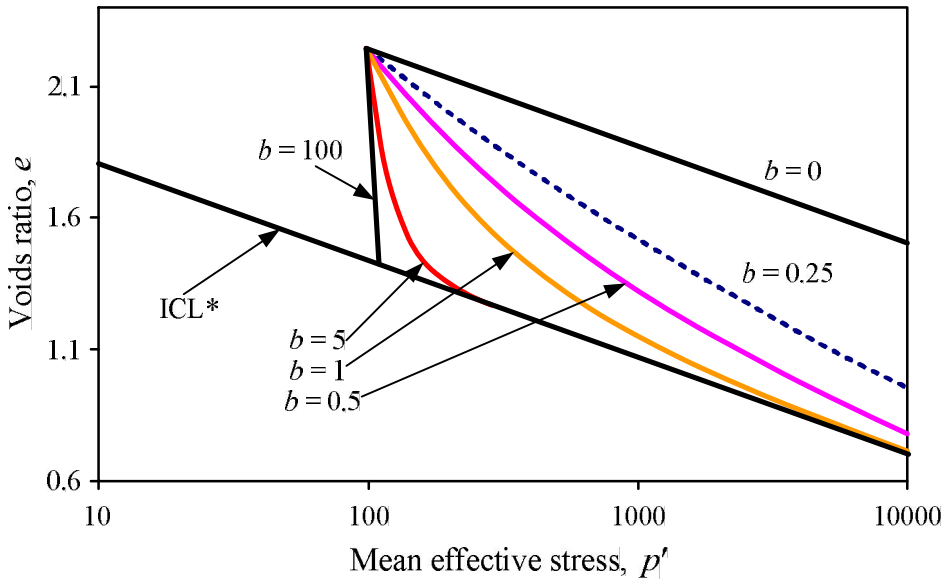

Figure 2.17 Influence of parameter b on isotropic compression behaviour (after Liu and Carter, 2002)

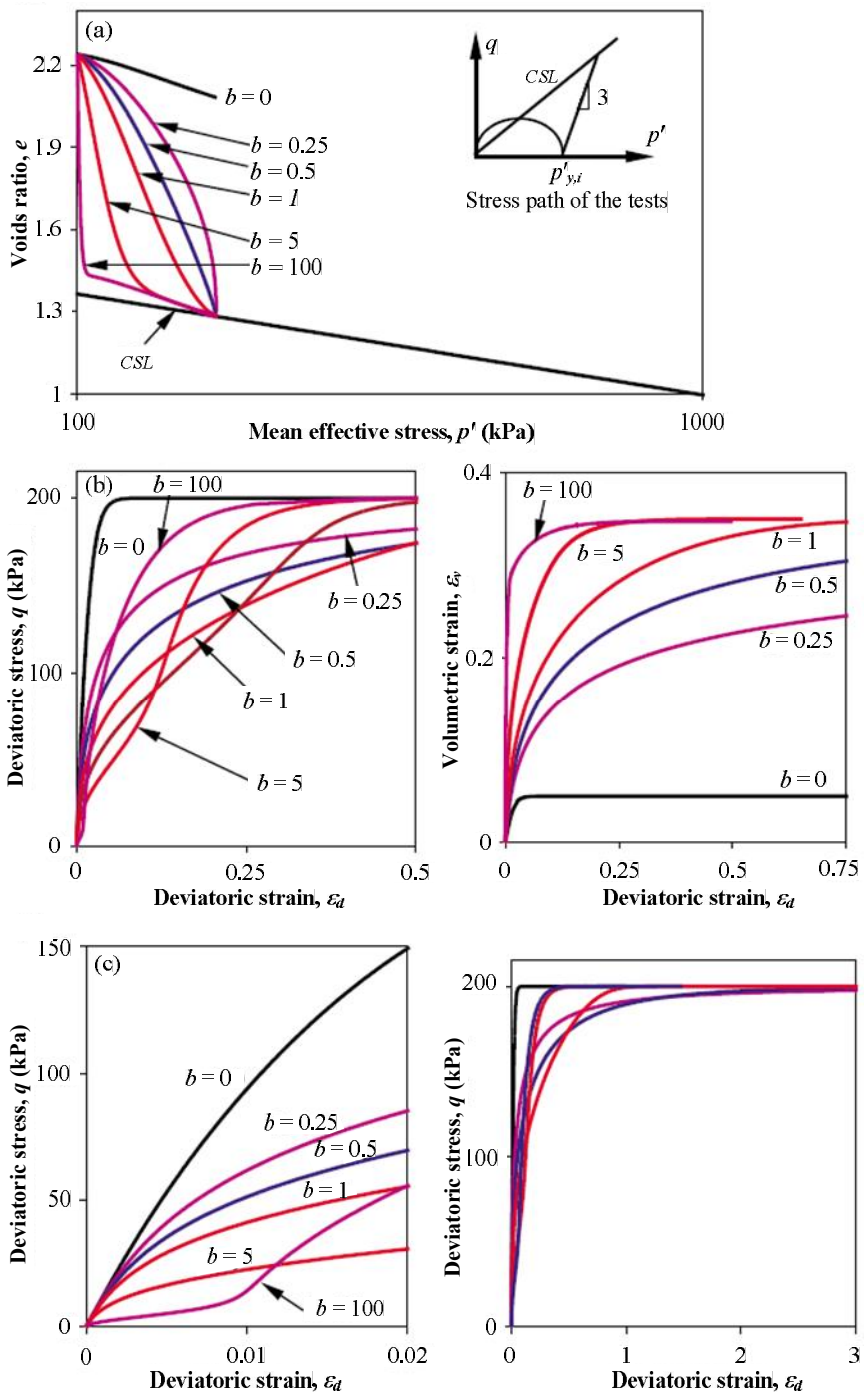

Figure 2.18 Influence of destructuring index b on the shearing behaviour of soil (a) Stress path in the $e - \ln p'$ plane (b) Stress and strain relationship (c) Deviatoric stress and strain relationship at different scales (after Liu and Carter, 2002)

The soil structure is assumed to influence the plastic direction via the modified flow rule. Based on the literature, a structured clay with positive Δe generally has a lower value for the strain increment ratio $d\varepsilon_d^p / d\varepsilon_v^p$ than the corresponding destructured soil at the same virgin yielding stress state (e.g., Graham and Li, 1985; Cotecchia, 1996; Cotecchia and Chandler, 1997). The flow rule for structured clay is,

$$\frac{d\varepsilon_d^p}{d\varepsilon_v^p} = \frac{k\eta}{M^{*2} - \eta^2}, \tag{2.26}$$

where k is a flow rule multiplier, which describes the influence of soil structure on the plastic direction. In the SCC model, the flow rule multiplier is assumed to depend on the Δe as following equation,

$$k = 2\left(1 - \omega \Delta e\right), \tag{2.27}$$

where ω is a model parameter which is satisfied the constraint as:

$$0 \le \omega \le \frac{1}{\Delta e_i}. \tag{2.28}$$

This flow rule have been adopted by the other research for modelling the behaviour of partially saturated clays (Alonso et al. 1990). McDowell and Hau (2004) have presented the value of flow rule multiplier equal to $0.7M^*$ for simulating stiff clay behaviour with non-associated model.

Following the yield surface for structured clay and modified flow rule, the elastic and plastic stress-strain response of the SCC model can be derived in the compliance relation as follows:

$$\begin{Bmatrix} \delta\varepsilon_v^e \\ \delta\varepsilon_d^e \end{Bmatrix} = \begin{bmatrix} \frac{1}{K'} & 0 \\ 0 & \frac{1}{3G'} \end{bmatrix} \begin{Bmatrix} \delta p' \\ \delta q \end{Bmatrix}, \tag{2.29}$$

$$\begin{Bmatrix} \delta\varepsilon_v^p \\ \delta\varepsilon_d^p \end{Bmatrix} = \frac{\left(\lambda^* - \kappa^*\right) + b\Delta e\left(\frac{M^*}{M^* - \eta}\right)}{\left(1+e\right)p'\left(M^{*2} + \eta^2\right)} \begin{bmatrix} \left(M^{*2} - \eta^2\right) & 2\eta \\ \left(1-\omega\Delta e\right)\eta & \frac{2\left(1-\omega\Delta e\right)\eta^2}{\left(M^{*2} - \eta^2\right)} \end{bmatrix} \begin{Bmatrix} \delta p' \\ \delta q \end{Bmatrix}. \tag{2.30}$$

2.6.1 Shortcoming of SCC model

Although, the influence of soil structure often produces anisotropy in the mechanical response of soil to change stress, destructuration usually leads to the reduction of anisotropy. In order to concentrate on introducing the physical concepts of the framework and to avoid unnecessary complexity of mathematical formulation, only the isotropic effects of soil structure are considered in the SCC model framework.

The SCC model can predict the impressive results for the soils which are not affected by cohesion intercept like natural soft clay. However there are some imperfections for using the SCC model with the highly cemented clay. Those are from (1) the effect of cohesion on the shape of yield surface, (2) The destructuration due to shear deformation and (3) The effect of soil structure to plastic potential. Although the

influence of structure and destructuration on the volumetric deformation is taken care in the SCC model, the effect of cohesion intercept on the stress-strain behaviour and the strain softening behaviour are ignored. However, based on the literature reviews, the cohesion intercept and strain softening are main characteristics, which are usually observed from testing on the structured stiff clays and artificially structured clays. The cohesion intercept and strain softening behaviour are one of the topics of this research. They are solved by the proposed model in Chapter III.

The prediction of soil behaviour in overconsolidated state is one of the imperfections of the SCC model. The SCC model overestimates the failure stresses on the 'dry' side (i.e. states to the left of the critical state line). This is due to the assumption of the elastic response inside the yield surface. Based on this assumption, the lack of smooth transition between elastic and plastic behaviours is usually obtained when modelling the soil in overconsolidated state. Moreover, the modelling of soils under repeated loading is another deficiency in the SCC model. The problem for stress-strain-strength characteristic of overconsolidated structured clay is solved by incorporating the bounding surface plasticity theory into the formulation of critical state model for structured clay, which is presented in Chapter IV.

2.7 Summary

The critical state framework and its extensive theory have been reviewed in this chapter. The advancement of soil models based on the critical state framework are summarised and discussed. The effect of soil structure is one important topic, which is the main problem of geotechnical practitioner for working with structured soils such as natural and cemented clays. Gen and Nova (1993) presented a concept for

modelling the behaviour of bonding materials that has a strong influence on some recent developed models for structured clay in the last two decade. There are great progresses on the development of soil model for structured clay by the advanced and practical trends. One of the practical soil model based on the critical state framework is the SCC model proposed by Liu and Carter (2002). The SCC model can be successfully explained the naturally structured clay behaviour. The intrinsic parameters from the MCC model are adopted together with the additional parameters for describing the effect of soil structure. It is interesting that its model parameters are derived from the comparison of test results between reconstituted and structured states. Most of them can be obtained directly from the conventional laboratory. However the SCC model needs to be improved for better simulation; those are the effect of cohesion on the shape of yield surface, the destructuration due to shear deformation, the effect of soil structure to plastic potential and the lack of smooth transitional between elastic to plastic behaviours. Those topics are overcome by the proposed model of this research, which is presented in the next chapters.

2.8 References

Adachi, T., and Oka, F. (1982). Constitutive equations for normally consolidated clay based on elasto-viscoplasticity. **Soils and Foundations**. 22(4): 57-70.

Al-Tabbaa, A., and Wood, D. M. (1989). An experimentally based 'bubble' model for clay. **Proceedings of the 3rd International Symposium on Numerical Models in Geomechanics (NUMOG III)** (pp. 91-99).

Asaoka, A., Nakano, N., and Noda, T. (2000). Superloading yield surface concept for highly structured soil behaviour. **Soils and Foundations**. 40(2): 99-110.

Baudet, B., and Stallebrass, S. (2004). A constitutive model for structured clays. **Geotechnique**. 54(4): 269-278.

Borja, R. I., and Lee, S. R. (1990). Cam-Clay plasticity, Part I: Implicit integration of elasto-plastic constitutive relations. **Computer Methods in Applied Mechanics and Engineering**. 78(1): 49-72.

Borjia, R. I., and Kavazanjian, E. J. (1985). A constitutive model for the stress-strain-time behaviour of wet clays. **Geotechnique**. 35(3): 283-298.

Britto, A. M., and Gunn, M. J. (1987). **Critical state soil mechanics via finite elements**. New York: Halsted Press.

Burland, J. B. (1965). Correspondence on 'On the Yielding of Soils'. **Geotechnique**. 15(2): 211-214.

Burland, J. B. (1990). On the compressibility and shear strength of natural soils. **Geotechnique**. 40(3): 329–378.

Callisto, L., and Rampello, S. (2004). An interpretation of structural degradation for three natural clays. **Canadian Geotechnical Journal**. 41: 392-407.

Chazallon, C., and Hicher, P. Y. (1995). An elastoplastic model with damage for bonded geornaterials. **Numerical models in Geomechanics, NUMOG V** (pp. 21-26).

Cotecchia, F. (1996). The effect of the structure on the properties of and Italian Pleistocene clay. **Ph.D. Thesis**, University of London.

Cotecchia, F., and Chandler, R. J. (1997). The influence of structure on the pre-failure behaviour of a natural clay. **Geotechnique**. 47(3): 523-544.

Cotecchia, F., and Chandler, R. J. (2000). A general framework for the mechanical behaviour of clays. **Geotechnique**. 50(4): 431-447.

Dafalias, Y. F. (1986). Bounding surface plasticity. I: Mathermatical foundation and hypoplasticity. **Journal of Engineering Mechanics, ASCE**. 112(9): 966-987.

Dafalias, Y. F., and Herrmann, L. R. (1980). Bounding surface formulation of the soil plasticity. **Soil Mechanics-Transient and Cyclic Loads**: Wiley, New York. 253-282.

Dafalias, Y. F., and Herrmann, L. R. (1986). Bounding surface plasticity. II: Application to isotropic cohesion soil. **Journal of Engineering Mechanics, ASCE**. 112(12): 1263-1291.

Dafalias, Y. F., Manzari, M. T., and Papadimitriou, A. G. (2006). SANICLAY: simple anisotropic clay plasticity model. **International Journal for Numerical and Analytical Methods in Geomechanics**. 30(12): 1231-1257.

Dafalias, Y. F., and Popov, E. P. (1975). A model of non-linearly hardening materials for complex loading. **Acta Mechanica**. 21: 173-192.

Desai, C. S. (2001). **Mechanics of Materials and Interface: The Disturbed State Concept**. CRC Press.

Gajo, A., and Muir Wood, D. (2001). A new approach to anisotropic, bounding surface plasticity: general formulation and simulations of natural and reconstituted clay behaviour. **International Journal for Numerical and Analytical Methods in Geomechanics**. 25: 207-241.

Gens, A., and Nova, R. (1993). Conceptual bases for constitutive model for bonded soil and weak rocks. **Geotechnical Engineering of Hard Soil-Soft Rocks**: Balkema.

Gens, A., and Potts, D. M. (1988). Critical state models in computational geomechanics. **Engineering Computationals**. 5(3): 178-197.

Graham, J., and Li, E. C. C. (1985). Comparison of natural and remolded plastic clay. **Journal of Geotechnical Engineering, ASCE**. 111(7): 865-881.

Hanzawa, H., and Adachi, K. (1983). Overconsolidation of alluvial clays. **Soils and Foundations**. 23(4): 106-118.

Hashiguchi, K. (1980). Constitutive equations of elastoplastic materials with elastic-plastic translation. **Journal of Applied Mechanics, ASME**. 47: 266-272.

Hashiguchi, K. (1989). Subloading surface model in unconventional plasticity. **International Journal of Solids and Structures**. 25(8): 917-945.

Hashiguchi, K., and Chen, Z. P. (1998). Elastoplastic constitutive equation of soils with the subloading surface and the rotational hardening. **International Journal for Numerical and Analytical Methods in Geomechanics**. 22(3): 197-227.

Hashiguchi, K., and Ueno, M. (1977). Elastoplastic constitutive laws of granular materials. Constitutive equations of Soils **Proceedings 9th International Conference on Soil Mechanics and Foundation Engineering, Special Session 9, JSSMFE** (pp. 73-82), Tokyo.

Horpibulsuk, S. (2001). Analysis and Assessment of Engineering Behavior of Cement Stabilized Clays. **Ph.D. dissertation**, Saga University, Saga, Japan.

Horpibulsuk, S., Miura, N., and Bergado, D. T. (2004). Undrained shear behaviour of cement admixed clay at high water content. **Journal of Geotechnical and Geoenvironmental Engineering, ASCE**. 130(10): 1096-1105.

Horpibulsuk, S., Miura, N., and Nagaraj, T. S. (2005). Clay-water/cement ratio identity of cement admixed soft clay. **Journal of Geotechnical and Geoenvironmental Engineering, ASCE**. 131(2): 187-192.

Horpibulsuk, S., Shibuya, S., Fuenkajorn, K., and Katkan, W. (2007). Assessment of engineering properties of Bangkok clay. **Canadian Geotechnical Journal**. 44(2): 173-187.

Huang, J. T., and Airey, D. W. (1998). Properties of an artificially cemented carbonate sand. **Journal of Geotechnical and Geoenvironmental Engineering, ASCE**. 124(6): 492-499.

Hvorslev, M. J. (1937). Uder die Festigkeitseigenschaften gestörter bindiger Böden. **Ingeniorvidenskabelige Skrifter, A.** Copenhagen.

Ismail, M. A., Joer, H. A., Randolph, M. F., and Sin, W. H. (2002). Effect of cement type on shear behaviour of cemented calcareous soil. **Journal of Geotechnical Engineering, ASCE**. 128(6): 520-529.

Kasama, K., Ochiai, H., and Yasufuku, N. (2000). On the stress-strain behaviour of lightly cemented clay based on an extended critical state concept. **Soils and Foundations**. 40(5): 37-47.

Kavvadas, M., and Amorosi, A. (2000). A constitutive model for structured soils. **Geotechnique**. 50(3): 263-273.

Khong, C. D. (2004). Development and numerical evaluation of unified critical state models. **Ph.D. Thesis**, University of Nottingham, UK.

Kutter, B. L., and Sathialingam, N. (1992). Elastic-viscoplastic modelling of the rate-dependent behaviour of clays. **Geotechnique**. 42(3): 427-441.

Lee, K., Chan, D., and Lam, K. (2004). Constitutive model for cement treated clay in a critical state framework. **Soils and Foundations**. 44(3): 69-77.

Leroueil, S., Tavenas, F., Brucy, F., La Rochelle, P., and Roy, M. (1979). Behavior of destructured natural clays. **Journal of Geotechnical Engineering, ASCE**. 105(6): 759-778.

Leroueil, S., Tavenas, F., Samson, L., and Morin, P. (1983). Preconsolidation pressure of Champlain clay Part II: Laboratory determination. **Canadian Geotechnical Journal**. 20(4): 803-816.

Leroueil, S., and Vaughan, P. R. (1990). The general and congruent effects of structure in natural soils and week rock. **Geotechnique**. 40: 467-488.

Liu, M. D., and Carter, J. P. (1999). Virgin compression of structured soils. **Geotechnique**. 49(1): 43–57.

Liu, M. D., and Carter, J. P. (2000). Modeling the destructuring of soils during virgin compression. **Geotechnique**. 50(4): 479–483.

Liu, M. D., and Carter, J. P. (2002). A structured Cam Clay model. **Canadian Geotechnical Journal**. 39: 1313–1332.

Liu, M. D., and Carter, J. P. (2003). Volumetric deformation of natural clays. **International Journal of Geomechanics, ASCE**. 3(2): 236-252.

Lorenzo, G., and Bergado, D. T. (2004). Fundamental parameters of cementadmixed clay: new approach. **Journal of Geotechnical and Geoenvironmental Engineering, ASCE**. 130(10): 1042-1050.

McDowell, G. R., and Hau, K. W. (2003). A simple non-associated three surface kinematic hardening model. **Geotechnique**. 53(4): 433-437.

McDowell, G. R., and Hau, K. W. (2004). A generalised Modified Cam clay model for clay and sand incorporating kinematic and bounding surface plasticity. **Granular Matter**. 6: 11-16.

Mitchell, J. K. (1996). **Fundamentals of Soil Behavior**. New York: John Willey & Sons Inc.

Mrŏz, Z. (1967). On Description of anisotropic work hardening. **Journal of the Mechanics and Physics of Solids**. 15(3): 163-175.

Mrŏz, Z. (1969). An attempt to describe the behaviour of metals under cyclic loads using a more general work hardening model. **Acta Mechanica**. 7: 169-212.

Mrŏz, Z., Norris, V. A., and Zienkiewicz, O. C. (1978). Anisotropic hardening model for soils and its application to cyclic loading. **International Journal for Numerical and Analytical Methods in Geomechanics**. 2(3): 203-221.

Mrŏz, Z., Norris, V. A., and Zienkiewicz, O. C. (1979). Application of an anisotropic hardening model in the analysis of elastoplastic deformation of soils. **Geotechnique**. 29(1): 1-34.

Mrŏz, Z., Norris, V. A., and Zienkiewicz, O. C. (1981). An anisotropic, critical state model for soils subject to cyclic loading. **Geotechnique**. 31(4): 451-469.

Oka, F., Leroueil, S., and Tavenas, F. (1989). A constitutive model for natural soft clay with strain softening. **Soils and Foundations**. 29(3): 54-66.

Prévost, J. H. (1977). Mathematical modelling of monotonic and cyclic undrained clay behaviour. **International Journal for Numerical and Analytical Methods in Geomechanics**. 1(2): 195-216.

Rendulic, L. (1937). Ein Grundgesetz der Tonmechanik und sien experimenteller Beweis. **Der Bauingenieur** 18: 459-467.

Roscoe, K. H., and Burland, J. B. (1968). On the generalised stress-strain behaviour of wet clay. **Engineering plasticity**. 535-609.

Roscoe, K. H., and Schofield, A. N. (1963). Mechanical behaviour of an idealised wet clay. **Proceedings of the European Conference on Soil Mechanics and Foundation Engineering** (pp. 47-54).

Rotta, G. V., Consoli, N. C., Prietto, P. D. M., Coop, M. R., and Graham, J. (2003). Isotropic yielding in an artificially cemented soil cured under stress. **Geotechnique**. 53(5): 493-501.

Rouainia, M., and Muir Wood, D. (2000). A kinematic hardening constitutive model for natural clays with loss of structure. **Geotechnique**. 50(2): 153-164.

Schofield, A. N., and Wroth, C. P. (1968). **Critical State Soil Mechanics**. London: MacGraw-Hill.

Shibuya, S. (2000). Assessing structure of aged natural sedimentary clays. **Soils and Foundations**. 40(3): 1-16.

Srinivasa Murthy, B. R., Vatsala, A., and Nagaraj, T. S. (1988). Can Cam-clay model be generalized. **Journal of Geotechnical Engineering, ASCE**. 114(5): 601-613.

Srinivasa Murthy, B. R., Vatsala, A., and Nagaraj, T. S. (1991). Revised Cam-clay model. **Journal of Geotechnical Engineering, ASCE**. 117(6): 851-871.

Stallebrass, S. E. (1990). Modelling the efects of recent stress history on the behaviour of overconsolidated soils. **Ph.D. thesis**, City University, London.

Stallebrass, S. E., and Taylor, R. N. (1997). The development and evaluation of a constitutive model for the prediction of ground movements in overconsolidated clay. **Geotechnique**. 47: 235-253.

Suebsuk, J., Horpibulsuk, S., and Liu, M. D. (2008). A modified Structure Cam Clay model. **Research and Development Journal of The Engineering Institute of Thailand**. 19(1): 1-8.

Tamagnini, C., and D'Elia, M. (1999). A simple bounding surface for bonded clays. **Pre-failure deformation Characteristics of Geomaterials**. Jamiolkowski, Lancellotta, and L. Presti, eds. Rotterdam: Balkema. 565-572.

Vatsala, A., Nora, R., and Srinivasa Murthy, B. R. (2001). Elastoplastic model for cemented soils. **Journal of Geotechnical and Geoenvironmental Engineering, ASCE**. 127(8): 678-687.

Wheeler, S. J., Näätänen, A., Karstunen, M., and Lojander, M. (2003). An anisotropic elasto-plastic model for soft clays. **Canadian Geotechnical Journal**. 40(2): 403-418.

Whittle, A. J. (1993). Evaluation of a constitutive model for overconsolidated clays. **Geotechnique**. 43(2): 289-313.

Whittle, A. J., and Kavvadas, M. J. (1994). Formulation of MIT-E3 constitutive model for overconsolidated clays. **Journal of Geotechnical Engineering, ASCE**. 120(1): 199–224.

Wissa, A. E. Z., Ladd, C. C., and Lambe, T. W. (1965). Effective stress strength parameters of stabilized soils. **Proceedings of 6th International Conference on Soil Mechanics and Foundation Engineering** (pp. 412-416).

Yu, H. S., Khong, C. D., and Wang, J. (2007). A unified plasticity model for cyclic behaviour of clay and sand. **Mechanics Research Communications**. 34: 97-114.

CHAPTER III

A GENERALISED CRITICAL STATE MODEL FOR STRUCTURED CLAY

3.1 Introduction

The inherent nature and diversity of the geotechnical process involved in soil formation are responsible for the wide variation in soil structure. Natural clay can be designated as "structured clay" (Leonard, 1972; Leroueil et al., 1979; Mitchell, 1996; Shibuya, 2000; etc.). The term "soil structure" is determined by both the particle associations and arrangements (fabric) and inter-particle forces (soil-cementation or bonding). The resistance of soil structure is responsible for the difference in the engineering behaviour of natural soils between the structured and destructured (remoulded) states (Leroueil et al., 1979; Hanzawa and Adachi, 1983; Leroueil et al., 1983; Leroueil and Vaughan, 1990; Mitchell, 1996; Shibuya, 2000; Horpibulsuk et al., 2007). The development of soil structure during the depositional and post-depositional processes has been reported by many researchers (Locat and Lefebvre, 1985; Mitchell, 1986; Schmertmann, 1991).

To improve soft ground with a chemical admixture such as the in-situ deep mixing technique, the natural clay is disturbed by mixing wings and mixed with cement or lime. The natural structure is destroyed and taken over by the cementation structure. The cement- or lime-admixed clay is thus designated as "artificially structured clay". The mechanical properties of artificially structured clay have been

investigated extensively (Wissa et al., 1965; Clough et al., 1981; Uddin, 1995; Horpibulsuk, 2001; Miura et al., 2001; Nagaraj and Miura, 2001; Ismail et al., 2002; Horpibulsuk et al., 2004a; Horpibulsuk et al., 2004b; and others).

In recent years, the rapid advances in computer hardware and the associated reduction in cost have resulted in a marked increase in the use of numerical methods to analyse geotechnical problems. The ability of such methods to provide realistic predictions depends on the accuracy of the constitutive model used to represent the mechanical behaviour of the soil. There has been great progress in constitutive modelling of the behaviour of soil with natural structure, such as those proposed by Gens and Nova (1993) and Vatsala et al. (2001). Some frontier research in understanding and modelling the degradation of soil structure includes a kinematic hardening model (Kavvadas and Amorosi, 2000; Rouainia and Muir Wood, 2000; Baudet and Stallebrass, 2004). Most of the previous constitutive models are, however, generally complicated and their model parameters are difficult to identify in practice and do not take into account the key features of artificially structured clay, especially the crushing of soil-cementation structure (Horpibulsuk et al., 2010).

Recently, there have been many models for structured clay developed based on the Modified Cam Clay (MCC) model due to its simple pattern recognition. Chai et al. (2004) have introduced the influence of structure on the compression behaviour and then modified the equation to predict plastic volumetric strain of the MCC model. Their model can simulate the volumetric deformation behaviour of naturally structured clay well. Liu and Carter (2002) and Carter and Liu (2005) introduced a simple predictive model, the Structured Cam Clay (SCC) model, for naturally structured clay. It has been formulated elegantly by introducing the influence of

structure on the volumetric deformation behaviour and the plastic strain direction into the MCC model. The influence of structure on volumetric deformation is taken into account by the additional voids ratio that is sustained by the soil structure (Δe). The destructuring law due to volumetric deformation has been proposed as a decreasing function of the Δe. The concept of the development of the non-associated flow rule adopted in the SCC model is similar to that made by McDowell and Hau (2003) for hard clay and sand, and by Horpibulsuk et al. (2010) for artificially structured clay. Both the SCC model and the model proposed by Chai et al. (2004) have not considered the influence of structure on strength characteristics (especially cohesion) and softening behaviour when stress states are on virgin yielding state. Cohesion is significant especially for stiff naturally structured clays (Callisto and Rampello, 2004) and artificially structured clays (Wissa et al., 1965; Clough et al., 1981). To explain the influence of structure on strength characteristics, Gens and Nova (1993), Kasama et al. (2000) and Lee et al. (2004) have introduced the modified effective stress concept. Based on this concept and the critical state framework, Kasama et al. (2000) have introduced a model that can predict the strength characteristics for artificially structured clay in normally and lightly over-consolidated states well. However, their model cannot describe the strain softening in virgin yielding state, which is generally observed as the soil-cementation structure is crushed (Miura et al., 2001; Nagaraj and Miura, 2001; Vatsala et al., 2001; Horpibulsuk et al., 2004b; Horpibulsuk et al., 2005). In the models proposed by Chai et al. (2004), Kasama et al., (2000) and Lee et al. (2004), the associated flow rule was adopted. Thus, those models cannot explain the influence of structure on the plastic strain direction, unlike the SCC model.

To form a model suitable for structured clay based on the critical state framework, the influence of structure and destructuring on the yield function, hardening rule and plastic potential must be incorporated. Recently, Horpibulsuk et al. (2010) have summarised the main features of cemented clay behaviour and introduced the SCC model for cemented clay. In the model, the effective stress concept, yield function, hardening rule and plastic potential have been developed to take into account the effect of structure. Their model can simulate shear behaviour for both normally and lightly over-consolidated states. Some modifications are needed, however, to simply and practically implement the model for numerical analysis and to better capture the main features of the artificially structured clay with the model parameters simply obtained from a conventional laboratory.

In present study, attempts are made to develop a generalised constitutive model based on the critical state framework for destructured, naturally structured and artificially structured clays. The proposed model, designated as the Modified Structured Cam Clay (MSCC) model, is formulated based on the SCC model for cemented clay (Horpibulsuk et al., 2010). In this research, based on a quantitative examination of test data describing the behaviour of cemented soils, the application of the modified effective stress concept to describe the compression and shear behaviour of structured clays is illustrated, and the yield function, hardening rule and plastic potential are developed based on the modified effective stress concept. A new plastic potential that reliably describes the effect of soil structure is introduced. A new general destructuring law that describes the degradation and crushing of the structure is also proposed. In this law, the destructuring is assumed to depend on the plastic distortional strain. Both new plastic potential and destructuring law better explain and

simulate the structured clay behaviour than those of the original models (Liu and Carter, 2002; Horpibulsuk et al., 2010). The MSCC model is verified by simulating the undrained and drained shear behaviour of destructured, naturally structured and artificially structured clays under a wide range of pre-shear consolidation pressure (both in normally and over-consolidated states). The naturally structured clays are Osaka clay (Adachi et al., 1995) and Marl clay (Anagnostopoulos et al., 1991), and the artificially structured clays are cemented Araike clay (Horpibulsuk, 2001; Horpibulsuk et al., 2004b) and cemented Bangkok clay (Uddin, 1995). The simulated shear behaviour of the same clay in both destructured and structured states using the same destructured model parameters is illustrated by the test results of destructured and artificially structured Ariake clay. This shows an advantage of the MSCC model using the destructured state as a reference.

3.2 Conceptual framework of the MSCC model

The MSCC model is developed by generalising the theoretical framework of the SCC model (Liu and Carter, 2002; Carter and Liu, 2005; Horpibulsuk et al., 2010). The major aim of formulating the MSCC model is to provide a constitutive model that is suitable for the routinely solving boundary value problems encountered in geotechnical engineering practice. Therefore, it is necessary to keep the model relatively simple. The model parameters can be simply determined from conventional compression and triaxial tests. The formulation of proposed model in this study is represented in the triaxial stress space via the well known state parameters (q and p').

3.2.1 Modified effective stress concept and destructuring law

The influence of structure is regarded akin to the effect of an increase in the effective stress and yield stress and, therefore, the yield surface (Gens and Nova, 1993; Kasama et al., 2000; Kavvadas and Amorosi, 2000; Rouainia and Muir Wood, 2000; Horpibulsuk, 2001; Baudet and Stallebrass, 2004; Lee et al., 2004; Horpibulsuk et al., 2010). For artificially structured clay, the increase in the yield stress with cement content is clearly understood from the compression and shear test results (Miura et al., 2001; Horpibulsuk et al., 2004a; Horpibulsuk et al., 2004b; etc.). Consequently, two samples of artificially structured clay under the same current stress (pre-shear consolidation pressure) but with different degrees of cementation show different stress-strain and strength characteristics due to the differences in the structural state and yield surface. Thus, the modified mean effective stress concept for structured clay is presented in the form:

$$\overline{p}' = (p + p_b') - u \,, \tag{3.1a}$$

$$\overline{p}' = p' + p_b' \,, \tag{3.1b}$$

where $\overline{p}'$ is the modified mean effective stress of structured clay or explicit mean effective stress and p_b' is the mean effective stress that increases due to structure (structure strength). When no cementation exists, the p_b' is null and the $\overline{p}' = p'$. Thus, the modified stress ratio can be expressed as follows:

$$\bar{\eta} = \frac{q}{p' + p'_b} . \tag{3.2}$$

Due to the p'_b caused by structure, the structured clay samples can stand without applied confining stress. Considering that the strength envelope moves toward the right, which establishes a zero cohesion intercept, the relationship between deviatoric stress and mean effective stress can be proposed as follows,

$$q = M(p' + p'_b), \tag{3.3}$$

where M is the gradient of the failure envelope in the $q - p'$ plane. Due to the destructuring, p'_b decreases when the stress state is on the yield surface.

Based on the isotropic compression behaviour of structured clays, the SCC model is formulated on the fundamental assumption that both hardening and destructuring of natural soils depends on plastic volumetric deformation. It has been demonstrated the model predicts accurate results for natural soil with weak or no cementation (Liu and Carter, 1999; Liu and Carter, 2000a; Liu and Carter, 2002). However, for stiff structured clay, the destructuring is mainly related to the plastic strain, which depends on two parts: those are from volumetric deformation and shear deformation (Kavvadas and Amorosi, 2000; Rouainia and Muir Wood, 2000; Cotecchia, 2003; Baudet and Stallebrass, 2004; Lee et al., 2004; Kimoto and Oka, 2005). The destructuring mechanism is the process of reducing the structure strength, p'_b, due to the degradation and crushing of the structure. In this study, the simplified destructuring, is assumed to be related directly to the plastic deviatoric strain, ε_d^p.

The p_b' is constant up to the virgin yielding. During virgin yielding (when plastic deviatoric strain occurs), the p_b' gradually decreases due to the degradation of structure until the failure state. This failure state is defined as the peak strength state in which the soil structure begins to be crushed. Thus, beyond this state, a sudden decrease in p_b' occurs and continues to the critical state where the soil structure is completely removed ($p_b' = 0$). Figure 3.1 explains the reduction in p_b' due to destructuring as the plastic deviatoric strain increases. The reduction in p_b' due to the degradation of structure (pre-failure) and the crushing of soil-cementation structure (post-failure) is proposed in terms of plastic deviatoric strain as follows,

$$p_b' = p_{b0}' \exp\left(-\varepsilon_d^p\right), \text{ for pre-failure (degradation of soil structure)} \quad (3.4)$$

$$p_b' = p_{b,f}' \exp\left[-\xi\left(\varepsilon_d^p - \varepsilon_{d,f}^p\right)\right], \text{ for post-failure (crushing of soil structure)} \quad (3.5)$$

where p_{b0}' is the initial structure strength, $p_{b,f}'$ is the structure strength at failure (peak strength), $\varepsilon_{d,f}^p$ is the plastic deviatoric strain at failure and ξ is the destructuring index due to shear deformation. From equations. (3.4) and (3.5), it is noted that the change in p_b' depends upon the plastic deviatoric strain, which is governed by the effective stress path and the plastic potential.

The state boundary surface was first proposed by Roscoe et al. (1958) for destructured (remoulded) clay. It is a normalised unique curve (Roscoe and Hvorslev surfaces) in q / p_e' and p' / p_e', where p_e' is the equivalent stress. The state boundary

surface separates states that soils can achieve from states that soils can never achieve (Atkinson and Bransby, 1978). It is known that this original state boundary surface cannot describe structured clay behaviour (Cotecchia and Chandler, 2000; Callisto and Rampello, 2004). The state boundary surface for structured clay can be generated based on the modified effective stress concept as shown in Figure 3.2 (test results were from Horpibulsuk et al., 2004b). The $\overline{p}'_y$ is the explicit mean effective yield stress, which is the sum of p'_y and p'_b. p'_y is the equivalent stress for undrained shearing. During virgin yielding (normally consolidated state), $\overline{p}'_y$ is equal to ($p'_0 + p'_b$), where p'_0 is the pre-shear effective stress or the yield stress in the isotropic compression condition. For the overconsolidated state, $\overline{p}'_y$ is constant and equal to ($p'_{y,i} + p'_b$), where $p'_{y,i}$ is the initial mean effective yield stress obtained from the compression curve. In this figure, p'_b is assumed to be p'_{b0} because the reduction in p'_b due to the degradation of structure is insignificant in the pre-failure state for cemented clay (Horpibulsuk et al., 2010). The degradation is insignificant because the change in plastic deviatoric strain is usually small in the pre-failure state for stiff (artificially) structured clay (Horpibulsuk, 2001; Horpibulsuk et al., 2004b; Horpibulsuk et al., 2010). It is found that the normalised modified effective stress paths for various cement contents during virgin yielding can be represented by a unique curve. This surface can be referred to as the modified Roscoe surface. These results show that the undrained stress paths on the state boundary surface are of the same shape and consistent with one another. Samples inside the state boundary surface, especially $\overline{p}' / \overline{p}'_y < 0.7$, fail on the same failure line, which designated as the

modified Hvorslev surface. The state boundary surface and the modified effective stress concepts are fundamental to the development of the MSCC model.

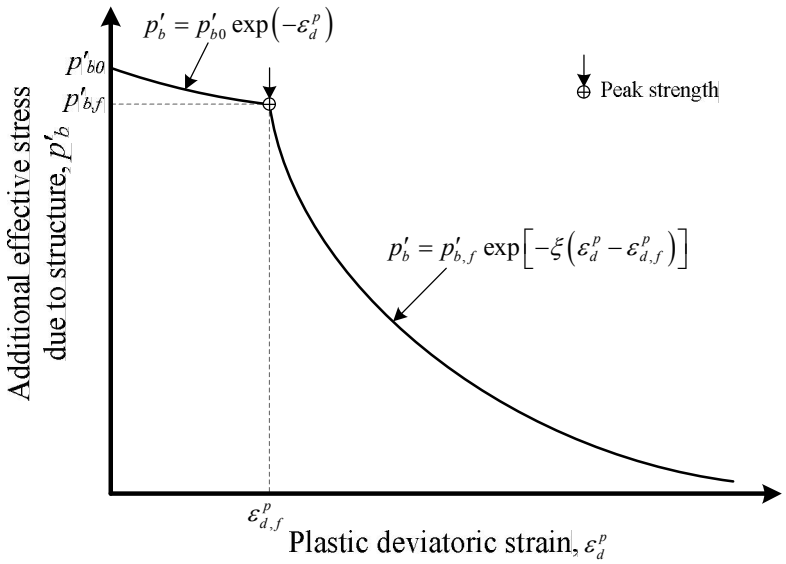

Figure 3.1 Schematic diagram of reduction in the p'_b due to destructuring process

3.2.2 Material idealisation

Structured soils usually possess anisotropic mechanical properties, and destructuring usually leads to the reduction of anisotropy. It is observed that the variation of mechanical properties of some artificially structured clays is basically isotropic (Huang and Airey, 1998; Rotta et al., 2003). To concentrate on introducing the effect of structure and destructuring and to avoid the unnecessary complexity of mathematical details, only the isotropic effects of soil structure are considered in the development of the MSCC model.

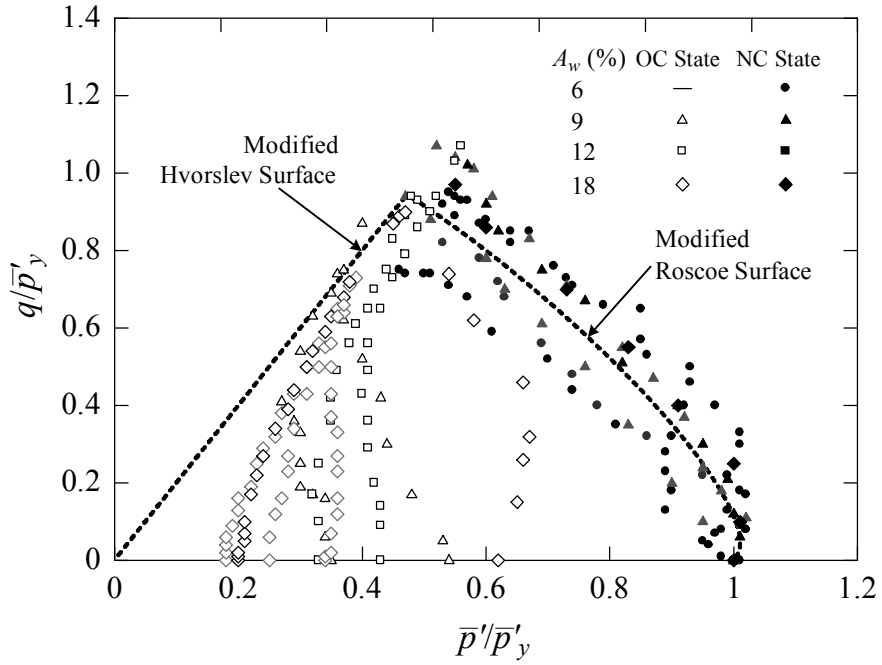

Figure 3.2 Test paths in $q/\overline{p}'_y$: $\overline{p}'/\overline{p}'_y$ space for an undrained test on artificially structured clay at 6%, 9%, 12% and 18% cement.
(data from Horpibulsuk et al., 2004b)

In the MSCC model, structured clay is idealised as an isotropic material with elastic and virgin yielding behaviours. The yield surface varies isotropically with plastic volumetric deformation. Soil behaviour is assumed to be elastic for any stress excursion inside the current yield surface. Virgin yielding and destructuring occur for stress variation originating on the yield surface. During virgin yielding, the current stress of structured clay stays on the yield surface.

Based on an examination of a large body of experimental data, material idealisation for the compression behaviour of structured clay is introduced in Figure 3.3a. Due to the structure, the structured clay can be stable above the intrinsic compresion line (ICL) of remoulded clay. In other words, the structured clay

possesses a higher voids ratio than the destructured clay at the same effective vertical stress (Horpibulsuk, 2001). This stable state is defined as meta-stable (Mitchell, 1996). The compression strain of the structured clay is negligible up to the yield stress, $p'_{y,i}$, because of the structure. Beyond this yield stress, there is sudden compression with a relatively high magnitude, which is indicated by the steep slope and caused by the destructuring. For further loading, the difference in the voids ratio between structured and destructured states (Δe) decreases with stress level and finally diminishes at a very high effective stress. Therefore, the virgin compression behaviour during the destructuring process of structured clay can be expressed by the following equation,

$$e = e^* + \Delta e, \tag{3.6}$$

where e is the voids ratio of structured clay and e^* is the voids ratio of destructured clay at the same stress state. The ICL of destructured clay is generally expressed in the form,

$$e^* = e^*_{IC} - \lambda^* \ln p', \tag{3.7}$$

where e^*_{IC} is the voids ratio at a reference mean effective stress (1 kPa) of the ICL and λ^* is the gradient of the ICL.

It has been proved that the compression equation for the additional voids ratio (Δe) of naturally structured clay proposed by Liu and Carter (1999; 2000a) is also applicable for artificially structured clay (Horpibulsuk et al., 2010). The following compression equation for structured clay is proposed:

$$e = e^{*} + \Delta e_i \left(\frac{p'_{y,i}}{p'_0} \right)^b , \tag{3.8}$$

where b is the destructuring index due to volumetric deformation, Δe_i is the additional voids ratio at the isotropic yield stress (Figure 3.3a) and p'_0 is the stress history or isotropic yield stress.

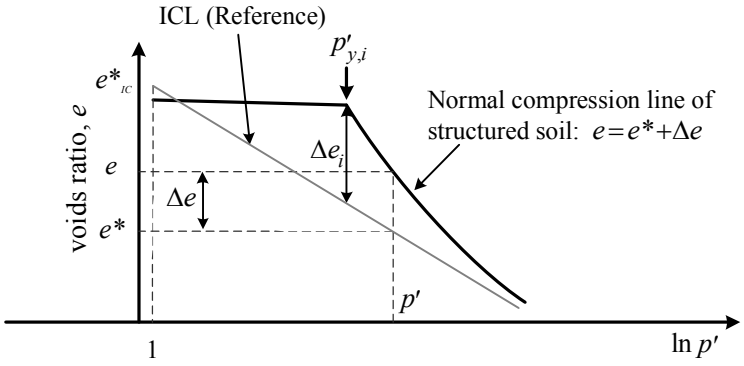

(a) Compression behaviour of structured soil

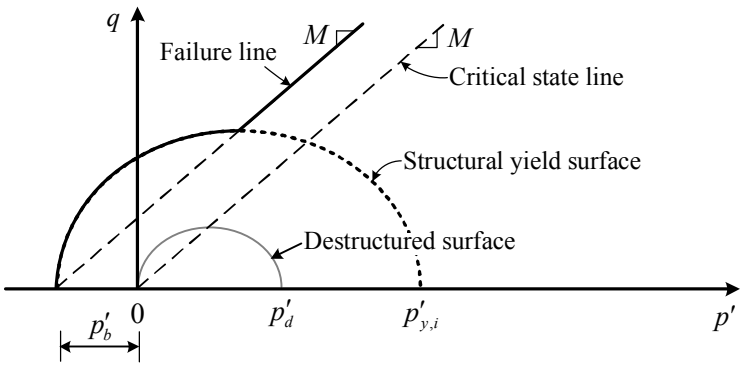

(b) Structural yield and destructured surfaces

Figure 3.3 Material idealisation for the MSCC model

Based on the state boundary surface for structured clay, the yield loci are of the same shape and consistent with one another. The yield surface of the MSCC model is assumed to be elliptical for both structured and destructured clays (anisotropic effect is not considered). By considering the effect of structure on the yield surface, the proposed yield function of the MSCC model in $q - p'$ plane is given by (Figure 3.3b),

$$F = q^2 - M^2 \left(p' + p'_b \right) \left(p'_0 - p' \right) = 0 . \tag{3.9}$$

The MSCC model assumes that the gradient of the failure envelope and the critical state line is the same. This concept has been employed in the previous works, such as those by Muir-Wood (1990); Kasama et al. (2000); and Lee et al., (2004). The structural and destructured yield surfaces are thus similar in shape (*vide* Figure 3.3b).

3.2.3 Stress states inside yield surface

As stated in the material idealisation, only elastic deformation occurs for stress excursions within the virgin yielding boundary. The elastic response of structured clay obeys Hooke's law, i.e.,

$$\delta\varepsilon_v^e = \frac{\delta p'}{K'} , \tag{3.10a}$$

$$\delta\varepsilon_d^e = \frac{\delta q}{3G'} , \tag{3.10b}$$

where K' is the bulk modulus and G' is the shear modulus. When shear modulus is constant, K' and Poisson's ratio, μ', are related to p', G' and the elastic swelling

index, κ, as follows:

$$K' = \frac{p'(1+e)}{\kappa}, \tag{3.11}$$

$$\mu' = \frac{3K' - 2G'}{6K' + 2G'}. \tag{3.12}$$

It was observed experimentally that the elastic deformation stiffness, $E' = 3(1-2\mu')K'$, generally increases with structure strength (e.g., Huang and Airey, 1998; Horpibulsuk et al., 2004b, etc.). This is reflected by equation (3.11) where the bulk modulus is linked to κ, which depends on structure strength.

3.2.4 Stress states on yield surface

Destructuring occurs with stress states on the yield surface for both hardening and softening behaviours. For models in the Cam Clay family, the plastic strain direction is determined from the plastic potential. Even though the MSCC model employs a yield surface with a shape similar to that of the MCC model, the original plastic potential is not used in the proposed model because the plastic potential of the MCC model generally produces too much plastic deviatoric strain and therefore leads to overprediction of the earth pressure at rest (McDowell, 2000; McDowell and Hau, 2003). It was also shown that the plastic deviatoric strain predicted by the original plastic potential is not suitable for artificially structured clay (Horpibulsuk et al., 2010). The plastic potential proposed by McDowell and Hau (2003) is modified by accounting for the structure effect. The plastic potential in the MSCC model is thus introduced as follows;

$$g = q^2 + \frac{M^2}{1-\psi}\left[\left(\frac{p'+p'_b}{p'_p+p'_b}\right)^{\frac{2}{\psi}}\left(p'_p+p'_b\right)^2 - \left(p'+p'_b\right)^2\right] = 0\,, \tag{3.13}$$

where p'_p is the parameter that describes the magnitude of the plastic potential and ψ is the parameter that describes the shape of the plastic potential. It should be noted that the critical state strength *M*, a parameter widely used in the Critical State Soil Mechanics, may vary with the Lode angle, θ, in three dimensional stress space depending on the methodology used for model generalisation (Khalili and Liu, 2008). A simple and accurate function that represents *M* in terms of the θ has been proposed by Sheng et al. (2000) as follows:

$$M(\theta) = M_{\max}\left(\frac{2\alpha^4}{1+\alpha^4-\left(1-\alpha^4\right)\sin 3\theta}\right)^{1/4}, \tag{3.14}$$

where $M_{\max}$ is the slope of the critical state line under triaxial compression ($\theta = -30^\circ$) and the parameter α depends on a friction angle of soil at the critical state line, ϕ', as follows:

$$\alpha = \frac{3-\sin\phi'}{3+\sin\phi'}, \tag{3.15}$$

With this generalisation, the plastic potential is applicable for general stress states. The shape of the plastic potential is shown in Figure 3.4 for various ψ-values and $p'_b = 0.2p'_p$ and M = 1.2. For a completely destructured state (p'_b = 0), this plastic potential becomes that of the MCC model if $\psi = 2$ is assumed.

For stress states on the yield surface and with $\bar{\eta} < M$ ($\delta p_0' > 0$), both volumetric hardening and destructuring occur. The plastic volumetric strain increment, $\delta\varepsilon_v^p$, for the MSCC model is derived from the assumption that the plastic volumetric strain depends on the change in stress history, $\delta p_0'$ and the current shear stress. The plastic volumetric strain increase during hardening is derived from equation (3.8) as follows:

$$\delta\varepsilon_v^p = \left\{ \left(\lambda^* - \kappa\right) + b\Delta e \left[\frac{M}{M - \bar{\eta}} \right] \right\} \frac{\delta p_0'}{\left(1+e\right) p_0'} . \tag{3.16}$$

The term $\dfrac{M}{M - \bar{\eta}}$ is introduced to take into account the effect of current shear stress. The derivation of this equation has been provided by Liu and Carter (2002; 2003). The effect of destructuring on the $\delta\varepsilon_v^p$ is reflected in the parameter *b* and thus also in the $\delta p_0'$.

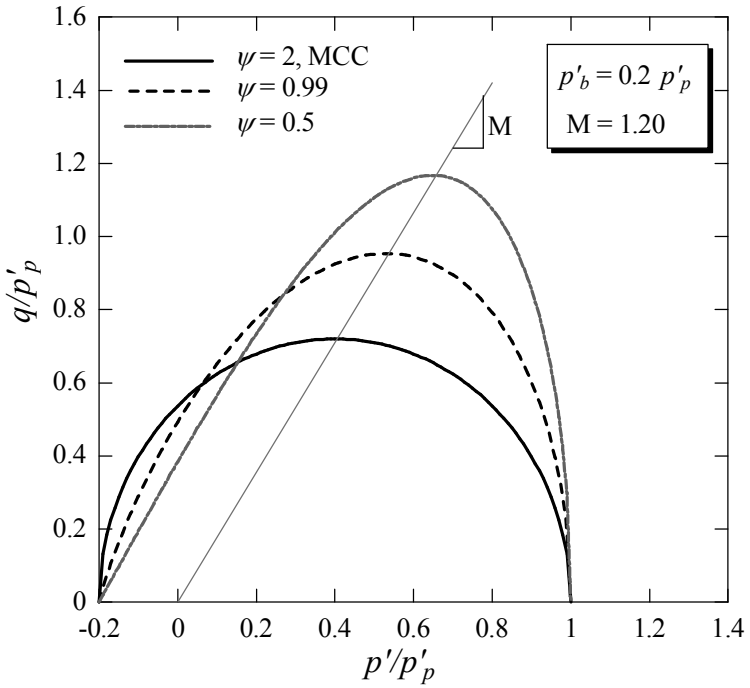

Figure 3.4 Shape of the plastic potential for the MSCC model

During the softening process ($\bar{\eta} > M$ and $\delta p_0' < 0$), the effect of current shear stress is not significant. The plastic volumetric strain increment during softening is thus proposed as follows:

$$\delta\varepsilon_v^p = \left\{\left(\lambda^* - \kappa\right) + b\Delta e\right\}\frac{\delta p_0'}{\left(1+e\right)p_0'}. \tag{3.17}$$

From the plastic potential (Equation 3.13) and the hardening rule (Equations 3.16 and 3.17), the hardening and the softening behaviours can be modelled in the same way as for other models in the Cam Clay family (Muir Wood, 1990; Liu and Carter, 2000b; Liu and Carter, 2003). When the stress state is on the yield surface with $\bar{\eta} < M$, hardening occurs (the yield surface expands) due to the

positive flow rule. Softening occurs when the stress state is on the yield surface with $\bar{\eta} > M$ where the flow rule becomes negative, which causes the yield surface to shrink.

The effect of ψ and ξ on the shear behaviour is illustrated in Figures 3.5 and 3.6 using the model parameters listed in Table 3.1. The parameter ψ significantly affects the plastic strain direction and, therefore, the stress-strain-strength relationships. The effect of ψ on the stress-strain-strength relationships for a particular destructuring rate (a particular ξ of 30) is shown in Figure 3.5. It is noted that as ψ decreases, the plastic deviatoric strain at failure, $\varepsilon_{d,f}^{p}$, decreases while the strength and stiffness increase. Figure 3.6 shows the effect of ξ on the strain-softening behaviour for ψ with a value of 0.1. As ξ increases, the p_b' at post failure decreases; thus, the deviatoric stress decreases more rapidly.

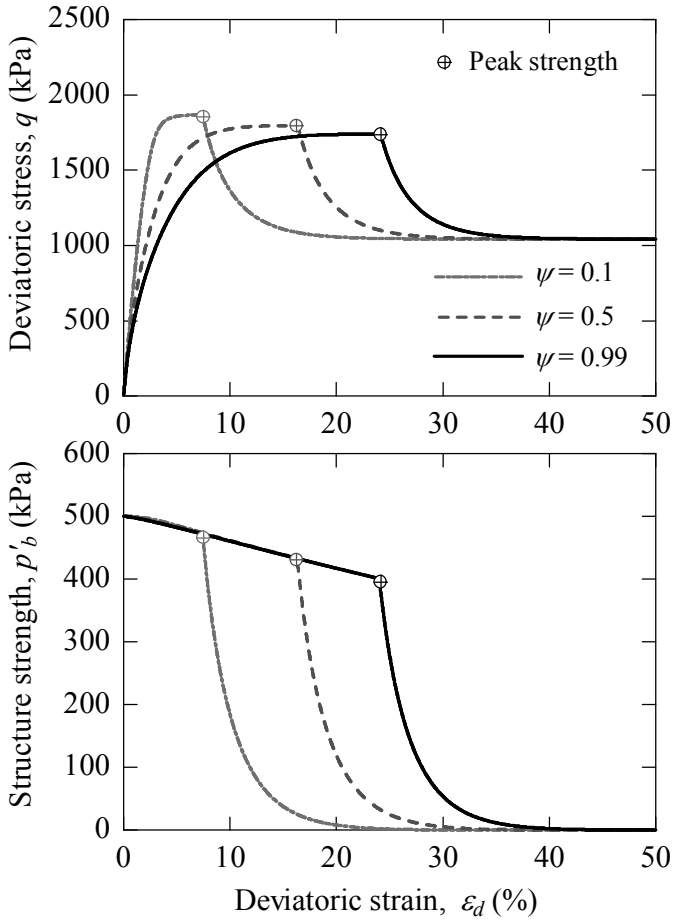

Figure 3.5 Parametric study on the parameter ψ

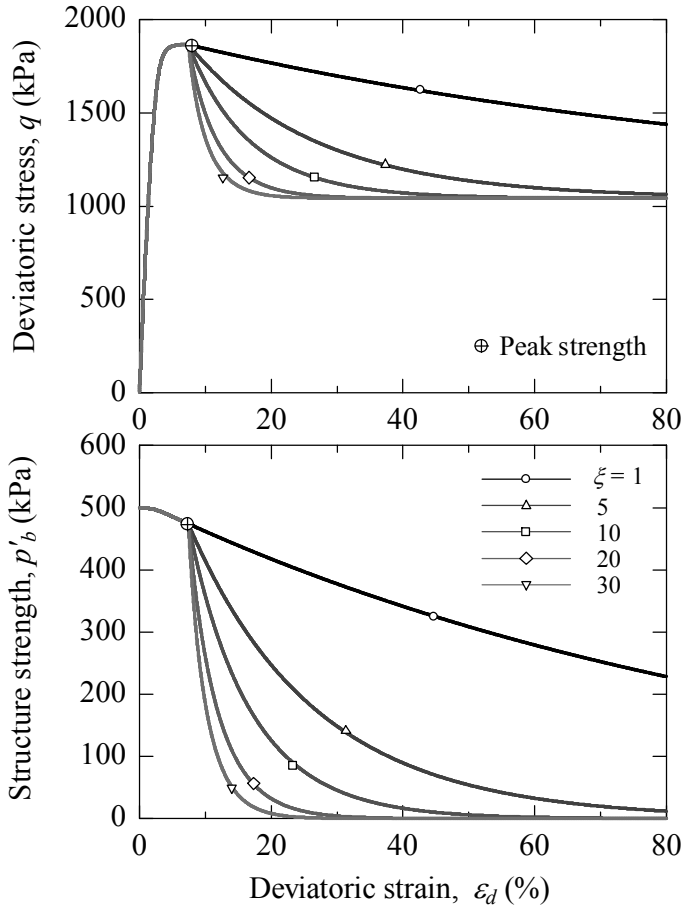

Figure 3.6 Parametric study on the parameter ξ

Table 3.1 Parameters of the MSCC model for parametric study

Model Parameters	Values	Physical meaning
λ^*	0.16	Gradient of intrinsic compression in the e-ln p' plane
κ	0.001	Current Gradient of unloding-reloading line in e-ln p' plane
e^*_{IC}	2.86	Voids ratio at reference stress (p' = 1 kPa) of intrinsic compression line
b	0.3	Destructured index due to volumetric deformation
Δe_i	0.75	Additional void ratio at the start of virgin yielding
M	1.10	Gradient of critical state ratio in the $q - p'$ plane
p'_{b0}	500	Initial of bonding strength in the $q - p'$ plane (kPa)
$p'_{y,i}$	600	Initial yield stress of isotropic compression line of cemented soil (kPa)
ψ	0.1-0.99	Parameter define the shape of plastic potential
ξ	1-30	Destructured index due to shear deformation
G'	30,000	Shear modulus in terms of effective stress (kPa)
σ'_c	600	Confining pressure (kPa)

3.3 Application and verification of the MSCC model

In this section, the MSCC model is employed to simulate the compression and shear behaviour of naturally and artificially structured clays. The capability of the MSCC model is evaluated based on comparisons between model simulations and experimental data. The following clays are evaluated: a destructured clay (Ariake clay), two naturally structured clays (Osaka and Marl clays) and two artificially structured clays (cemented Ariake and Bangkok clays). Some basic and engineering properties of the natural Osaka and Marl clays and of the destructured Ariake and Bangkok clays are presented in Table 3.2.

Table 3.2 Physical properties of the simulated clays

Properties	Osaka clay	Marl clay	Ariake clay	Bangkok clay
Reference	Adachi et al. (1995)	Anagnostopoulos et al. (1991)	Horpibulsuk et al. (2004b)	Uddin (1995)
Specific density	2.67-2.70	2.72	2.70	2.67-2.69
Natural water content	65-72%	20-21%	135-150%	81.60-86.00
Liquid limit	69.2-75.1%	24-38%	120%*	103%**
Plasticity index	41.9-50.6%	2.5-12%	63%	60%
Liquidity	0.75-1.13	-	1.24-1.47	0.62
Sensitivity	14.5	-	-	7.3
Activity	0.54	0.75-1.25[b]	-	0.87
Clay fraction	44%[a]	13-24%	55%	69%
Silt fraction	49%	75-87%	44%	28%
Sand fraction	7%	< 12%	1%	3%
Confining pressure	20-235 kPa	98-4,000 kPa	50-4,000 kPa	50-600 kPa
In-situ voids ratio	1.67-1.92	0.55-0.60	3.65-4.05	2.20-2.44
Strain rate of shearing (mm/min)	0.0061-0.00632[c]	0.009[c,d]	0.0075[c], 0.0025[d]	0.009[c], 0.0018[d]
Sample type	Intact	Intact	Cemented	Cemented

Remarks: [a] Less than 2μ m, [b] Clay-sized fraction, [c] Undrained test, [d] Drained test,
* Water content = 180% before mixed with cement and
** Water content = 120% before mixed with cement

The model parameter values are listed in Tables 3.3 and 3.4 for the naturally and artificially structured clays, respectively. Parameters e^*_{IC}, λ^*, κ, $p'_{y,i}$, b and Δe_i were determined from the results of isotropic compression test and G' was approximated from the $q-\varepsilon_d$ curve. The parameters denoted by an asterisk were tested from a remoulded sample (Burland, 1990). In the absence of the ICL, parameters e^*_{IC} and λ^* can be approximated from the intrinsic state line in terms of the liquid limit voids ratio (Nagaraj et al., 1998), which was achieved by Horpibulsuk et al. (2010). The values of the strength parameters M and p'_{b0} were obtained by plotting the peak strength in the $q-p'$ plane. The value for ψ was estimated from the simulation of anisotropic compression test results of structured clay with different η values. The parameter ψ is determined as shown in Figure 3.7 for the artificially

structured Bangkok clay. In the absence of the anisotropic compression test results, ψ can be estimated from the stress-strain relationship. It is found that the ψ value decreases with the degree of cementation. The ψ -value is close to 2.0 for the naturally structured clays as shown in Table 3.3. It is 2.0 for Osaka and 1.5 for Marl clays. Because ξ is a parameter that reflects the rate of strain softening, it is estimated from the stress-strain relationship at post-failure.

Table 3.3 MSCC model parameters for the naturally structured clays

Model Parameters	**Naturally structured clays**	
	Osaka	**Marl**
λ^*	0.147	0.025
κ	0.027	0.009
e^*_{IC}	1.92	0.67
b	0.6	0.7
Δe_i	0.62	0.085
M	1.15	1.30
p'_{b0} (kPa)	30	300
$p'_{y,i}$ (kPa)	100	4,150
G' (kPa)	3,000	45,000
ξ	1	1
ψ	2	1.5

Table 3.4 MSCC model parameters for the artificially structured clays

Model Parameters	Ariake Clay				Bangkok Clay		
	A_w=0%	A_w=6%	A_w=9%	A_w=18%	A_w=5%	A_w=10%	A_w=15%
λ^*	0.44	0.44	0.44	0.44	0.26	0.26	0.26
κ	0.08	0.06	0.024	0.001	0.02	0.01	0.005
e^*_{IC}	4.37	4.37	4.37	4.37	2.86	2.86	2.86
b	-	0.15	0.01	0.001	0.02	0.01	0.01
Δe_i	-	1.50	2.25	2.65	0.55	0.60	0.75
M	1.58	1.60	1.45	1.35	1.13	1.13	1.13
p'_{b0} (kPa)	-	50	100	650	60	400	500
$p'_{y,i}$ (kPa)	-	50	200	1,800	150	430	600
G' (kPa)	4,000	6,000	8,000	40,000	14,000	16,000	30,000
ξ	-	10	10	30	10	30	30
ψ	2.0	1.8	0.5	0.1	1.5	0.2	0.1

Table 3.5 MCC model parameters for the natural Osaka and cemented Ariake clays

Model Parameters	Natural Osaka Clay	Cemented Ariake Clay (A_w=9%)
λ^*	0.147	0.44
κ^*	0.027	0.024
e^*_{IC}	1.92	4.37
M	1.15	1.45
p'_c (kPa)	100	200
G' (kPa)	3,000	8,000

Table 3.6 SCC model parameters for the natural Osaka and cemented Ariake clays

Model Parameters	Natural Osaka Clay	Cemented Ariake Clay (A_w=9%)
λ^*	0.147	0.44
κ	0.027	0.024
e^*_{IC}	1.92	4.37
b	0.6	0.01
Δe_i	0.62	2.25
M	1.15	1.45
$p'_{y,i}$ (kPa)	100	200
G' (kPa)	3,000	8,000
ψ	2.0	0.5

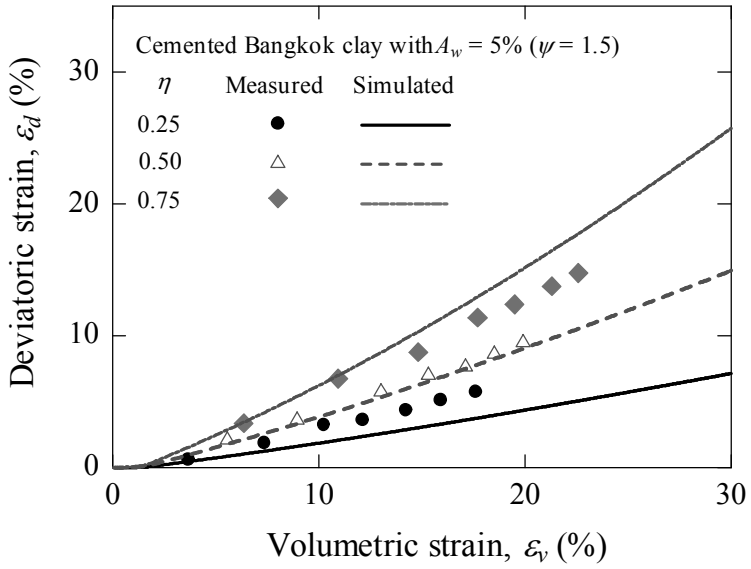

Figure 3.7 Determination of the ψ for artificially structured Bangkok clay (data from Uddin, 1995)

Based on the parameters presented in Tables 3.3 and 3.4, the isotropic compression behaviours of all four structured clays were simulated and compared with experimental data as shown in Figure 3.8. The compression behaviour of both naturally structured and artificially structured clays are well represented.

A comparison of the model simulations and experimental data for isotropically consolidated undrained triaxial (CIU) tests on Osaka clay is shown in Figure 3.9. A comparison of the model simulations and experimental data for isotropically consolidated drained triaxial (CID) tests on Marl clay is shown in Figure 3.10. Unlike a completely destructured clay, natural Osaka clay shows strain softening in the ($q - \varepsilon_d$) relationship in both normally consolidated states and overconsolidated states. This type of behaviour is frequently found in naturally structured soils (Burland, 1990; Carter and Liu, 2005) and has been captured satisfactorily by the MSCC model. The

model simulations and experimental data for the two sets of tests on natural soils are in very good agreement.

The capacity of the MSCC model to describe the influence of cementation is verified by simulating both undrained and drained shear behaviour of artificially structured Ariake clay and Bangkok clay under different pre-shear consolidated pressures and cement contents. Comparisons between the test data and model simulations are shown in Figures 3.11 through 3.15 for the destructured and artificially structured Ariake clay, and in Figures 3.16 and 3.17 for the artificially structured Bangkok clay. It is interesting to note that the same destructured parameters can be used to simulate the shear behaviour of clay in destructured and structured states.

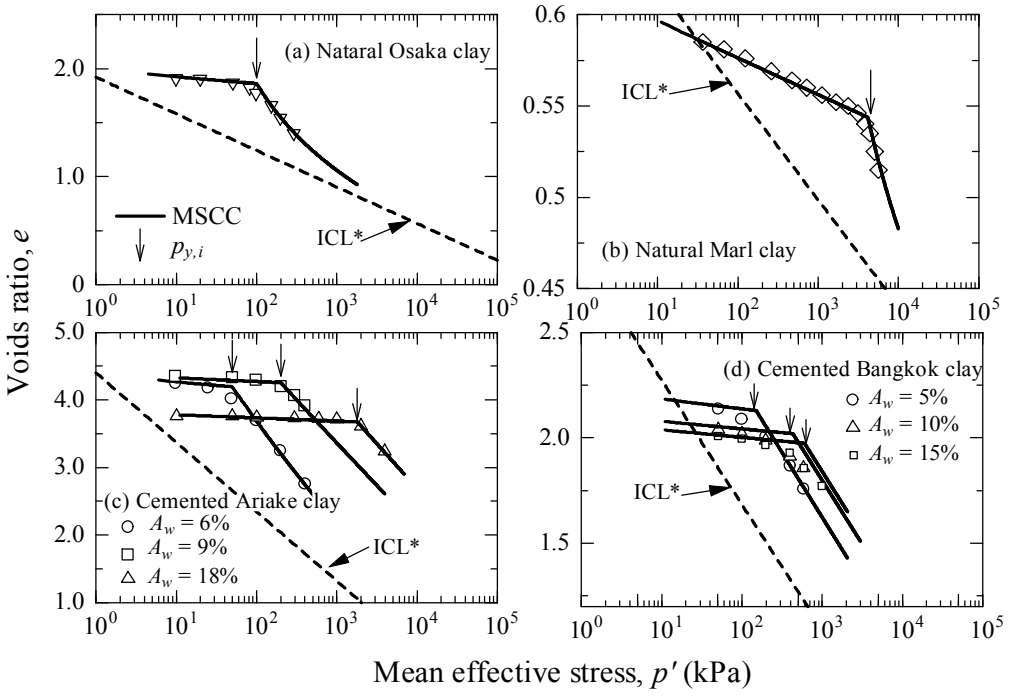

Figure 3.8 Simulation of isotropic compression curves of studied structured clays

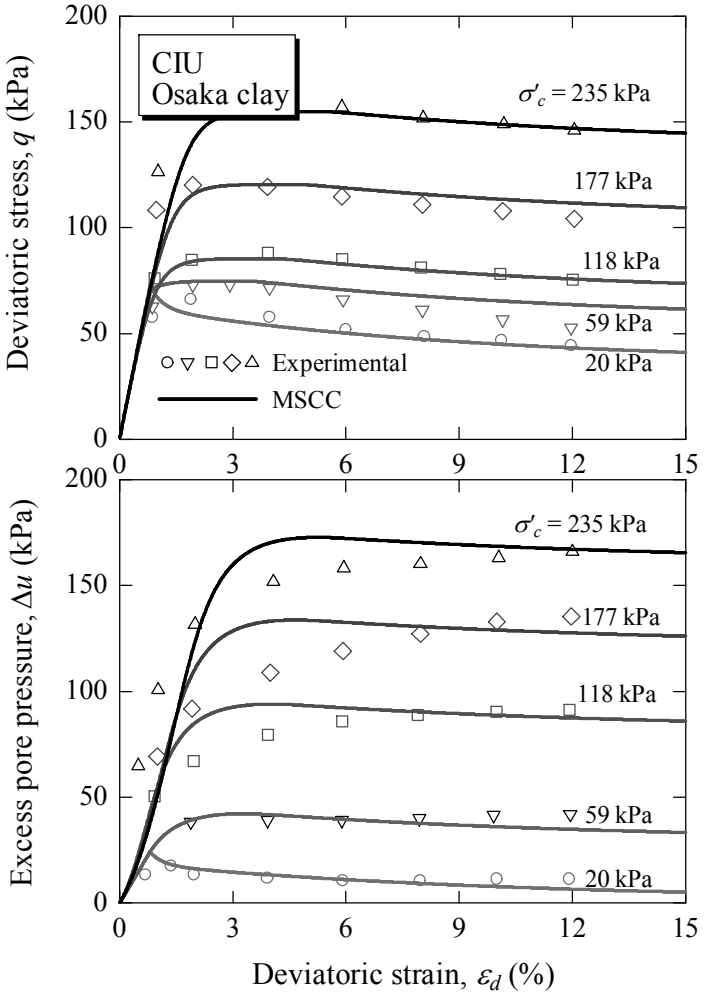

Figure 3.9 Comparison of experimental and simulated CIU test results of natural Osaka clay

The critical state (very large strain) of the structured clay cannot be measured due to the limitation of the triaxial apparatus. For the simulation, this state can however be presented where the structure strength (p'_b) is completely removed. Overall, the general patterns of the behaviour of artificially structured clays, i.e., the increase in stiffness and peak strength with cementation and the rapidness of the reduction in deviatoric stress during strain softening, have been captured. The model

simulations cover a wide range of cement contents (from 0 to 18% by weight) and a wide range of pre-shear consolidated pressures (50 kPa to 3,000 kPa) and are made with the model parameter values that are determined based on their physical meanings.

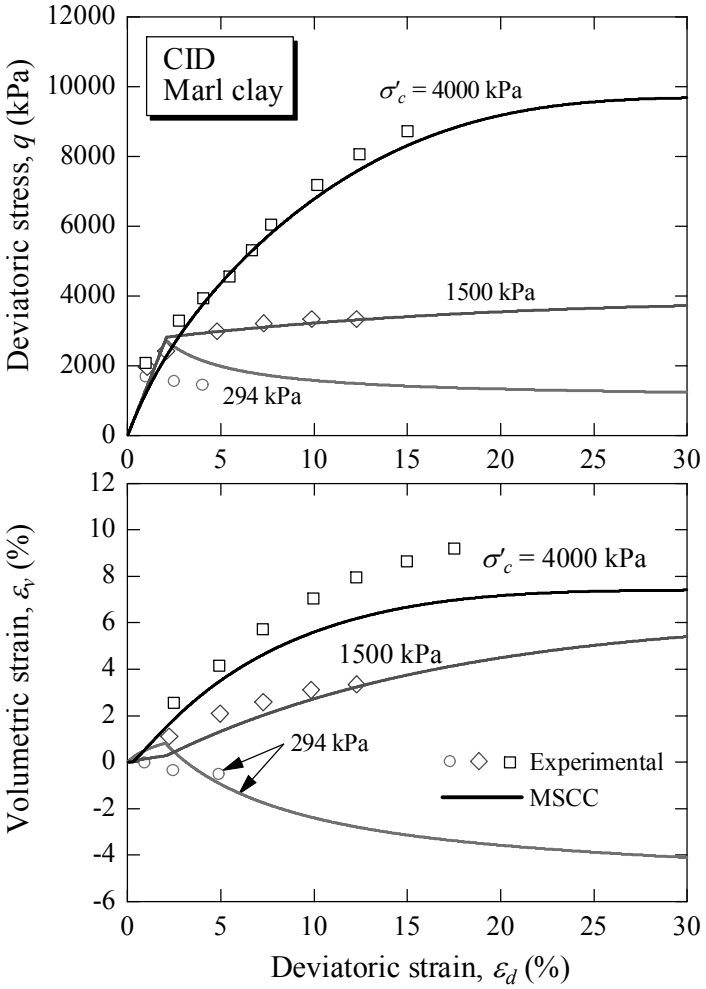

Figure 3.10 Comparison of experimental and simulated on CID test results of natural Marl clay

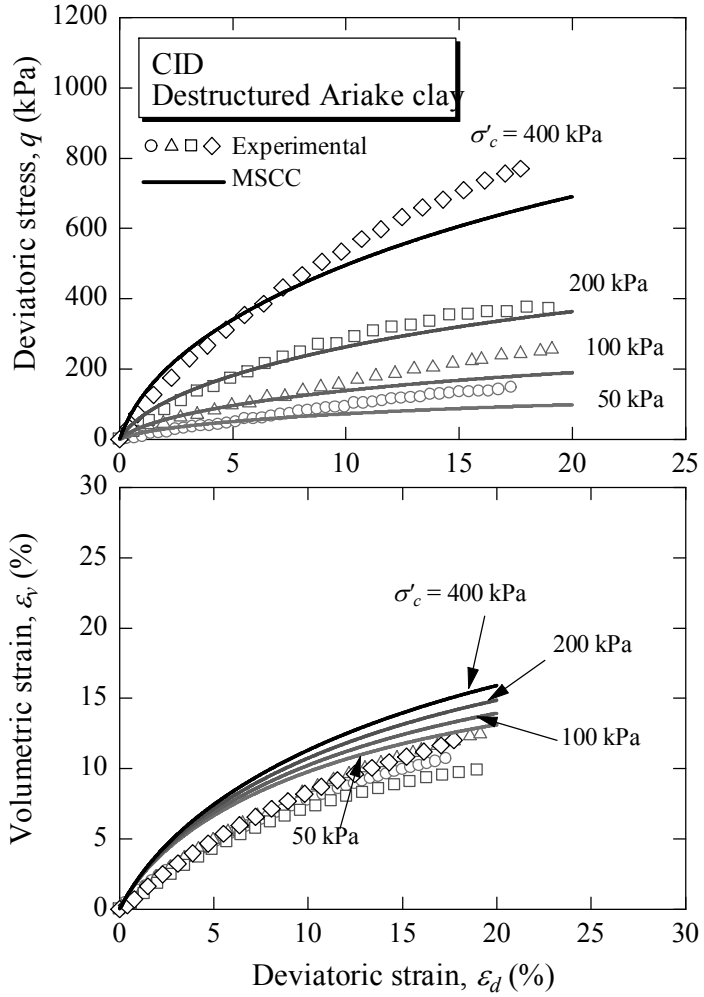

Figure 3.11 Comparison of experimental and simulated CID test results of destructured Ariake clay

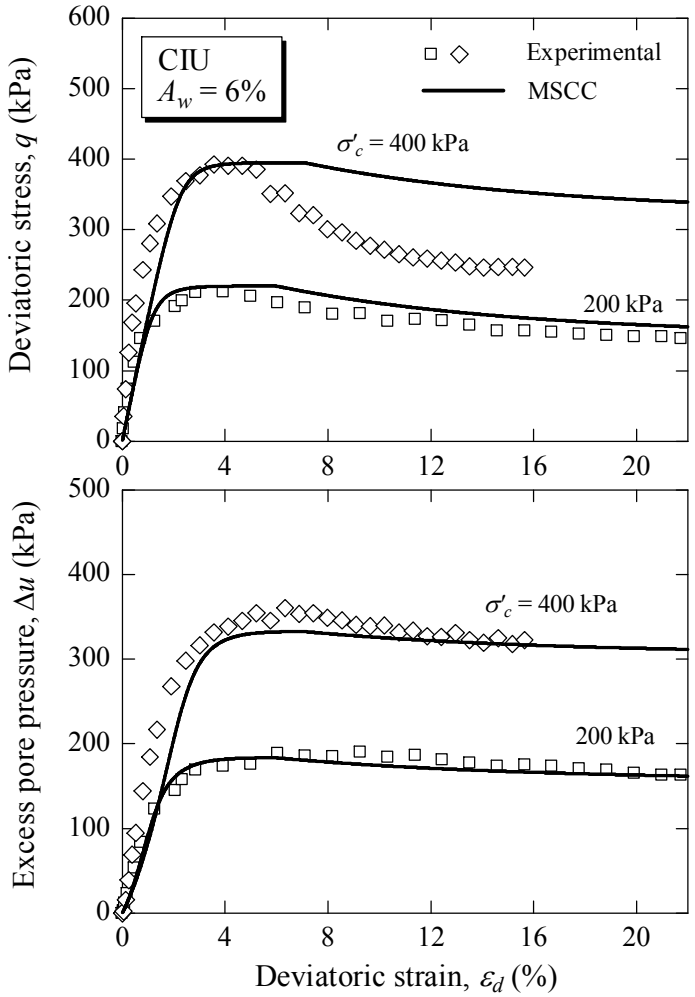

Figure 3.12 Comparison of experimental and simulated CIU test results of 6% cement Ariake clay

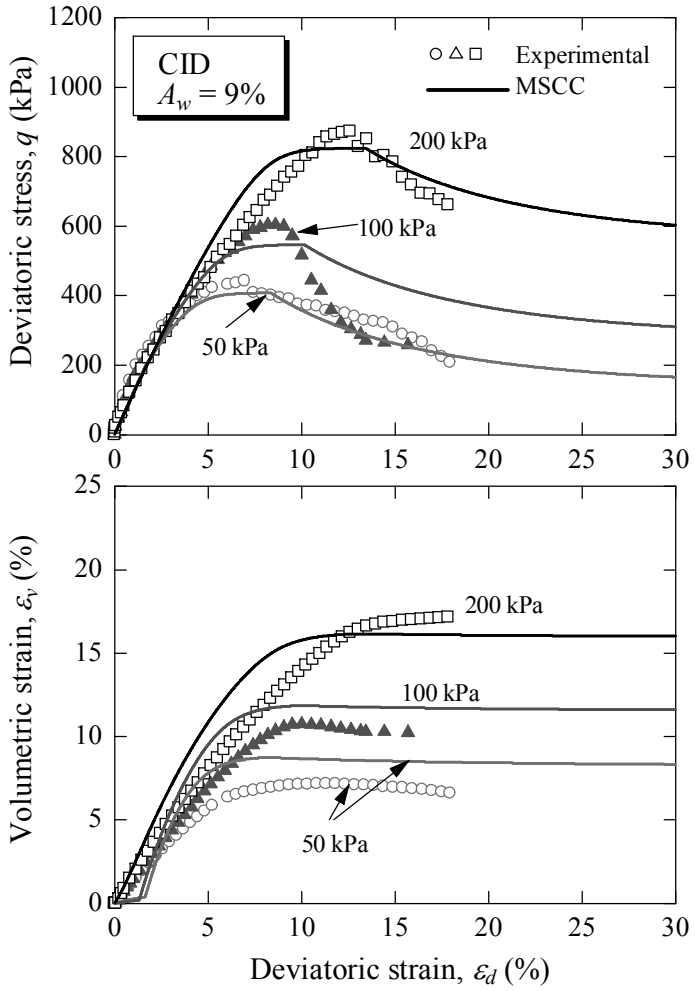

Figure 3.13 Comparison of experimental and simulated CID test results of 9% cement Ariake clay

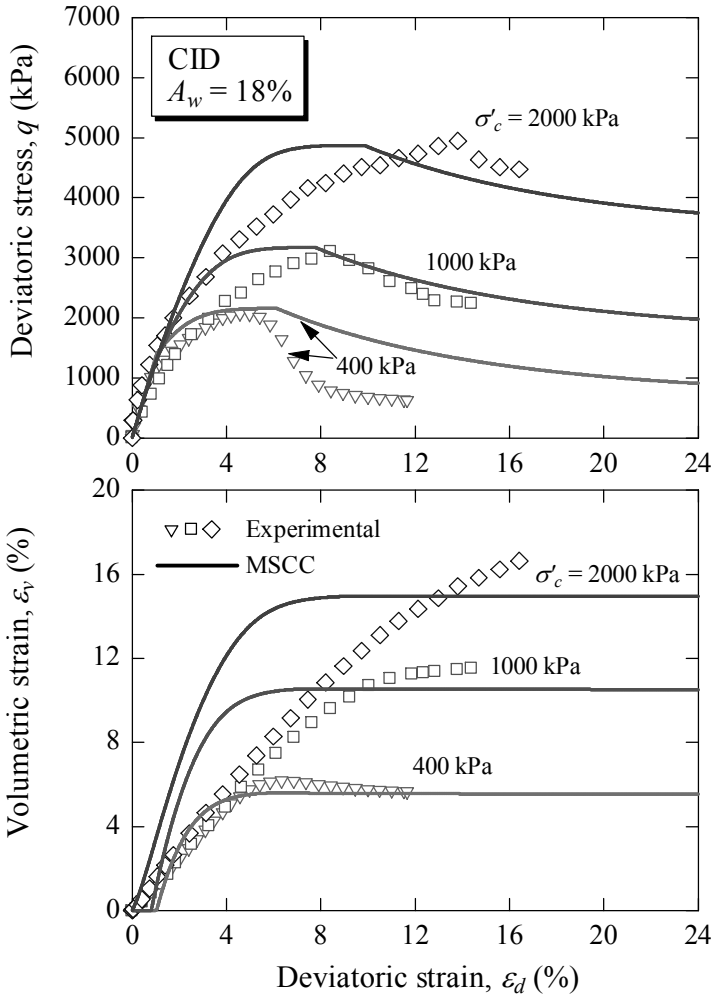

Figure 3.14 Comparison of experimental and simulated CID test results of 18% cement Ariake clay

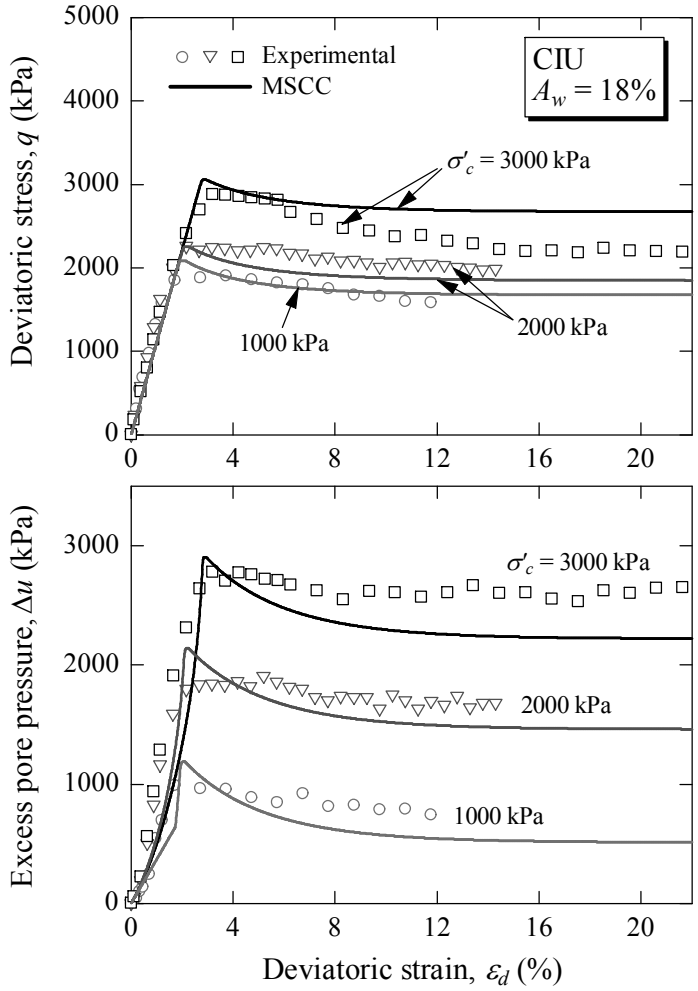

Figure 3.15 Comparison of experimental and simulated CIU test results of 18% cement Ariake clay

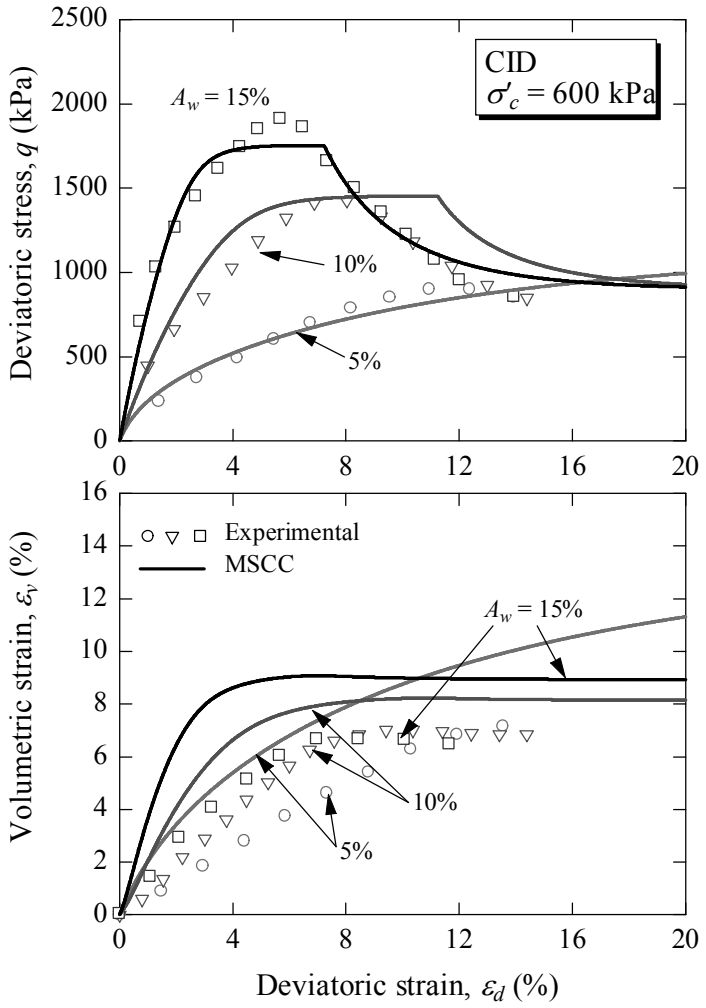

Figure 3.16 Comparison of experimental and simulated CID test results of cemented Bangkok clay under σ'_3 = 600 kPa ($\sigma'_3 > p'_y$) for A_w = 5 to 15%

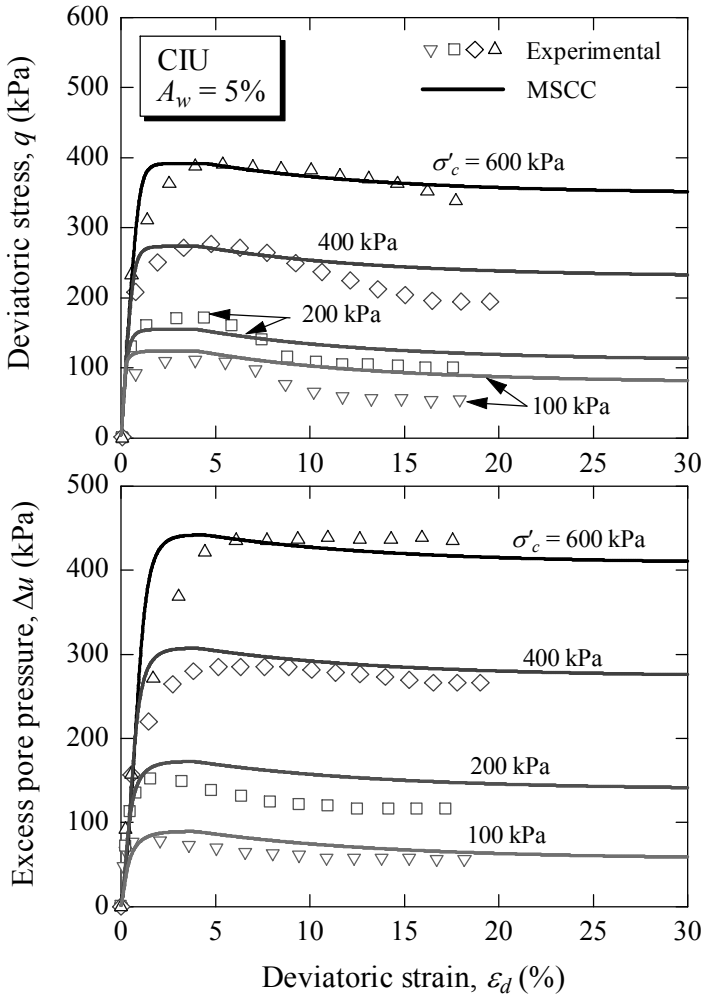

Figure 3.17 Comparison of experimental and simulated CIU test results of 5% cement Bangkok clay

3.4 Discussions

Based on the modified effective stress concept, yield function, hardening rule and the plastic potential proposed, the methodology for simulating the stress-strain behaviour of structured clay is simpler and provides better quantitative and qualitative performance than the MCC model and the original SCC model. As seen in the comparisons of the simulations shown in Figures 3.18 and 3.19, the performance of

the MSCC model is significantly better than that of the SCC and MCC models. It is found that the destructuring law proposed in terms of plastic deviatoric strain provides a reasonably good simulation. The values of model parameters for the MCC and the SCC are given in Tables 3.5 and 3.6, respectively.

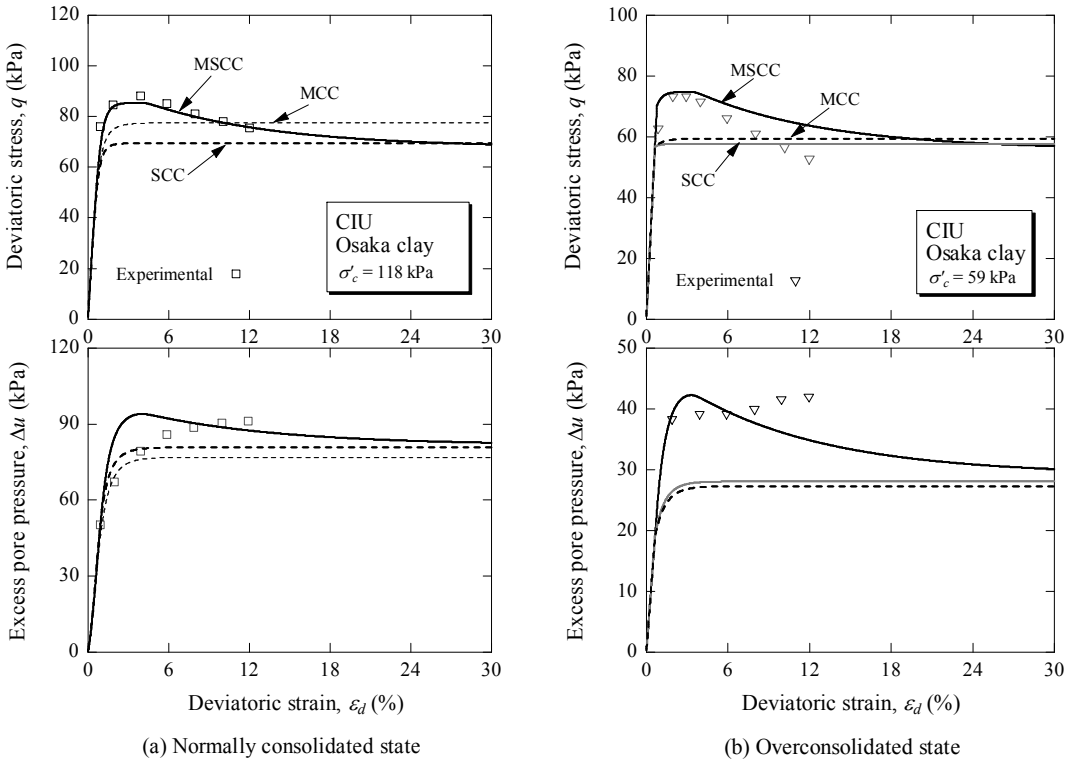

Figure 3.18 Comparisons of experimental and simulated on CIU test results of natural Osaka clay for different models

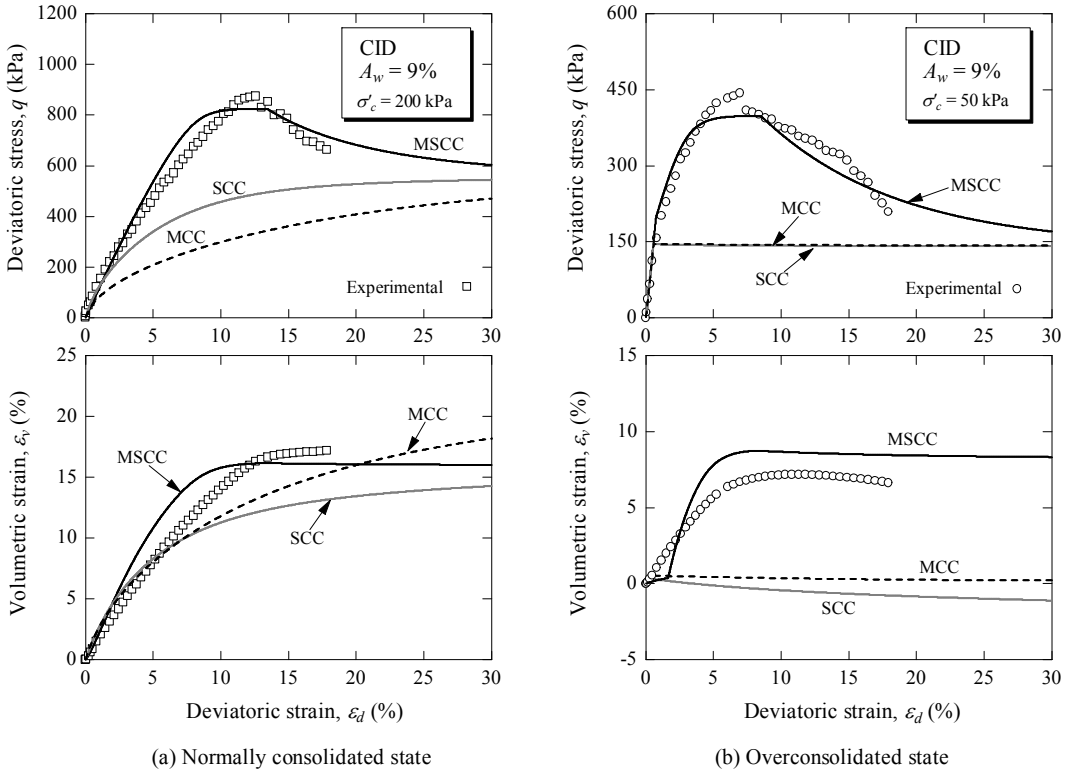

(a) Normally consolidated state (b) Overconsolidated state

Figure 3.19 Comparisons of experimental and simulated on CID test results of cemented Ariake clay for different models

This model can be simply implemented into a numerical analysis. The MSCC model is identical to the MCC model when clay is in a destructured state, i.e., $\Delta e = 0$ and $p'_b = 0$. A study of the microstructure of some structured clays has shown that some elements of structure remain in the clay even at very large strains or a destructured state (e.g., Cotecchia and Chandler, 1998; Fearon and Coop, 2000). The MSCC model also follows this premise. Even though the critical state lines in the $q - p'$ plane are the same for destructured and structured states, the critical state lines in $e - \ln p'$ plane are not the same.

In the MSCC model, the structured soil is treated as an isotropic elastic-virgin yielding material. The two mechanisms are separated by the current yield surface. The soil shows purely elastic behaviour when the stress state is inside the yield surface. When the stress state reaches the yield surface, the plastic behaviour occurs. At this point, there is a sharp change in the stiffness of the soil response, as shown in the simulated results. Further development to obtain more precise simulation can be easily attained by implementing a hardening equation during subloading into the model. The implementation of a simple and predictive hardening equation in the original SCC model has been successfully achieved for natural clay by Suebsuk et al. (2008). However, the MSCC model is extended in Chapter IV to represent the subyielding behaviour by incorporating with the bounding surface theory.

It is seen from the shearing test results that there is some discrepancy between the model simulations and the experimental data in the volumetric deformation (e.g., Figures 3.13, 3.14 and 3.16). This discrepancy may be inherited from the Modified Cam Clay model, which does not accurately simulate the behavior of destructured Ariake clay (Figure 3.11). Further study on this topic is needed, perhaps with considering the influence of anisotropy. Some frontier research accounting for the influence of anisotropy has been reported in works by Rouainia and Muir Wood (2000), Wheeler et al. (2003), Dafalias et al. (2006) and Taiebat et al. (2009). If the influence of anisotropy on the yield loci is considered, the destructuring law should be extended to include the reduction of anisotropy and isotropy during the destructuring process.

The MSCC model is developed based on the simple predictive SCC model with the purpose to solve some practical geotechnical problems. Although the model

has 11 parameters, 6 parameters are the same as those used in the MCC model to describe the basic mechanical properties of soil. The other parameters can be determined or estimated relatively conveniently from conventional laboratory tests on structured clay specimens. For practical use, the application of MSCC model in a numerical analysis for solving geotechnical boundary value problems is presented in Chapter V. Recently, some important works in numerical analysis with constitutive models for structured soils such as those by Zhao et al. (2005), Karstunen et al. (2005) and Liyanapathirana et al. (2009) have been published.

3.5 Conclusions

In this study, the MSCC model is developed by extending the simple predictive SCC model. In the MSCC model, the destructuring law due to shearing is proposed to describe the effect of degradation and crushing of the soil-cementation structure on the reduction in p_b'. Destructuring begins when the stress state is on the virgin yielding. p_b' gradually decreases due to the degradation of the structure until the failure state. It rapidly decreases when the stress state reaches the failure state and is completed removed at the critical state due to the crushing of the soil-cementation structure. The effect of structure and destructuring is incorporated into the effective stress concept, yield function, hardening rule and plastic potential to describe the mechanical behaviour of structured clay during strain hardening and softening. The methodology of modelling the shear behaviour of structured clay is simple, as in other models of the Cam Clay family.

Simulations were performed using the MSCC model for different clays with both natural and artificial structures under different pre-shear consolidated pressures,

drainage conditions and cement contents, and these simulations were compared with experimental data. Overall, a reasonable description of the influence of various types of soil structures on soil behaviour has been achieved. It is seen that the MSCC model has unified the clay behaviour in destructured, naturally structured and artificially structured states into one consistent theoretical framework. Because the MSCC model is simple and the model parameters can be determined from conventional laboratory tests, the model has the potential to solve geotechnical engineering problems involving various types of structured soils.

3.6 References

Adachi, T., Oka, F., Hirata, T., Hashimoto, T., Nagaya, J., Mimura, M., and Pradhan, T. B. S. (1995). Stress-strain behavior and yielding characteristics of eastern Osaka clay. **Soils and Foundations**. 35(3): 1-13.

Anagnostopoulos, A. G., Kalteziotis, N., and Tsiambaos, G. K. (1991). Geotechnical properties of the Carinth Canal marls. **Geotechnical and Geological Engineering**. 9: 1-26.

Atkinson, J. H., and Bransby, P. L. (1978). **The mechanics of soils. An introduction to critical state soil mechanics**. McGraw-Hill.

Baudet, B., and Stallebrass, S. (2004). A constitutive model for structured clays. **Geotechnique**. 54(4): 269-278.

Burland, J. B. (1990). On the compressibility and shear strength of natural soils. **Geotechnique**. 40(3): 329–378.

Callisto, L., and Rampello, S. (2004). An interpretation of structural degradation for three natural clays. **Canadian Geotechnical Journal**. 41: 392-407.

Carter, J. P., and Liu, M. D. (2005). Review of the Structure Cam Clay model. Soil Constitutive models: evaluation, selection, and calibration. **ASCE, Geotechnical special publication**. 128: 99-132.

Chai, J. C., Miura, N., and Zhu, H. H. (2004). Compression and consolidation characteristics of structured natural clays. **Canadian Geotechnical Journal**. 41(6): 1250-1258.

Clough, G. W., Sitar, N., Bachus, R. C., and Rad, N. S. (1981). Cemented sands under static loading. **Journal of Geotechnical Engineering, ASCE**. 107(GT6): 799-817.

Cotecchia, F. (2003). Mechanical behaviour of the stiff clays from the Montemesola Basin in relation to their geological history and structure. **Proceedings of the international conference on the characterization and engineering properties of natural soils** (pp. 817-850), Lisse.

Cotecchia, F., and Chandler, R. J. (1998). One-dimentional compression of a natural clay: structural changes and mechanical effects. **The geotechnics of hard soils-soft rocks**. A. Evangelista and L. Picarelli, eds. Rotterdam: Balkema. 103-113.

Cotecchia, F., and Chandler, R. J. (2000). A general framework for the mechanical behaviour of clays. **Geotechnique**. 50(4): 431-447.

Dafalias, Y. F., Manzari, M. T., and Papadimitriou, A. G. (2006). SANICLAY: simple anisotropic clay plasticity model. **International Journal for Numerical and Analytical Methods in Geomechanics**. 30(12): 1231-1257.

Fearon, R. E., and Coop, M. R. (2000). Reconstitution: what makes an appropriate reference material? **Geotechnique**. 50(4): 314-333.

Gens, A., and Nova, R. (1993). Conceptual bases for constitutive model for bonded soil and weak rocks. **Geotechnical Engineering of Hard Soil-Soft Rocks**: Balkema.

Hanzawa, H., and Adachi, K. (1983). Overconsolidation of alluvial clays. **Soils and Foundations**. 23(4): 106-118.

Horpibulsuk, S. (2001). Analysis and Assessment of Engineering Behavior of Cement Stabilized Clays. **Ph.D. dissertation**, Saga University, Saga, Japan.

Horpibulsuk, S., Bergado, D. T., and Lorenzo, G. A. (2004a). Compressibility of cement admixed clays at high water content. **Geotechnique**. 54(2): 151-154.

Horpibulsuk, S., Liu, M. D., Liyanapathirana, D. S., and Suebsuk, J. (2010). Behaviour of cemented clay simulated via the theoretical framework of Structured Cam Clay model. **Computers and Geotechnics**. 37(1-2): 1-9.

Horpibulsuk, S., Miura, N., and Bergado, D. T. (2004b). Undrained shear behaviour of cement admixed clay at high water content. **Journal of Geotechnical and Geoenvironmental Engineering, ASCE**. 130(10): 1096-1105.

Horpibulsuk, S., Miura, N., and Nagaraj, T. S. (2005). Clay-water/cement ratio identity of cement admixed soft clay. **Journal of Geotechnical and Geoenvironmental Engineering, ASCE**. 131(2): 187-192.

Horpibulsuk, S., Shibuya, S., Fuenkajorn, K., and Katkan, W. (2007). Assessment of engineering properties of Bangkok clay. **Canadian Geotechnical Journal**. 44(2): 173-187.

Huang, J. T., and Airey, D. W. (1998). Properties of an artificially cemented carbonate sand. **Journal of Geotechnical and Geoenvironmental Engineering, ASCE**. 124(6): 492-499.

Ismail, M. A., Joer, H. A., Randolph, M. F., and Sin, W. H. (2002). Effect of cement type on shear behaviour of cemented calcareous soil. **Journal of Geotechnical Engineering, ASCE**. 128(6): 520-529.

Karstunen, M., Krenn, H., Wheeler, S. J., Koskinen, M., and Zentar, R. (2005). The effect of anisotropy and destructuring on the behaviour of Murro test embankment. **International Journal of Geomechanics, ASCE**. 5(2): 87-97.

Kasama, K., Ochiai, H., and Yasufuku, N. (2000). On the stress-strain behaviour of lightly cemented clay based on an extended critical state concept. **Soils and Foundations**. 40(5): 37-47.

Kavvadas, M., and Amorosi, A. (2000). A constitutive model for structured soils. **Geotechnique**. 50(3): 263-273.

Khalili, N., and Liu, M. D. (2008). On generalization of constitutive models from two dimensions to three dimensions. **International Journal for Numerical and Analytical Methods in Geomechanics**. 32: 2045-2065.

Kimoto, S., and Oka, F. (2005). An elasto-viscoplastic model for clay considering destructuralization and consolidation analysis of unstable behaviour. **Soils and Foundations**. 45(2): 29-43.

Lee, K., Chan, D., and Lam, K. (2004). Constitutive model for cement treated clay in a critical state framework. **Soils and Foundations**. 44(3): 69-77.

Leonard, G. A. (1972). Discussion of 'Shallow foundation'. **Proceedings of ASCE Spec. Conf. on Perf. of Earth and Earth supported Struct., ASCE** (pp. 169-173), New York.

Leroueil, S., Tavenas, F., Brucy, F., La Rochelle, P., and Roy, M. (1979). Behavior of destructured natural clays. **Journal of Geotechnical Engineering, ASCE**. 105(6): 759-778.

Leroueil, S., Tavenas, F., Samson, L., and Morin, P. (1983). Preconsolidation pressure of Champlain clay Part II: Laboratory determination. **Canadian Geotechnical Journal**. 20(4): 803-816.

Leroueil, S., and Vaughan, P. R. (1990). The general and congruent effects of structure in natural soils and week rock. **Geotechnique**. 40: 467-488.

Liu, M. D., and Carter, J. P. (1999). Virgin compression of structured soils. **Geotechnique**. 49(1): 43–57.

Liu, M. D., and Carter, J. P. (2000a). Modeling the destructuring of soils during virgin compression. **Geotechnique**. 50(4): 479–483.

Liu, M. D., and Carter, J. P. (2000b). On the volumetric deformation of reconstituted soils. **International Journal for Numerical and Analytical Methods in Geomechanics**. 24(2): 101–133.

Liu, M. D., and Carter, J. P. (2002). A structured Cam Clay model. **Canadian Geotechnical Journal**. 39: 1313–1332.

Liu, M. D., and Carter, J. P. (2003). Volumetric deformation of natural clays. **International Journal of Geomechanics, ASCE**. 3(2): 236-252.

Liyanapathirana, D. S., Carter, J. P., and Airey, D. W. (2009). Drained bearing response of shallow foundations on structured soils. **Computers and Geotechnics**. 36: 493-502.

Locat, J., and Lefebvre, G. (1985). The compressibility and sensitivity of an artificially sedimented clay soil: the Grande-Baleine marine clay. **Quebec. Marine Geotechnology**. 6(1): 1-27.

McDowell, G. R. (2000). A family of yield loci based on micro mechanics. **Soils and Foundations**. 40(6): 133-137.

McDowell, G. R., and Hau, K. W. (2003). A simple non-associated three surface kinematic hardening model. **Geotechnique**. 53(4): 433-437.

Mitchell, J. K. (1986). Practical problems from surprising soil behavior. **Journal of Geotechnical Engineering, ASCE**. 112(3): 259-289.

Mitchell, J. K. (1996). **Fundamentals of Soil Behavior**. New York: John Willey & Sons Inc.

Miura, N., Horpibulsuk, S., and Nagaraj, T. S. (2001). Engineering behavior of Cement stabilized clays. **Soils and Foundations**. 41(5): 33-45.

Muir Wood, D. (1990). **Soil Behaviour and Critical State Soil Mechanics**. Cambridge, UK: Cambridge University Press.

Nagaraj, T. S., and Miura, N. (2001). **Soft Clay Behaviour – Analysis and Assessment**. Netherlands: A.A.Balkema.

Nagaraj, T. S., Pandian, N. S., and Narasimha Raju, P. S. R. (1998). Compressibility behavior of soft cemented soils. **Geotechnique**. 48(2): 281-287.

Roscoe, K. H., Schofield, A. N., and Wroth, C. P. (1958). On the yielding of soils. **Geotechnique**. 8: 22-53.

Rotta, G. V., Consoli, N. C., Prietto, P. D. M., Coop, M. R., and Graham, J. (2003). Isotropic yielding in an artificially cemented soil cured under stress. **Geotechnique**. 53(5): 493-501.

Rouainia, M., and Muir Wood, D. (2000). A kinematic hardening constitutive model for natural clays with loss of structure. **Geotechnique**. 50(2): 153-164.

Schmertmann, J. H. (1991). The mechanical aging of soils. **Journal of Geotechnical Engineering, ASCE**. 119(9): 1288-1330.

Sheng, D., Sloan, S. W., and Yu, H. S. (2000). Aspects of finite element implementation of critical state models. **Computational Mechanics**. 26(2): 185-196.

Shibuya, S. (2000). Assessing structure of aged natural sedimentary clays. **Soils and Foundations**. 40(3): 1-16.

Suebsuk, J., Horpibulsuk, S., and Liu, M. D. (2008). Modeling the volumetric deformation of naturally structured clays during subyielding. **Proceedings of The 12th International Conference of International Association for Computer Methods and Advances in Geomechanics (IACMAG)** (pp. 883-890), GOA, India.

Taiebat, M., Dafalias, Y. F., and Peek, P. (2009). A destructuration theory and its application to SANICLAY model. **International Journal for Numerical and Analytical Methods in Geomechanics**. 34(10): 1009-1040.

Uddin, K. (1995). Strength and Deformation Behavior of Cement–Treated Bangkok Clay. **D.Eng. Thesis**, Asian Institute of Technology, Bangkok, Thailand.

Vatsala, A., Nora, R., and Srinivasa Murthy, B. R. (2001). Elastoplastic model for cemented soils. **Journal of Geotechnical and Geoenvironmental Engineering, ASCE**. 127(8): 678-687.

Wheeler, S. J., Näätänen, A., Karstunen, M., and Lojander, M. (2003). An anisotropic elasto-plastic model for soft clays. **Canadian Geotechnical Journal**. 40(2): 403-418.

Wissa, A. E. Z., Ladd, C. C., and Lambe, T. W. (1965). Effective stress strength parameters of stabilized soils. **Proceedings of 6th International Conference on Soil Mechanics and Foundation Engineering** (pp. 412-416).

Zhao, J., Sheng, D., Rouainia, M., and Sloan, S. W. (2005). Explicit stress integration of complex soil models. **International Journal for Numerical and Analytical Methods in Geomechanics**. 29: 1209-1229.

CHAPTER IV

A CRITICAL STATE MODEL FOR STRUCTURED CLAYS IN OVERCONSOLIDATED STATE

4.1 Introduction

Reconstituted clay behaviour has been studied for the last four decades. The critical state theory is one of the major developments of the constitutive model for clays. The models of the Cam Clay family such as the Cam Clay (CC) model (Roscoe and Schofield, 1963) and the Modified Cam Clay (MCC) model (Roscoe and Burland, 1968) are used widely to describe clay behaviour in the reconstituted state. The models give good agreement between experimental and model simulation results. However, recent studies (Leroueil et al., 1979; Burland, 1990; Leroueil and Vaughan, 1990; Cotecchia and Chandler, 1997; Cotecchia and Chandler, 2000; Shibuya, 2000; Horpibulsuk et al., 2007) have shown that natural clay is structured, and its behaviour is different than its behaviour in the reconstituted state. Cement stabilised clay is also identified as artificially structured clay (Miura et al., 2001; Horpibulsuk et al., 2004a; Horpibulsuk et al., 2004b). The critical state theory, which is widely accepted for simulating clay behaviour (Schofield and Wroth, 1968; Muir Wood, 1990), has been extended to simulate structured clay behaviour by considering the effect of soil structure (Gens and Nova, 1993; Kasama et al., 2000; Kavvadas and Amorosi, 2000; Rouainia and Muir Wood, 2000; Liu and Carter, 2002; Baudet and Stallebrass, 2004; Lee et al., 2004). Taiebat et al. (2009) have proposed a model taking into account the

effect of destructuring and anisotropy on the stress-strain response. The Structured Cam Clay (SCC) model (Liu and Carter, 2002) is a simple and predictive critical state model for structured clays. It was formulated simply by introducing the influences of soil structure on the volumetric deformation and the plastic deviatoric strain into the MCC model. A key assumption of the SCC model is that both the hardening rule and destructuring of structured clay are dependent on plastic volumetric deformation. A simple elliptical yield surface with a non-associated flow rule is used for predicting the behaviour of clays in naturally structured states. The SCC model successfully captures many important features (particularly volumetric hardening/destructuring) of the naturally structured clay behaviour with insignificant cohesion.

However, the cohesion and strain softening, which are generally very significant for naturally structured stiff clays (Burland, 1990; Leroueil and Vaughan, 1990; Cotecchia and Chandler, 2000) and artificially structured clays such as cement-stabilised clays (Wissa et al., 1965; Clough et al., 1981; Kasama et al., 2000; Horpibulsuk et al., 2004b), cannot be taken into account by the SCC model. For better simulation of cemented clays, the modified effective stress concept was introduced into the SCC model (Horpibulsuk et al., 2010).

Suebsuk et al. (2010) developed a general constitutive model based on the critical state framework for destructured, naturally structured and artificially structured clays. The proposed model is the Modified Structured Cam Clay (MSCC) model. It was formulated based on the SCC model for cemented clay (Horpibulsuk et al., 2010). In the MSCC model, the influence of soil structure and destructuring were introduced into the yield function, plastic potential, and hardening rule to describe the mechanical behaviour of structured clays. The soil structure increases the

mean effective yield stress under isotropic compression (p'_y) and structure strength (p'_b). The destructuring mechanism in the MSCC model is the process of reducing the structure strength, p'_b due to the degradation and the crushing of structure. The destructuring, is assumed to be related directly to the plastic deviatoric strain, ε_d^p . The destructuring behaviour of the MSCC model is divided into two parts for volumetric deformation and shearing. The destructuring due to shearing causes a reduction in structure strength that is directly related to the plastic deviatoric strain, ε_d^p . The strain softening can be described by the MSCC model when the stress states are on the state boundary surface.

In the MSCC model, a yield surface separates elastic behaviour (i.e., stress states inside the yield surface) from elastoplastic behaviour (i.e., stress states on the yield surface). However, in reality, even in the overconsolidated state, naturally structured clays, artificially structured clay and many geomaterials often exhibit a non-recoverable behaviour upon unloading and repeated loading (Burland, 1990), which results in overestimation of the soil strength and the lack of a smooth transition between elastic and elastoplastic behaviour. To obtain accurate predictions of the deformational response, it is necessary to improve the MSCC model to better simulate the soil behaviour in the overconsolidated state. It is noted herein that the traditional term “overconsolidated state” is also used for structured clay to indicate the relative position of the current stress in relation to its limit state surface or bounding surface that the yield stress (stress history) is caused by both mechanical and chemical effects.

There are two well-known theories that have been developed for clays in the overconsolidated state. One is the kinematic hardening or multi surface plasticity

theory, which was originally applied to metal (Iwan, 1967; Mrŏz, 1967). Recently, this concept has been extended to some soil models for geomaterials (e.g., Al-Tabbaa, 1987; Stallebrass, 1990; Kavvadas and Amorosi, 2000; Rouainia and Muir Wood, 2000; Puzrin and Kirschenboim, 2001; McDowell and Hau, 2003; Baudet and Stallebrass, 2004). However, the major setback of kinematic hardening model is that the numerical computation is complex and requires considerable memory for the configuration of the sub-yield and stress reversal surface. The other is the bounding surface plasticity theory, which was introduced by Dafalias and Popov (1975) and Dafalias (1975). Many models for overconsolidated soils were developed based on this theory (e.g., Bardet, 1986; Dafalias, 1986; Dafalias and Herrmann, 1987; Whittle, 1993; Yu et al., 2007). Moreover, the bounding surface plasticity has been extended for the unsaturated structured clay (Yang et al., 2008; Yang et al., 2010)

To keep a model simple for practical use, it is impossible to include all features of the soil behaviour in a model. A complex model with many features should be avoided because it may have hidden inaccuracies, numerical instabilities, lack of a converged solution and others errors (Wroth and Houlsby, 1985). In present study, the bounding surface theory was employed with the MSCC model to simulate the stress-strain behaviour of overconsolidated structured clays because this theory is simple and predictive. The proposed model is called the "Modified Structured Cam Clay with Bounding Surface Theory" (MSCC-B) model. The MSCC-B model is presented in a four-dimensional space consisting of the current stress state, the current voids ratio, the stress history and the current soil structure. The MSCC-B model requires six parameters in addition to the standard parameters from the MCC model. The five parameters (b, Δe_i, p'_{b0}, ξ and ψ) are the same as those of the MSCC model and

have clear physical meaning. A new constant material parameter, h, is proposed in the study to take into account the effect of the material type on the plastic hardening modulus in the overconsolidation state.

Finally, the MSCC-B model is evaluated in the light of the model performance. The MSCC-B model was implemented in a single element elastoplastic calculation for simulating the behaviour of structured clays in both naturally and artificially structured states. Test data over a wide range of the mean effective stress and degree of cementation under both drained and undrained shearings were used in the verification.

4.2 Formulation of the MSCC-B model

The bounding surface plasticity theory was introduced by Dafalias and Popov (1975); Dafalias (1975). The salient feature of the bounding surface formulation is that plastic deformation during subyielding is generally induced by the stress change inside the yield surface as well as by the stress change originating on the current yield surface. This stress change is caused by the expansion and contraction of the subsets of the yield surface. It results in the variation of the plastic modulus during loading. The subsets of the yield surface inside the current yield surface are referred to as the "loading surface". The loading surface varies isotropically with the change in plastic volumetric deformation. During virgin yielding, the bounding surface expands and coincides with the loading surface. For structured clay, the bounding surface is modified as the structural bounding surface, which is affected by the soil structure. The variation of the structural bounding surface is dependent on destructuring as well as hardening, both of which are assumed to be determined due to the change in plastic

volumetric deformation and plastic deviatoric deformation following that of classic plasticity (Schofield and Wroth, 1968; Liu and Carter, 2003).

Based on the bounding surface theory and the framework of the MSCC model, Figure 4.1 shows the schematic diagram for illustrating the change of stress state (e - $\ln p'$ plane and q-p' plane) under isotropic compression loading for path 1-6. Point 1 is an initial in-situ state for a clay whose structural bounding surface is defined by isotropic yield stress on SCL, p'_y and structure strength, p'_b. As loading continues along stress path 1-2, subyielding occurs, and the loading surface expands (inside the structural bounding surface). Supposing that the loading surface and the structural bounding surface coincide at point 2, that is, $p'_{c,2} = p'_{0j,2}$, virgin yielding commences at this point and continues along the path 2-3.

Unloading starts at point 3 and continues along the stress path 3-4, i.e., $\delta p'_c < 0$ and $p'_c \neq p'_{0j}$. Subsequently, the current loading surface enters inside the structural bounding surface. When the stress path changes direction again at point 4 with $\delta p'_c > 0$, reloading then commences and continues along stress path 4-5. The perfectly hysteresis loop is assumed for the MSCC-B model, and hence $p'_{c,3} = p'_{c,5}$. At point 5, the loading surface coincides with the structural bounding surface, i.e., $p'_{c,5} = p'_{oj,5}$. In this case, virgin yielding recommences at point 5 and continues for loading along stress path 5-6. For isotropic condition, the expansion and contraction of the loading surface is only dependent on the plastic deformation. The change of stress state under shearing can be explained in the same way, but p'_{b0} decreases due to the destructuring law (Equations 3.4 and 3.5). The plastic deviatoric strain influences the stress path direction when $\eta > 0$.

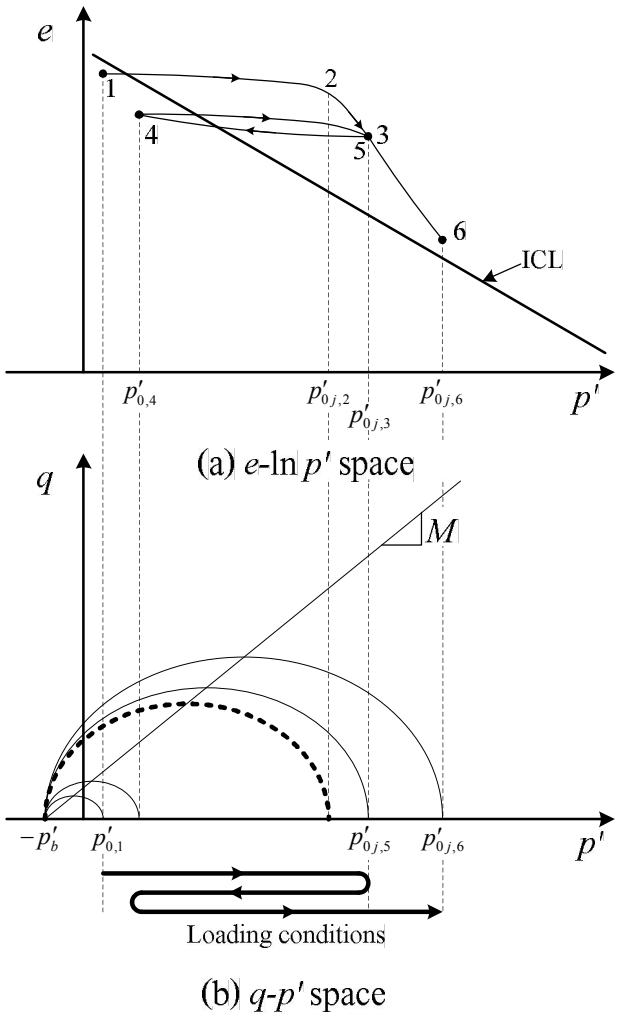

Figure 4.1 Idealisation of bounding surface plasticity model for isotropic compression of structured clays

4.2.1 Bounding surface theory with radial mapping technique

The bounding surface theory for modelling the elastoplastic deformation of material with the radial mapping technique (Whittle, 1993; Yu et al., 2007) was extended for this study. The structural bounding surface is defined by the stress history, p'_{0j}, and structure strength, p'_b. The clay behaviour is divided into the virgin yielding ($p'_c = p'_{0j}$) and subyielding ($p'_c < p'_{0j}$), where p'_c is a reference size of

loading surface. Similar to the MSCC model, the equation for the structural bounding surface is assumed to be elliptical and can be expressed as follows:

$$F = q^2 - M^2\left(p' + p'_b\right)\left(p'_{0j} - p'\right) = 0\,. \tag{4.1}$$

The loading surface is defined as the surface on which the current stress state remains. For simplicity, the loading surface is assumed to be the same shape as the structural bounding surface and with an aspect ratio similarly equal to *M*.

4.2.2 Plastic potential

The plastic potential adopted in the MSCC-B model is the same as that proposed in the MSCC model as shown in equation (3.13).

4.2.3 Destructuring law

The volumetric hardening and destructuring rules presented in the previous chapter (Equation 3.16) were adopted in the formulation of the hardening modulus for the MSCC-B model with the assumption that $p'_{0j} = p'_0$ and $\delta p'_{0j} = \delta p'_0$. The destructuring laws due to shearing presented in a previous chapter (Equations 3.4 and 3.5) are used in the MSCC-B model.

4.2.4 Mapping rule

The mapping rule is an essential part of a bounding surface theory based on which the stiffness of soil deformation during subyielding is defined. A detailed discussion on the significance of mapping rule can be found in a paper by Yang et al. (2010). The original radial mapping technique was modified for structured clay in this study since this method is both simple and effective for many conventional stress paths. The image stress point on the structural bounding surface is used for

determining the plastic volumetric strain. The schematic diagram for the mapping rule is shown in Figure 4.2. An association between any stress point and the image stress point is described by the intersection of the structural bounding surface with the straight line passing through the origin and the current stress state, based on the assumption that the hardening modulus at the current stress point (H) is related to the hardening modulus at its corresponding image stress point (H_j) as well as to the ratio of the image stress ratio (α). The variation of α is assumed to be a function of both the current stress state (q, p') and the image stress state (q_j, p'_j) as follows:

$$\alpha = \sqrt{\frac{\left(p' / p'_j\right)^2 + \left(q / q_j\right)^2}{2}}, \tag{4.2}$$

with $0 \le \alpha \le 1$. α for any p' and q can be computed from equation (4.2) when p'_j and q_j are known. The p'_j and q_j values for any p'_{0j} are determined from the structural bounding surface (Equation 4.1). The parameter α becomes the unique value ($\alpha = \frac{p'}{p'_j} = \frac{q}{q_j} = \frac{p'_0}{p'_{0j}}$) at the critical state when p'_b is zero due to the complete removal of cementation structure (destrucuturing).

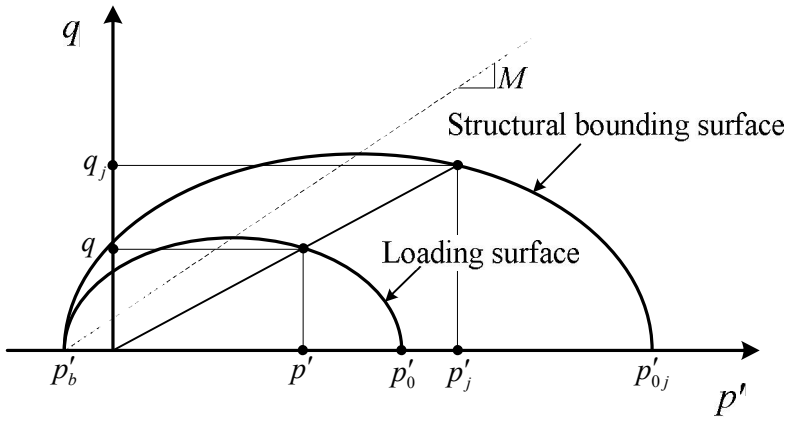

Figure 4.2 Mapping rule for the MSCC-B model

4.2.5 Hardening modulus

a) Hardening modulus at an image stress point (H_j)

Based on the state boundary surface theory, the variation of the structural bounding surface ($\delta p'_{0j}$) is related to the plastic volumetric strain increment ($\delta\varepsilon_v^p$). It is developed based on equation (3.16) as follows:

$$\delta p'_{0j} = \frac{(1+e)\, p'_{0j}}{(\lambda^* - \kappa) + \left(\frac{M}{M-\bar{\eta}}\right) b\Delta e} \delta\varepsilon_v^p . \tag{4.3}$$

The differential form of the structural bounding surface is

$$\frac{\partial F}{\partial p'}\delta p'_j + \frac{\partial F}{\partial q}\delta q_j + \frac{\partial F}{\partial p'_{0j}}\delta p'_{0j} = 0 . \tag{4.4}$$

Differentiating equation (4.1) with respect to p'_{0j},

$$\frac{\partial F}{\partial p'_{0j}} = -M^2\left(p' + p'_b\right). \tag{4.5}$$

Substituting equations (4.3) and (4.5) into equation (4.4),

$$\frac{\partial F}{\partial p'}\delta p'_j + \frac{\partial F}{\partial q}\delta q_j - M^2\left(p' + p'_b\right)\frac{\left(1+e\right)p'_{0j}}{\left(\lambda^* - \kappa\right) + \left(\dfrac{M}{M-\bar{\eta}}\right)b\Delta e}\delta\varepsilon_v^p = 0. \tag{4.6}$$

The plastic strain increment in the subyielding state is defined in terms of the hardening modulus, yield function and plastic potential in the same way as that in the virgin yielding state as previously successfully done by Dafalias and Herrmann (1980), Bardet (1986); Yu et al. (2007). Thus,

$$\delta\varepsilon_v^p = \frac{1}{H_j}\left(\frac{\partial F}{\partial p'}\delta p'_j + \frac{\partial F}{\partial q}\delta q_j\right)\left(\left.\frac{\partial G}{\partial p'}\right|_j\right). \tag{4.7}$$

Substituting equation (4.7) into equation (4.6),

$$H_j = M^2\left(p' + p'_b\right)\frac{\left(1+e\right)p'_{0j}}{\left(\lambda^* - \kappa\right) + \left(\dfrac{M}{M-\bar{\eta}}\right)b\Delta e}\left(\left.\frac{\partial G}{\partial p'}\right|_j\right), \tag{4.8}$$

where $\left.\frac{\partial G}{\partial p'}\right|_j$ are given as

$$\left.\frac{\partial G}{\partial p'}\right|_j = \frac{M^2}{1-\psi}\left(\frac{2\left(\frac{p'_j + p'_b}{p'_p + p'_b}\right)\left(p'_p + p'_b\right)^2}{\psi\left(p'_j + p'_b\right)} - 2\left(p'_j + p'_b\right)\right). \tag{4.9}$$

b) Hardening modulus at the stress point (H)

A specific feature of the bounding surface theory is that the hardening modulus (H) is not only dependent on the location of the image point but also on a function of the distance from the stress point to the structural bounding surface with the following requirements (Dafalias and Herrmann, 1987; Khalili et al., 2005; Yu et al., 2007):

$$H = +\infty \quad \text{if} \quad \alpha = 0, \tag{4.10a}$$

$$H = H_j \quad \text{if} \quad \alpha = 1. \tag{4.10b}$$

The restriction imposed by equations (4.10a, b) ensures that the clay behaviour is almost purely elastic when the stress state is far away from the structural bounding surface and that the stress point and the structural bounding surface move together when the current stress state lies on the structural bounding surface. The hardening modulus for the MSCC-B model under monotonic loading conditions is proposed to satisfy the restriction equations (4.10a, b) as follows:

$$H = H_j + \left(h \cdot H_{j,i}\right) \cdot \frac{(1-\alpha)^2}{\alpha}, \tag{4.11}$$

where h is the non-dimensional parameter describing the effect of material characteristics on H and $H_{j,i}$ is the initial hardening modulus at the image stress point, which is calculated by equation (4.8).

4.2.3 Model parameters

There are 12 parameters for the MSCC-B model. Six parameters (λ^*, e_{IC}^*, κ, M, p_0', G' or ν') are the basic parameters adopted from the MCC model. The other five parameters (b, Δe_i, p_{b0}', ξ and ψ) are the structural parameters describing the hardening and destructuring behaviour for the original MSCC model. The last parameter is h, which is newly presented in this paper to describe the effect of the material characteristics on the hardening modulus in the overconsolidated state. The parameters denoted by a superscript * are the parameters tested with reconstituted samples (Burland, 1990). The details of the parameter determination can be found in the papers by Horpibulsuk et al. (2010) and Suebsuk et al. (2010). A new parameter h is presented in this paper to describe the effect of the material characteristics on the hardening modulus in the overconsolidated state.

The effect of h on the shear behaviour is illustrated in Figures 4.3 and 4.4 using the model parameters listed in Table 4.1. Figure 4.3a shows the effect of h on the undrained stress path. It is clear that h significantly affects the hardening and destructuring behaviour for structured soil in the overconsolidated state. An increase

in h increases both the stiffness and strength of the clay, as shown in Figures 4.3a and 4.3b. A higher h results in a higher maximum deviatoric stress, which tends to overestimate the soil strength (*vide* Figure 4.3b). The smoothness of the excess pore pressure-deviatoric strain curve is illustrated in Figure 4.3c for various h. At the same deviatoric stress, a decrease in h leads to a larger deformation produced by the shearing. Figure 4.4 presents the influence of h on the relationship between $\alpha - \varepsilon_v^p$ under drained shearing. The parameter h insignificantly affects the soil stiffness when it is smaller than 1.

Table 4.1 Parameters for a parametric study on the effect of h

Model Parameters	Physical Meaning	Value	Unit
λ^*	Gradient of ICL in e-ln p' plane	0.147	-
e^*_{IC}	Voids ratio at reference stress (p' = 1 kPa) on ICL	1.92	-
κ	Gradient of unloading-reloading line of SCL in e-ln p'	0.027	-
b	Non-dimension parameter describing the destructuring by volumetric plastic strain	0.6	-
Δe_i	Additional of voids ratio between ICL and SCL at yield stress	1.92	-
$p'_{y,i}$	Mean effective yield stress on SCL	100	kPa
M	Gradient of critical state line in q-p' plane	1.2	-
G'	Shear modulus	3,000	kPa
ψ	Non-dimension constant parameter define the shape of plastic potential	2.0	-
p'_{b0}	Initial structure strength on in q-p' plane	20	kPa
ξ	Non-dimension constant parameter describing the destructuring by shearing	10	-

The parametric studies (Figures 4.3 and 4.4) show that the destructuring depends on both ε_v^p and ε_d. Its behaviour can be predicted by equations 3.4, 3.5 and 3.16. The plastic volumetric strain occurs at the early stage of loading. If α < 1, the stress state stays inside the structural bounding surface, and the destructuring is caused by the change in plastic volumetric strain due to $\delta p_c'$ and the degradation of soil structure due to the deviatoric strain. The destructuring gradually occurs as shown by the smooth stress-strain relationship. When α = 1, the loading surface and structural bounding surface coincide, and the MSCC-B and MSCC models are the same.

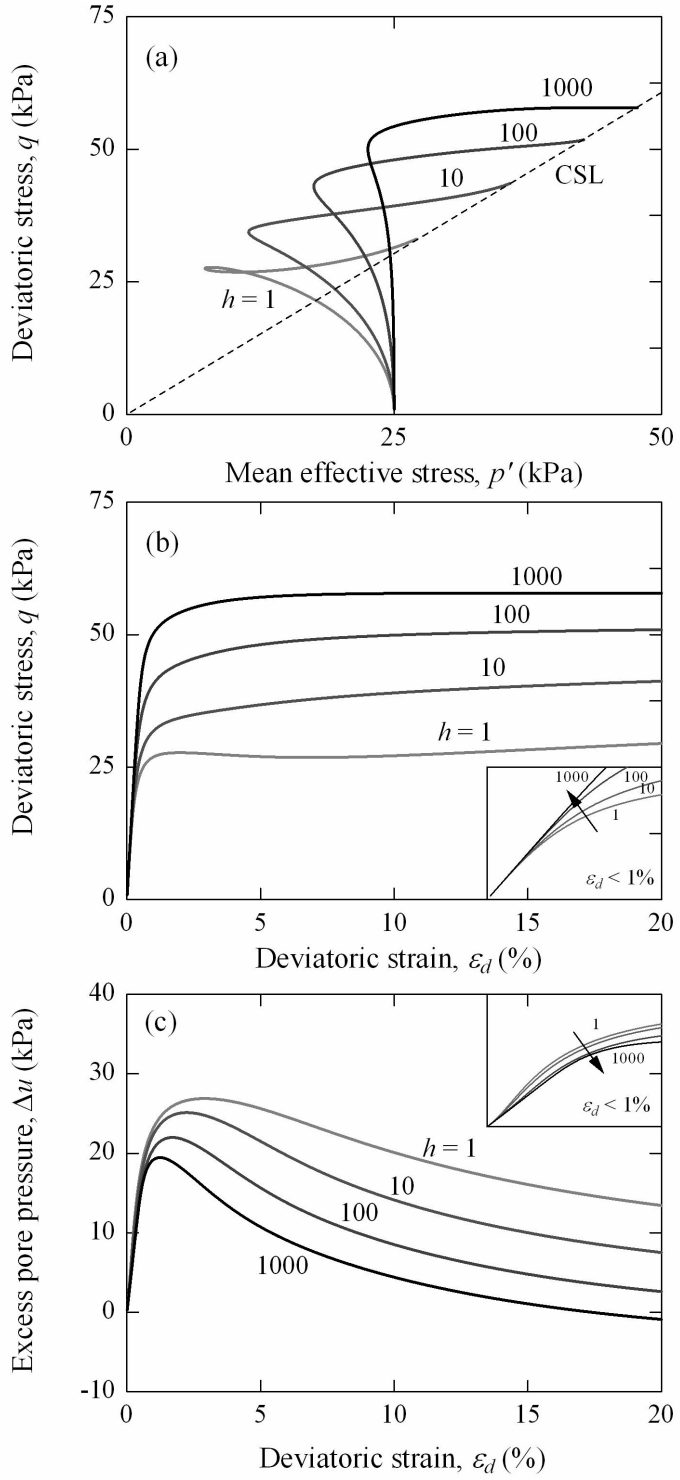

Figure 4.3 Influence of h on the soil behaviour under the undrained shearing test

(a) the stress path, (b) the stress-strain behaviour and

(c) the development of excess pore pressure

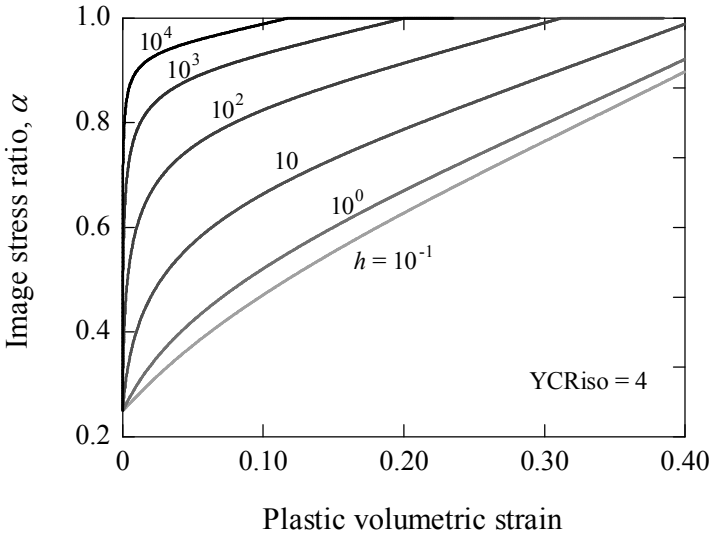

Figure 4.4 Influence of h on the $\alpha - \varepsilon_v^p$ curve under the drained shearing test

4.3 Performance of the MSCC-B model

In this section, the MSCC-B model is verified by a comparison between measured and simulated data. The tested results for intact Pappadai clay (Cotecchia and Chandler, 2000; Cotecchia, 2003) and cemented Ariake clay (Horpibulsuk, 2001; Horpibulsuk et al., 2004b) were used for this verification. The physical properties of both clays are presented in Table 4.2. The testing programmes of the Pappadai and cemented Ariake clays are summarised in Tables 4.3. The model parameters were obtained with the following steps:

a) The isotropic compression test results of structured samples and reconstituted (remoulded) samples were taken to determine compression parameters. The λ^* and e_{IC}^* were determined from the intrinsic compression line, ICL (Burland, 1990). The three additional structural parameters ($p'_{y,i}$, Δe_i and b) were determined

from the structured compression line, SCL (Liu and Carter, 2002; Suebsuk et al., 2010). The κ was determined from the unload-reloading line of the structured sample.

b) Undrained and drained shearing test results of isotropic consolidated structured clay were taken to determine the parameters (M, p'_{b0}, G', ψ, ξ and h) at various isotropic yield stress ratios (YSRiso). The gradient of critical state line M and initial structure strength p'_{b0} was obtained from the stress path (*vide* Figure 3.3b). The shear modulus G' was approximated from the q-ε_d curve. The parameters ψ and ξ are dependent on the type of clays and the degree of cementation (Suebsuk et al., 2010). The parameter ψ were estimated from the shape of the structural bounding surface. For natural clay, the plastic potential is approximately elliptical, and ψ can be taken as 2. For cemented clay, it is usually less than 2 (Suebsuk et al., 2010). The parameter ξ was estimated from the stress-strain response, and its value is $1 \le \xi \le 100$ (Suebsuk et al., 2010). The parameter h was obtained by plotting the simulated α-ε_v^p curve compared with measured data.

Tables 4.4 and 4.5 present the input parameters selected for intact Pappadia clay and cemented Ariake clay, respectively.

Table 4.2 Physical properties of the base clays

Properties	Pappadai clay	Ariake clay
Reference	Cotecchia and Chandler (2000); Cotecchia (1996)	Horpibulsuk (2001); Horpibulsuk et al. (2004b)
Specific density	2.73	2.70
Natural water content (%)	29.8-32.6	135-150*
Liquid limit (%)	65	120
Plasticity index (%)	35	63
Activity	0.42-0.72	1.24-1.47
Clay fraction (%)	50	55
Silt fraction (%)	-	44
Sand fraction (%)	-	1
In-situ voids ratio	0.68-0.90	3.65-4.05
Sample type	Intact	Cemented

Remarks: * Water content = 180% before mixed with cement

Table 4.3 Testing programme for triaxial test on the base clays

Base clay	Sample No	YSRiso	*p′* before shearing (kPa)	*e* before shearing	Shearing condition	Strain or displacement rate
Intact Pappadai clay	TN14	4.52	500	0.875	D	0.2-0.6%/day*
	TN15	2.825	800	0.8725	D	0.189%/day*
	TN18	1.50	1,500	0.839	D	0.4%/day*
	TN17	1.00	2,500	0.766	D	0.189%/day*
	TN5	3.22	700	0.895	U	4%/day*
	TN3	2.167	1,042	0.862	U	4.3%/day*
	TN11	1.40	1,600	0.856	U	5%/day*
Cemented Ariake clay	AW6-50	1.40	50	4.098	D	0.0025**
	AW18-400	5.00	400	3.673	D	0.0025**
	AW18-500	4.00	500	3.668	D	0.0025**
	AW18-1000	2.00	1,000	3.657	D	0.0025**
	AW9-100	3.70	100	3.650	U	0.0075**
	AW9-200	1.85	200	3.589	U	0.0075**
	AW18-200	10.0	200	3.707	U	0.0075**
	AW18-400	5.0	400	3.673	U	0.0075**

Remarks: U = Undrained test, D = Drained test, * $d\varepsilon_a / dt$ and ** mm/min

Table 4.4 Parameters of the MSCC-B model for intact Pappadai clay

Test type	Parameter/symbol	Unit	Value
Isotropic compression test	λ^*	-	0.206
	e^*_{IC}	-	3.17
	κ	-	0.009
	b	-	0.1
	Δe_i	-	0.32
	$p'_{y,i}$	kPa	2300
	h	-	1000
Drained or Undrained shearing test	M	-	0.83
	G'	kPa	40,000
	p'_{b0}	kPa	480
	ξ	-	10
	ψ	-	2.0

Table 4.5 Parameters of the MSCC-B model for cemented Ariake clay

Test type	Parameter/symbol	Unit	A_w = 6%	A_w = 9%	A_w = 18%
Isotropic compression test	λ^*	-	0.44	0.44	0.44
	e^*_{IC}	-	4.37	4.37	4.37
	κ	-	0.06	0.03	0.01
	b	-	0.05	0.01	0.001
	Δe_i	-	2.0	2.5	2.72
	$p'_{y,i}$	kPa	70	370	2,000
	h	-	100	800	1000
Drained or Undrained shearing test	M	-	1.44	1.73	1.32
	G'	kPa	4,000	8,000	40,000
	p'_{b0}	kPa	50	75	730
	ξ	-	10	10	10
	ψ	-	0.9	0.5	0.1

4.3.1 Isotropic compression

Figure 4.5 shows the comparison between the measured and simulated data for the isotropic compression of intact Pappadai clay. The tested data can be captured well by the model simulation. The smooth $e - \ln p'$ curve for pre- and post-yield states is seen. The meta-stable voids ratio, which cannot be degraded with the increase in confining pressure, is predicted by the MSCC-B model. The lower the b, the smaller the destructuring. Figure 4.6 compares the model simulation results of the

isotropic compression curves with the measured data for the cemented Ariake clay at different cement contents. The simulations were performed with a single set of intrinsic parameters. The results show that samples with higher cement content exhibit smaller destructuring, which is controlled by b. The MSCC-B model simulation broadly matches the experimental results better than the original MSCC model, which cannot simulate the subyielding behaviour. From the comparisons, it is seen that the destructuring by shearing does not affect the isotropic compression response, and thus the simulation of isotropic compression is only controlled by six parameters (λ^*, e^*_{IC}, κ, $p'_{y,i}$, b and Δe_i).

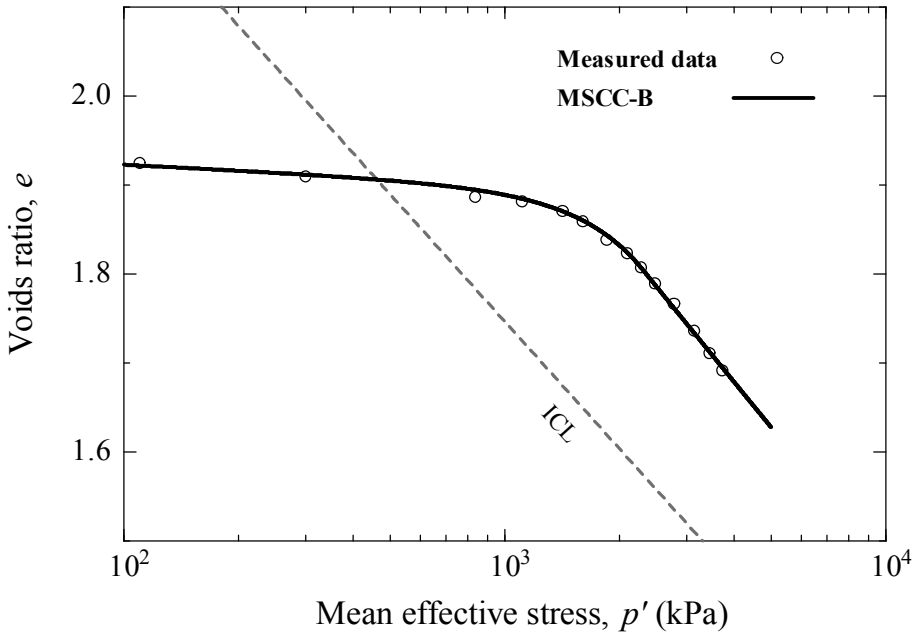

Figure 4.5 Comparison of measured and simulated isotropic compression tests of intact Pappadai clay

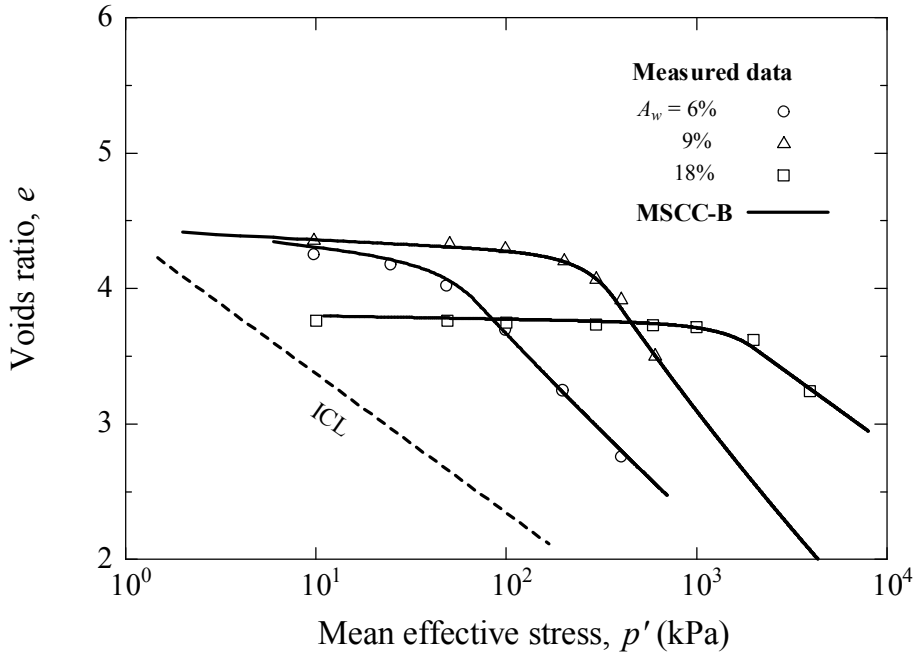

Figure 4.6 Comparison of measured and simulated isotropic compression tests of cemented Ariake clay

4.3.2 Drained triaxial shearing

The results of the model simulation of isotropically consolidated drained compression (CID) shearing of the intact Pappadai clay are shown in Figure 4.7. For moderate to large deviatoric strain (ε_d = 0.1-20%), a constant shear modulus is assumed throughout this simulation. The MSCC-B model gives more realistic predictions than those predicted by the original MSCC model. The smooth stress-strain relationship can be captured by the MSCC-B model. By comparison of the stress ratio-deviatoric strain curve and volumetric strain-deviatoric strain curve, it is seen that the MSCC-B model provides a very good simulation.

Figures 4.8 and 4.9 present the comparison of measured and simulated data for the cemented Ariake clay at different cement contents. The test data covers

the range of cement contents from 6% to 18% with the variation of confining stress from 50 kPa to 1000 kPa. The smooth stress-strain response was simulated along the loading path. The MSCC-B model gives good results for the stress-strain curve and the volumetric deformation curve.

4.3.3 Undrained triaxial shearing

Figure 4.10 compares the measured and simulated results of the intact Pappadai clay with various YSRiso from 7.50 to 1.50. Figures 4.11 and 4.12 compare the measured and simulated results of the cemented Ariake clay at various YSRiso and cement contents. It is found that the deviatoric stress and excess pore pressure versus deviatoric strain can be predicted well by the MSCC-B model.

From the simulation of compressibility and shearing for naturally and artificially structured clays, it is concluded that the MSCC-B model can describe the influence of artificial cementation structure on soil behaviour.

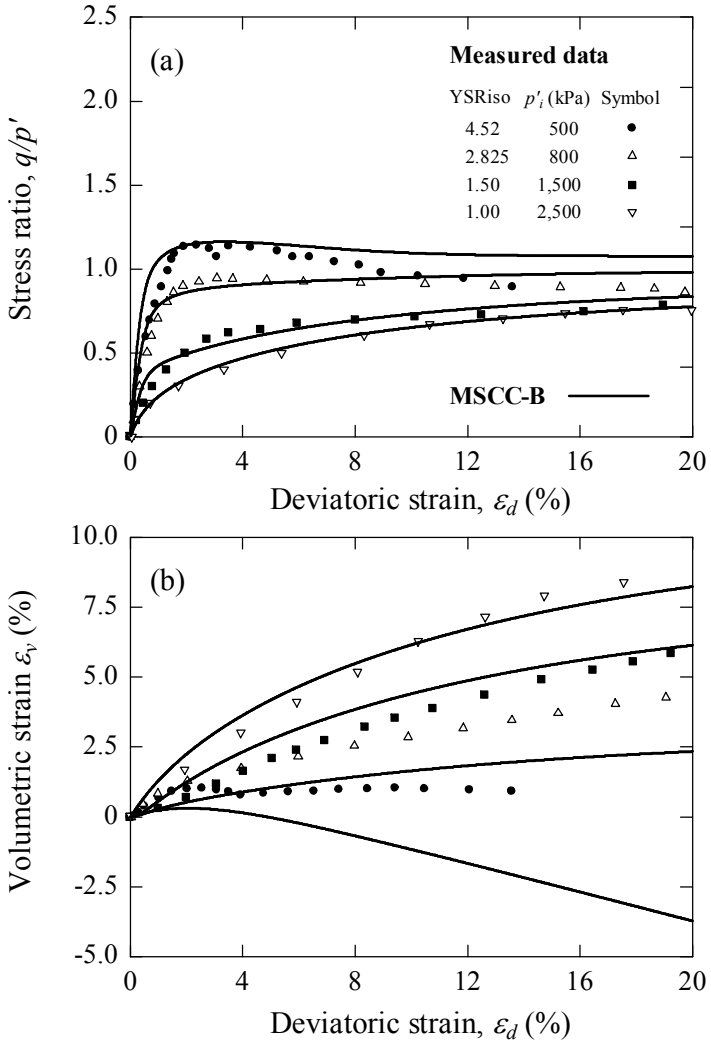

Figure 4.7 Comparison of measured and simulated CID test of intact Pappadai clay (a) stress ratio-deviatoric strain curve and (b) volumetric strain-deviatoric strain curve

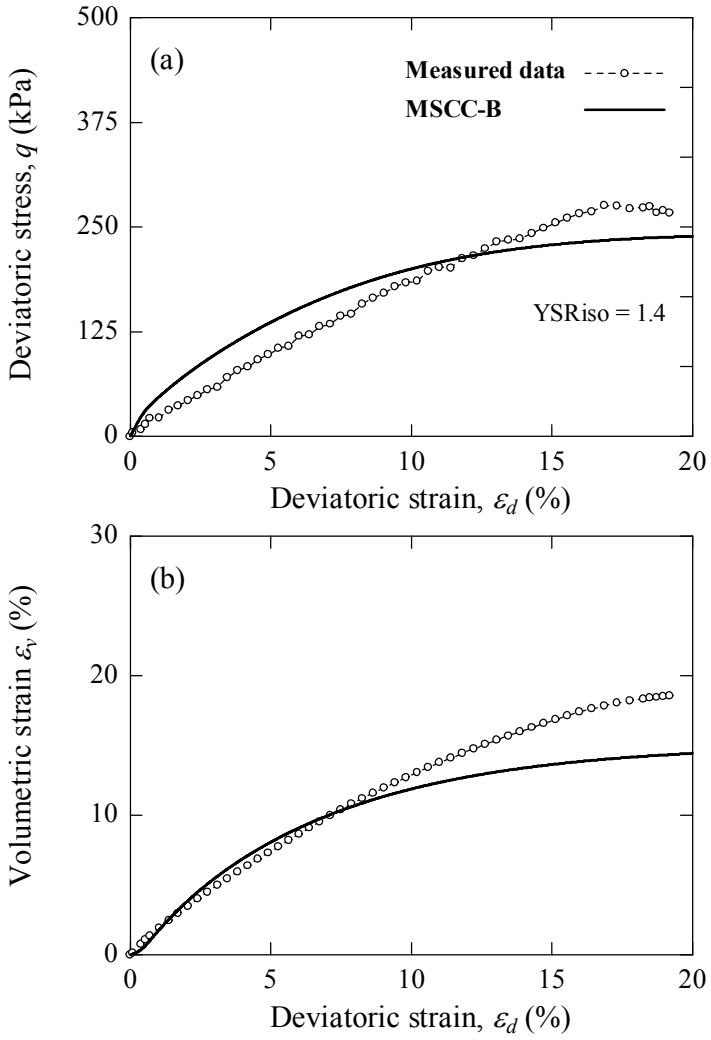

Figure 4.8 Comparison of measured and simulated CID test of cemented Ariake clay with 6% cement content (a) stress ratio-deviatoric strain curve and (b) volumetric strain-deviatoric strain curve

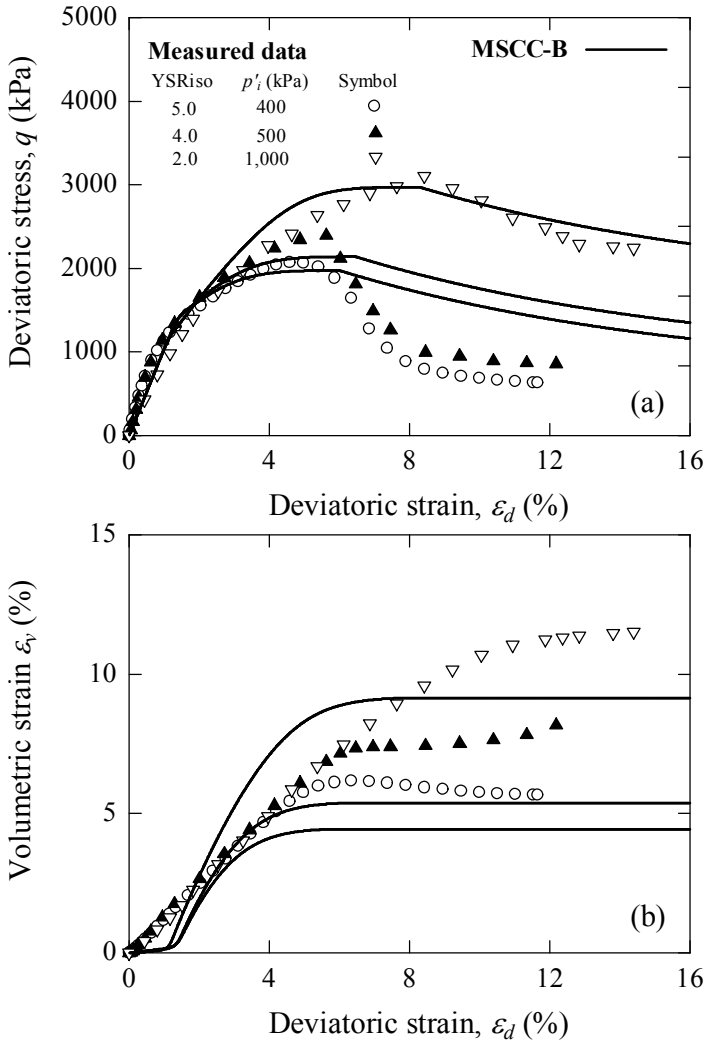

Figure 4.9 Comparison of measured and simulated CID test of cemented Ariake clay with 18% cement content. (a) Stress ratio-deviatoric strain curve (b) Volumetric strain-deviatoric strain curve

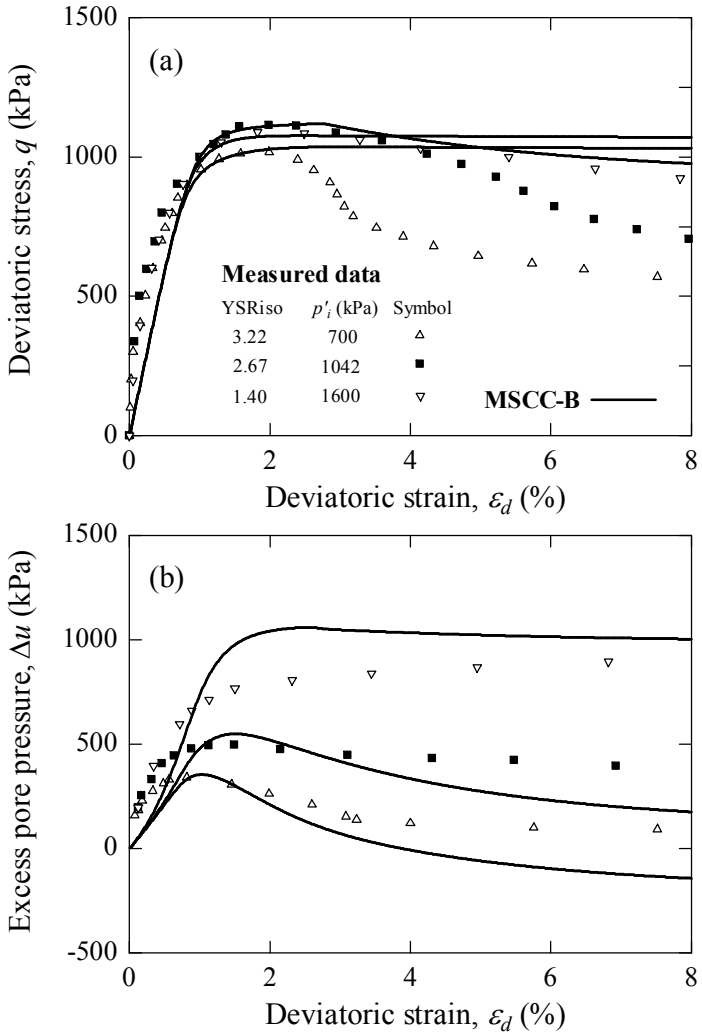

Figure 4.10 Comparison of measured and simulated CIU test results of intact Pappadai clay (a) deviatoric stress-deviatoric strain curve and (b) excess pore pressure-deviatoric strain curve

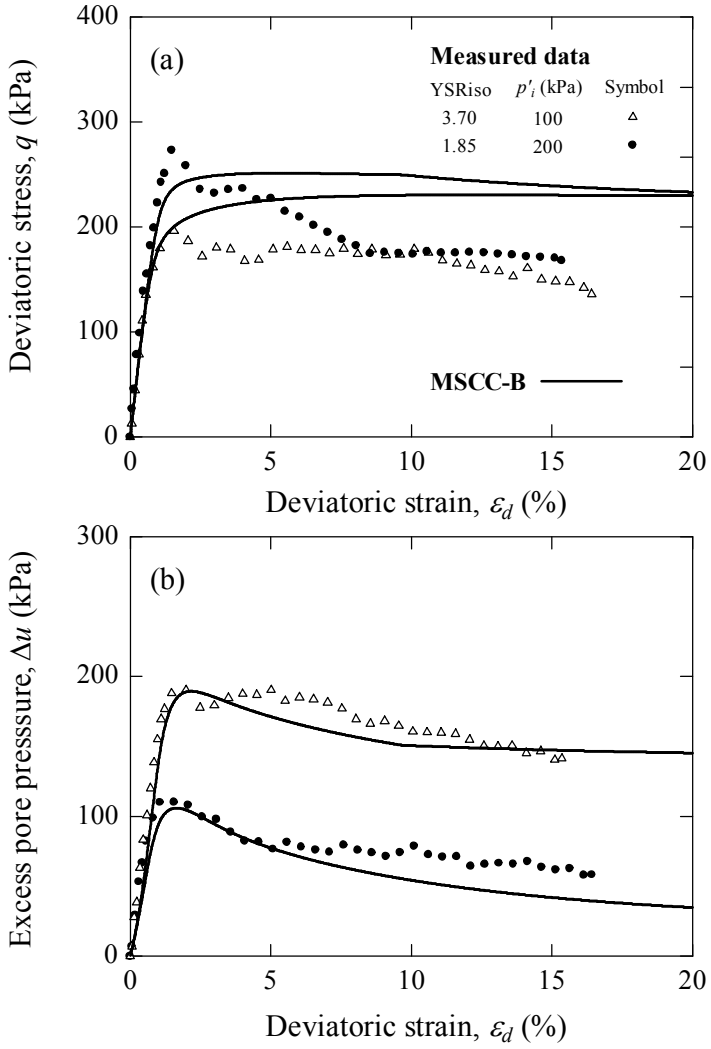

Figure 4.11 Comparison of measured and simulated CIU test of cemented Ariake clay with 9% cement content. (a) deviatoric stress-deviatoric strain curve and (b) excess pore pressure-deviatoric strain curve

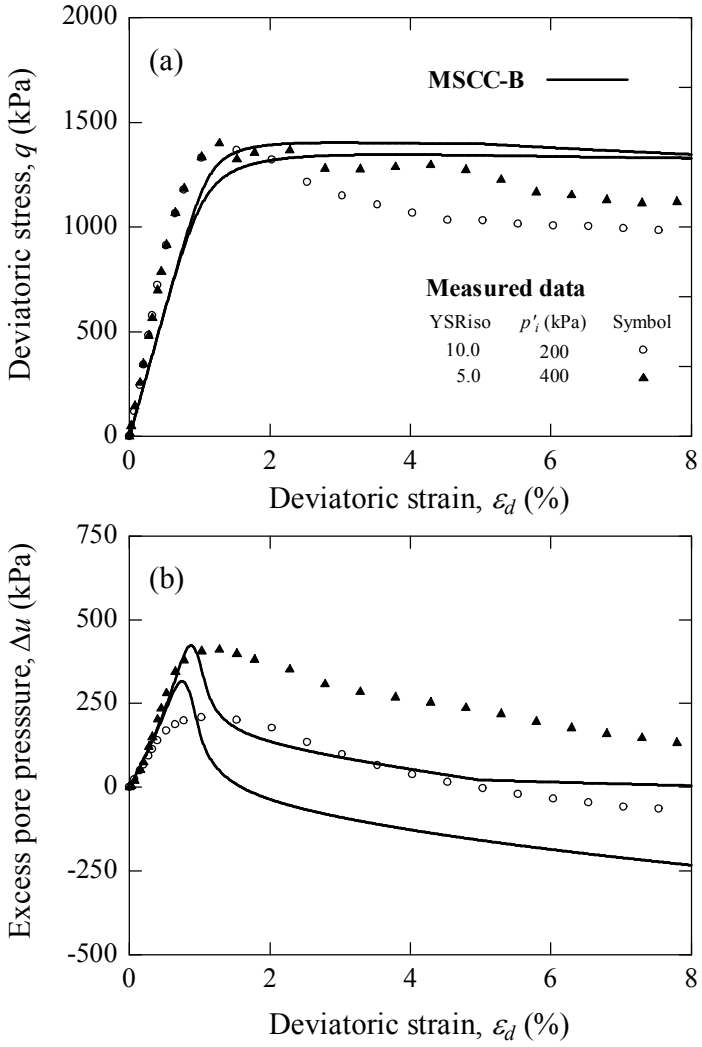

Figure 4.12 Comparison of measured and simulated CIU test of cemented Ariake clay with 18% cement content (a) deviatoric stress-deviatoric strain curve and (b) excess pore pressure-deviatoric strain curve

4.4 Performance of the MSCC-B model compared with the original MSCC model

To demonstrate the improvement of MSCC-B model, simulations of structured soil behaviour made by the MSCC-B model are compared with those of the original MSCC model as shown in Figures 4.13 to 4.15 for Pappadai clay. It is seen that there are the following improvement in model simulation for MSCC-B.

a) The plastic deformation of soil within the yield surface is captured. This is especially important for highly overconsolidated soils.

b) The peak strength and the smooth transition from hardening to softening behaviours, for both drained or undrained situations, have been better represented by the boundary surface theory. This improves the overall accuracy of stress and strain relationship.

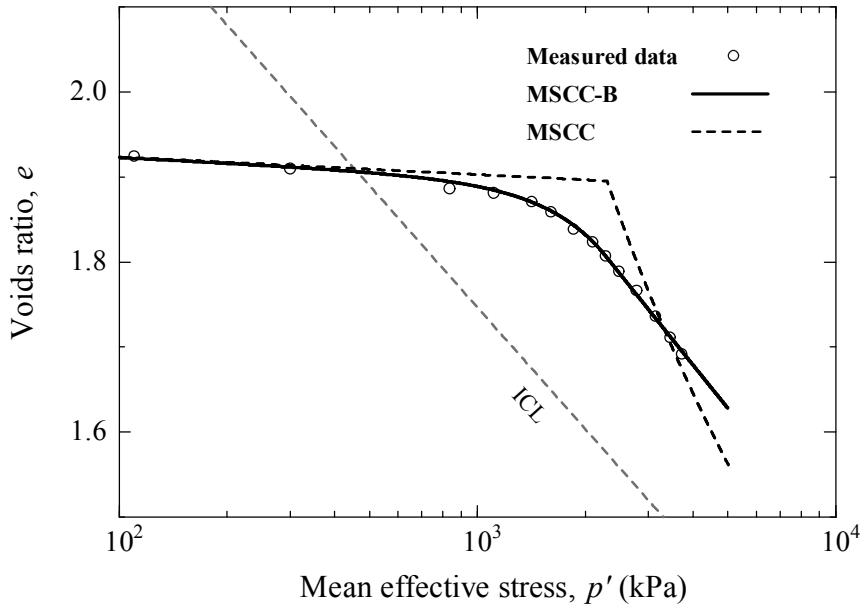

Figure 4.13 Comparisons of experimental and simulated on isotropic compression test results of intact Pappadai clay by MSCC and MSCC-B models

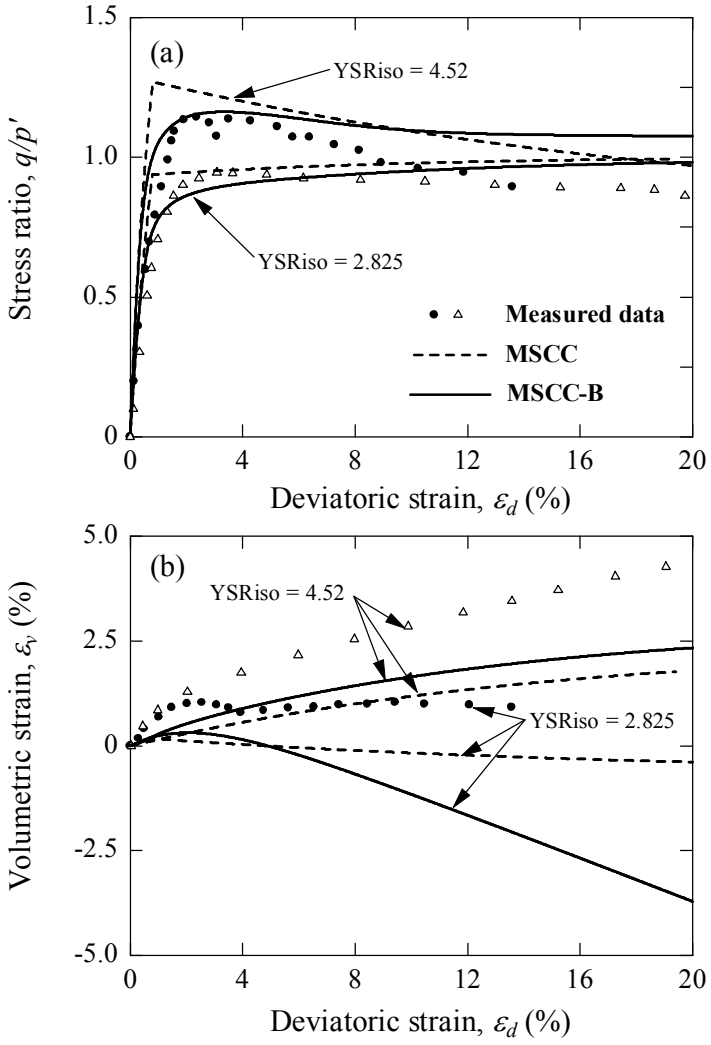

Figure 4.14 Comparisons of experimental and simulated on CID test results of intact Pappadai clay by MSCC and MSCC-B models

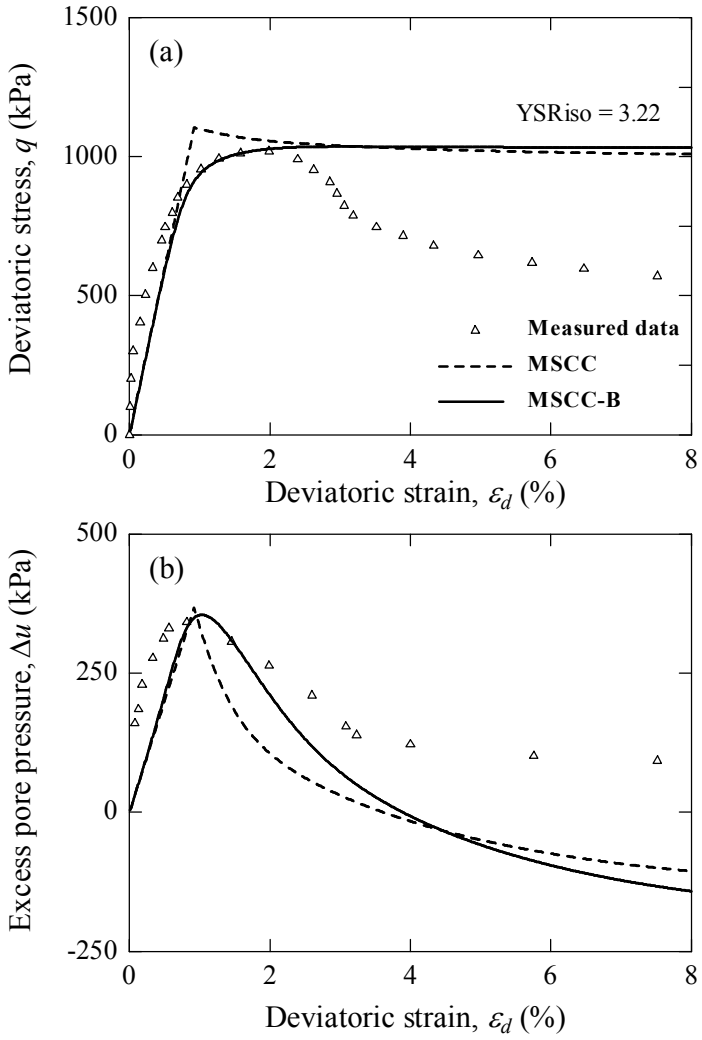

Figure 4.15 Comparisons of experimental and simulated on CIU test results of intact Pappadai clay by MSCC and MSCC-B models

4.5 Conclusions

Based on an extensive review of the available experimental data, a critical state model with bounding surface theory to describe the mechanical behaviour of naturally and artificially structured clays in the overconsolidated state was proposed. A fundamental hypothesis of the development is that the hardening and destructuring of structured clay are dependent on both the plastic volumetric strain and deviatoric

strain. The key feature of the MSCC-B model is that the plastic deformation for stress state inside the yield surface can be well-captured.

The hardening modulus for structured clay was formulated based on the bounding surface theory with the radial mapping technique. It is suitable for describing the compression and shearing behaviours of natural clays and cement-stabilised clays under monotonic loading in the overconsolidated state. The MSCC-B model can simulate the stress-strain-strength relationships of structured clays well over a wide range of YSRiso. Generally speaking, a reasonable good agreement between the model performance and experimental data is achieved. The model can be used as a powerful tool for simulating structured clay behaviour in the overconsolidated state.

4.6 References

Al-Tabbaa, A. (1987). Permeability and stress-strain response of speswhite kaolin. **Ph.D. Thesis**, University of Cambridge, Cambridge, UK.

Bardet, J. P. (1986). Bounding surface plasticity model for sands. **Journal of Engineering Mechanics, ASCE**. 112(11): 1198-1217.

Baudet, B., and Stallebrass, S. (2004). A constitutive model for structured clays. **Geotechnique**. 54(4): 269-278.

Burland, J. B. (1990). On the compressibility and shear strength of natural soils. **Geotechnique**. 40(3): 329–378.

Clough, G. W., Sitar, N., Bachus, R. C., and Rad, N. S. (1981). Cemented sands under static loading. **Journal of Geotechnical Engineering, ASCE**. 107(GT6): 799-817.

Cotecchia, F. (1996). The effect of the structure on the properties of and Italian Pleistocene clay. **Ph.D. Thesis**, University of London.

Cotecchia, F. (2003). Mechanical behaviour of the stiff clays from the Montemesola Basin in relation to their geological history and structure. **Proceedings of the international conference on the characterization and engineering properties of natural soils** (pp. 817-850), Lisse.

Cotecchia, F., and Chandler, R. J. (1997). The influence of structure on the pre-failure behaviour of a natural clay. **Geotechnique**. 47(3): 523-544.

Cotecchia, F., and Chandler, R. J. (2000). A general framework for the mechanical behaviour of clays. **Geotechnique**. 50(4): 431-447.

Dafalias, Y. F. (1975). On the cyclic and anisotropy plasticity. **Ph.D. Thesis**, The University of California at Berkeley.

Dafalias, Y. F. (1986). Bounding surface plasticity. I: Mathermatical foundation and hypoplasticity. **Journal of Engineering Mechanics, ASCE**. 112(9): 966-987.

Dafalias, Y. F., and Herrmann, L. R. (1980). Bounding surface formulation of the soil plasticity. **Soil Mechanics-Transient and Cyclic Loads**: Wiley, New York. 253-282.

Dafalias, Y. F., and Herrmann, L. R. (1987). Bounding surface plasticity. II: Application to isotropic cohesion soil. **Journal of Engineering Mechanics, ASCE**. 112(12): 1263-1291.

Dafalias, Y. F., and Popov, E. P. (1975). A model of non-linearly hardening materials for complex loading. **Acta Mechanica**. 21: 173-192.

Gens, A., and Nova, R. (1993). Conceptual bases for constitutive model for bonded soil and weak rocks. **Geotechnical Engineering of Hard Soil-Soft Rocks**: Balkema.

Horpibulsuk, S. (2001). Analysis and Assessment of Engineering Behavior of Cement Stabilized Clays. **Ph.D. dissertation**, Saga University, Saga, Japan.

Horpibulsuk, S., Bergado, D. T., and Lorenzo, G. A. (2004a). Compressibility of cement admixed clays at high water content. **Geotechnique**. 54(2): 151-154.

Horpibulsuk, S., Liu, M. D., Liyanapathirana, D. S., and Suebsuk, J. (2010). Behaviour of cemented clay simulated via the theoretical framework of Structured Cam Clay model. **Computers and Geotechnics**. 37(1-2): 1-9.

Horpibulsuk, S., Miura, N., and Bergado, D. T. (2004b). Undrained shear behaviour of cement admixed clay at high water content. **Journal of Geotechnical and Geoenvironmental Engineering, ASCE**. 130(10): 1096-1105.

Horpibulsuk, S., Shibuya, S., Fuenkajorn, K., and Katkan, W. (2007). Assessment of engineering properties of Bangkok clay. **Canadian Geotechnical Journal**. 44(2): 173-187.

Iwan, D. W. (1967). On a class of models for the yielding behaviour of continuous and composite systems. **Journal of Applied Mechanics, ASME**. 34: 612-617.

Kasama, K., Ochiai, H., and Yasufuku, N. (2000). On the stress-strain behaviour of lightly cemented clay based on an extended critical state concept. **Soils and Foundations**. 40(5): 37-47.

Kavvadas, M., and Amorosi, A. (2000). A constitutive model for structured soils. **Geotechnique**. 50(3): 263-273.

Khalili, N., Habte, M. A., and Valliappan, S. (2005). A bounding surface plasticity model for cyclic loading of granular soils. **International Journal for Numerical Methods in Engineering**. 63(14): 1939-1960.

Lee, K., Chan, D., and Lam, K. (2004). Constitutive model for cement treated clay in a critical state framework. **Soils and Foundations**. 44(3): 69-77.

Leroueil, S., Tavenas, F., Brucy, F., La Rochelle, P., and Roy, M. (1979). Behavior of destructured natural clays. **Journal of Geotechnical Engineering, ASCE**. 105(6): 759-778.

Leroueil, S., and Vaughan, P. R. (1990). The general and congruent effects of structure in natural soils and week rock. **Geotechnique**. 40: 467-488.

Liu, M. D., and Carter, J. P. (2002). A structured Cam Clay model. **Canadian Geotechnical Journal**. 39: 1313–1332.

Liu, M. D., and Carter, J. P. (2003). Volumetric deformation of natural clays. **International Journal of Geomechanics, ASCE**. 3(2): 236-252.

McDowell, G. R., and Hau, K. W. (2003). A simple non-associated three surface kinematic hardening model. **Geotechnique**. 53(4): 433-437.

Miura, N., Horpibulsuk, S., and Nagaraj, T. S. (2001). Engineering behavior of Cement stabilized clays. **Soils and Foundations**. 41(5): 33-45.

Mrŏz, Z. (1967). On Description of anisotropic work hardening. **Journal of the Mechanics and Physics of Solids**. 15(3): 163-175.

Muir Wood, D. (1990). **Soil Behaviour and Critical State Soil Mechanics**. Cambridge, UK: Cambridge University Press.

Puzrin, A. M., and Kirschenboim, E. (2001). Kinematic hardening model for overconsolidated clays. **Computers and Geotechnics**. 28: 1-36.

Roscoe, K. H., and Burland, J. B. (1968). On the generalised stress-strain behaviour of wet clay. **Engineering plasticity**. 535-609.

Roscoe, K. H., and Schofield, A. N. (1963). Mechanical behaviour of an idealised wet clay. **Proceedings of the European Conference on Soil Mechanics and Foundation Engineering** (pp. 47-54).

Rouainia, M., and Muir Wood, D. (2000). A kinematic hardening constitutive model for natural clays with loss of structure. **Geotechnique**. 50(2): 153-164.

Schofield, A. N., and Wroth, C. P. (1968). **Critical State Soil Mechanics**. London: MacGraw-Hill.

Shibuya, S. (2000). Assessing structure of aged natural sedimentary clays. **Soils and Foundations**. 40(3): 1-16.

Stallebrass, S. E. (1990). Modelling the efects of recent stress history on the behaviour of overconsolidated soils. **Ph.D. thesis**, City University, London.

Suebsuk, J., Horpibulsuk, S., and Liu, M. D. (2010). Modified Structured Cam Clay: a generalised critical state model for destructured, naturally structured and artificially structured clays. **Computers and Geotechnics**. 37(7-8): 956-968.

Taiebat, M., Dafalias, Y. F., and Peek, P. (2009). A destructuration theory and its application to SANICLAY model. **International Journal for Numerical and Analytical Methods in Geomechanics**. 34(10): 1009-1040.

Whittle, A. J. (1993). Evaluation of a constitutive model for overconsolidated clays. **Geotechnique**. 43(2): 289-313.

Wissa, A. E. Z., Ladd, C. C., and Lambe, T. W. (1965). Effective stress strength parameters of stabilized soils. **Proceedings of 6th International Conference on Soil Mechanics and Foundation Engineering** (pp. 412-416).

Wroth, C. P., and Houlsby, G. T. (1985). Soil mechanics; characterization of the properties and calculation processes. **Boletim Geotechnico** (pp. 167-179), Univ. Nova Lisboa, Seccao Autonoma de Geotecnia da Caparica, Portugal.

Yang, C., Cui, Y. J., Pereira, J. M., and Huang, M. S. (2008). A constitutive model for unsaturated cemented soils under cyclic loading. **Computers and Geotechnics**. 35(6): 853-859.

Yang, C., Huang, M. S., and Cui, Y. J. (2010). Constitutive Model of Unsaturated Structured Soils under Cyclic Loading. **Unsaturated Soils, Proceedings of the fifth international conference on unsaturated soils** (pp. 987-992).

Yu, H. S., Khong, C. D., and Wang, J. (2007). A unified plasticity model for cyclic behaviour of clay and sand. **Mechanics Research Communications**. 34: 97-114.

CHAPTER V

APPLICATION OF THE MODIFIED STRUCTURED CAM CLAY MODEL IN FINITE ELEMENT ANALYSIS

5.1 Introduction

The most widely used procedure for determining stress-strain-strength characteristics of naturally and artificially soil is the triaxial compression test. The conventional triaxial tests on artificially structured soils have been carried out for investigation of the mechanical behaviour and verification of the constitutive model during the last two decades (Huang and Airey, 1998; Kasama et al., 2000; Miura et al., 2001; Ismail et al., 2002; Uddin and Buensuceso, 2002; Horpibulsuk et al., 2004; Kamruzzaman et al., 2009). In the conventional triaxial test, the cylindrical soil specimen with a height to diameter of 2 is assumed to be subjected to the axial and radial compression stresses, which represent the three principal stresses. The axial and radial strains are determined from the measured volume change and axial deformation. The soil specimen would satisfy that assumption when it deforms uniformly during the test and there is no shear stress, τ developed in the specimen. However, many effects can lead to the inhomogeneous behaviour during the triaxial test such as geometry, end restraint, insufficient drainage, membrane effects, self weight, instability of soil structure and etc. These effects cause the instability of

material and the geometric instability of the deformation. Several numerical studies have been carried out to investigate the inhomogeneous stress-strain behaviour of reconstituted clay. Some studies of the finite element analysis have performed by using the Modified Cam Clay (MCC) model (e.g., Carter, 1982; Airey, 1991; Sheng et al., 1997). The MCC model has a limitation for describing the influence of soil-cementation structure and destructuring, which are the main aspects controlling the structured clays behaviour (Cotecchia and Chandler, 2000; Callisto and Rampello, 2004; Horpibulsuk et al., 2010). The instability of material is related to the strain hardening or softening characteristics due to either the destructuring or crushing of soil-cementation structure processes. An advancement of critical state models for structured clays have been presented recently based on the MCC model (Asaoka et al., 2000; Kavvadas and Amorosi, 2000; Rouainia and Muir Wood, 2000; Liu and Carter, 2002; Baudet and Stallebrass, 2004; Lee et al., 2004; Horpibulsuk et al., 2010; Suebsuk et al., 2010).

Liyanapathirana et al. (2005) have studied the influence of destructuring process on the inhomogeneous behaviour of triaxial specimen of naturally structured clay by a finite element analysis using the Structured Cam Clay (SCC) model (Liu and Carter, 2002). For the simulation of the inhomogeneous soil behaviour of artificially structured clay in a triaxial test, a realistic constitutive model is required. Such a model should take into account for the important features of structured soil behaviour. Although the SCC model can present the volumetric hardening and destructuring of structured clay behaviour well, it has limitations for predicting the strain softening behaviour and does not consider the cohesion effect, which are the key features of highly structured and cemented soil (Horpibulsuk et al., 2010).

The Modified Structured Cam Clay (MSCC) model (Suebsuk et al., 2010) is one of the simple and rational models, which can well predict the volumetric hardening and softening processes of destructured and structured clays. Although the MSCC model shows a good performance in single soil element analysis, the applications to boundary value problems are limited. The implementation of the MSCC model into numerical analysis, such as finite element method, is therefore required for an application in geotechnical practices.

The aim of the present study is to extend the MSCC model into the generalised stress space by the assumption that the shape of failure surface in deviatoric plane follows the function proposed by Sheng et al. (2000). The continuum Jacobian of the MSCC model have been formulated and implemented into the finite element code to study the inhomogeneous stress-strain-strength behaviour influenced by an increase in the degree of soil cementation structure. The MSCC model formulated with a continuum Jacobian has been coded into the commercial finite element program, ABAQUS (2009) by the user subroutine, named UMAT. The generalised MSCC model has been used to study a triaxial compression test of cemented clays specimen with various cement contents under drained and undrained conditions by a couple hydro-mechanic finite element analysis. The influence of structural properties on degree of inhomogeneity is studied. The simulation has been made to illustrate the effect of soil cementation structure under various cement contents and initial stress states. The triaxial specimen with a height to diameter ratio of 2 and axisymetric problem has been considered for the simulation. The distribution of stress and strain in the cemented specimen for different structural properties is compared with those of the reconstituted specimen under various isotropic yield stress ratios (YSRiso,

p'_y / p'_i). Finally, the key aspects of finite element simulation of cemented clay are summarised and discussed.

5.2 General formulation for finite element implementation

The key procedure in finite element analysis of material non-linearity involves integrating the stress-strain relations to obtain the unknown increment in the stresses. These relations define as a set of ordinary differential equations. However, the finite element deals with the incremental calculation, so the differential equations cannot be directly used in the finite element procedures. Methods for integrating those equations are required. Existing approaches for integrating stress-strain relations at Gauss point can be classified as explicit or implicit schemes. In an implicit scheme, the yield surface, plastic potential gradients and hardening law are evaluated at unknown stress states and the resulting system of non-linear equations must be solved iteratively. A Newton scheme is popularly used for this purpose. However, in the Newton scheme, the second derivatives of the yield function and plastic potential are required to implement the iteration. This leads to inconvenient formulation for complex plasticity model such as critical state model. In an explicit integration scheme, the yield surface, plastic potential gradients and hardening law are all evaluated at known stress states and no iteration is strictly necessary to predict the final stresses. The explicit scheme employs the standard elastoplastic constitutive law and requires only first derivatives of the yield function and plastic potential. It has an advantage of being more straightforward to implement for finite element analysis. The explicit scheme has also successfully been applied to many critical state soil models (Potts and Gens, 1985; Britto and Gunn, 1987; Sheng et al., 2000; Luccioni et al., 2001; Sheng and Sloan,

2001; Zhao et al., 2005). The explicit stress integration is adopted in the present study. The general formulation for explicit scheme is presented in this section.

5.2.1 Stiffness equation and stress integration

During a typical step or iteration of an elastoplastic finite element analysis, the forces are applied in increments and the corresponding nodal displacement increments are found from the global stiffness equations. The following system of ordinary differential equations is to be solved,

$$d\sigma = \left[D_{ep} \right] d\varepsilon \,, \tag{5.1}$$

$$dh = d\lambda A \,, \tag{5.2}$$

where $d\sigma$ and $d\varepsilon$ are the rate of stress and strain, respectively, dh is the rate of hardening parameter. The elastoplastic stiffness matrix, $\left[D_{ep} \right]$ and plastic multiplier, $d\lambda$ can be defined by a set of equation as follows,

$$\left[D_{ep} \right] = \left[D_e \right] - \frac{\left[D_e \right] \left\{ \frac{\partial G}{\partial \sigma} \right\} \left\{ \frac{\partial F}{\partial \sigma} \right\}^T \left[D_e \right]}{\left\{ \frac{\partial F}{\partial \sigma} \right\}^T \left[D_e \right] \left\{ \frac{\partial G}{\partial \sigma} \right\} + H}, \tag{5.3}$$

$$[D_e]=\begin{bmatrix} K+\frac{4}{3}G & K-\frac{2}{3}G & K-\frac{2}{3}G & 0 & 0 & 0 \\ & K+\frac{4}{3}G & K-\frac{2}{3}G & 0 & 0 & 0 \\ & & K+\frac{4}{3}G & 0 & 0 & 0 \\ & & & G & 0 & 0 \\ & & & & G & 0 \\ sym. & & & & & G \end{bmatrix}, \tag{5.4}$$

$$d\lambda=\frac{\left\{\frac{\partial F}{\partial \sigma}\right\}^T [D_e] d\varepsilon}{\left\{\frac{\partial F}{\partial \sigma}\right\}^T [D_e]\left\{\frac{\partial G}{\partial \sigma}\right\}+H}, \tag{5.5}$$

$$H=-\frac{1}{d\lambda}\frac{\partial F}{\partial k}dh, \tag{5.6}$$

$$\text{and } A=-\frac{H}{\partial F/\partial h}. \tag{5.7}$$

In the above equations, $[D_e]$ is the elastic stiffness matrix, K is the elastic bulk modulus, G is the elastic shear modulus and H is the hardening modulus.

To integrate Equations 5.1 and 5.2 numerically, it is convenient to introduce a pseudo time, *T*, defined by

$$T=\left(t-t_0\right)/\Delta t, \tag{5.8}$$

where t_0 is the time at the start of the load increment, $t_0 + \Delta t$ is the time at the end of the load increment, and $0 \le T \le 1$. Since $dT / dt = 1/\Delta t$, Equations 5.1 and 5.2 can be rewritten as follows:

$$\frac{d\sigma'}{dT} = \left[D_{ep} \right] \Delta\varepsilon = \Delta\sigma'_e - \Delta\lambda \left[D_e \right] \left\{ \frac{\partial G}{\partial \sigma} \right\}, \tag{5.9}$$

$$\frac{dh}{dT} = d\lambda \Delta t A = \Delta\lambda A, \tag{5.10}$$

where

$$\Delta\lambda = \frac{\left\{ \frac{\partial F}{\partial \sigma} \right\}^T \left[D_e \right] \Delta\varepsilon}{\left\{ \frac{\partial F}{\partial \sigma} \right\}^T \left[D_e \right] \left\{ \frac{\partial G}{\partial \sigma} \right\} + H} = \frac{\left\{ \frac{\partial F}{\partial \sigma} \right\}^T \Delta\sigma_e}{\left\{ \frac{\partial F}{\partial \sigma} \right\}^T \left[D_e \right] \left\{ \frac{\partial G}{\partial \sigma} \right\} + H}. \tag{5.11}$$

Equations 5.9 and 5.10 define a classical initial value problem to be integrated over the pseudo-time interval $T = 0$ to 1.

5.2.2 Isotropic hardening plasticity implementation

The algorithm for an explicit integration (Euler's forward scheme) with a continuum Jacobian is summarised as follows. All quantities are assumed to be given at time, *t*, that is, at the start of the time increment:

(i) Determine the yield function, $F = f(\sigma, h)$.

(ii) Determine if actively yielding, Is $F > 0$?

(iii) Determine the plastic multiplier,

$$F > 0,\ \ \Delta\lambda = \frac{\left\{\frac{\partial F}{\partial \sigma}\right\}^T [D_e]\Delta\varepsilon}{\left\{\frac{\partial F}{\partial \sigma}\right\}^T [D_e]\left\{\frac{\partial G}{\partial \sigma}\right\} + H} \quad \text{or} \quad F < 0,\ \ \Delta\lambda = 0\,. \tag{5.12}$$

(iv) Determine stress and isotropic hardening increments,

$$\{\Delta\sigma\} = [D_e]\{\Delta\varepsilon^e\} = [D_e]\left\{\Delta\varepsilon - \Delta\lambda \cdot \frac{\partial G}{\partial \sigma}\right\}, \tag{5.13}$$

$$\Delta h = f\left(\Delta\varepsilon_v^p\right). \tag{5.14}$$

(v) Update all quantities to the end of the time increment, using Euler's forward scheme,

$$\sigma_{t+\Delta t} = \sigma + \Delta\sigma\,, \tag{5.15}$$

$$\varepsilon^p_{t+\Delta t} = \varepsilon^p + \Delta\varepsilon^p\,, \tag{5.16}$$

$$h_{t+\Delta t} = h + \Delta h\,. \tag{5.17}$$

(vi) Determine Jacobian,

$$[J] = [D_e] - \frac{[D_e]\left\{\frac{\partial G}{\partial \sigma}\right\}\left\{\frac{\partial F}{\partial \sigma}\right\}^T [D_e]}{\left\{\frac{\partial F}{\partial \sigma}\right\}^T [D_e]\left\{\frac{\partial G}{\partial \sigma}\right\} + H}. \tag{5.18}$$

(vii) End.

5.3 Generalisation of the MSCC model into the three-dimensional stress space

The q and p' are used to describe the formulation of MSCC model entirely in Chapter III, which are related to the conventional triaxial test. However, the geotechnical applications deal with either the two-dimensional (axisymmetry or plain strain) or three-dimension problems that the stresses and strains are in the generalised form. Thus, to extend the MSCC model to a generalised stress space, the stress state is reformulated in this section. The yield surface and plastic potential shapes extended in deviatoric plane are presented and the variations of those surfaces over stress change are derived.

5.3.1 Yield surface and plastic potential shapes

In the finite element formulation, the MSCC model has generalised into the three dimensional stress space by making some assumption about the shapes of the yield and the plastic potential surfaces in the deviatoric plane. The simplest generalisation is to assume a circular shape (Roscoe and Burland, 1968). However, it is well known that a circle does not provide a good representation of the failure condition for soils whereas a Mohr-Coulomb type of failure criterion is more appropriate. The yield surface and plastic potential functions presented in Chapter III have introduced by the Lode angle (θ) as follows,

$$F = \frac{q^2}{\left(p_0' + p_b'\right)^2} + \frac{M^2\left(p' + p_b'\right)\left(p_0' - p'\right)}{\left(p_0' + p_b'\right)^2} = 0\,, \tag{5.19}$$

$$G = \frac{q^2}{\left(p_p' + p_b'\right)^2} + \frac{M^2}{1-\psi}\left(\left(\frac{p' + p_b'}{p_p' + p_b'}\right)^{\frac{2}{\psi}} - \left(\frac{p' + p_b'}{p_p' + p_b'}\right)^2\right) = 0\,. \tag{5.20}$$

The gradient of critical state line (M) is expressed as a function of θ, which is assumed to satisfy the failure envelope proposed by Sheng et al. (2000) as follows:

$$M = M_{\max}\left[\frac{2\alpha^4}{1+\alpha^4 - \left(1-\alpha^4\right)\sin 3\theta}\right]^{\frac{1}{4}}, \tag{5.21}$$

where $\alpha = \dfrac{3-\sin\phi'}{3+\sin\phi'}$, ϕ' is a friction angle of the soil at critical state and $M_{\max}$ is a gradient of critical state line under triaxial compression test ($\theta = -30°$) in the q'-p plane. The shapes of the yield and plastic potential surfaces in the deviatoric plane are shown in Figure 5.1.

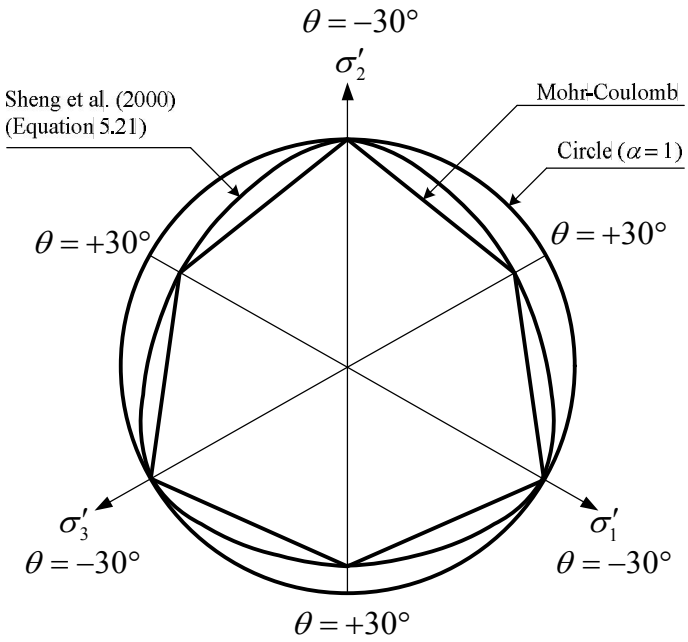

Figure 5.1 The shapes of the yield surface and plastic potential in deviatoric plane

5.3.2 Derivation of yield and plastic potential equations in the generalised form

Based on the yield and plastic potential equations for the MSCC model proposed in Chapter III, the differentiating values with respect to stress, σ, are derived by the application of chain rule as follows,

$$\frac{\partial F}{\partial \sigma} = \frac{\partial F}{\partial p'}\frac{\partial p'}{\partial \sigma} + \frac{\partial F}{\partial q}\frac{\partial q}{\partial \sigma} + \frac{\partial F}{\partial M}\frac{\partial M}{\partial \theta}\frac{\partial \theta}{\partial \sigma}, \tag{5.22}$$

where

$$\frac{\partial F}{\partial p'} = M^2 \frac{\left(2p' + p'_b - p'_0\right)}{\left(p'_0 + p'_b\right)^2},$$

$$\frac{\partial p'}{\partial \sigma} = \frac{1}{3}\begin{bmatrix}1 & 1 & 1 & 0 & 0 & 0\end{bmatrix},$$

$$\frac{\partial F}{\partial q} = \frac{2q}{\left(p_0' + p_b'\right)^2},$$

$$\frac{\partial q}{\partial \sigma} = \frac{3}{2q}\left[\left(\sigma_x - p'\right) \quad \left(\sigma_y - p'\right) \quad \left(\sigma_z - p'\right) \quad 2\tau_{xy} \quad 2\tau_{zx} \quad 2\tau_{yz}\right],$$

$$\frac{\partial F}{\partial M} = 2M\frac{\left(p'^2 + p'p_b' - p'p_0 - p_b'p_0'\right)}{\left(p_0' + p_b'\right)^2},$$

$$\frac{\partial M}{\partial \theta} = \frac{3\sqrt[4]{2}}{4} M_{\max} \frac{\alpha\left(\alpha^4 - 1\right)\cos 3\theta}{\left[1 + \alpha^4 - \left(1 - \alpha^4\right)\sin 3\theta\right]^{\frac{5}{4}}},$$

$$\frac{\partial \theta}{\partial \sigma} = \frac{9}{2\cos\left(3\theta\right)q^3}\left[\frac{3\det s}{q}\left\{\frac{\partial q}{\partial \sigma}\right\} - \left\{\frac{\partial \det s}{\partial \sigma}\right\}\right],$$

$$\frac{\partial \det s}{\partial \sigma_x} = 2p'^2 - \frac{2}{3}\sigma_x\left(\sigma_y + \sigma_z\right) - \frac{1}{3}\left(\sigma_y^2 + \sigma_z^2\right) + \frac{1}{3}\left(\tau_{xy}^2 + \tau_{zx}^2 - 2\tau_{yz}^2\right),$$

$$\frac{\partial \det s}{\partial \sigma_y} = 2p'^2 - \frac{2}{3}\sigma_y\left(\sigma_x + \sigma_z\right) - \frac{1}{3}\left(\sigma_x^2 + \sigma_z^2\right) + \frac{1}{3}\left(\tau_{xy}^2 + \tau_{yz}^2 - 2\tau_{zx}^2\right),$$

$$\frac{\partial \det s}{\partial \sigma_z} = 2p'^2 - \frac{2}{3}\sigma_z\left(\sigma_y + \sigma_x\right) - \frac{1}{3}\left(\sigma_y^2 + \sigma_x^2\right) + \frac{1}{3}\left(\tau_{yz}^2 + \tau_{zx}^2 - 2\tau_{xy}^2\right),$$

$$\frac{\partial \det s}{\partial \tau_{xy}} = -2\tau_{xy}\left(\sigma_z - p'\right) + 2\tau_{zx}\tau_{yz},$$

$$\frac{\partial \det s}{\partial \tau_{zx}} = -2\tau_{zx}\left(\sigma_y - p'\right) + 2\tau_{yz}\tau_{xy},$$

$$\frac{\partial \det s}{\partial \tau_{yz}} = -2\tau_{yz}\left(\sigma_x - p'\right) + 2\tau_{zx}\tau_{xy}.$$

In case of $\alpha = 1.0$ (circular), $M = M_{\max}$, hence,

$$\frac{\partial F}{\partial \sigma_x} = \frac{M_{\max}^2 \left(2p' + p_b' - p_0'\right)}{3\left(p_0' + p_b'\right)^2} + \frac{3\left(\sigma_x - p'\right)}{\left(p_0' + p_b'\right)^2}, \tag{5.23a}$$

$$\frac{\partial F}{\partial \sigma_y} = \frac{M_{\max}^2 \left(2p' + p_b' - p_0'\right)}{3\left(p_0' + p_b'\right)^2} + \frac{3\left(\sigma_y - p'\right)}{\left(p_0' + p_b'\right)^2}, \tag{5.23b}$$

$$\frac{\partial F}{\partial \sigma_z} = \frac{M_{\max}^2 \left(2p' + p_b' - p_0'\right)}{3\left(p_0' + p_b'\right)^2} + \frac{3\left(\sigma_z - p'\right)}{\left(p_0' + p_b'\right)^2}, \tag{5.23c}$$

$$\frac{\partial F}{\partial \tau_{xy}} = \frac{6\tau_{xy}}{\left(p_0' + p_b'\right)^2}, \tag{5.23d}$$

$$\frac{\partial F}{\partial \tau_{zx}} = \frac{6\tau_{zx}}{\left(p_0' + p_b'\right)^2}, \tag{5.23e}$$

$$\frac{\partial F}{\partial \tau_{yz}} = \frac{6\tau_{yz}}{\left(p_0' + p_b'\right)^2}. \tag{5.23f}$$

$$\frac{\partial G}{\partial \sigma} = \frac{\partial G}{\partial p'}\frac{\partial p'}{\partial \sigma} + \frac{\partial G}{\partial q}\frac{\partial q}{\partial \sigma} + \frac{\partial G}{\partial M}\frac{\partial M}{\partial \theta}\frac{\partial \theta}{\partial \sigma}, \tag{5.24}$$

where

$$\frac{\partial G}{\partial p'} = \frac{2M^2}{(1-\psi)}\left(\frac{\left(\dfrac{p'+p'_b}{p'_p+p'_b}\right)^{\frac{2}{\psi}}}{\psi\left(p'+p'_b\right)} - \frac{\left(p'+p'_b\right)}{\left(p'_p+p'_b\right)^2}\right),$$

$$\frac{\partial p'}{\partial \sigma} = \frac{1}{3}\begin{bmatrix}1 & 1 & 1 & 0 & 0 & 0\end{bmatrix},$$

$$\frac{\partial G}{\partial q} = \frac{2q}{\left(p'_p+p'_b\right)^2},$$

$$\frac{\partial q}{\partial \sigma} = \frac{3}{2q}\begin{bmatrix}\left(\sigma_x - p'\right) & \left(\sigma_y - p'\right) & \left(\sigma_z - p'\right) & 2\tau_{xy} & 2\tau_{zx} & 2\tau_{yz}\end{bmatrix},$$

$$\frac{\partial G}{\partial M} = \frac{2M}{(1-\psi)}\left(\left(\frac{p'+p'_b}{p'_p+p'_b}\right)^{\frac{2}{\psi}} - \frac{\left(p'+p'_b\right)^2}{\left(p'_p+p'_b\right)^2}\right).$$

In case of $\alpha = 1.0$ (circular), $M = M_{\max}$, hence,

$$\frac{\partial G}{\partial \sigma_x} = \frac{2M^2}{3(1-\psi)}\left(\frac{\left(\dfrac{p' + p'_b}{p'_p + p'_b} \right)^{\frac{2}{\psi}}}{\psi\left(p' + p'_b\right)} - \frac{\left(p' + p'_b\right)}{\left(p'_p + p'_b\right)^2} \right) + \frac{3\left(\sigma_x - p'\right)}{\left(p'_p + p'_b\right)^2}, \tag{5.25a}$$

$$\frac{\partial G}{\partial \sigma_y} = \frac{2M^2}{3(1-\psi)}\left(\frac{\left(\dfrac{p' + p'_b}{p'_p + p'_b} \right)^{\frac{2}{\psi}}}{\psi\left(p' + p'_b\right)} - \frac{\left(p' + p'_b\right)}{\left(p'_p + p'_b\right)^2} \right) + \frac{3\left(\sigma_y - p'\right)}{\left(p'_p + p'_b\right)^2}, \tag{5.25b}$$

$$\frac{\partial G}{\partial \sigma_z} = \frac{2M^2}{3(1-\psi)}\left(\frac{\left(\dfrac{p' + p'_b}{p'_p + p'_b} \right)^{\frac{2}{\psi}}}{\psi\left(p' + p'_b\right)} - \frac{\left(p' + p'_b\right)}{\left(p'_p + p'_b\right)^2} \right) + \frac{3\left(\sigma_z - p'\right)}{\left(p'_p + p'_b\right)^2}, \tag{5.25c}$$

$$\frac{\partial G}{\partial \tau_{xy}} = \frac{6\tau_{xy}}{\left(p'_p + p'_b\right)^2}, \tag{5.25d}$$

$$\frac{\partial G}{\partial \tau_{zx}} = \frac{6\tau_{zx}}{\left(p'_p + p'_b\right)^2}, \tag{5.25e}$$

$$\frac{\partial G}{\partial \tau_{yz}} = \frac{6\tau_{yz}}{\left(p'_p + p'_b\right)^2}. \tag{5.25f}$$

The hardening modulus for the MSCC model can be formulated as follows,

$$H = -\frac{1}{d\lambda}\frac{\partial F}{\partial k}dk = -\frac{1}{d\lambda}\frac{\partial F}{\partial p_0'}dp_0', \tag{5.26}$$

where

$$\frac{\partial F}{\partial p_0'} = -\frac{2q^2 - M^2 p' p_0' + 3M^2 p' p_b' - M^2 p_b' p_0' + M^2 p_b'^2 + 2M^2 p'^2}{\left(p_0' + p_b'\right)^3},$$

$$dp_0' = \frac{p_0'\left(1+e\right)}{\left(\lambda^* - \kappa\right) + b\Delta e\left(\dfrac{M}{M-\bar{\eta}}\right)} d\lambda \frac{\partial G}{\partial p'},$$

$$\frac{\partial G}{\partial p'} = \frac{2M^2}{1+\psi}\left(\frac{\left(\dfrac{p'+p_b'}{p_p'+p_b'}\right)^{\frac{2}{\psi}}}{\psi\left(p'+p_b'\right)} - \frac{\left(p'+p_b'\right)}{\left(p_p'+p_b'\right)^2}\right).$$

5.4 Numerical model

The implemented MSCC model described above has been used in the numerical study of triaxial specimen of cemented clays. The structural properties for the MSCC model have been calibrated from the triaxial compression test of cemented Ariake clays. They were carried out under various cement contents and initial stress states (Horpibulsuk, 2001; Horpibulsuk et al., 2004). The inhomogeneous stress and strain behaviour during volumetric hardening and softening of triaxial test due to the effect of soil-cementation structure is studied. A couple hydro-mechanic analysis was used in the calculation, which is provided by the commercial finite element program, ABAQUS (2009). The pore pressure development is governed by the continuity equation, which is coupled to the equilibrium equation through the rate of volume change and the effective stress theory. This is the couple Biot-type consolidation (Small et al., 1976). The MSCC model was coded in FORTRAN90 following the Euler's forward algorithm as presented in section 5.2.2 and then it was implemented into the unified finite element program, ABAQUS via a user subroutine, namely UMAT.

In order to investigate the effect of structural properties on the inhomogeneous stress and strain behaviour in triaxial specimen, the parameters such as the aspect ratio of specimen, the type and number of element and the boundary conditions are kept constant.

5.4.1 Model configuration and boundary condition

The radial x-y plane of a quarter triaxial specimen, 0.025 unit in radius and 0.05 unit in height, is discretised into 50 elements with 8-node axisymmetric bi-quadratic elements. The pore pressure is set as the third degree of freedom at the

corner nodes. The model configuration is set up as shown in Figure 5.2. The top boundary is only allowed to have vertical movement, while the fixed boundary conditions are used for the horizontal displacement at the left end and the vertical displacement at the bottom end. Particularly, the boundary on the right corner of a specimen is set as horizontal fixed for perfectly rough contact and is set as free end for idealised smooth contact. The degree of inhomogeneity is investigated by comparing the stress and strain behaviour of perfectly rough contact case with that of the idealised smooth contact case. During the drained condition, the top and right boundaries are set as permeable, whereas all boundaries are set as impermeable under undrained condition. An global axial strain (ε_a) of 30% is motivated for soil sample at different rates dependent on the test condition. The strain rate are set as 5×10^{-9} m/s for drained condition and 5×10^{-4} m/s for undrained condition. The local stress path and stress strain curves were investigated at certain points within the specimen. Those are element No.1, 5, 23 and 45 as shown in Figure 5.2.

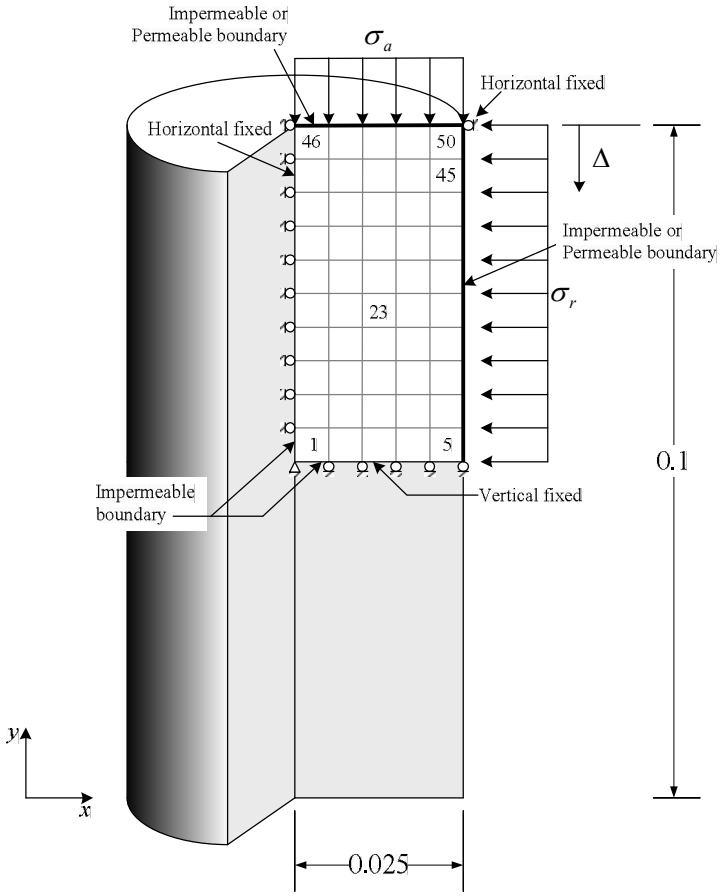

Figure 5.2 Finite element model configuration

5.4.2 Soil model parameters

The model properties for cemented Ariake clay with different cement contents are listed in the Table 5.1. The determination and physical meaning for each parameter are clearly described in the paper by Suebsuk et al. (2010). The intrinsic properties for reconstituted Ariake clay tested are denoted by an asterisk. The other properties are dependent on the soil cementation structure, which were determined from laboratory test results. The initial condition for the simulation is listed for various yield stress ratios in the Table 5.2

Table 5.1 The MSCC model parameters for Ariake clay

Parameters	Ariake clay		
	A_w = 0% (ref.)	A_w = 6%	A_w = 9%
λ^*	0.44	0.44	0.44
κ	0.03	0.01	0.008
M	1.58	1.60	1.45
μ	0.25	0.25	0.25
$p'_{y,i}$	200	50	200
e^*_{IC}	4.37	4.37	4.37
Δe_i	-	1.5	2.25
b	-	0.15	0.01
ψ	2.0	1.8	0.5
p'_{b0}	-	10	100
ξ	-	10	10
k	1×10^{-9}	1×10^{-9}	1×10^{-9}

Table 5.2 Initial condition for the simulation

Initial value	NC	OC			
(a) Uncemented and 9% cement content					
Initial mean effective stress (kPa)	200	100	67	50	40
Coefficient of earth pressure, K_0	1.0				
YSRiso	1.0	2.0	3.0	4.0	5.0
(b) 6% cement content					
Initial mean effective stress (kPa)	50	25	16.7	12.5	10
Coefficient of earth pressure, K_0	1.0				
YSRiso	1.0	2.0	3.0	4.0	5.0

5.5 Numerical results and discussions

5.5.1 Drained triaxial shearing

The end restraint in the case of perfect rough contact regards akin to an additional confinement at the ends of a specimen (Sheng et al., 1997). It prevents the soil mass from moving outwards freely therefore inducing shear stress, τ_{xy}. The distribution of the τ_{xy} within a specimen tested at global axial strain, $\varepsilon_a = 0.3$ under drained condition is shown in Figure 5.3 for different cemented states and YSRiso. In Figure 5.3a (uncemented state), the τ_{xy} develops from the end edges into a specimen in a X-shape and increases with increasing the global axial strain. It is seen that the τ_{xy} decreases with increasing in the YSRiso. It is because the higher confinement for lower the YSRiso prevents the lateral deformation of soil mass. This leads to the small displacement at the ends of specimen. Normally consolidated (NC) specimen shows that the higher τ_{xy} at end edge and more concentrated displacement in the centre of the specimen than those of overconsolidated (OC) specimen. For cemented soil (6% and 9% cement), sample with higher cement content show the higher τ_{xy} at the end edge. In the same way, the τ_{xy} is diminished at the centre of the uncemented and cemented specimens. The X-shape concentration of τ_{xy} leads to the localisation of shear deformation and eventually the formation of shear band (Lade, 1982). The occurrence of the τ_{xy} causes the non-uniform deviatoric stress, plastic volumetric strain and plastic deviatoric strain. At large global axial strain, both of the uncemented and cemented specimens deform in the same way as a barrel shape. In contrast, the τ_{xy} does not develop in the *x-y* plane during the idealised case with perfectly smooth

contact, which means that the axial and radial stresses are the principal stresses and the specimen deforms uniformly along the loading path.

The distributions of deviatoric stress, plastic volumetric strain and deviatoric strain for uncemented and 6% and 9% specimens in normally consolidated state are shown in Figures 5.4, 5.5 and 5.6, respectively. The stress and strain behaviours of both uncemented and cemented specimen are of the same pattern. The non-uniformity increases as the global axial strain and cement content increase. The centre of the specimen experiences both the largest deviatoric stress and the largest deviatoric strain. However the stress concentration occurs at the end edges of a specimen. For OC state (YSRiso = 5.0), the distributions of deviatoric stress, plastic volumetric strain and deviatoric strain for uncemented and 6% and 9% cement specimens are shown in Figures 5.7, 5.8 and 5.9, respectively. Compared to the NC state, the specimens in OC state display higher displacement at the middle than that at the end edge. Another observation from the OC specimen is that the inhomogeneity of volumetric deformation (degree of consolidation) due to the end restraint decreases as the strength of soil cementation structure increases.

The local stress-strain and volumetric behaviours for uncemented and 6% and 9% cement specimens in NC and OC states are shown in Figures 5.10, 5.11 and 5.12, respectively. The development of τ_{xy} leads to the difference in deviatoric strain for each local element. For uncemented specimen, the inhomogeneous behaviour increases with increasing the YSRiso. The inhomogeneous behaviour of cemented specimen increases with increasing the YSRiso and the cement content. At the same stress state, the specimen with 9% cement content (Figure 5.12) displays more pronounced inhomogeneous behaviour when compared to the uncemented specimen

(Figure 5.10). The inhomogeneous behaviour of specimen starts when the stress state of local element reaches the 60-75% of peak strength state ($\bar{\eta} > M$). The local elements show the different peak strengths on the $q - \varepsilon_d$ curves, whereas the maximum deviatoric stress is at the element No. 45. Compared to the idealised perfectly smooth contact, the local stress-strain and volumetric behaviours increase the degree of inhomogeneity with increasing the isotropic yield stress ratio (YSRiso) and the strength degree of soil cementation structure.

The strain softening of soil particle induces the inhomogeneous behaviour; therefore, the development of the shear band and strain localisation of soil specimen. Because of the localisation of soil sample is directly related to the development of inhomogeneous deviatoric strain caused by end restraint or insufficient drainage. In other words, the inhomogeneous behaviour of triaxial specimen increases from the difference in residual deviatoric stress at each local element on the soil specimen, which is caused by the strain softening.

In order to understand the influence of soil structure on the degree of inhomogeneous, the local stress-strain and volumetric behaviours of 0% and 9% cement specimens at the same initial condition are demonstrated in Figure 5.10 and 5.12, respectively. The cemented specimens with higher structure strength, and Δe show more stress inhomogeneities than the uncemented specimen.

(a) Uncemented state ($p'_{y,i}$ = 200 kPa)

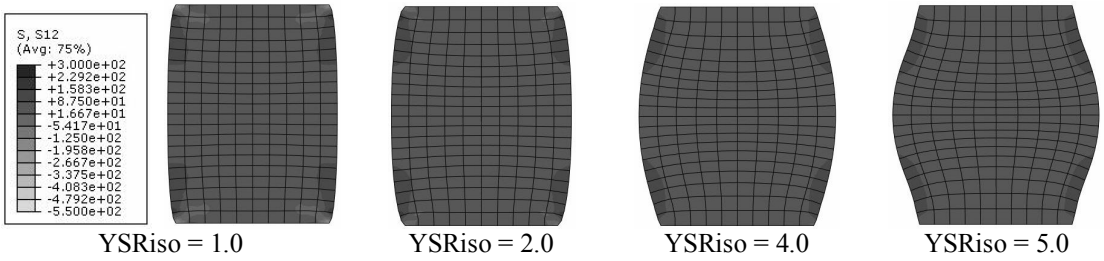

(b) Cemented Ariake clay with 6% cement content ($p'_{y,i}$ = 50 kPa)

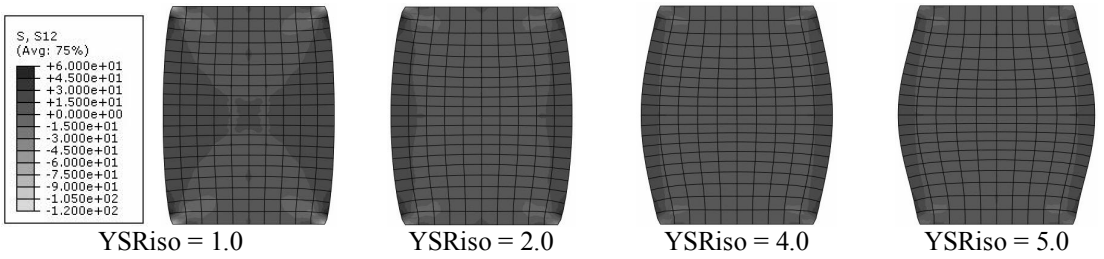

(c) Cemented Ariake clay with 9% cement content ($p'_{y,i}$ = 200 kPa)

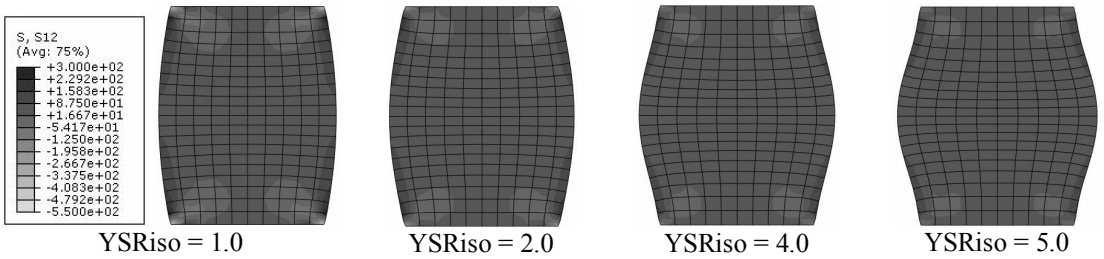

Figure 5.3 Distribution of shear stress, τ_{xy} in uncemented and cemented Ariake clay specimen under drained triaxial compression test with various cement content and YSRiso (at ε_a = 30%)

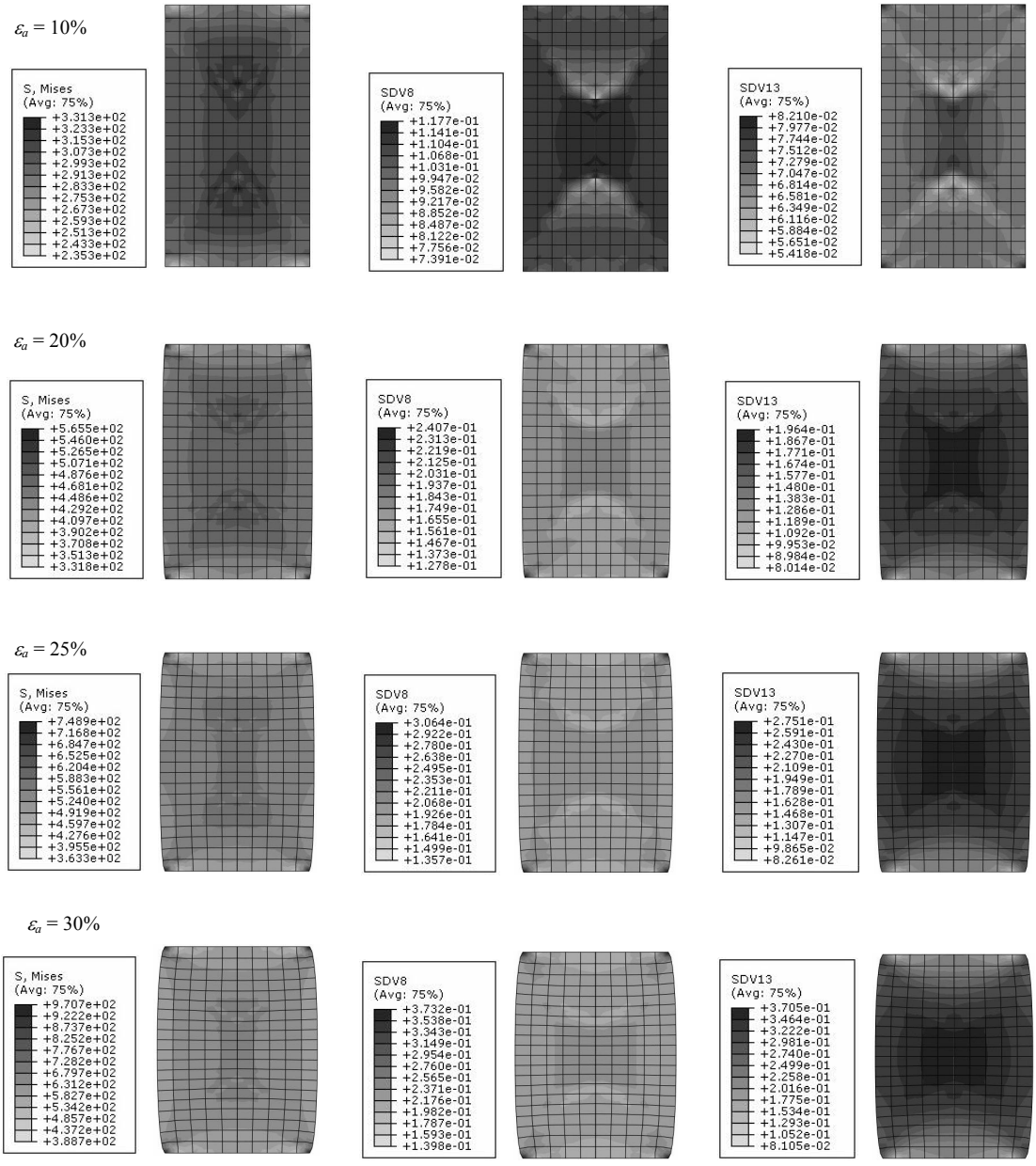

(a) Deviatoric stress, q (b) Plastic volumetric strain, ε_v^p (c) Plastic deviatoric strain, ε_d^p

Figure 5.4 Distribution of (a) deviatoric stress, (b) plastic volumetric strain and (c) plastic deviatoric strain under drained triaxial test of normally consolidated uncemented Ariake clay (YSRiso = 1.0)

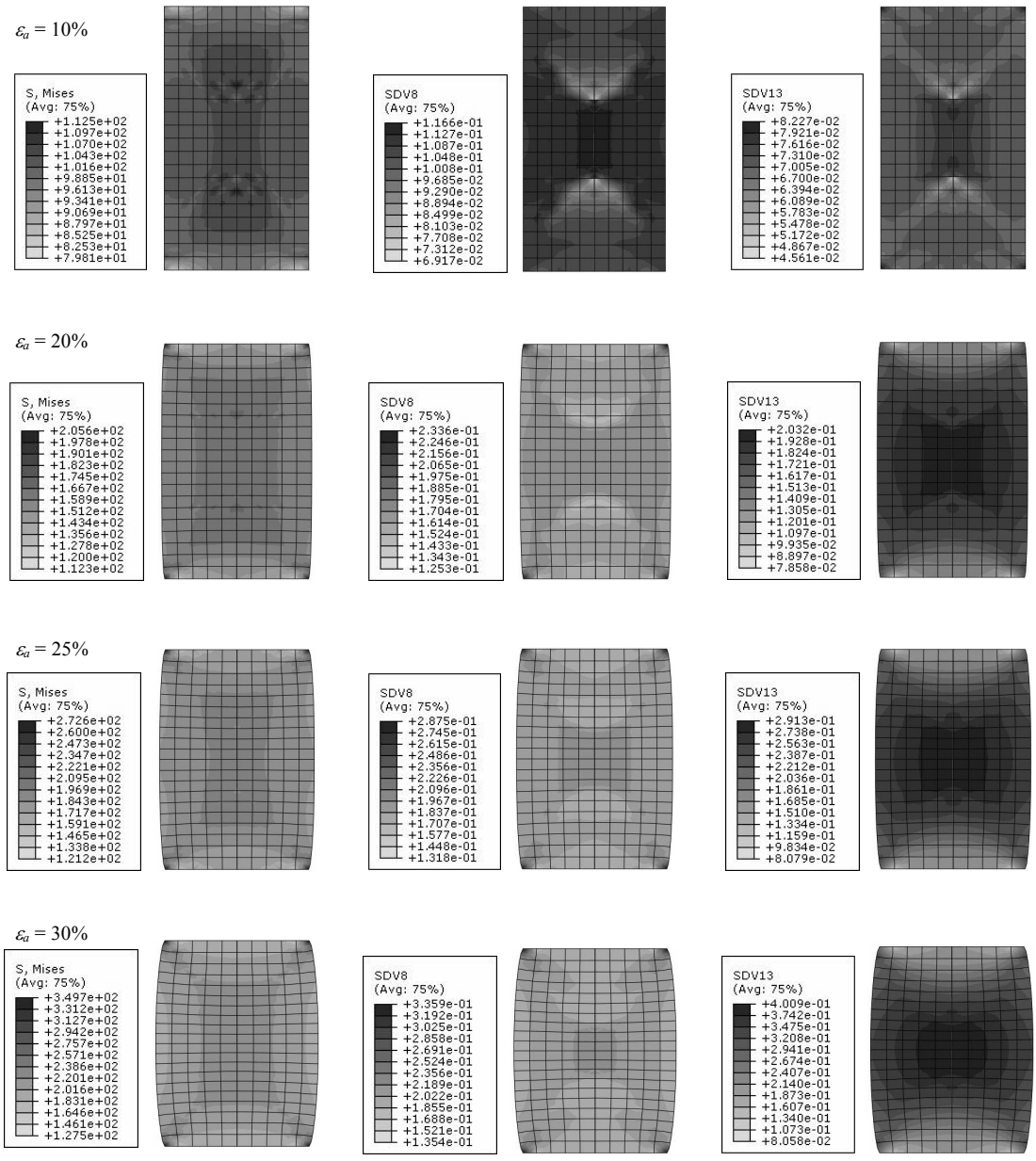

(a) Deviatoric stress, q (b) Plastic volumetric strain, ε_v^p (c) Plastic deviatoric strain, ε_d^p

Figure 5.5 Distribution of (a) deviatoric stress, (b) plastic volumetric strain and (c) plastic deviatoric strain under drained triaxial test of normally consolidated cemented Ariake clay with 6% cement content (YSRiso = 1.0)

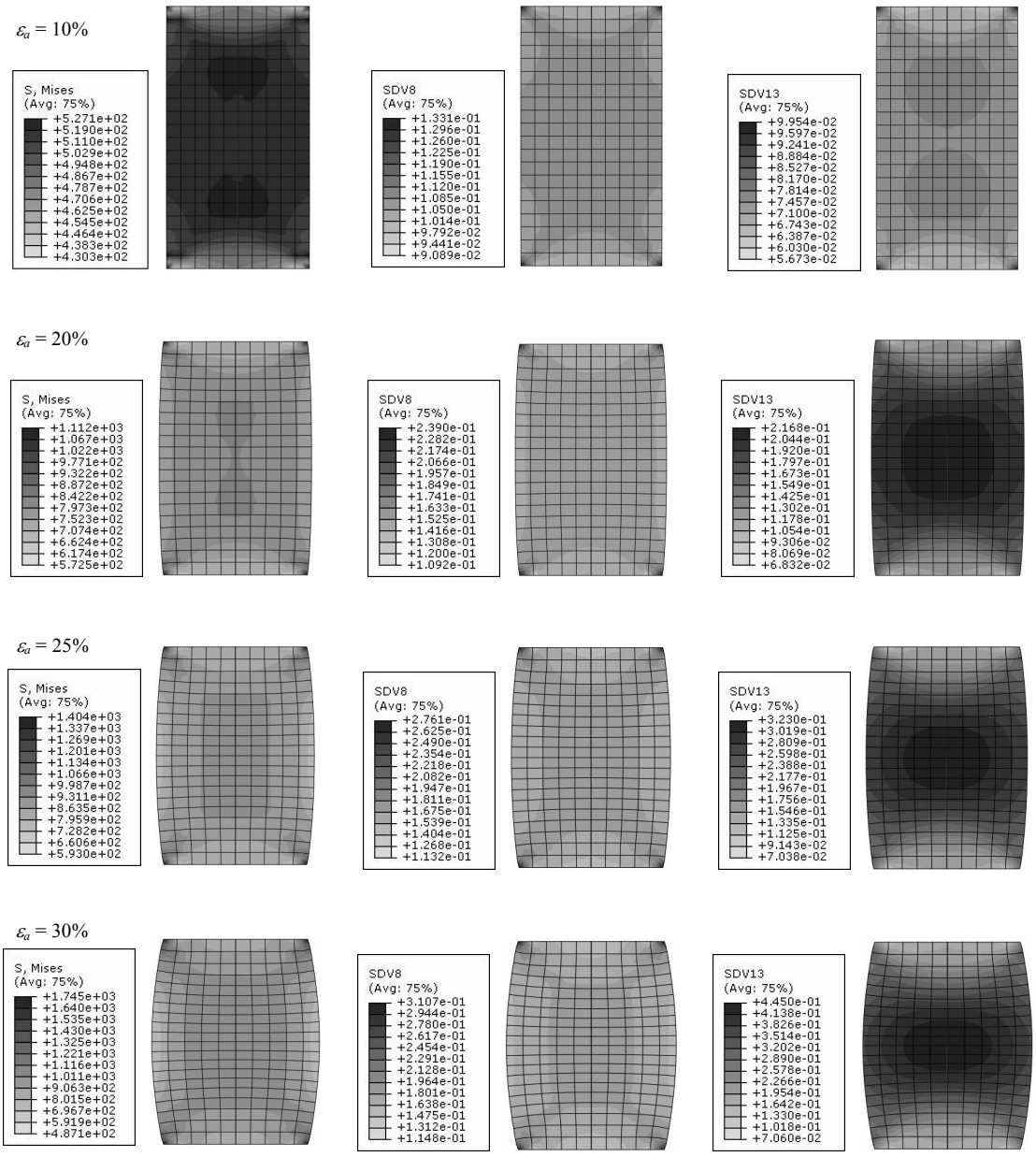

(a) Deviatoric stress, q (b) Plastic volumetric strain, ε_v^p (c) Plastic deviatoric strain, ε_d^p

Figure 5.6 Distribution of (a) deviatoric stress, (b) plastic volumetric strain and (c) plastic deviatoric strain under drained triaxial test of normally consolidated cemented Ariake clay with 9% cement content (YSRiso = 1.0)

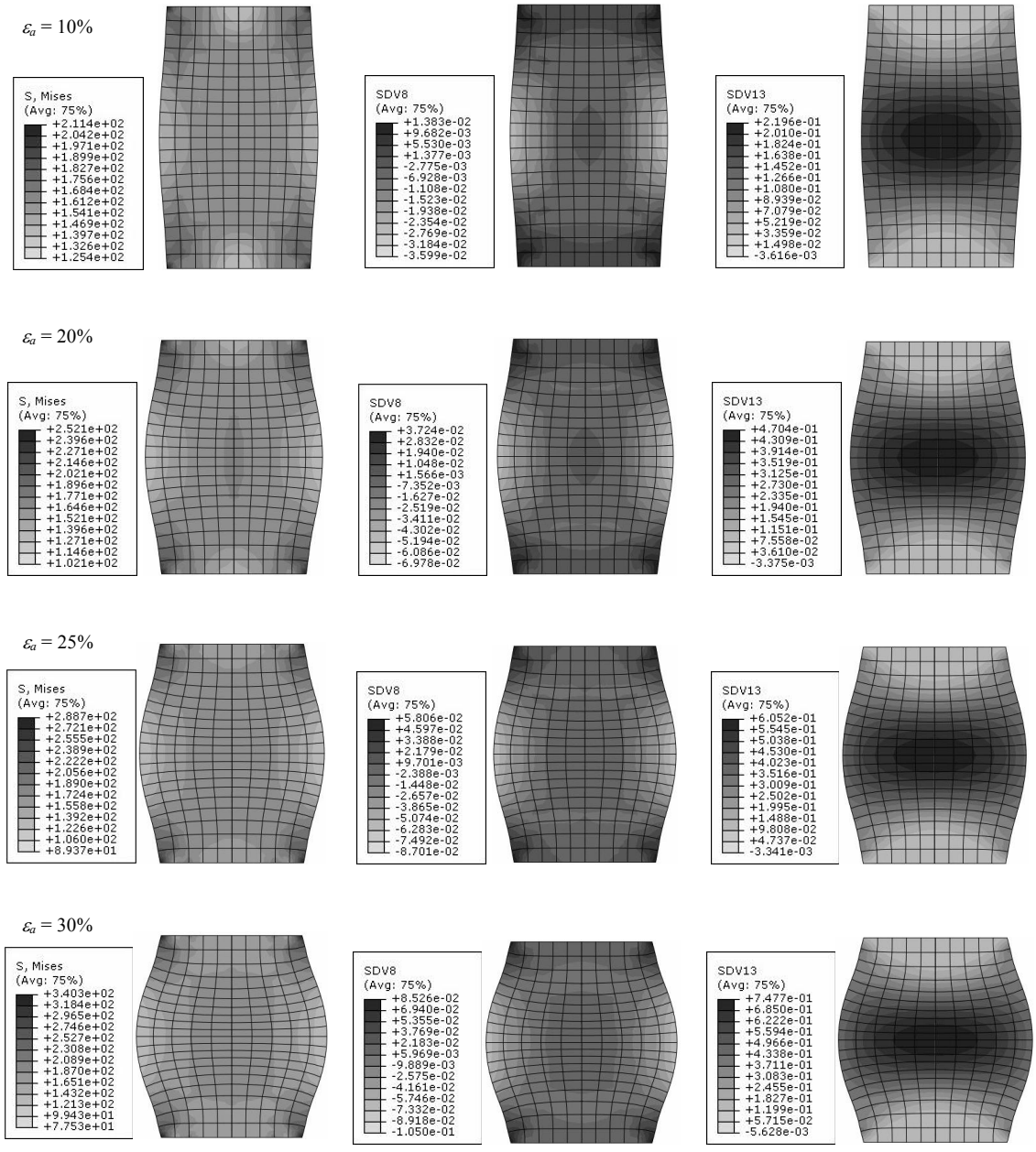

(a) Deviatoric stress, q (b) Plastic volumetric strain, ε_v^p (c) Plastic deviatoric strain, ε_d^p

Figure 5.7 Distribution of (a) deviatoric stress, (b) plastic volumetric strain and (c) plastic deviatoric strain under drained triaxial test of overconsolidated uncemented Ariake clay (YSRiso = 5.0)

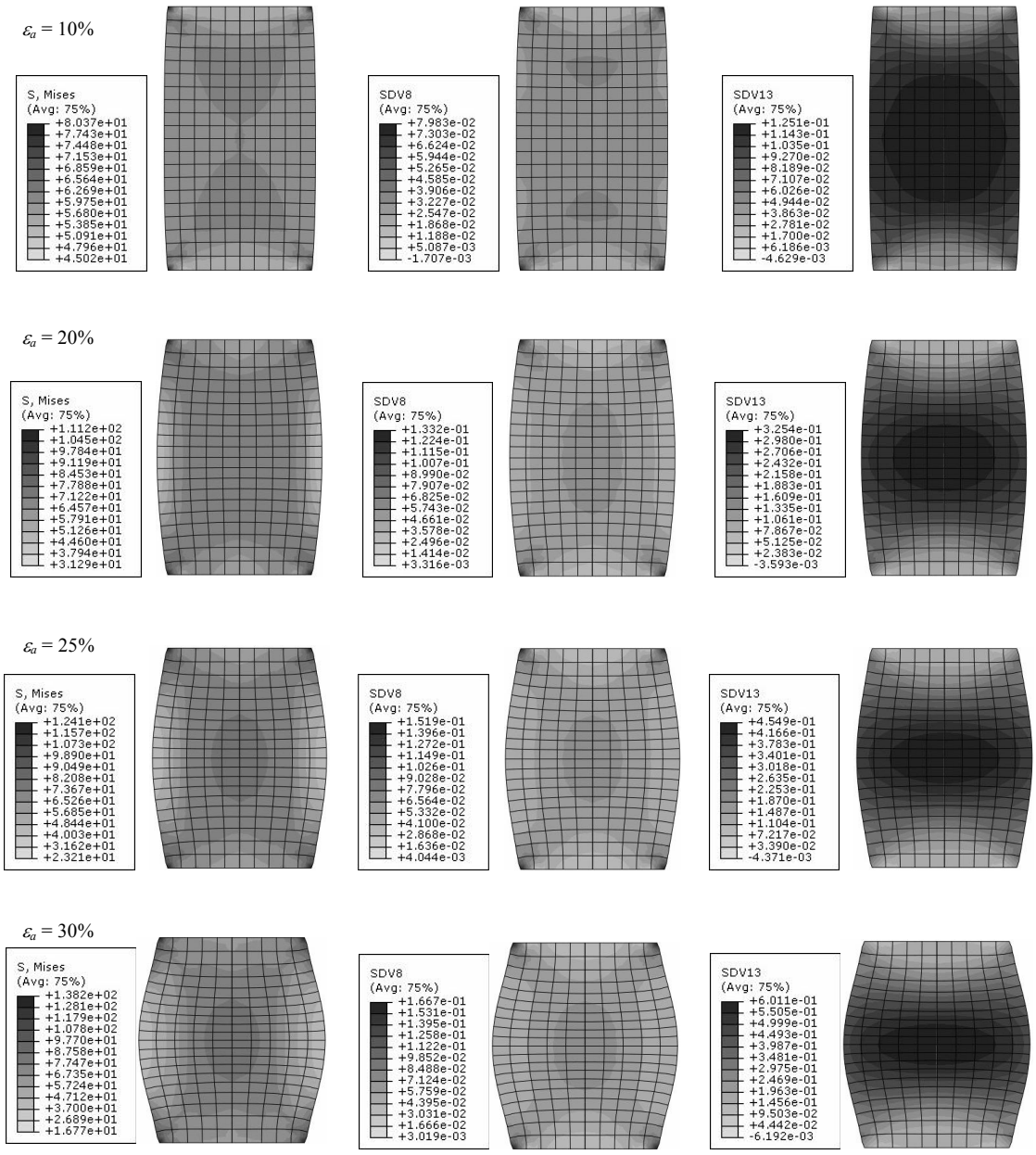

(a) Deviatoric stress, q (b) Plastic volumetric strain, ε_v^p (c) Plastic deviatoric strain, ε_d^p

Figure 5.8 Distribution of (a) deviatoric stress, (b) plastic volumetric strain and (c) plastic deviatoric strain under drained triaxial test of overconsolidated cemented Ariake clay with 6% cement content (YSRiso = 5.0)

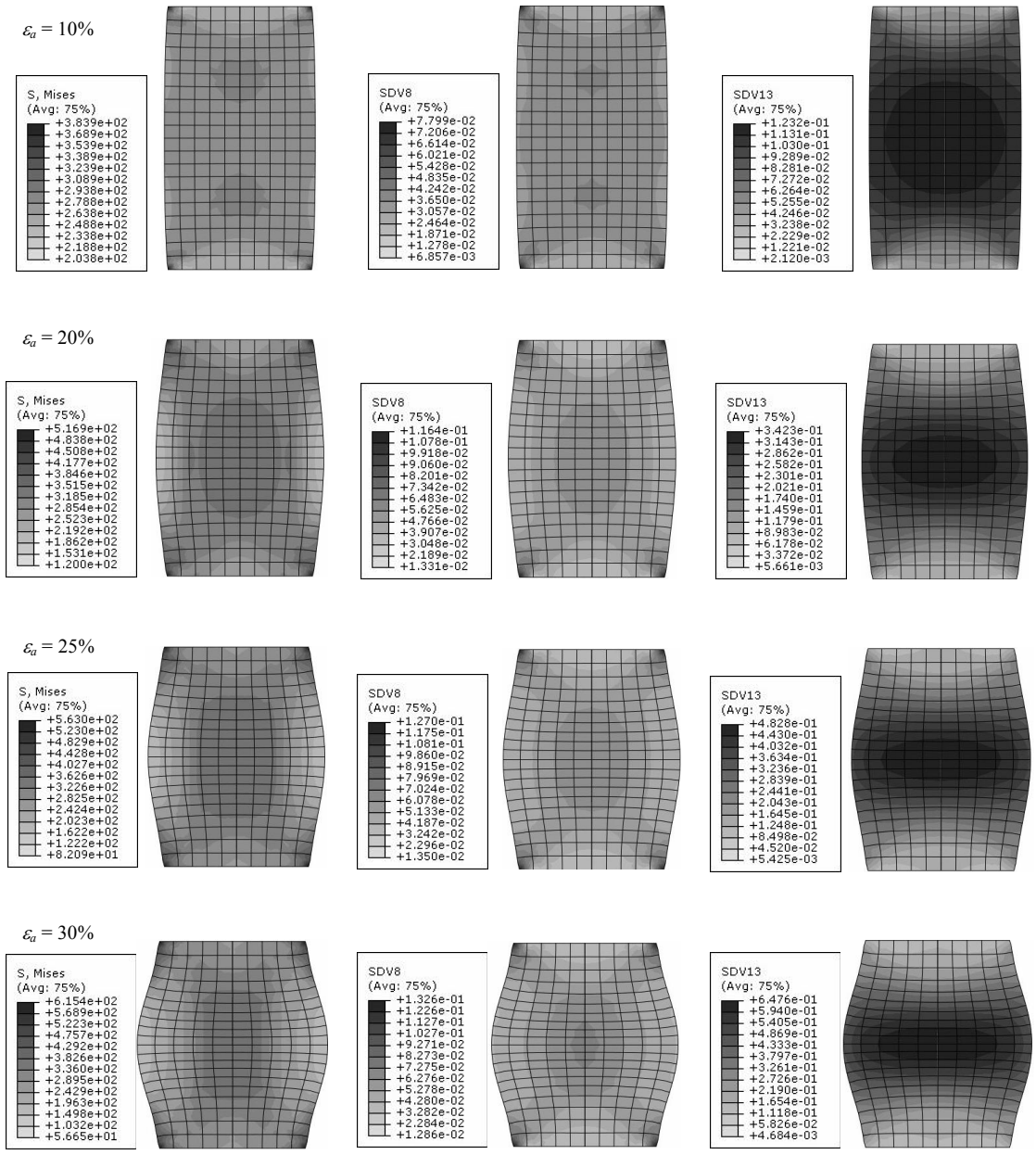

(a) Deviatoric stress, q (b) Plastic volumetric strain, ε_v^p (c) Plastic deviatoric strain, ε_d^p

Figure 5.9 Distribution of (a) deviatoric stress, (b) plastic volumetric strain and (c) plastic deviatoric strain under drained triaxial test of overconsolidated cemented Ariake clay with 9% cement content (YSRiso = 5.0)

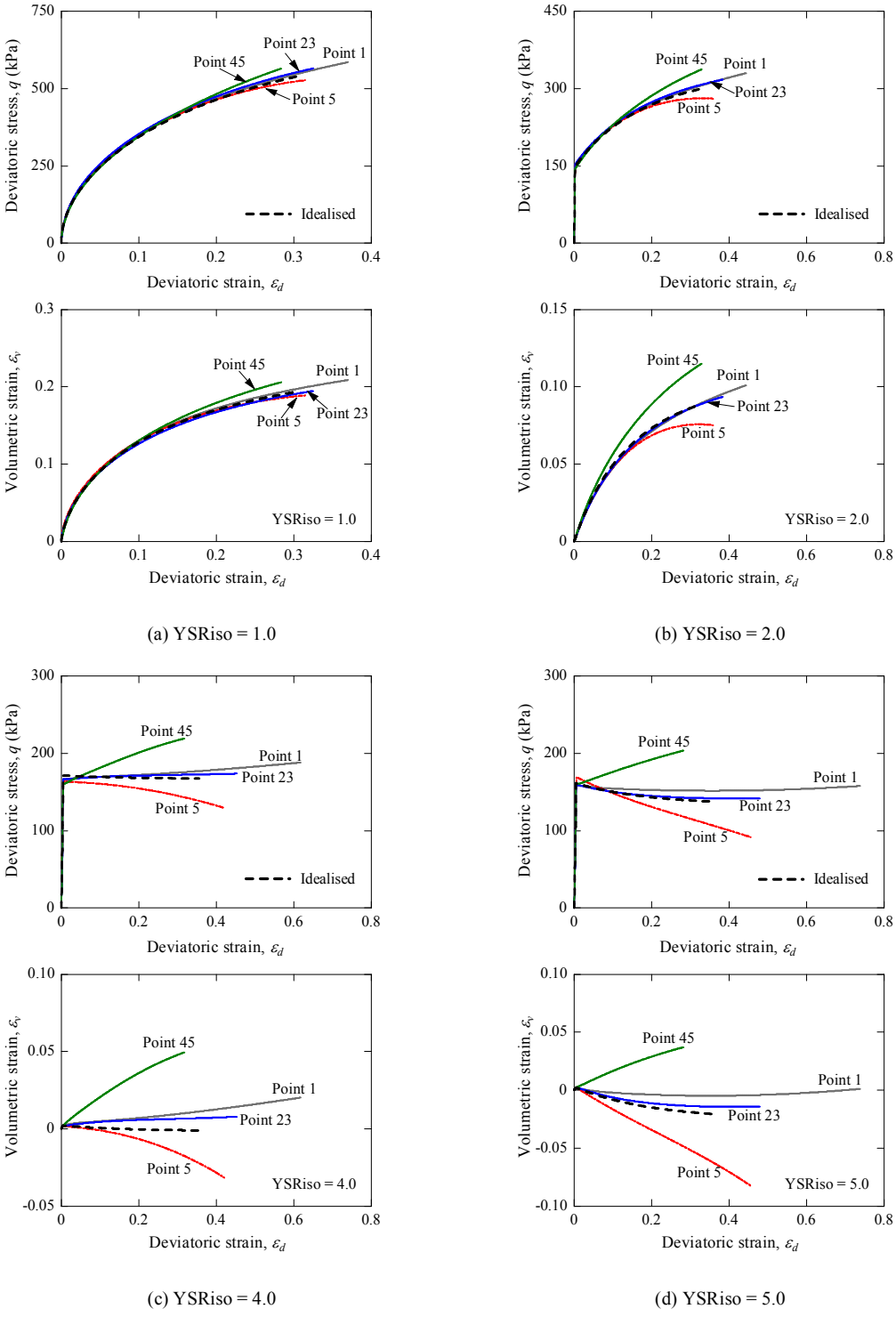

(a) YSRiso = 1.0

(b) YSRiso = 2.0

(c) YSRiso = 4.0

(d) YSRiso = 5.0

Figure 5.10 Comparison of deviatoric stress and volumetric strain development for uncemented Ariake clay under drained triaxial test at YSRiso = 1.0 to 5.0

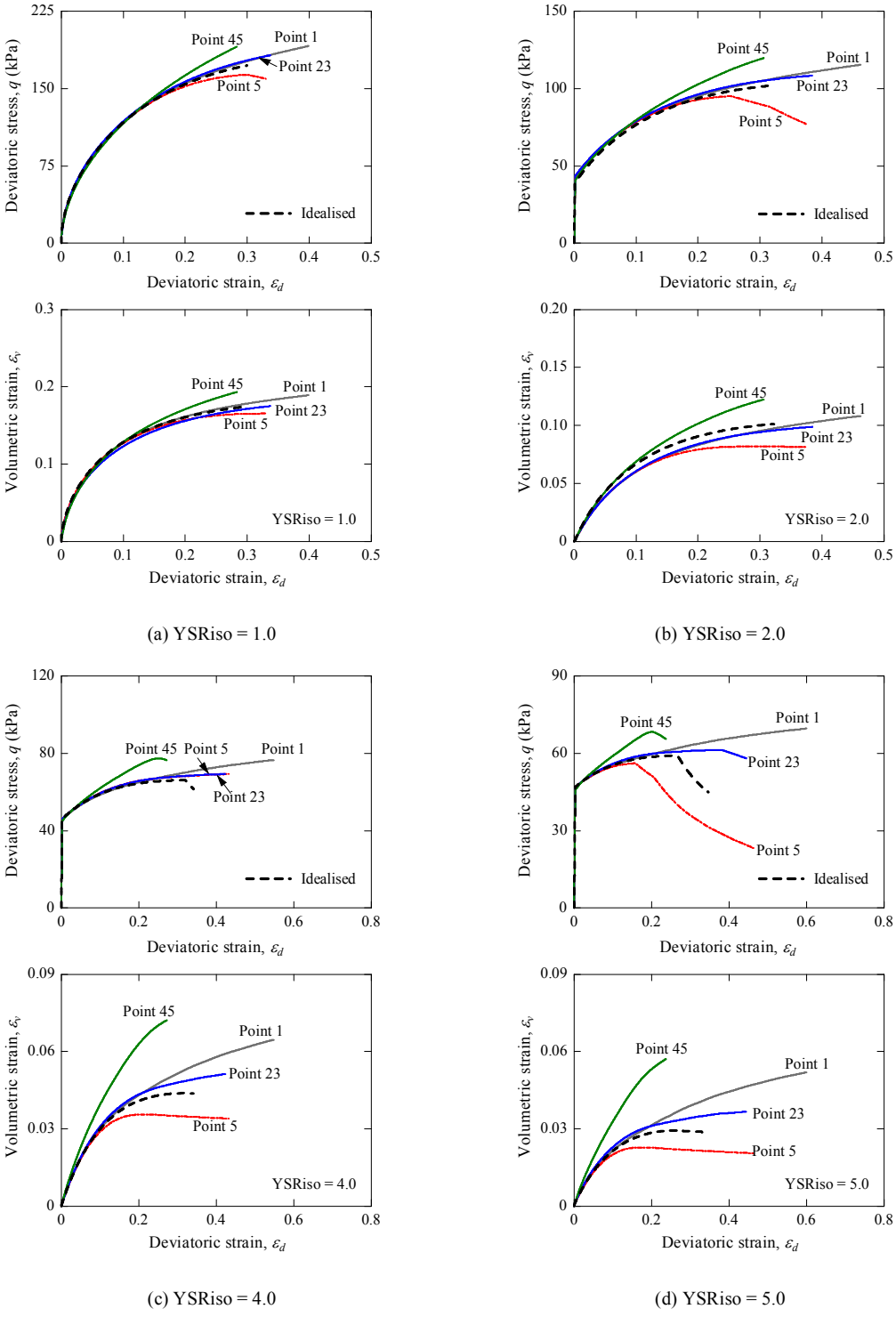

(a) YSRiso = 1.0

(b) YSRiso = 2.0

(c) YSRiso = 4.0

(d) YSRiso = 5.0

Figure 5.11 Comparison of deviatoric stress and volumetric strain development for cemented Ariake clay (A_w = 6%) under drained triaxial test at YSRiso = 1.0 to 5.0

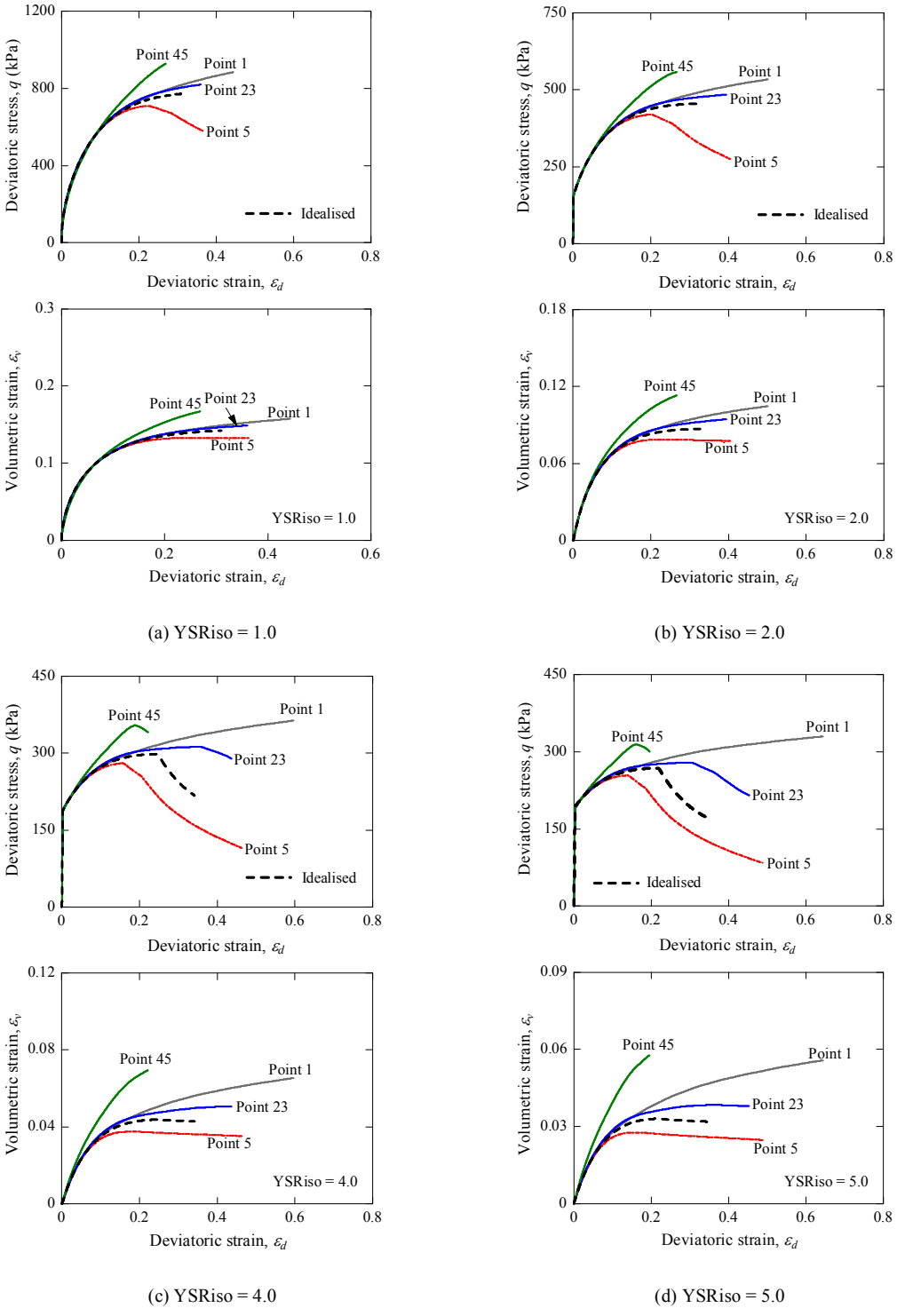

(a) YSRiso = 1.0

(b) YSRiso = 2.0

(c) YSRiso = 4.0

(d) YSRiso = 5.0

Figure 5.12 Comparison of deviatoric stress and volumetric strain development for cemented Ariake clay (A_w = 9%) under drained triaxial condition at YSRiso = 1.0 to 5.0

5.5.2 Undrained triaxial shearing

For perfectly rough contact end, the specimen under undrained condition deforms in similar pattern to that under the drained condition. The distributions of τ_{xy} observed in the undrained condition are lower than those of the drained condition as shown in Figure 5.13 for various YSRiso and cement content. In contrast, the specimen with YSRiso = 2.0 shows the higher τ_{xy} than that with YSRiso = 1.0 and the τ_{xy} decreases with the increasing the YSRiso. Although the centre of a specimen displays less pronounced axial deformation when compared to that in the drained condition, the τ_{xy} observed in the undrained condition increases with increasing the cementation structure strength.

The distribution of deviatoric stress, excess pore pressure and plastic deviatoric strain of soil mass in NC state are shown in Figures 5.14, 5.15 and 5.16 for uncemented specimen, 6% and 9% cement specimens, respectively. For OC state (YSRiso = 5.0), the distribution of deviatoric stress, plastic volumetric strain and deviatoric strain of uncemented specimen, 6% and 9% cement specimens are shown in Figures 5.17, 5.18 and 5.19, respectively. The distribution of the deviatoric stress under undrained condition is more uniform than that under drained condition at low global axial strain. At the end edge of a specimen, pronounced stress concentration due to the end boundary is clearly seen. This concentration increases with increasing the strength of soil cementation structure but decreases with increasing the YSRiso. The excess pore pressure and deviatoric strain have observed in a specimen as the X-shape. The negative excess pore water pressure is occured at the centre of a specimen in OC state at medium to large global axial strain.

The local stress-strain and development of excess pore pressure of soil mass under undrained test for uncemented, 6% and 9% cement content are shown in Figures 5.20, 5.21 and 5.22, respectively. The inhomogeneity of undrained specimen starts when the local stress state reaches the peak strength state. All local elements (No.1, 5, 13 and 45) show the strain softening behaviour for the NC specimen. The degree of inhomogeneity for the $q-\varepsilon_d$ curves under the undrained tests is less than those observed from the drained test at the same stress state (YSRiso). As the simulated results, the increase in soil cementation structure shows less pronounced inhomogeneous behaviour of stress under undrained test when compared to the excess pore pressure and deviatoric strain.

(a) Uncemented Ariake clay ($p'_{y,i}$ = 200 kPa)

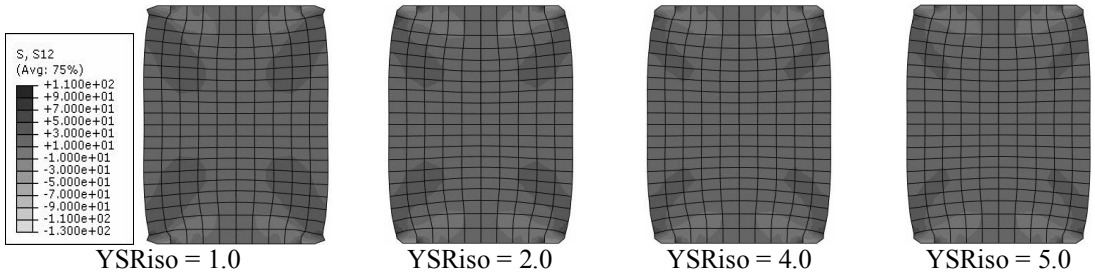

(b) Cemented Ariake clay with 6% cement content ($p'_{y,i}$ = 50 kPa)

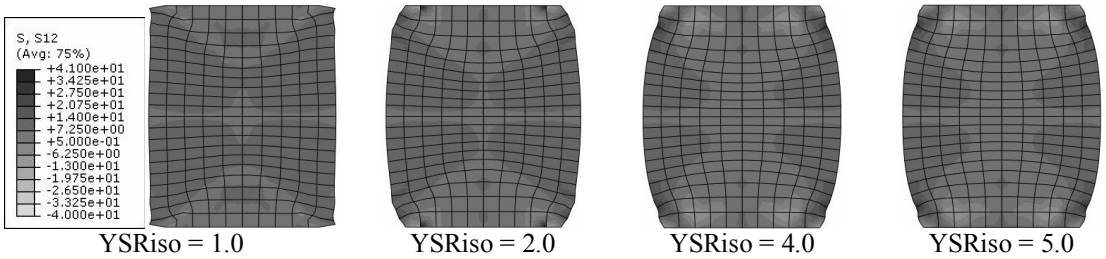

(c) Cemented Ariake clay with 9% cement content ($p'_{y,i}$ = 200 kPa)

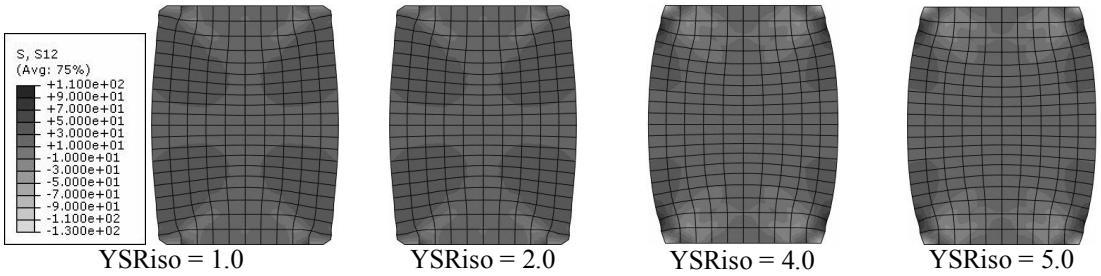

Figure 5.13 Distribution of shear stress, τ_{xy} in uncemented and cemented Ariake clay specimen under undrained triaxial compression test with various cement content and YSRiso (at ε_a = 25 %)

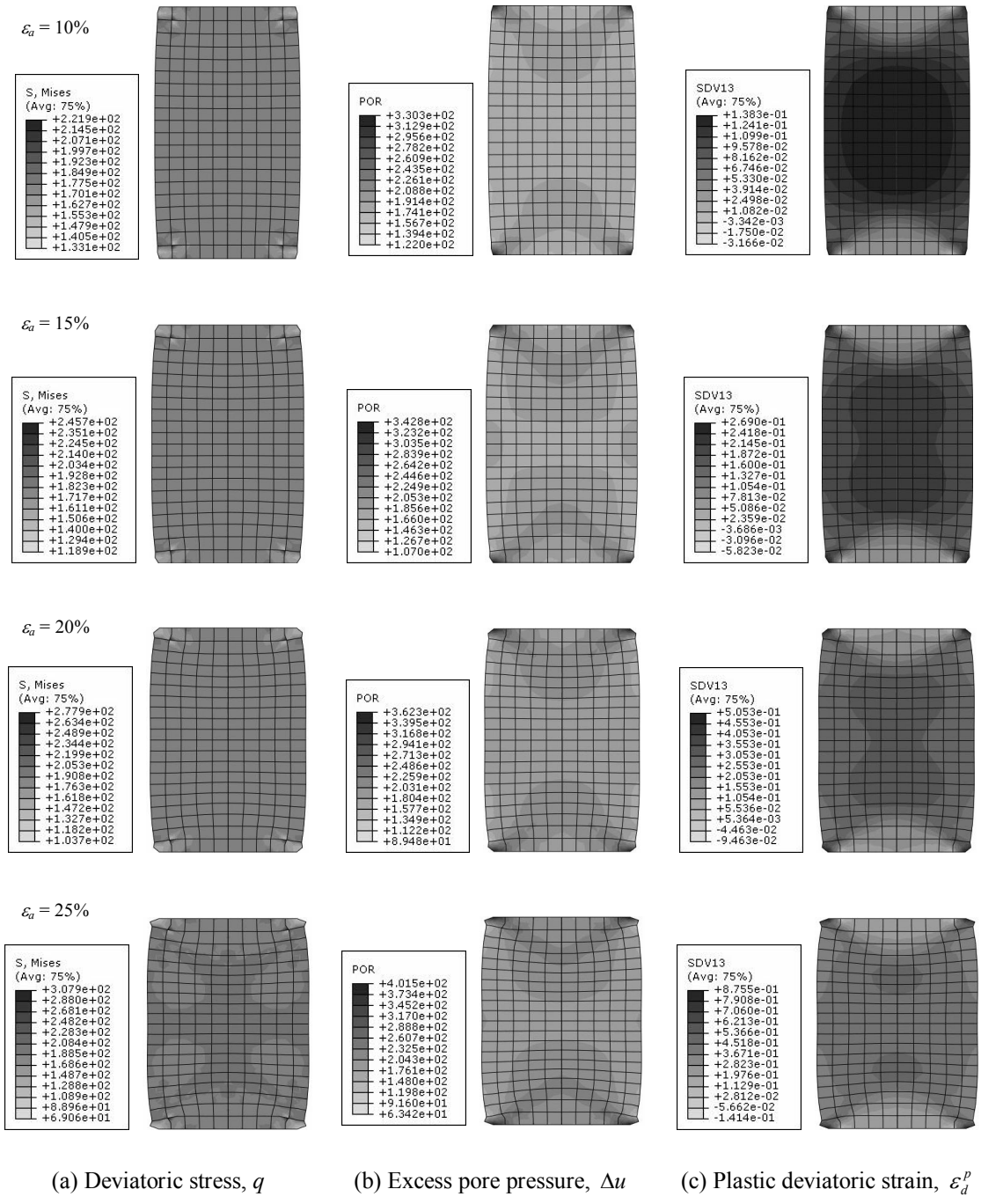

(a) Deviatoric stress, q (b) Excess pore pressure, Δu (c) Plastic deviatoric strain, ε_d^p

Figure 5.14 Distribution of (a) deviatoric stress, (b) excess pore pressure and (c) plastic deviatoric strain under undrained triaxial test of normally consolidated uncemented Ariake clay (YSRiso = 1.0)

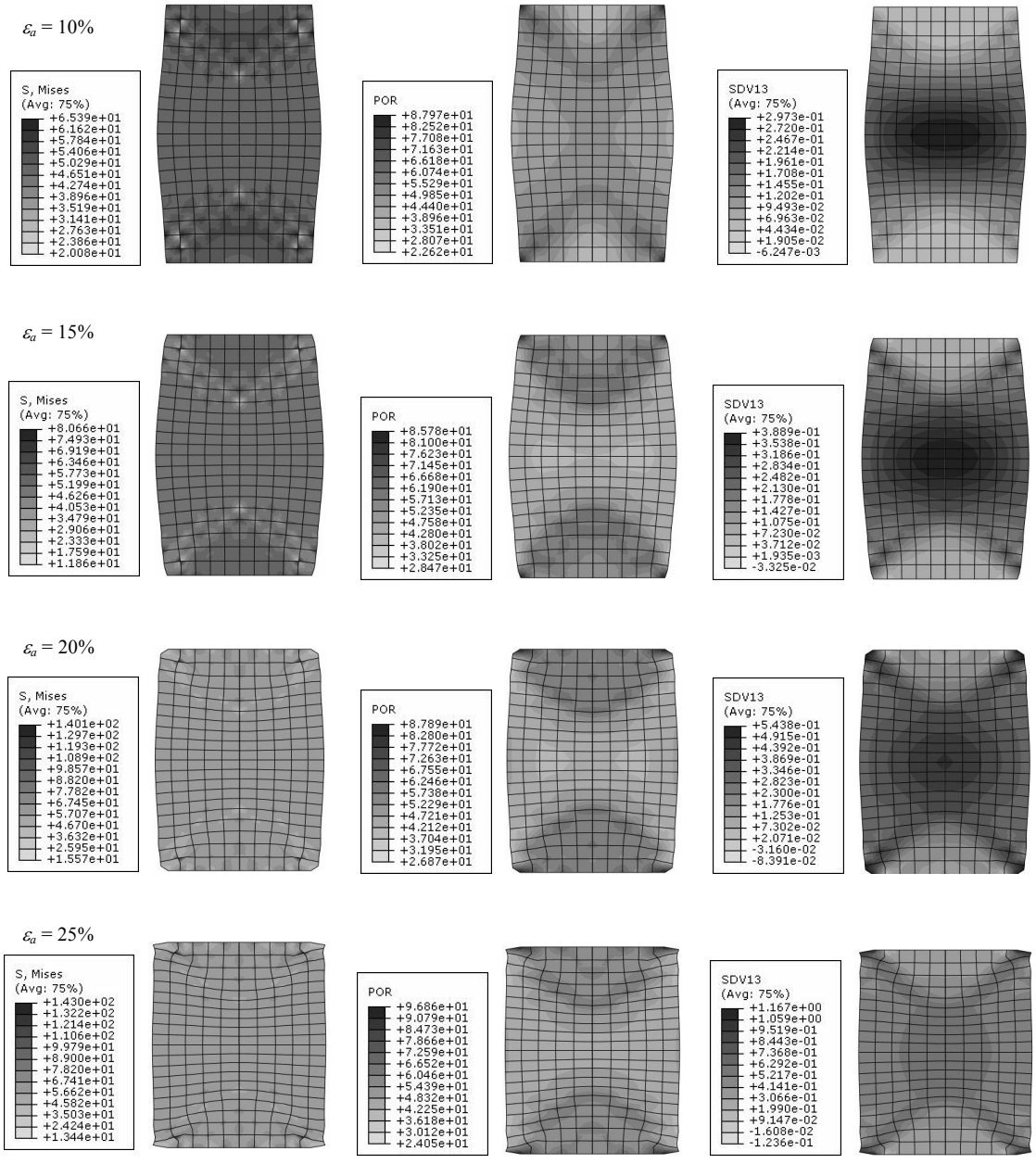

(a) Deviatoric stress, q (b) Excess pore pressure, Δu (c) Plastic deviatoric strain, ε_d^p

Figure 5.15 Distribution of (a) deviatoric stress, (b) excess pore pressure and (c) plastic deviatoric strain under undrained triaxial test of normally consolidated cemented Ariake clay with 6% cement content (YSRiso = 1.0)

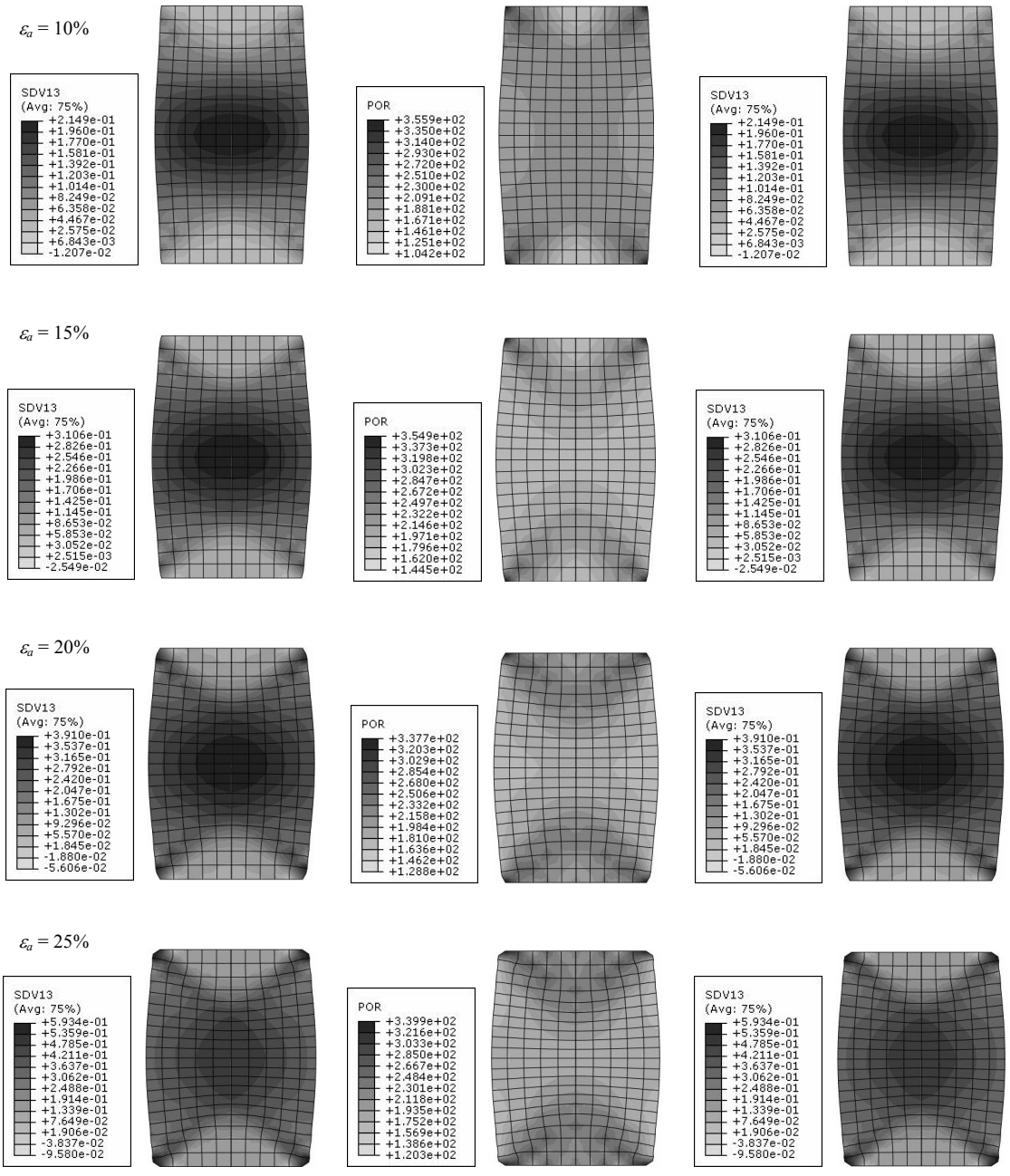

(a) Deviatoric stress, q (b) Excess pore pressure, Δu (c) Plastic deviatoric strain, ε_d^p

Figure 5.16 Distribution of (a) deviatoric stress, (b) excess pore pressure and (c) plastic deviatoric strain under undrained triaxial test of normally consolidated cemented Ariake clay with 9% cement content (YSRiso = 1.0)

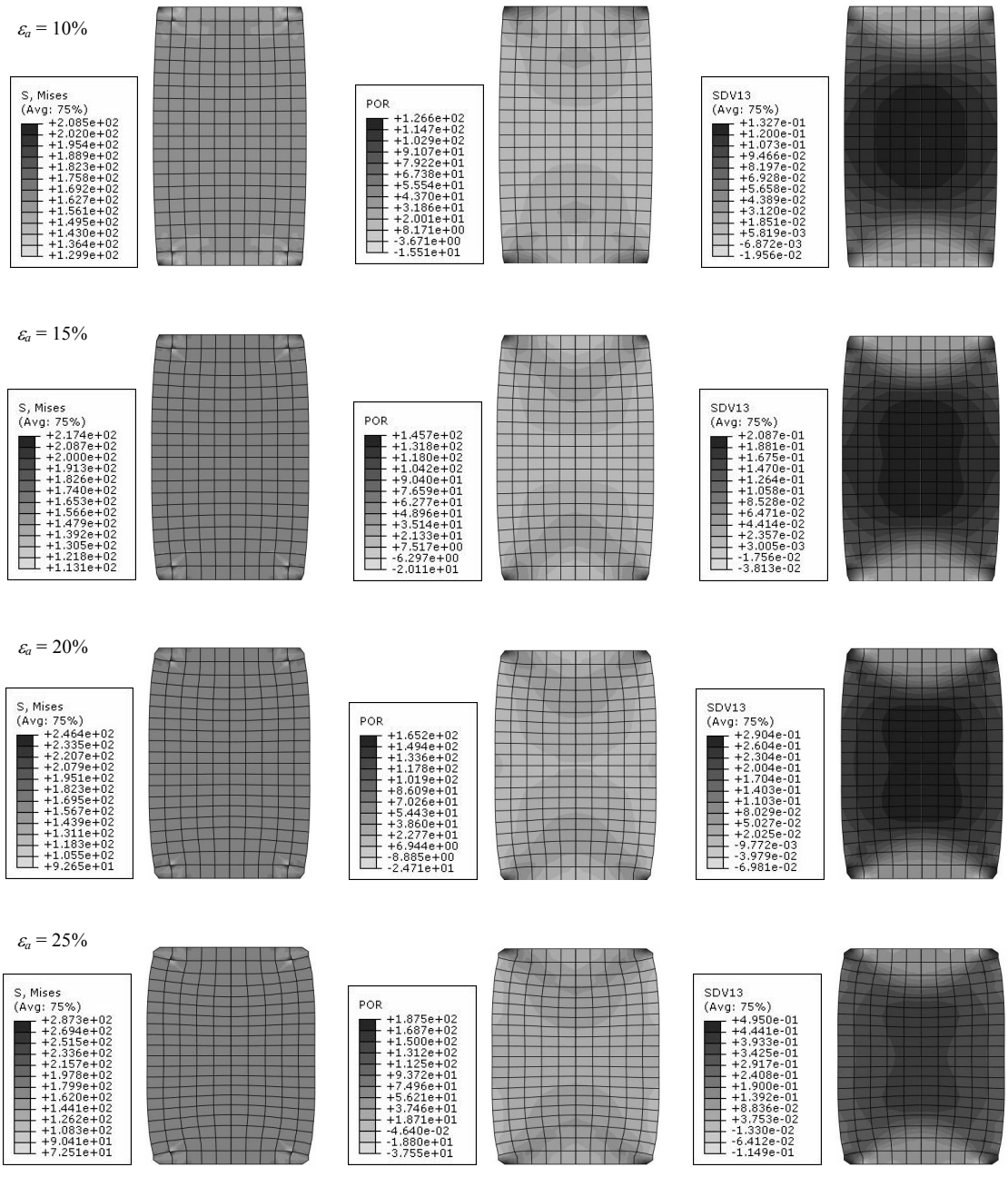

(a) Deviatoric stress, q (b) Excess pore pressure, Δu (c) Plastic deviatoric strain, ε_d^p

Figure 5.17 Distribution of (a) deviatoric stress, (b) excess pore pressure and (c) plastic deviatoric strain under undrained triaxial test of overconsolidated uncemented Ariake clay (YSRiso = 5.0)

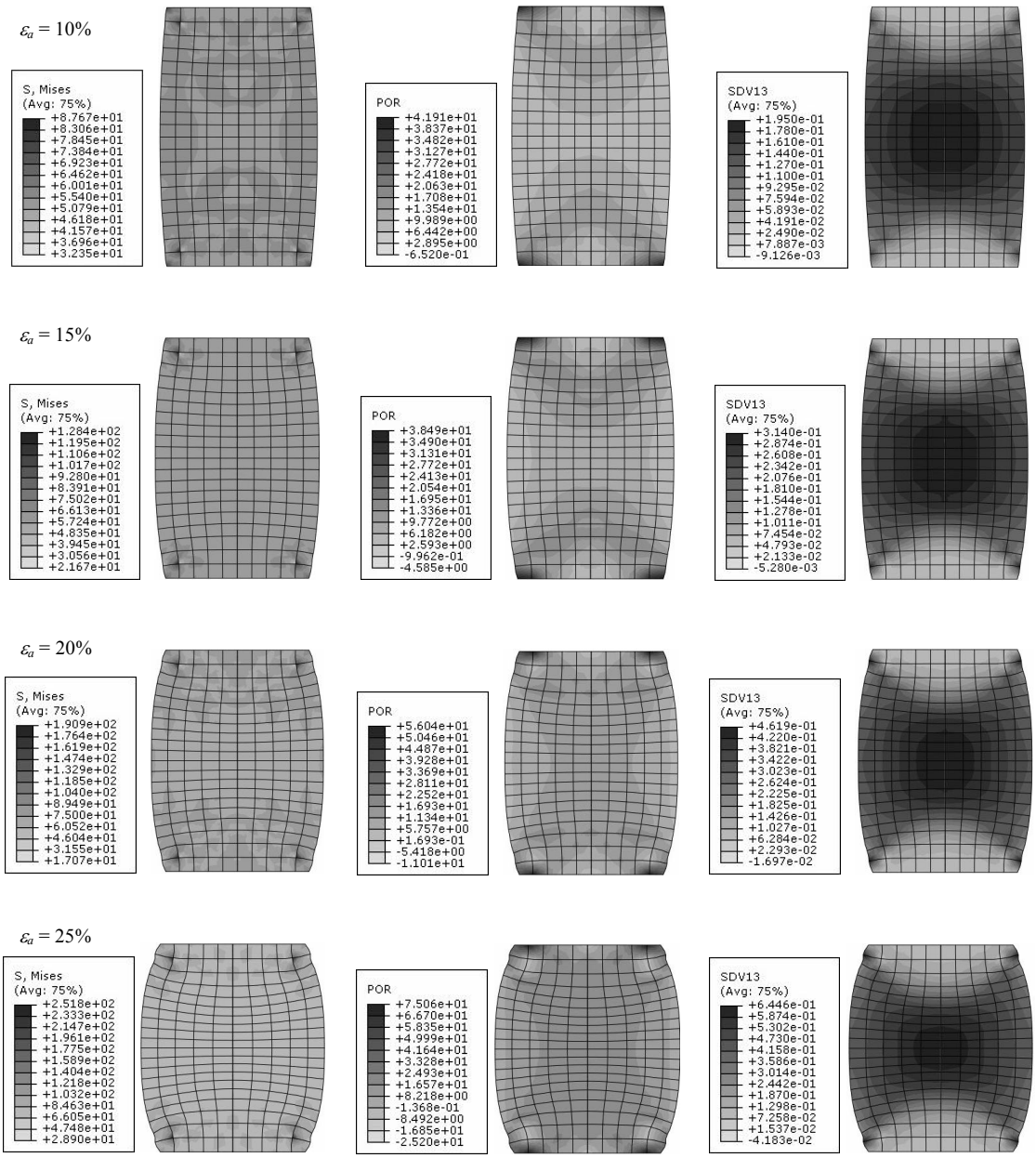

(a) Deviatoric stress, q (b) Excess pore pressure, Δu (c) Plastic deviatoric strain, ε_d^p

Figure 5.18 Distribution of (a) deviatoric stress, (b) excess pore pressure and (c) plastic deviatoric strain under undrained triaxial test of overconsolidated cemented Ariake clay with 6% cement content (YSRiso = 5.0)

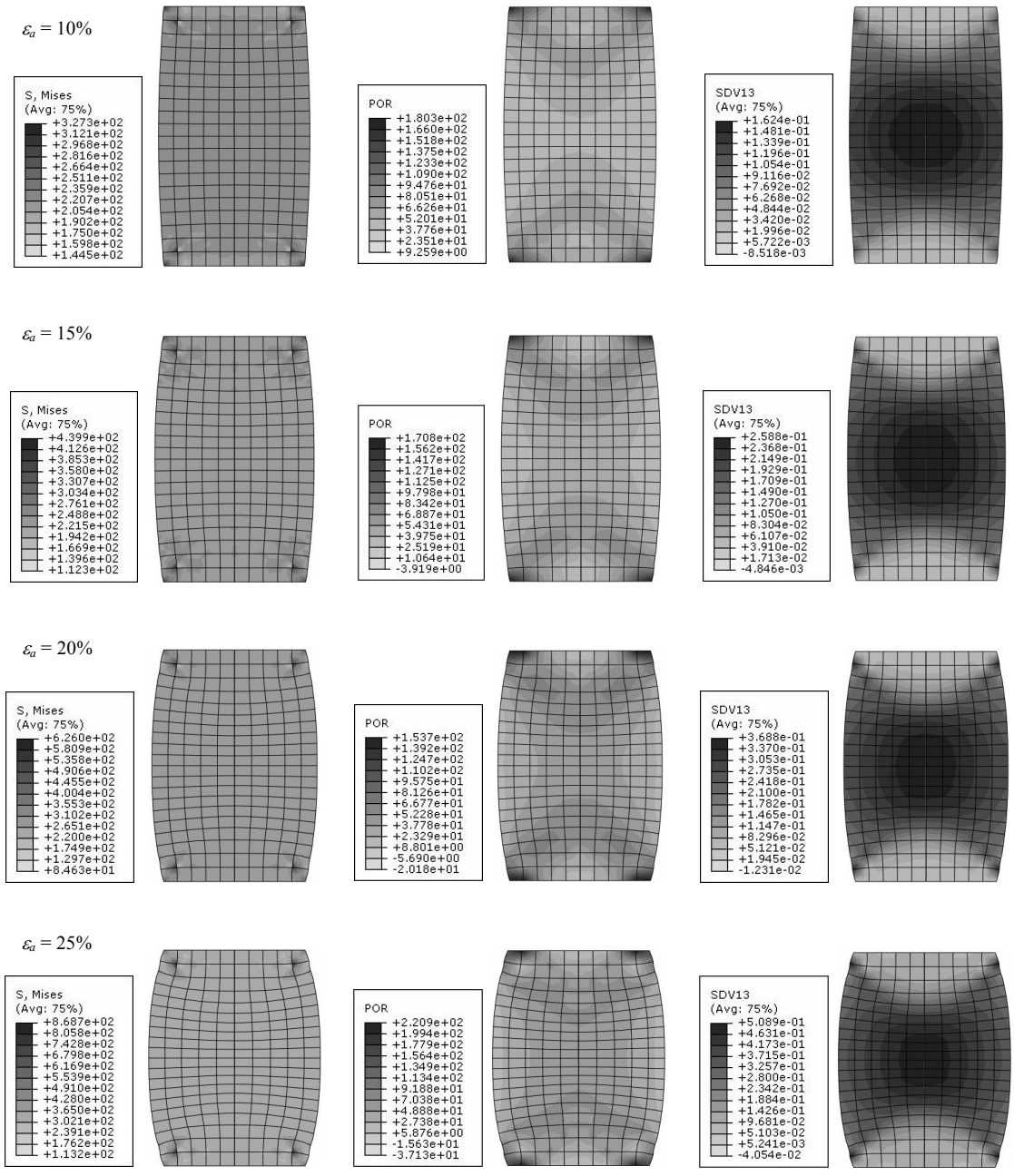

(a) Deviatoric stress, q (b) Excess pore pressure, Δu (c) Plastic deviatoric strain, ε_d^p

Figure 5.19 Distribution of (a) deviatoric stress, (b) excess pore pressure and (c) plastic deviatoric strain under undrained triaxial test of overconsolidated cemented Ariake clay with 9% cement content (YSRiso = 5.0)

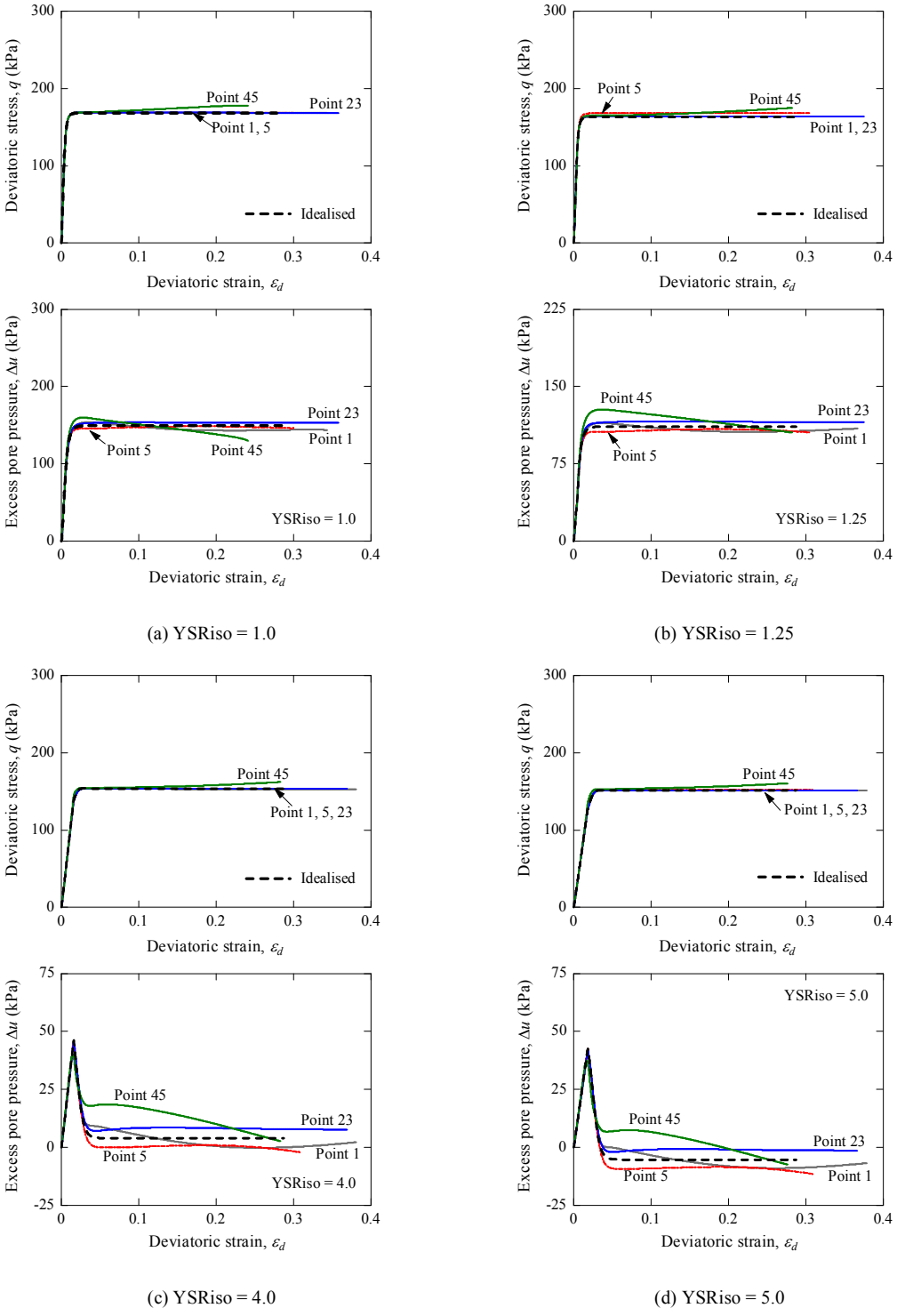

(a) YSRiso = 1.0

(b) YSRiso = 1.25

(c) YSRiso = 4.0

(d) YSRiso = 5.0

Figure 5.20 Comparison of deviatoric stress and excess pore pressure development for uncemented Ariake clay under undrained triaxial test at YSRiso = 1.0 to 5.0

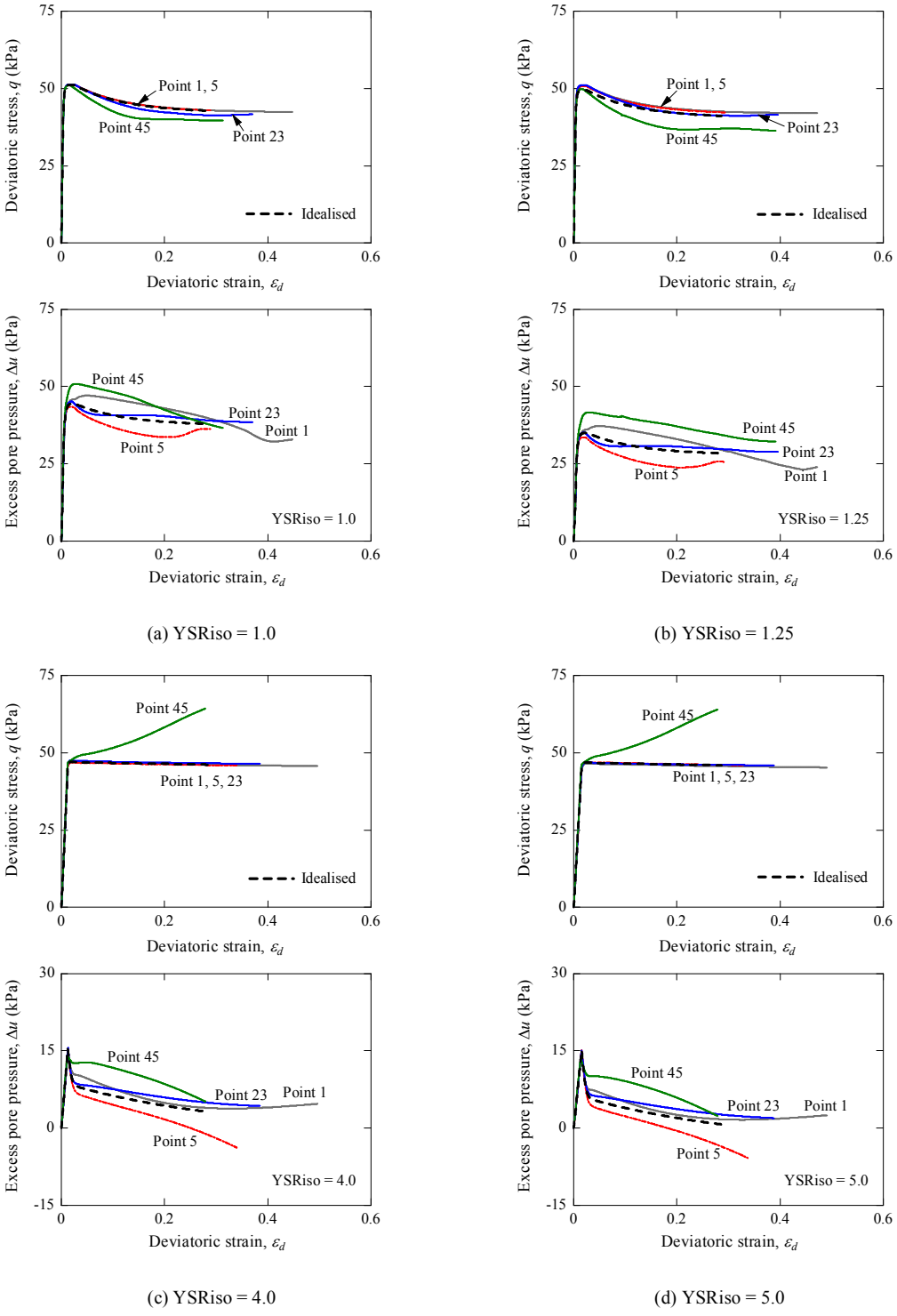

(a) YSRiso = 1.0

(b) YSRiso = 1.25

(c) YSRiso = 4.0

(d) YSRiso = 5.0

Figure 5.21 Comparison of deviatoric stress and excess pore pressure development for cemented Ariake clay (A_w = 6%) under undrained triaxial test at YSRiso = 1.0 to 5.0

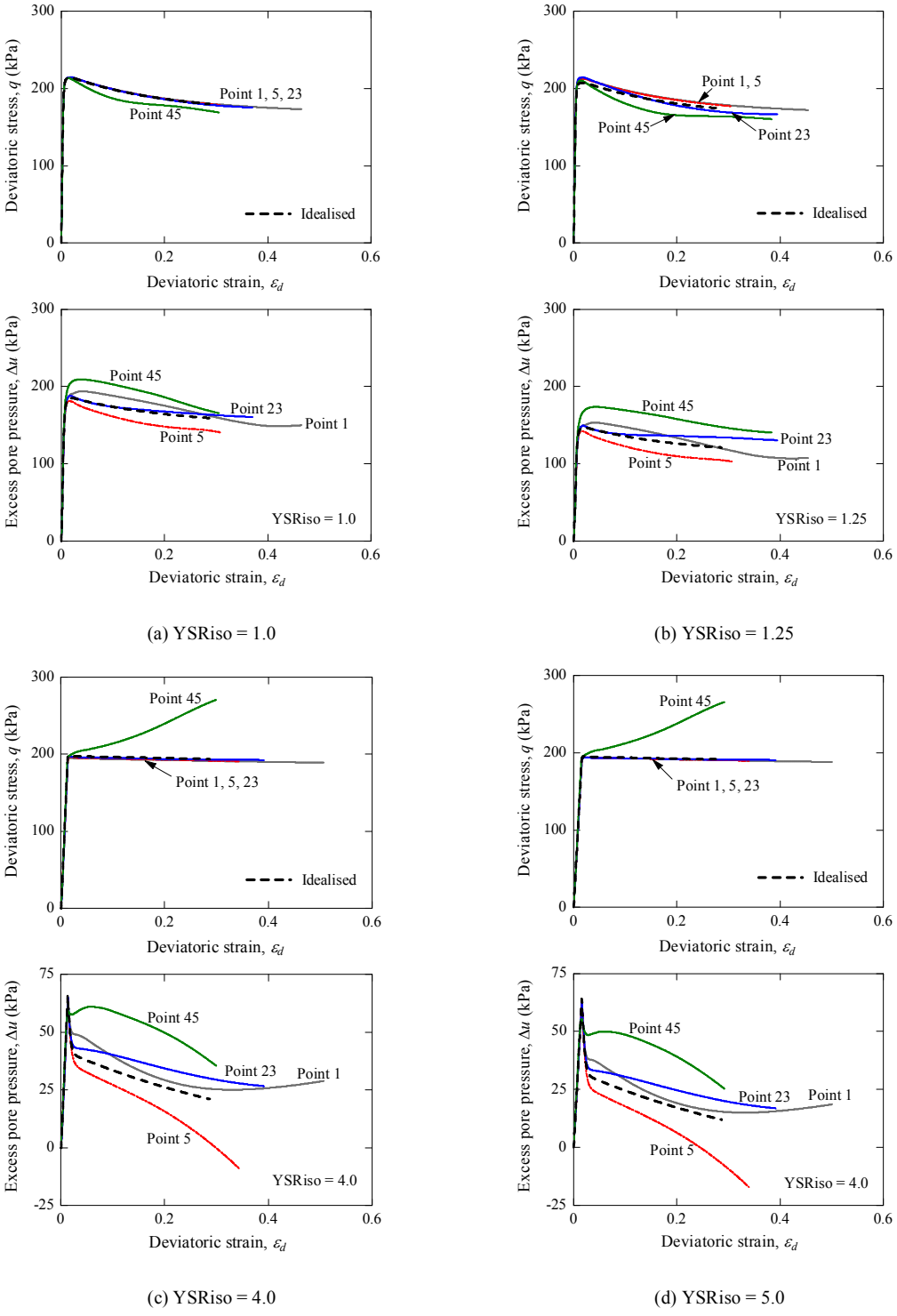

Figure 5.22 Comparison of deviatoric stress and excess pore pressure development for cemented Ariake clay (A_w = 9%) under undrained triaxial test at YSRiso = 1.0 to 5.0

5.6 Conclusions

A critical state plasticity model for structured clays, the MSCC model has been implemented into the commercial finite element program, ABAQUS (2009). The implemented MSCC model has been adopted for simulating the triaxial compression test of uncemented and cemented Ariake clays. The inhomogeneous triaxial behaviour of cemented clay caused by end restraint and insufficient drainage has been investigated via axisymetric finite element analysis under drained and undrained conditions. The finite element analysis with MSCC model can well capture the behaviour of cemented clay Ariake clay under both drained and undrained conditions. The local element behaviour at X shape concentration of stress show more significant stress inhomogeneity with increasing the structural properties (higher degree of cementation) and this leads to the strain localisation of the specimen. Both end restraint in drained and undrained tests and insufficient drainage in drained test can cause inhomogeneous barrel-shape deformation of the specimen at large strains. It is concludes that the increase in the global axial strain induces the inhomogeneity in the specimen. The degree of inhomogeneity of stress-strain behaviour is dependent on the initial stress state before shearing and structural properties of specimen. The simulation results show that the increasing in cement content leads to the significantly difference in the stress-strain behaviour at the local element level under drained and undrained conditions.

5.7 References

ABAQUS. (2009). **Abaqus 6.9 Theory Manual**. RI, USA.: Dassault Systèmes Simulia Corp.

Airey, D. W. (1991). Finite element analyses of triaxial tests with different end and drainage conditions. **Proceedings of the 7th International Conference on Computer Methods and Advances in Geomechanics** (pp. 225-230).

Asaoka, A., Nakano, N., and Noda, T. (2000). Superloading yield surface concept for highly structured soil behaviour. **Soils and Foundations**. 40(2): 99-110.

Baudet, B., and Stallebrass, S. (2004). A constitutive model for structured clays. **Geotechnique**. 54(4): 269-278.

Britto, A. M., and Gunn, M. J. (1987). **Critical state soil mechanics via finite elements**. New York: Halsted Press.

Callisto, L., and Rampello, S. (2004). An interpretation of structural degradation for three natural clays. **Canadian Geotechnical Journal**. 41: 392-407.

Carter, J. P. (1982). Predictions of the non-homogeneous behaviour of clay in the triaxail test. **Geotechnique**. 32(1): 55-58.

Cotecchia, F., and Chandler, R. J. (2000). A general framework for the mechanical behaviour of clays. **Geotechnique**. 50(4): 431-447.

Horpibulsuk, S. (2001). Analysis and Assessment of Engineering Behavior of Cement Stabilized Clays. **Ph.D. dissertation**, Saga University, Saga, Japan.

Horpibulsuk, S., Liu, M. D., Liyanapathirana, D. S., and Suebsuk, J. (2010). Behaviour of cemented clay simulated via the theoretical framework of Structured Cam Clay model. **Computers and Geotechnics**. 37(1-2): 1-9.

Horpibulsuk, S., Miura, N., and Bergado, D. T. (2004). Undrained shear behaviour of cement admixed clay at high water content. **Journal of Geotechnical and Geoenvironmental Engineering, ASCE**. 130(10): 1096-1105.

Huang, J. T., and Airey, D. W. (1998). Properties of an artificially cemented carbonate sand. **Journal of Geotechnical and Geoenvironmental Engineering, ASCE**. 124(6): 492-499.

Ismail, M. A., Joer, H. A., Randolph, M. F., and Sin, W. H. (2002). Effect of cement type on shear behaviour of cemented calcareous soil. **Journal of Geotechnical Engineering, ASCE**. 128(6): 520-529.

Kamruzzaman, A. H. M., Chew, S. H., and Lee, F. H. (2009). Structuration and destructuration behavior of cement-treated singapore marine clay. **Journal of Geotechnical and Geoenvironmental Engineering, ASCE**. 135(4): 573-589.

Kasama, K., Ochiai, H., and Yasufuku, N. (2000). On the stress-strain behaviour of lightly cemented clay based on an extended critical state concept. **Soils and Foundations**. 40(5): 37-47.

Kavvadas, M., and Amorosi, A. (2000). A constitutive model for structured soils. **Geotechnique**. 50(3): 263-273.

Lade, P. V. (1982). Localization effects in triaxial tests on sand. **Proceedings of the International Union of Theoretical and Applied Mechanics. Symposium on Deformation and Failure of Granular Materials** (pp. 461-472), Rotterdam.

Lee, K., Chan, D., and Lam, K. (2004). Constitutive model for cement treated clay in a critical state framework. **Soils and Foundations**. 44(3): 69-77.

Liu, M. D., and Carter, J. P. (2002). A structured Cam Clay model. **Canadian Geotechnical Journal**. 39: 1313–1332.

Liyanapathirana, D. S., Carter, J. P., and Airey, D. W. (2005). Numerical modeling of Nonhomogenous behaviour of structured soils during triaxial tests. **International Journal of Geomechanics, ASCE**. 5(1): 10-23.

Luccioni, D. C., Pestana, J. M., and Taylor, R. L. (2001). Finite element implementation of non-inear elastoplastic constitutive laws using local and global explicit algorithms with automatic error control. **International Journal for Numerical Methods in Engineering**. 50: 1191-1212.

Miura, N., Horpibulsuk, S., and Nagaraj, T. S. (2001). Engineering behavior of Cement stabilized clays. **Soils and Foundations**. 41(5): 33-45.

Potts, D. M., and Gens, A. (1985). A critical assessment of methods of correcting for drift from the yield surface in elastoplastic finite element analysis. **International Journal for Numerical and Analytical Methods in Geomechanics**. 9: 149-159.

Roscoe, K. H., and Burland, J. B. (1968). On the generalised stress-strain behaviour of wet clay. **Engineering plasticity**. 535-609.

Rouainia, M., and Muir Wood, D. (2000). A kinematic hardening constitutive model for natural clays with loss of structure. **Geotechnique**. 50(2): 153-164.

Sheng, D., and Sloan, S. W. (2001). Loading stepping schemes for critical state models. **International Journal for Numerical and Analytical Methods in Geomechanics**. 50: 67-93.

Sheng, D., Sloan, S. W., and Yu, H. S. (2000). Aspects of finite element implementation of critical state models. **Computational Mechanics**. 26(2): 185-196.

Sheng, D., Westerberg, B., Mattsson, H., and Axelsson, K. (1997). Effects of end restraint and strain rate in triaxial tests. **Computers and Geotechnics**. 21(3): 163-182.

Small, J. C., Booker, J. R., and Davies, E. H. (1976). Elasto-plastic consolidation of soil. **International Journal of Solids and Structures**. 12: 431-448.

Suebsuk, J., Horpibulsuk, S., and Liu, M. D. (2010). Modified Structured Cam Clay: A Generalised Critical State Model for Destructured, Naturally Structured and Artificially Structured Clays. **Computers and Geotechnics**. 37(7-8): 956-968.

Uddin, K., and Buensuceso, B. R. (2002). Lime treated clay: salient engineering properties and a concept model. **Soils and Foundations**. 42(5): 79-89.

Zhao, J., Sheng, D., Rouainia, M., and Sloan, S. W. (2005). Explicit stress integration of complex soil models. **International Journal for Numerical and Analytical Methods in Geomechanics**. 29: 1209-1229.

CHAPTER VI

CONCLUSIONS AND RECOMMENDATIONS

6.1 Summary and conclusions

This thesis is made to meet three main objectives. The first is to develop the generalised critical state model for structured clays based on the Structured Cam Clay model (Liu and Carter, 2002) for explanation of clay behaviour in different structured states. The second is to improve a generalised model for structured clay for better simulation of the stress-strain behaviour in overconsolidated state. The third is to implement the developed model into the finite element code to study the inhomogeneous stress-strain behaviour influenced by the strength of soil cementation structure. In the following sections, the conclusions obtained from the study are summarised.

6.1.1 Modified effective stress concept

The modified or explicit mean effective stress presented in Chapter III has been successfully adopted to generate the state boundary surface for structured clay in the $q/\overline{p}'_y - p'/\overline{p}'_y$ plane. The normalised stress paths for cemented Ariake clay with various cementation structure have been represented by two unique curves referred to as the modified Roscoe surface for soil in virgin yielding state and the modified Hvorslev surface for soil in overconsolidated state.

This concept can be used as a powerful method to predict the stress-strain-strength of structured clay, which cannot be explained by the conventional state boundary surface concept.

6.1.2 Destructuring law

The destructuring is the removal of structure strength, p_b' during the loading path. The simple destructuring law has been proposed based on the general idealisation proposed by Gen and Nova (1993) in the exponential function. The destructuring processes have been represented by Equations 3.4 and 3.5. When the stress state is on the virgin yielding, the destructuring is caused by the degradation of soil cementation. The sudden crushing of soil structure occurs when the stress state reaches the failure envelope. The destructuring is assumed to be related directly to the plastic deviatoric strain and does not occur for loading in the elastic range.

6.1.3 Yield surface and plastic potential for structured clay

The elliptical shape of the MCC model and modified effective stress concept are adopted for the development of yield surface (*vide* Eq. 3.9). The plastic potential of the MSCC model was developed from that proposed by McDowell and Hau (2003) and presented by Equation 3.13. The shape of plastic potential is controlled by the simple parameter ψ. When $\psi = 2$, the plastic potential shape is the elliptical function.

6.1.4 The MSCC model

The generalised critical state plasticity model for structured clay, the MSCC model, has been formulated in the triaxial stress space based on the modified effective stress concept, the destructuring law, yield surface, plastic potential and the conventional assumptions of the Structured Cam Clay model. The structured clay was modelled as the elastic-virgin yielding material. The loading inside the yield surface was assumed to be elastic. The yield surface and plastic potential introduced by the structure strength were adopted for the formulation of the elastoplastic stiffness. The yield surface was assumed as a simple elliptical shape for simplicity while the shape of the plastic potential was justified using experimental evidence. The five conventional parameters from MCC model were used in the MSCC model. The other five additional structural parameters can be simply obtained from the laboratory tests on structured samples.

The generalised MSCC model has been verified by comparing the MSCC model simulation result with a series of triaxial test results of various naturally and cemented clays and the SCC and MCC model simulation results. It was found that the simulated results by the MSCC model were consistently better than those by the SCC and MCC models for both normally and overconsolidated states under both drained and undrained loading conditions. In particular, the MSCC model can capture reasonably well the strain hardening and softening behaviours affected by soil-cementation structure

6.1.5 The MSCC-B model

In Chapter IV, an extended MSCC model for better simulation of overconsolidated structured clay designated as the Modified Structured Cam Clay model with bounding surface theory (MSCC-B) was proposed. The model has been formulated based on the bounding surface plasticity theory and the SCC framework. A new parameter, h has been introduced into the extended model for representing the influence of soil-cementation structure on the hardening modulus. The new features of the MSCC-B are specially useful when analysing the structured clay in the overconsolidated state, the MSCC-B model is the same as the original MSCC model when the structured soil is in normally consolidated state.

The formulation of the radial mapping rule and the modification of hardening modulus equation were described in details. The single element simulations of the triaxial tests on the overconsolidated clays in both naturally structured and artificially structured states were carried out to validate and assess the performance of the MSCC-B model. It was found that the MSCC-B model gave a good prediction for the stress state of soil inside the boundary surface. The pre-failure behaviours (stress-strain-strength) of overconsolidated structured clays have been captured well by the MSCC-B model. The smooth change from the elastic to plastic behaviour of the soil and the more realistic direction of the stress path under undrained condition were observed.

6.1.6 Finite element implementation of the MSCC model

The MSCC model has been implemented into the finite element program on a coupled hydro-mechanical analysis. A commercial unified finite element program, ABAQUS was chosen for this study. In Chapter V, the implementation

procedures of the MSCC model into finite element code was described. This included the formulation of the model in a generalised stress space, stress integration scheme and verification of the implemented model.

The implemented MSCC model in finite element analysis was used to simulate the inhomogeneous stress-strain behaviour of triaxial compression test influenced by soil cementation structure. It was seen that the increase in the strength of soil-cementation structure increased the inhomogeneity in the specimen. The inhomogeneity of stress-strain behaviour is dependent on the initial stress state before shearing and structural properties of soil mass. For chemical stabilised soil, the increase in cement or lime content leads to the significant difference in the stress-strain behaviour at local element level under drained and undrained conditions.

6.2 Recommendations for future work

The single element and finite element analyses of MSCC model presented in this research study have demonstrated the very good predictive capabilities for structured clays. However, the model limits only for monotonic loading and clayey soil, some extension of the model and numerical analysis for actual structures field problems are still required before the general validity of the series of MSCC models can be fully established.

6.2.1 Further modifications

The MSCC and MSCC-B presented in Chapters III and IV needs to be modified so that the yield function and plastic potential can be presented in the normalisation form. In critical state model, the yield function and plastic potential are usually expressed in terms of stress invariants, q and p'. Since the value of the yield

function is normally used to determine if a stress state is elastic ($F < 0$) or plastic ($F > 0$), it is appropriate to scale these functions against a stress parameter so that their values are not significant influenced by the magnitudes of the stresses. The condition, $F < 0$ and $F > 0$ are always checked using a specified yield surface tolerance, which is typically in the range 10^{-6}-10^{-12}. For a state boundary surface for structured clay (Suebsuk et al., 2010), a normalisation parameter is the explicit isotropic preconsolidation pressure, $\overline{p}_0' = p_0' + p_b'$. The yield surface and plastic potential should be modified into the normalisation stress plane plot of $p'/\overline{p}_0'$ versus $q/\overline{p}_0'$. This leads to the accuracy of the yield function or plastic potential that they are less dependent on the stress magnitudes. In the other hand, the boundary surface is static in the normalised stress plane.

For the stress integration scheme, the Euler's forward algorithm has been adopted in the finite element implementation. The finite element simulation of element tests shows a good prediction at very small increment. However based on the study, the Euler's forward algorithm was highly sensitive to the increment size and required very small increment to achieve acceptable accuracy. It is because at the end of each subincrement in the explicit integration process, the stresses may diverge from the yield condition so that $F > TOL$. The extent of this violation, which is commonly known as yield surface "drift", depends on the accuracy of the integration scheme and the non-linearity of the constitutive relations. These problems can be solved by the modified Euler scheme with automatic substeping and drift correction (Sloan et al., 2001).

6.2.2 An extended MSCC model for unloading and reloading

The MSCC-B model proposed in Chapter IV can be extended for predicting the unloading and reloading simplicity by making some modification on the hardening modulus. The unloading hardening modulus proposed by McVay and Taesiri (1985) with a simple form and good performance can be adopted in the formulation of MSCC-B model. The unloading hardening modulus equation is,

$$H = H_U \times \frac{1}{(1-\alpha)}, \tag{6.1}$$

where α is the image stress ratio and H_U is an unloading hardening parameter. For reloading, the equation of virgin hardening modulus can be replaced by the simple equation proposed by Khong (2004), which defined as follows,

$$H = H_j + H_R \times \frac{(1-\alpha)}{\alpha} \times \left(1+\varepsilon_d^p\right)^k, \tag{6.2}$$

where H_j and γ are the same as the virgin loading, H_R is an reloading hardening parameter and *k* is a non-dimension parameter controlling the shakedown behaviour.

6.3 References

Gens, A., and Nova, R. (1993). Conceptual bases for constitutive model for bonded soil and weak rocks. **Geotechnical Engineering of Hard Soil-Soft Rocks**: Balkema.

Khong, C. D. (2004). Development and numerical evaluation of unified critical state models. **Ph.D. Thesis**, University of Nottingham, UK.

Liu, M. D., and Carter, J. P. (2002). A structured Cam Clay model. **Canadian Geotechnical Journal**. 39: 1313–1332.

McDowell, G. R., and Hau, K. W. (2003). A simple non-associated three surface kinematic hardening model. **Geotechnique**. 53(4): 433-437.

McVay, M., and Taesiri, Y. (1985). Cyclic behaviour of pavement base materials. **Journal of Geotechnical Engineering, ASCE**. 111(1): 1-17.

Sloan, S. W., Abbo, A. J., and Sheng, D. (2001). Refined explicit integration of elastoplastic models with automatic error control. **Engineering Computations**. 18: 121-154.

Suebsuk, J., Horpibulsuk, S., and Liu, M. D. (2010). Modified Structured Cam Clay: a generalised critical state model for destructured, naturally structured and artificially structured clays. **Computers and Geotechnics**. 37(7-8): 956-968.

APPENDIX A

THE INPUT PARAMETERS FOR THE MSCC MODEL

Table A.1 The input parameters for the MSCC model

No.	Input parameters	Physical meaning
1	RLAM	Gradient of intrinsic compression in the *e*-ln *p*' plane
2	RKAP	Current Gradient of unloding-reloading line in *e*-ln *p*' plane
3	VOIDIC	Voids ratio at reference stress (p' = 1 unit) of intrinsic compression line
4	PCS0	Initial yield stress of isotropic compression line of cemented soil
5	BINDEX	Destructured index due to volumetric deformation
6	DEI	Additional void ratio at the start of virgin yielding
7	ASPTM	Gradient of critical state ratio in the $q - p'$ plane
8	PBS0	Initial of bonding strength in the $q - p'$ plane
9	XNUE or EG	Poisson's ratio or shear modulus
10	KINDEX	Destructured index due to shear deformation
11	WINDEX	Parameter define the shape of plastic potential
12	PHI	Friction angle of the soil at critical state for defining the shape of yield surface and plastic potential in deviatoric plane

APPENDIX B

THE SOURCE CODE OF THE MSCC MODEL

```
************************************************************************************
** UMAT FOR ABAQUS/STANDARD INCORPORATING MODIFIED STRUCTURED CAM CLAY
** PLASTICICTY WITH LARGE DEFORMATION FORMULATION
** FOR PLAIN STRAIN AND AXI-SYMMETRIC ELEMENT.
** EXPLICIT INTERGRATION WITH CONTINUUM JACOBIAN
**
** AUTHOR: Jirayut Suebsuk
** EMAIL: j.suebsuk@gmail.com
**
************************************************************************************
**
**    Update 19/10/2010
**    1) To normalise the yield surface and plastic potential by modified
**         effective stress
**    2) Failure envelope of Sheng et al. (2000) is adopted.
**
* UMAT SUBROUTINE
      SUBROUTINE UMAT(STRESS,STATEV,DDSDDE,SSE,SPD,SCD,
     1 RPL,DDSDDT,DRPLDE,DRPLDT,
     2 STRAN,DSTRAN,TIME,DTIME,TEMP,DTEMP,PREDEF,DPRED,CMNAME,
     3 NDI,NSHR,NTENS,NSTATV,PROPS,NPROPS,COORDS,DROT,PNEWDT,
     4 CELENT,DFGRD0,DFGRD1,NOEL,NPT,LAYER,KSPT,KSTEP,KINC)
C
      INCLUDE 'ABA_PARAM.INC'
C
      CHARACTER*80 CMNAME
C
C
C
C
C
C
```

```
C
      DIMENSION STRESS(NTENS),STATEV(NSTATV),
     1 DDSDDE(NTENS,NTENS),DDSDDT(NTENS),DRPLDE(NTENS),
     2 STRAN(NTENS),DSTRAN(NTENS),TIME(2),PREDEF(1),DPRED(1),
     3 PROPS(NPROPS),COORDS(3),DROT(3,3),DFGRD0(3,3),DFGRD1(3,3)
C
      PARAMETER (M=3,N=3,ID=3,ZERO=0.D0,ONE=1.D0,TWO=2.D0,THREE=3.D0,
     +     FOUR=4.D0,FIVE=5.D0,SIX=6.D0,NINE=9.D0,
     +     TOLER=0.D-6,HTOL=1.E-9)
C
      DIMENSION XIDEN(M,N),DIFF(4),DIFG(4),DPSTRAN(4),XNVE(4),
     +     DESTRAN(4),DSTRESS(4),
     +     STR(M,N),DSTR(M,N),XNDIR(M,N),DYPROD(4,4),
     +     DV(4),DDS(4,4),DPROD(4),DLAM(4)
C
C -------------------------------------------------------------------------
C TRANFER STRESS AN STRAIN TO CONVENTIONAL DEFINITION IN SOIL MECHANICS
C (COMPRESSION IS POSITIVE)
      DO I=1,NTENS
        STRESS(I)=-STRESS(I)
        STRAN(I)=-STRAN(I)
        DSTRAN(I)=-DSTRAN(I)
      END DO
C -------------------------------------------------------------------------
C SPECIFIC MATERIAL PROPERTIES
      RLAM=0.44
      RKAP=0.008
      VOIDIC=4.428
      PCS0=200.0
      BINDEX=0.15
      DEI=2.25
      ASPTMAX=1.58
      PBS0=100.0
      XNUE=0.3
```

```
      KINDEX=10.0
      WINDEX=1.5
      ALPHA=1.0
C
C ZERO MATRICES
      DO I=1,4
      DO J=1,4
       DDS(I,J)=0.0
      END DO
      END DO
      DO I=1,NTENS
       DLAM(I)=0.0
       DO J=1,NTENS
        DYPROD(I,J)=0.0
       END DO
      END DO
C      DEBUG3=0.0
      PBSF=STATEV(14)
      EQPF=STATEV(15)
C
C DEFINE PCS
      IYIELD = STATEV(6)
      IF (IYIELD .GT. 0) THEN
       PCS=STATEV(3)
       PPS=STATEV(9)
      ELSE
       PCS=PCS0
       PPS=PCS
       CAPYIELD=0
      END IF
C
C SET UP THE ELSTIC MATRIX AND IDENTITY MATRIX
C DDS = [C]
```

```
C XIDEN = [I]
C DYPROD = DYADIC PRODUCT
      SIG11=STRESS(1)
      SIG22=STRESS(2)
      SIG33=STRESS(3)
      SIG12=STRESS(4)
      SIG1=(ONE/TWO)*(STRESS(1)+STRESS(2))+
     &     SQRT((ONE/FOUR)*(STRESS(1)-STRESS(2))**TWO+STRESS(4)**TWO)
      SIG2=STRESS(3)
      SIG3=(ONE/TWO)*(STRESS(1)+STRESS(2))-
     &     SQRT((ONE/FOUR)*(STRESS(1)-STRESS(2))**TWO+STRESS(4)**TWO)
      SMEAN=(SIG1+SIG2+SIG3)/THREE
      SR3J2=SQRT((ONE/TWO)*((SIG1-SIG2)**TWO+(SIG3-SIG1)**TWO+
     &     (SIG2-SIG3)**TWO))
      IF ((SIG1-SIG3) .EQ. 0.) THEN
        BB=0.
      ELSE
        BB=(SIG2-SIG3)/(SIG1-SIG3)
      END IF
      THETA=ATAND((ONE/SQRT(THREE))*(TWO*BB-ONE))
      ASPTM=ASPTMAX*(((TWO*ALPHA**FOUR)/(ONE+ALPHA**FOUR-
     &     (ONE-ALPHA**FOUR)*SIND(THREE*THETA)))**(ONE/FOUR))
      DEBUG3=THETA
      ETA=SR3J2/SMEAN
      IF (STATEV(1) .GT. 0.0) THEN
        VOID=STATEV(1)
        DES=STATEV(2)
        PBS=STATEV(10)
        CAPYIELD=STATEV(16)
      ELSE
        !Compression curve for structured clay
        VOID=VOIDIC-(RLAM-RKAP)*LOG(PCS)-RKAP*LOG(SMEAN)
     &      +DEI*(PCS0/PCS)**BINDEX
```

```
C       VOIDR=VOIDIC-(RLAM-RKAP)*LOG(PCS)-RKAP*LOG(SMEAN)
        VOIDR=VOIDIC-RLAM*LOG(SMEAN)
        DES=VOID-VOIDR
        IF (DES .LT. 0.0) THEN
          DES=0.0
        END IF
        PBS=PBS0
      END IF
      ETABAR=SR3J2/(SMEAN+PBS)
      IF (XNUE .GT. 0.0) THEN
        EMOD=THREE*(ONE-TWO*XNUE)*(ONE+VOID)*SMEAN/RKAP
        EBULK3=EMOD/(ONE-TWO*XNUE)
        EG2=EMOD/(ONE+XNUE)
        EG=EG2/TWO
        ELAM=(EBULK3-EG2)/THREE
      ELSE
        EBULK3=THREE*(ONE+VOID)*SMEAN/RKAP
        EG2=EG*TWO
        ELAM=(EBULK3-EG2)/THREE
      END IF
C
      DO K1=1,3
        DO K2=1,3
          DDS(K2,K1)=ELAM
        END DO
        DDS(K1,K1)=EG2+ELAM
      END DO
      DDS(4,4)=EG
C
C DEFINE IDENTITY MATRIX
      DO 50 I=1,M
      DO 50 J=1,N
        IF(I .EQ. J) THEN
```

```
        XIDEN(I,J)=1.0D0
       ELSE
        XIDEN(I,J)=0.0D0
       END IF
50    CONTINUE
C
C ---------------------------------------------------------------------
C DETERMINE IF THE YIELDING CONDITION IS SATISFIED
     YF=(SR3J2**TWO-(ASPTM**TWO)*(SMEAN+PBS)*(PCS-SMEAN))/(PCS+PBS)**TWO
C
     DLAMBDA=0.
C
     IF (YF .GT. 0. .OR. IYIELD .GT. 0) THEN
C
     DFM=TWO*ASPTM*(SMEAN**TWO+SMEAN*PBS-SMEAN*PCS-PBS*PCS)
    &    /(PCS+PBS)**TWO
     DMT=((THREE*TWO**(ONE/FOUR)*ASPTMAX*ALPHA*(ALPHA**FOUR-ONE)*
    &    COSD(THREE*THETA))/(FOUR*(ONE+ALPHA**FOUR+(ONE-ALPHA**FOUR)*
    &    SIND(THREE*THETA))**(FIVE/FOUR)))
     DTS1=(NINE/(TWO*COSD(THREE*THETA)*SR3J2**THREE))
     DIFF(1)=(ASPTM**TWO)*(TWO*SMEAN+PBS-PCS)/(THREE*(PCS+PBS)**TWO)
    &        +(THREE/(PCS+PBS)**TWO)*(SIG11-SMEAN)+
    &        DFM*DMT*DTS1*(NINE*DETS*(SIG11-SMEAN)/(TWO*SR3J2**TWO)-
    &        TWO*SMEAN**TWO+TWO*SIG11*(SIG22+SIG33)/THREE+
    &        (SIG22**TWO+SIG33**TWO)/THREE-(SIG12**TWO)/THREE)
     DIFF(2)=(ASPTM**TWO)*(TWO*SMEAN+PBS-PCS)/(THREE*(PCS+PBS)**TWO)
    &        +(THREE/(PCS+PBS)**TWO)*(SIG22-SMEAN)+
    &        DFM*DMT*DTS1*(NINE*DETS*(SIG22-SMEAN)/(TWO*SR3J2**TWO)-
    &        TWO*SMEAN**TWO+TWO*SIG22*(SIG11+SIG33)/THREE+
    &        (SIG11**TWO+SIG33**TWO)/THREE-(SIG12**TWO)/THREE)
     DIFF(3)=(ASPTM**TWO)*(TWO*SMEAN+PBS-PCS)/(THREE*(PCS+PBS)**TWO)
    &        +(THREE/(PCS+PBS)**TWO)*(SIG33-SMEAN)+
    &        DFM*DMT*DTS1*(NINE*DETS*(SIG33-SMEAN)/(TWO*SR3J2**TWO)-
```

```
     &       TWO*SMEAN**TWO+TWO*SIG33*(SIG22+SIG11)/THREE+
     &       (SIG22**TWO+SIG11**TWO)/THREE-(-TWO*SIG12**TWO)/THREE)
      DIFF(4)=(SIX*SIG12/(PCS+PBS)**TWO+
     &       DFM*DMT*DTS1*(NINE*DETS*(TWO*SIG12)/(TWO*SR3J2**TWO)+
     &       TWO*SIG12*(SIG33-SMEAN)))
      !Plastic potential
C     DGM=(TWO*ASPTM/(ONE-WINDEX))*(((SMEAN+PBS)/(PPS+PBS))
C    &       **(TWO/WINDEX)-((SMEAN+PBS)/(PPS+PBS))**TWO)
      DIFG(1)=((TWO*ASPTM**TWO)/(THREE*(ONE-WINDEX)))
     &       *(((((SMEAN+PBS)/(PPS+PBS))**(TWO/WINDEX))
     &       /(WINDEX*(SMEAN+PBS)))-(SMEAN+PBS)/(PPS+PBS)**TWO)
     &       +(THREE/((PPS+PBS)**TWO))*(SIG11-SMEAN)+
     &       DGM*DMT*DMT*(NINE*DETS*(SIG11-SMEAN)/(TWO*SR3J2**TWO)-
     &       TWO*SMEAN**TWO+TWO*SIG11*(SIG22+SIG33)/THREE+
     &       (SIG22**TWO+SIG33**TWO)/THREE-(SIG12**TWO)/THREE)
      DIFG(2)=((TWO*ASPTM**TWO)/(THREE*(ONE-WINDEX)))
     &       *(((((SMEAN+PBS)/(PPS+PBS))**(TWO/WINDEX))
     &       /(WINDEX*(SMEAN+PBS)))-(SMEAN+PBS)/(PPS+PBS)**TWO)
     &       +(THREE/((PPS+PBS)**TWO))*(SIG22-SMEAN)+
     &       DGM*DMT*DTS1*(NINE*DETS*(SIG22-SMEAN)/(TWO*SR3J2**TWO)-
     &       TWO*SMEAN**TWO+TWO*SIG22*(SIG11+SIG33)/THREE+
     &       (SIG11**TWO+SIG33**TWO)/THREE-(SIG12**TWO)/THREE)
      DIFG(3)=((TWO*ASPTM**TWO)/(THREE*(ONE-WINDEX)))
     &       *(((((SMEAN+PBS)/(PPS+PBS))**(TWO/WINDEX))
     &       /(WINDEX*(SMEAN+PBS)))-(SMEAN+PBS)/(PPS+PBS)**TWO)
     &       +(THREE/((PPS+PBS)**TWO))*(SIG33-SMEAN)+
     &       DGM*DMT*DTS1*(NINE*DETS*(SIG33-SMEAN)/(TWO*SR3J2**TWO)-
     &       TWO*SMEAN**TWO+TWO*SIG33*(SIG22+SIG11)/THREE+
     &       (SIG22**TWO+SIG11**TWO)/THREE-(-TWO*SIG12**TWO)/THREE)
      DIFG(4)=(SIX*SIG12/(PPS+PBS)**TWO+
     &       DGM*DMT*DTS1*(NINE*DETS*(TWO*SIG12)/(TWO*SR3J2**TWO)+
     &       TWO*SIG12*(SIG33-SMEAN)))
C
```

```
C THEN DETERMINE THE PLASTIC MULTIPLIER
      CALL KMLT1(DDS,DSTRAN,DV,NTENS)
C
      CALL DOTPROD(DV,DIFF,TERM1,NTENS)
C
      CALL KMLT1(DDS,DIFG,DV,NTENS)
C
      CALL DOTPROD(DIFF,DV,TERM2,NTENS)
C
      !Hardening modulus
      A1=(TWO*SR3J2**TWO-(ASPTM**TWO)*SMEAN*PCS+THREE*(ASPTM*TWO)
     &   *SMEAN*PBS-(ASPTM**TWO)*PBS*PCS+(ASPTM**TWO)*(PBS**TWO)
     &   +TWO*(ASPTM**TWO)*(SMEAN**TWO))/(PCS+PBS)**THREE
C     Modified date 09/09/2010
      A2=PCS*(ONE+VOID)/(RLAM-RKAP+BINDEX*DES)
      IF (PBSF .GT. 0.0 .AND. CAPYIELD .GT. 0) THEN
        A2=PCS*(ONE+VOID)/(RKAP)
      END IF
      A3=((TWO*ASPTM**TWO)/(ONE-WINDEX))*(((SMEAN+PBS)/(PPS+PBS))
     &   **(TWO/WINDEX)/(WINDEX*(SMEAN+PBS))
     &   -(SMEAN+PBS)/(PPS+PBS)**TWO)
      TERM3=(A1*A2*A3)
C
      DLAMBDA=(TERM1/(TERM2+TERM3))
      IF (TERM3 .LT. 0.0) THEN
       !OC YIELD
        IYIELD=1
        IF (CAPYIELD .GT. 0) THEN
          IYIELD=2
        END IF
        IF (PBSF .GT. 0.0) THEN
        ELSE
          PBSF=PBS
```

```
          EQPF=STATEV(13)
         END IF
       ELSE
        !CAP YIELD
         IYIELD=3
         CAPYIELD=1
       END IF
C
       END IF
C -------------------------------------------------------------------------
C CALCULATE PLASTIC STRAIN INCREMENT
C
       DO K=1,4
        DPSTRAN(K)=DLAMBDA*DIFG(K)
       END DO
       DEVP=DLAMBDA*((TWO*ASPTM**TWO)/(ONE-WINDEX))
      &   *(((SMEAN+PBS)/(PPS+PBS))
      &   **(TWO/WINDEX)/(WINDEX*(SMEAN+PBS))
      &   -(SMEAN+PBS)/(PPS+PBS)**TWO)
       DEQP=DLAMBDA*(TWO*SR3J2/(PPS+PBS)**TWO)
C
C DETERMINE ELASTIC STRAIN INCREMENT
       DO K=1,4
        DESTRAN(K)=DSTRAN(K)-DPSTRAN(K)
       END DO
C
C DETERMINE STRESS INCREMENT
       CALL KMLT1(DDS,DESTRAN,DSTRESS,NTENS)
C -------------------------------------------------------------------------
C UPDATE ALL QUANTITIES USING EXPLICIT INTEGRATION
C
       DO K=1,NTENS
        STRESS(K)=STRESS(K)+DSTRESS(K)
```

```
      END DO
C -------------------------------------------------------------------------
C DETERMINE JACOBIAN
      IF (YF .GT. 0.0 .OR. IYIELD .GT. 0) THEN
        CALL KMLT1(DDS,DIFG,DPROD,NTENS)
        CALL DOTPROD(DIFF,DPROD,XNDN,NTENS)
C
        A1=(TWO*SR3J2**TWO-(ASPTM**TWO)*SMEAN*PCS+THREE*(ASPTM*TWO)
     &   *SMEAN*PBS-(ASPTM**TWO)*PBS*PCS+(ASPTM**TWO)*(PBS**TWO)
     &   +TWO*(ASPTM**TWO)*(SMEAN**TWO))/(PCS+PBS)**THREE
C
C     Modified date 09/09/2010
        A2=PCS*(ONE+VOID)/(RLAM-RKAP+BINDEX*DES)
        IF (PBSF .GT. 0.0 .AND. CAPYIELD .GT. 0) THEN
          A2=PCS*(ONE+VOID)/(RKAP)
        END IF
        A3=((TWO*ASPTM**TWO)/(ONE-WINDEX))*(((SMEAN+PBS)/(PPS+PBS))
     &   **(TWO/WINDEX)/(WINDEX*(SMEAN+PBS))
     &   -(SMEAN+PBS)/(PPS+PBS)**TWO)
        H=(A1*A2*A3)
        HARD=XNDN+H
C
        CALL KMLT1(DDS,DIFF,DV,NTENS)
        CALL DYADICPROD(DPROD,DV,DYPROD,NTENS)
        DO I=1,4
          DO J=1,4
            DYPROD(I,J)=DYPROD(I,J)/HARD
          END DO
        END DO
      END IF
C
      DO I=1,4
        DO J=1,4
```

```
        DDSDDE(I,J)=DDS(I,J)-DYPROD(I,J)
       END DO
     END DO
C
C -------------------------------------------------------------------------
C UPDATE STATE VARIABLES
     SIG11=STRESS(1)
     SIG22=STRESS(2)
     SIG33=STRESS(3)
     SIG12=STRESS(4)
     SIG1=(ONE/TWO)*(STRESS(1)+STRESS(2))-
    &     SQRT((ONE/FOUR)*(STRESS(1)-STRESS(2))**TWO+STRESS(4)**TWO)
     SIG2=STRESS(3)
     SIG3=(ONE/TWO)*(STRESS(1)+STRESS(2))+
    &     SQRT((ONE/FOUR)*(STRESS(1)-STRESS(2))**TWO+STRESS(4)**TWO)
     SMEAN=(SIG1+SIG2+SIG3)/THREE
     SR3J2=SQRT((ONE/TWO)*((SIG1-SIG2)**TWO+(SIG3-SIG1)**TWO+
    &     (SIG2-SIG3)**TWO))
     DEV=DSTRAN(1)+DSTRAN(2)+DSTRAN(3)
     DEQ=(SQRT(TWO)/THREE)*SQRT((DSTRAN(1)-DSTRAN(2))**TWO+
    &    (DSTRAN(2)-DSTRAN(3))**TWO+(DSTRAN(3)-DSTRAN(1))**TWO
    &    +SIX*DSTRAN(4)**TWO)
     EQ=STATEV(12)+DEQ
     EV=STATEV(17)+DEV
     IF ((SIG1-SIG3) .EQ. 0.) THEN
       BB=0.
     ELSE
       BB=(SIG2-SIG3)/(SIG1-SIG3)
     END IF
     THETA=ATAND((ONE/SQRT(THREE))*(TWO*BB-ONE))
     ASPTM=ASPTMAX*(((TWO*ALPHA**FOUR)/(ONE+ALPHA**FOUR-
    &     (ONE-ALPHA**FOUR)*SIND(THREE*THETA)))**(ONE/FOUR))
     IF (IYIELD .GT. 0) THEN
```

```
      EVP=STATEV(8)+DEVP
      EQP=STATEV(13)+DEQP
      PCSNEW=PCS+(ONE+VOID)*DEVP*PCS/(RLAM-RKAP+BINDEX*DES)
      IF (PBSF .GT. 0.0 .AND. CAPYIELD .GT. 0) THEN
       PCSNEW=PCS+(ONE+VOID)*DEVP*PCS/(RKAP)
      END IF
      IF (PBSF .GT. 0.0) THEN
       PBS=PBSF*EXP(-KINDEX*(EQP-EQPF))
      ELSE
       PBS=PBS0*EXP(-EQP)
      END IF
      !Determination of pp
      A1=((SR3J2**TWO)*WINDEX-(SR3J2**TWO)+
     &    TWO*(ASPTM**TWO)*SMEAN*PBS+(ASPTM**TWO)*(PBS**TWO)
     &    +(ASPTM**TWO)*(SMEAN**TWO))/((ASPTM**TWO)*(SMEAN+PBS)**TWO)
      A2=WINDEX/(TWO*(WINDEX-ONE))
      PPS=SMEAN*(A1**A2)+PBS*(A1**A2)-PBS
     ELSE
      EVP=0.0
      EQP=0.0
      PCSNEW=PCS
     END IF
     VOID=VOID-DEV*(ONE+VOID)
C     VOIDR=VOIDIC-(RLAM-RKAP)*LOG(PCSNEW)-RKAP*LOG(SMEAN)
     VOIDR=VOIDIC-RLAM*LOG(SMEAN)
     DES=VOID-VOIDR
     !Add on 28-08-2010
     IF (DES .LT. 0.0) THEN
      DES=0.0
     END IF
C
C STORE UPDATE STATE VARIABLES
     STATEV(1)=VOID
```

```
      STATEV(2)=DES
      STATEV(3)=PCSNEW
      STATEV(4)=YF
      STATEV(5)=DLAMBDA
      STATEV(6)=IYIELD
      STATEV(7)=ETA
      STATEV(8)=EVP
      STATEV(9)=PPS
      STATEV(10)=PBS
      STATEV(11)=ETABAR
      STATEV(12)=EQ
      STATEV(13)=EQP
      STATEV(14)=PBSF
      STATEV(15)=EQPF
      STATEV(16)=CAPYIELD
      STATEV(17)=EV
      STATEV(18)=DEBUG3
C
C
C -------------------------------------------------------------------------
C TRANFER STRESS AN STRAIN TO CONVENTIONAL DEFINITION IN SOIL MECHANICS
C (COMPRESSION IS POSITIVE)
      DO I=1,NTENS
        STRESS(I)=-STRESS(I)
        STRAN(I)=-STRAN(I)
        DSTRAN(I)=-DSTRAN(I)
      END DO
C
      RETURN
      END
```

```
**************************************************************************
* UTILITY SUBROUTINES
**************************************************************************
* MULTIPLY 4X4 MATRIX WITH 4X1 VECTOR
      SUBROUTINE KMLT1(DM1,DM2,DM,NTENS)
C
      INCLUDE 'ABA_PARAM.INC'
C
      PARAMETER (M=4)
C
      DIMENSION DM1(M,M),DM2(M),DM(M)
C
      DO 10 I=1,NTENS
        X=0.0
      DO 20 K=1,NTENS
        Y=DM1(I,K)*DM2(K)
        X=X+Y
20    CONTINUE
      DM(I)=X
10    CONTINUE
      RETURN
      END
* DOT PRODUCT OF TWO VECTOR
      SUBROUTINE DOTPROD(DM1,DM2,DM,NTENS)
C
      INCLUDE 'ABA_PARAM.INC'
C
      DIMENSION DM1(4),DM2(4)
C
      Y=0.0
      DO 20 K=1,NTENS
        X=DM1(K)*DM2(K)
        Y=X+Y
```

```
20    CONTINUE
      DM=Y
      RETURN
      END
* THE DYADIC PRODUCT OF TWO VECTORS
      SUBROUTINE DYADICPROD(DM1,DM2,DM3,NTENS)
C
      INCLUDE 'ABA_PARAM.INC'
C
      DIMENSION DM1(4),DM2(4),DM3(4,4)
C
      DO I=1,4
        DO J=1,4
          DM3(I,J)=DM1(I)*DM2(J)
        END DO
      END DO
C
      RETURN
      END
```

APPENDIX C

LIST OF PUBLICATIONS

INTERNATIOANAL JOURNAL

Horpibulsuk, S., Liu, M. D., Liyanapathirana, D. S., and Suebsuk, J. (2010). **Behaviour of cemented clay simulated via the theoretical framework of Structured Cam Clay model**. Computers and Geotechnics. 37(1-2): 1-9.

Suebsuk, J., Horpibulsuk, S., and Liu, M.D. (2010). **Modified Structured Cam Clay: A Generalised Critical State Model for Destructured, Naturally Structured and Artificially Structured Clays**. Computers and Geotechnics. 37(7-8): 956-968.

Suebsuk, J., Horpibulsuk, S., and Liu, M.D. (2011). **A critical state model for structured clay in overconsolidated state**. Computers and Geotechnics. (In press)

Suebsuk, J., Horpibulsuk, S., and Liu, M.D. (201?). **The influence of soil cementation structure on the inhomogeneous behaviour of triaxial compression test studied by the MSCC model**. Communicated to Computers and Geotechnics.

NATIONAL JOURNAL

Suebsuk, J., Horpibulsuk, S., and Liu, M.D. (2008). A modified Structure Cam Clay model. Research and Development Journal of The Engineering Institute of Thailand. 19(1): 1-8.

INTERNATIONAL CONFERENCE AND SYMPOSIUM

Horpibulsuk, S., Suebsuk, J., Liu, M.D., and Carter, J.P. (2006), **Simulation of the undrained shear behavior of cemented clay with the modified Structure Cam Clay model**, Proceeding of 6th International Symposium on Soil/Ground Improvement and Geosynthetics (ISGIS) (pp. 162-170). Thailand.

Suebsuk, J., Horpibulsuk, S. and Liu, M.D. (2007). **Simulation the undrained behavior of induced cemented clay with a Cemented Soil model**. Proceedings of PSU-UNS International Conference on Engineering and Environment - ICEE-2007. Phuket, Thailand. (CD version)

Horpibulsuk, S., Suebsuk, J., and Liu, M.D., (2007). **A Theoretical Study of the Pore Pressure Development of Cemented Soft Clays**. Earthquake Engineering Conference AEES 2007. Australia.

Liu, M.D., Horpibulsuk, S., Suebsuk, J., and Chinkulkijniwat, A. (2007). **A Theoretical Study of the Behaviour of Clays in Reconstituted, Naturally Structured and Cemented States**. Proceedings of 7th International Symposium on Geotechnical Engineering, Ground Improvement and Geosynthetics for Human Security and Environmental Preservation (pp. 469-483). Bangkok, Thailand.

Suebsuk, J., Horpibulsuk, S. and Liu, M.D. (2008). **Modeling the volumetric deformation of naturally structured clays during subyielding**. Proceedings of The 12th International Conference of International Association for Computer Methods and Advances in Geomechanics (IACMAG) (pp. 883-890). 1-6 October 2008, GOA, India.

Horpibulsuk, S., Suebsuk, J., Chinkulkijniwat, A. and Liu, M.D. (2009). **A study the compression behaviour of structured clays**. Proceedings of the International Symposium on Prediction and Simulation Methods for Geo-hazard (IS-Kyoto2009) (pp. 269-272). 25-27 May 2009, Kyoto, Japan.

Suebsuk, J., Horpibulsuk, S., Chinkulkijniwat, A. and Liu, M.D. (2009). **Modeling the behavior of artificially structured clays by the Modified Structured Cam clay model**. Proceedings of the International Symposium on Prediction and Simulation Methods for Geo-hazard (IS-Kyoto2009) (pp. 313-318). 25-27 May 2009, Kyoto, Japan.

Pan, J., Liu, M.D., Horpibulsuk, S., and Suebsuk, J. (2010). **A compression model of structured soils**. Proceedings of the 17th Southeast Asian Geotechnical Conference (SEAGC) (pp. 157-160). 13-15 May 2010, Taipei, Taiwan.

Suebsuk, J., Horpibulsuk, S. Liu, M.D. (2010). **Modified Structured Cam Clay model: theory and verification**. Proceedings of the international symposium and exhibition on geotechnical and geosynthetics engineering: challenges and opportunities in climate change. (pp. 419-434). 7-8 December, Bangkok, Thailand.

NATIONAL CONFERENCE AND SYMPOSIUM

Suebsuk, J., Horpibulsuk, S. and Liu, M.D., (2007). **The cemented soil model for cemented clay**. Proceedings of the 12th National Convention Thailand on Civil Engineering (NCCE) (vol.3, 189-196). 2-4 May 2007, Phitsanulok, Thailand.

Suebsuk, J., Horpibulsuk, S. and Liu, M.D. (2008). **A new hardening rule for natural cemented soil during subyielding**. Proceedings of 13th National Convention Thailand on Civil Engineering (NCCE). Thailand.

BIOGRAPHY

My name is Mr. Jirayut Suebsuk. I obatined my bachelor degree in Civil Engineering from the School of Civil Engineering, Srinakharinwirot University since 2002. I then worked as a civil engineer at the S. Inter & Associated Co., Ltd. from 2002 to 2003. In June 2003, I continued my master studies at the School of Civil Engineering, Suranaree University of Technology and received my Master's degree in Civil Engineering in May 2006. I started my Ph.D. study in June 2006. During my Ph.D. study, I worked as a teaching assistant at the School of Civil Engineering, giving courses on Engineering Statics and Soil Mechanics Laboratory during 2006-2009. I visited the Faculty of Engineering, University of Wollongong, NSW, Australia for research under the supervision of Dr. Martin D. Liu from April to October 2010. During my Ph.D. study, I published 3-international and 1-national journal papers, as well as 11-international and national conference papers.